RXE-92-01B

Individual Plant Examination Submittal:

Comanche Peak Steam Electric Station

Volume II: Back-End Analysis

By

H. C. da Silva, Jr.

October, 1992

Prepared by: Hugo C. da Silva Jr. 10-27-92

H. C. da Silva, Jr. Date
Senior Engineer

Reviewed by: S. D. Karpyak 10-27-92

S. D. Karpyak Date
Senior Engineer

W. G. Choe 10-27-92

W. G. Choe Date
Supervisor, LOCA Analysis

Approved by: H. G. Hamzehee 10/27/92

H. G. Hamzehee Date
Supervisor, Systems Analysis

Ansaf Husain 10/27/92

A. Husain Date
Director, Reactor Engineering

ACKNOWLEDGEMENT

Both the front-end and back-end components of the CPSES IPE were multi-discipline efforts. It is therefore appropriate to recognize contributions from all members of the IPE team, LOCA Analysis Group, and support staff. Specifically, it is important to mention: Chris Cragg, who binned the Level I sequences into PDS and streamlined the CET computation process; Dan Tirsun, who produced the ISLOCA analysis and the descriptions of the Level I functional sequences; Yu Shen, for his mathematically rigorous derivations which were used to compute several basic event probabilities; Dan Brozak, who reviewed and helped prepare the MAAP Parameter file development document and compiled all the plant data for Section 4.1 of this report; Steve Karpyak, who managed the report production; and Irene Reyes who did all the word processing.

Table of Contents

List of Tables

List of Figures

List of Acronyms

AF	-	Auxiliary Feedwater
ARV	-	Atmospheric Relief Valve
ASME	-	American Society of Mechanical Engineers
ASTM	-	American Society of Testing and Materials
ATU	-	Automatic Transfer Unit
ATWS	-	Anticipated Transient Without Scram
BATP	-	Boric Acid Transfer Pump
BOS	-	Blackout Signal
CACRS	-	Containment Air Recirculation and Cooling System
CAFTA	-	Computer Aided Fault Tree Analysis
CC	-	Component Cooling Water
CCI	-	Core Concrete Interaction
CCP	-	Centrifugal Charging Pump
CET	-	Containment Event Tree
CH	-	Chilled Water (Safety and Nonsafety)
CI	-	Instrument Air
CPSES	-	Comanche Peak Steam Electric Station
CS	-	Chemical and Volume Control System
CST	-	Condensate Storage Tank
CT	-	Containment Spray
CW	-	Circulating Water
CZ	-	Containment Isolation System
DCH	-	Direct Containment Heating
DHR	-	Decay Heat Removal
ECCS	-	Emergency Core Cooling System
EHC	-	Electro-Hydraulic Control
EOP	-	Emergency Operating Procedure
EP	-	Electrical Power
EPRI	-	Electric Power Research Institute
ERG	-	Emergency Response Guideline
ES	-	Reactor Protection System
ESF	-	Engineered Safeguards Feature
ESFAS	-	Engineered Safeguards Features Actuation System
FSAR	-	Final Safety Analysis Report
FTT	-	Fuel Transfer Tube
FW	-	Main Feedwater

HPME	-	High Pressure Melt Ejection
HRA	-	Human Reliability Analysis
HVAC	-	Heating Ventillation and Air Conditioning
IDCOR	-	Industrial Degraded Core Rulemaking Program
IPE	-	Individual Plant Examination
ISGTR	-	Induced Steam Generator Tube Rupture
LOCA	-	Loss of Coolant Accident
LOOP	-	Loss of Offsite Power
MAAP	-	Modular Accident Analysis Program
MCC	-	Motor Control Center
MS	-	Main Steam
MSIV	-	Main Steam Isolation Valve
MSLB	-	Main Steam Line Break
NRC	-	Nuclear Regulator Commission
NSAC	-	Nuclear Safety Analysis Center
P	-	Containment Hi-3 Signal
PDS	-	Plant Damage State
PORV	-	Power Operated Relief Valve
PRA	-	Probabilisitic Risk Assessment
RC/RCS	-	Reactor Coolant (System)
RCC	-	Rod Cluster Control Guide
RCP	-	Reactor Coolant Pump
RCPB	-	Reactor Coolant Pressure Boundary
RH	-	Residual Heat Removal
RV	-	Reactor Vessel
RWST	-	Refueling Water Storage Tank
S/G	-	Steam Generator
S	-	Safety Injection Signal
SGTR	-	Steam Generator Tube Rupture
SI	-	Safety Injection
SIP	-	Safety Injection Pump
SRV	-	Safety Relief Valve
STCP	-	Source Term Code Package
SW	-	Station Service Water
TDAFWP	-	Turbine Driven Auxiliary Feedwater Pump
TPCW	-	Turbine Plant Cooling Water

1. EXECUTIVE SUMMARY

The CPSES IPE was prepared in two volumes: Volume I presents the front-end analysis and Volume II presents the back-end analysis. The general issues common to the front-end and to the back-end were reported in Volume I along with the front-end analysis. Nevertheless, some areas require reporting from both the front-end and the back-end perspectives. In those cases, the front-end perspective is presented in Volume I and the back-end perspective is presented in Volume II. The sections which in Volume II contain the back-end findings, and in Volume I, contain the front-end findings are:

The deterministic part of the back-end analysis, i.e., the severe accident sequence analyses relevant to the CPSES IPE, utilizes the Modular Accident Analysis Program (MAAP 3.0B, Rev. 16, Ref. 10). The MAAP code is a well-known, fully integrated analytical tool for the analysis of severe accidents. The logic model and the probabilistic part of the CPSES back-end analysis are based on standard methodology, specifically the EPRI back-end generic framework (Ref.1).

1.4 Summary of Major Findings (Back-end)

The overall performance of the CPSES containment given a core melt accident[1] can be summarized by one of the following outcomes:

(1)	The containment will remain intact	40%
(2)	Late failures from steam generation	2%
(3)	Late failures from core-concrete interactions	49%
(4)	Early bypass (mostly due to SGTR)	8%
(5)	Early failures due to phenomena (HPME or ALPHA)	1%
	TOTAL	100%

[1] The overall core melt frequency is 5.72E-5 per year as reported in Volume I.

The main conclusion to be drawn from these findings is that the CPSES containment provides adequate protection to the public.

The principal concerns in that regard are the frequency and timing of potential early containment failures. With the exception of Steam Generator Tube Ruptures (SGTR), all other possible modes of early containment failure have frequencies nearly at or below the reporting cut-off levels of 1E-7. Although classified as early failures, most SGTR events would take several hours to reach core melt, allowing that time to be used for accident diagnosis and management.

Regarding the late containment failures, almost all are due to overpressurization from non-condensibles originating in a post dry-out core concrete attack. This type of failure is protracted over approximately 36 hours, allowing for effective accident management.

CPSES exhibits three specific design features that are the underlying causes for the good performance of the CPSES containment.

The first is the very large containment free volume, which renders the CPSES containment relatively invulnerable to early hydrogen burn events and to the direct containment heating (DCH) phenomena associated with high pressure melt ejection sequences. Calculations performed for the CPSES containment show that the containment would not reach the failure pressure even if a hydrogen burn from a 100% Zirconium oxidation were postulated. Furthermore, the assessment of the direct containment heating phenomena for CPSES, which is based on the conservative analyses for the Zion plant under the NUREG-1150 program, has shown that the CPSES containment is unlikely to fail as a result of a DCH overpressure transient.

The second and third important containment features are associated with the reactor cavity configuration. First, the reactor cavity has a large flat floor area of over 70 m^2 (800 ft^2). This results in a shallow debris bed of only a few inches thickness, which is coolable by an overlaying layer of water, and which would result in a slow concrete penetration rate if the debris is dry and not self cooled by convection to the atmosphere. Second, there is no curb at the containment floor elevation surrounding the reactor cavity exit for the instrument guide tubes that would prevent the return of water from the main containment floor to the reactor cavity. As a result, all the water injected into the containment or released inside the containment has to boil off before the debris in the reactor cavity can dry out. Accident sequences with failure of RWST injection dominate the plant damage states that dominate the

containment failures. Therefore, the absence of a reactor cavity curb means that even if only the RCS water inventory is released to the containment, this entire water inventory must boil off and be in the form of steam in the containment before the debris in the reactor cavity can dry out. After that, containment pressurization proceeds very slowly, due only to non-condensible gas generation in the core-concrete attack. This characteristic results in the protracted containment failures. Furthermore, any condensation or water injected into the containment by accident management would drain back to the reactor cavity and to the debris.

Finally, the back-end analysis did not reveal any vulnerabilities nor the need for any plant improvements.

4. BACK-END ANALYSIS

The back-end (sometimes called containment) analysis of the CPSES IPE utilizes the approach of a Level II probabilistic risk assessment (PRA), whose methods and results are summarized in this section. A Level II analysis involves two types of considerations: (1) analyses of physical processes during severe accidents, where degraded core and containment thermo-hydraulic variables are determined along with source terms for the accident progressions, and (2) a probabilistic component where the likelihood of the various outcomes is assessed. The relationship of a Level II analysis to a Level I (and a Level III, sometimes called site) analysis is shown schematically in Figure 4.0-1. The starting point for the Level II analysis is the plant damage states (PDS). These are the bins into which the core melt sequences determined in the Level I, or plant, analysis are collected. The guidelines for these bins are determined such that sequences in a given bin have similar accident progressions and outcomes of similar likelihood. For each PDS there is a containment event tree (CET). The path through each CET begins with a PDS and ends with a CET end-state which is defined by a containment failure mode, time and release fractions. These CET end-states are later binned into release categories. Thus, release categories represent types, quantities and timing of radioactive material releases.

This section begins in Section 4.1 with the summary of plant data requested in section 2.2.2.6 of NUREG-1335. That is followed in Section 4.2 by a description of plant models and methods utilized for the physical processes analyses. Section 4.3 describes the criteria and the results of the binning process whereby the Level I sequences are grouped into PDSs. Section 4.4 identifies the possible challenges to the CPSES containment, including those leading to containment bypass, early failures and late failures. It also examines the possible ways in which the containment might fail to perform its function by evaluating penetrations, evaluating the limits for liner tear at discontinuities and evaluating the ultimate strength of the containment to catastrophic failure. Section 4.5 presents CETs and the rationale for their development. Section 4.6 discusses the CET quantification which is the assessment of probabilities, and the phenomenological developments that define the accident progression. It includes an analysis of uncertainties to demonstrate the absence of hidden vulnerabilities and the overall robustness of the findings. Section 4.7 groups the CET end-states into release categories and provides the frequency, the type, timing and release fractions for the release categories.

Figure 4.0-1: Schematic Representation of PRA Levels

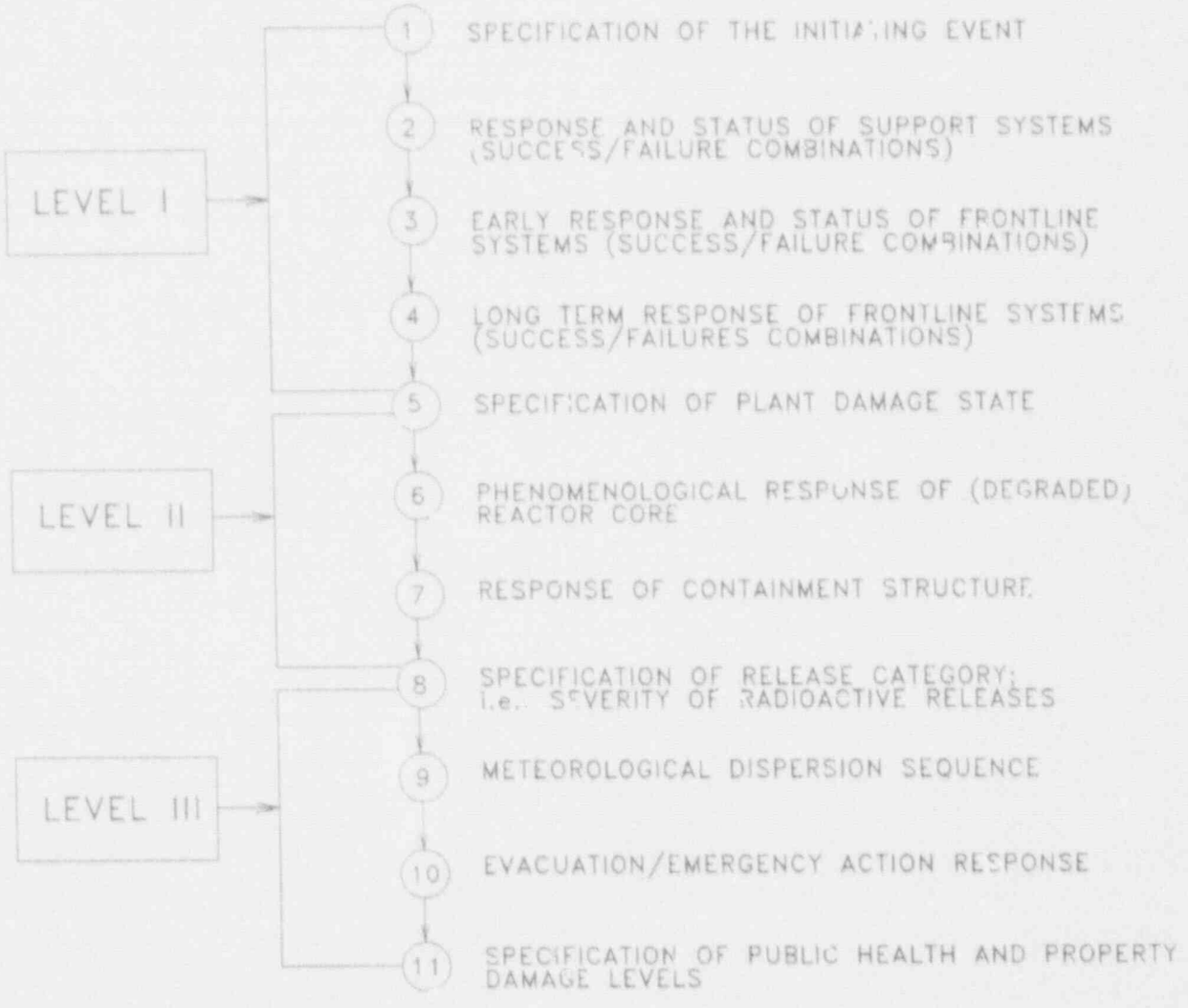

4.1 Plant Data and Plant Description

As discussed in Section 4.2, the severe accident sequences that are relevant to the CPSES IPE were analyzed using the MAAP code (Refs. 2,7,10). In order to perform those analyses, it was necessary to collect a substantial amount of plant data, which is summarized in the code's parameter file. A detailed derivation of this file is recorded in Reference 25. The present section summarizes some of that information by identifying and highlighting most of the component, system and structure data that is of significance in assessing severe accident progressions. Additional information including the sources and the derivation of the information presented in this section is available in Reference 25.

This section is organized into the four subsections suggested by Table A.1 of NUREG-1335, viz.:

- Reactor Core, Vessel and Primary System
- Containment System
- Emergency Core Cooling Systems (ECCS) and other water injection/recirculation systems
- Auxiliary Building

Each subsection contains a narrative followed by tabular data in that category. Figures that include the drawings requested in NUREG-1335 are at the end of the section.

4.1.1 Reactor Core, Vessel and Primary System Data

The reactor core consists of 193 fuel assemblies, each a 17 x 17 rod array with 264 fuel rods, 24 rod cluster control guide (RCC) thimbles and an incore instrumentation thimble. The fuel rods consist of slightly enriched UO_2 pellets. Fuel rod cladding is Zircaloy-4. The RCC guide thimbles and instrumentation thimbles are Zircaloy-4, with type-304 stainless steel sleeves positioned at each axial location of an Inconel-718 spring clip grid. The sleeves are fastened to the eight grids at approximately equal distances along the length of the column. The RCC guide thimbles are secured to the top and bottom nozzles to complete the assembly.

The reactor vessel is sufficiently described by the data in Tables 4.1.1-6, 7 and 8.

The primary system is described in Section 3.2.1-7 (Volume 1 of this report: Front-End Submittal). Additional reactor core, vessel and primary system data is summarized in Tables 4.1.1-1 through 12 as follows:

Table 4.1.1-1	Core Materials Weight and Volume
Table 4.1.1-2	Core Geometry
Table 4.1.1-3	Core Performance Characteristics
Table 4.1.1-4	Rod Cluster Control Assemblies
Table 4.1.1-5	Burnable Poison Rods
Table 4.1.1-6	Reactor Vessel (RV) Metal Masses
Table 4.1.1-7	RV Fluid Volumes
Table 4.1.1-8	RV Geometry
Table 4.1.1-9	RCS Fluid Volumes
Table 4.1.1-10	RCS Valve Data and Setpoints
Table 4.1.1-11	RCS Normal Full Power Operating Conditions
Table 4.1.1-12	RCS Metal Masses

In addition, the following drawings of the reactor coolant system are provided:

Figure 4.1-1	General Plant Schematic
Figure 4.1-2	Simplified Process Flow Diagram of the RCS
Figure 4.1-3	Main Components of the RCS
Figure 4.1-4	Primary Side Process Flow Diagram
Figure 4.1-5	Secondary Side Process Flow Diagram
Figure 4.1-6	Structural Plant Arrangement
Figure 4.1-7	Containment Cut View with Main RCS Components
Figure 4.1-8	General Reactor Vessel Assembly
Figure 4.1-9.1	Reactor Vessel Lower Internals Assembly
Figure 4.1-9.2	Lower Core Support Assembly
Figure 4.1-10	Bottom Mounted Reactor Vessel Instrumentation
Figure 4.1-11.1	Pressurizer (Cutaway)

Table 4.1.1-1: Core Materials Weight and Volume

Core Material Active Core, Cold	Density (lbm/in^3)	Volume (in^3)	Weight (lbm)
Fuel, UO_2	0.376	592,140	222,645
Zircaloy-4	0.237	198,281	46,993
Inconel-718	0.296	6,221	1,841
Stainless Steel-304	0.285	4,758	1,356

Table 4.1.1-2: Core Geometry

Core Average Active Fuel Height, in	144.0
Lattice Configuration	17 x 17
Lattice Pitch, in	0.496
Number of Fuel Assemblies	193
Region 1	65
Region 2	64
Region 3	64
Number of Rods per Assembly	264
Enrichments, w/o U-235	
Region 1	1.60
Region 2	2.40
Region 3	3.10
Outer Fuel Rod Diameter, in	0.374
Cladding Thickness, in	0.0225
Diametral Gap, in	0.0065
UO_2 Pellet Diameter, in	0.3225
Density (Percent of Theoretical)	95.0
Volume Fraction of UO_2 in Pellet Region	0.9880
Cladding Material	Zircaloy-4
Gap Material	Helium
Guide/Instrument Thimble Material	Zircaloy-4
Structural Grid Material	Inconel-718
Grid Sleeve Material	SS-304
Number of Grids over Height of Assembly	8

Table 4.1.1-3: Core Performance Characteristics

Heat Output, MWt	3,411
Heat Generated in Fuel, %	97.4
Coolant Average Temperature at HFP, °F	591
Operating Pressure, psia	2,250

Table 4.1.1-4: Rod Cluster Control Assemblies

Material	Ag-80%, In-15%, Cd-5%
Number of Fuel Assemblies Containing RCC Assemblies	53
Number of Absorber Rods per RCC Assembly	24

Table 4.1.1-5: Burnable Poison Rods

Material	Borosilicate Glass
Content, B_2O_3, w/o	12.5
Number in Core	944

Table 4.1.1-6: Reactor Vessel (RV) Metal Masses, lbm

Core Barrel	
Above the Top Elev. of the Core	39,694
Below the Top Elev. of the Core	124,315
Upper Plenum Internals	68,702
Upper Core Support Plate	39,500
RV Wall	
Above Upper Head Flange	202,302
Below Upper Head Flange	661,656
Lower Plenum Head	82,382

Table 4.1.1-7: RV Fluid Volumes, ft^3

RV Total Volume	4,571
Downcomer	936
Lower Plenum	889
Core + Bypass	844
Upper Plenum	959
Upper Head	903

Table 4.1.1-8: RV Geometry, in

Inner Diameter of RV Wall	
Above Nozzles	170.88
Below Nozzles	173.00
Spherical Radius of Lower Plenum Head	88.16
Thickness of Lower Plenum Head	5.52

Table 4.1.1-9: RCS Fluid Volumes, ft^3

Primary System Total Water Inventory	Approximately 12,000
RV Total Volume	4,571
Pressurizer (steam + water)	1,800
Pressurizer Surge Line	46
Hot Legs	317
Intermediate Legs	531
Cold Legs	332
Reactor Coolant Pumps	314
Steam Generator Inlet Plenums	670
Steam Generator Tubes	2,528
Steam Generator outlet Plenums	630
Secondary System	
Steam Generator (steam + water)	5,954
Nominal Main Steam Line Piping from SG to MSIV (per loop)	962

Table 4.1.1-10: RCS Valve Data and Setpoints

Pressurizer	
Number of Safety Valves	3
Safety Valve Setpoint, psia	2,500
Safety Valve Rated Flow, lbm/hr	420,000
Number of Power Operated Relief Valves	2
PORV Setpoint, psia	2,350
PORV Rated Flow, lbm/hr	210,000
Spray Setpoint, psia	2,300
Steam Generator (SG)	
Number of Safety Valves	5
SG Safety Valve Low Setpoint, psia	1,200
SG Safety Valve High Setpoint, psia	1,250
Avg SG Safety Valve Rated Flow, lbm/hr	911,779
Number of Power Operated Relief Valves	1
PORV Setpoint, psia	1,140
PORV Rated Flow, lbm/hr	735,370

Table 4.1.1-11: RCS Normal Full Power Operating Conditions

Primary System	
System Pressure, psia	2,250
Nominal Water Temperature, °F	591
Total Thermal Flow Rate, lbm/hr	142,000,000
Pressure Drops, psi	
Across Core	25.8
Across RV (including nozzles)	46.3
Secondary System	
SG Pressure, psia	1,000
Main Feedwater Flow per SG, lbm/hr	3,390,000
SG Water Mass, lbm	102,500

Table 4.1.1-12 RCS Metal Masses, lbm

Hot Leg (per loop)	15,972
Intermediate Leg (per loop)	23,800
Cold Leg (per loop)	14,964
Pressurizer Shell and Heaters	195,508
Pressurizer Surge Line	12,827
SG Total Shell	310,000
SG Lower Head & Tubesheet	180,800

4.1.2 Containment System

The key features of the containment are: (1) safeguards and isolation systems and (2) containment design and structures. These features are summarized in Tables 4.1.2-1 and 2, respectively.

4.1.2.1 Safeguards and Isolation Systems

The containment safeguards systems are the Containment Spray System (CT) and the Fan Coolers (FC) that are part of the Containment Air Cooling and Recirculation System (CACRS). The Containment Isolation System (CZ) is a system designed to provide integrity of the containment boundary. These systems are discussed in detail in the following sections.

Containment Spray System (CT)

The Containment Spray System is discussed in Section 3.2.1-5 (Volume I of this submittal: Front-End) and a diagram of the system is shown there, in Figure 3.2.1.5. Additional information on the CT system is provided here and in Table 4.1.2-1, Figure 4.1-19 and Figure 4.1-23.3.

The CT system consists of two separate, independent, and full capacity trains. Each train contains two spray pumps, one heat exchanger, two chemical eductors, spray headers, spray nozzles, associated piping, valves, and instrumentation. Failure of the CT system does not result in an initiating event.

The function of the CT system is to maintain the containment pressure within its design limit after the following initiating events:

- Loss-Of-Coolant-Accident (LOCA)
- Main Steam Line Break (MSLB) inside containment
- Feedwater Line Break (FWLB) inside containment

The CT pumps are provided with suction lines from both the Refueling Water Storage Tank (RWST) and the containment sumps. Thus, the system is capable of providing the containment with short term (injection mode) and long term (recirculation mode) cooling. Each pump train takes suction from the RWST via normally open motor-operated valve 1-HV-4758/4759. The CT system shares the RWST with

the Safety Injection System (SI), Residual Heat Removal System (RH) and Chemical and Volume Control System (CS). In addition, the RH, SI, and CT systems share RWST isolation valve 1SI-047. Following depletion of the RWST, the suction of the CT pump train is switched over to its respective containment sump via normally closed motor-operated valve 1-HV-4782/4783. The RH and CT systems share the containment sumps.

The design flow rate of each CT pump is 3000 gpm at 260 psid. The design of the system is such that both pumps per train are required to deliver enough flow to the spray header to remove an adequate amount of heat from the containment atmosphere. The pumps are powered from separate Class 1E 6.9kV buses. Each CT pump room contains two spray pumps and two associated room cooler units to ensure that the ambient room temperature remains within equipment qualification limits. The room cooler units are powered by Class 1E 480V Motor Control Centers (MCC) and are supplied chilled water by the Safety Chilled Water System (CH). CT pump miniflow protection is provided by normally open motor-operated valve 1-FV-4772-1/4772-2/4773-1/4773-2. The pump seals are cooled by the Component Cooling Water (CC) system; the pump bearings are cooled by the Station Service Water (SW) system. The pumps are actuated by a Safety Injection ("S") signal. The pumps also receive a confirmation start signal when containment pressure reaches the hi-3 ("P") setpoint. Following the "S" signal, the pumps operate in miniflow until the hi-3 setpoint is reached. At that point, the spray header isolation valves 1-HV-4776,4777 open and the miniflow valves close.

Each pump is equipped with as associated chemical eductor which delivers a 28-30 weight percent solution of sodium hydroxide to the pump suction. One chemical additive tank provides gravity flow to each eductor venturi section. Success of the chemical addition system is not considered essential for system operation.

Each pump discharges to a header which routes flow to its respective heat exchanger. The CC system supplies cooling to the shell side of the heat exchanger via normally closed motor-operated valve 1-HV-4574/4575. The valve is opened automatically by a "P" signal. Upon discharge from the heat exchanger, flow is routed to the spray header via normally closed motor-operated isolation valve 1-HV-4776/4777. The spray headers route flow to ring headers located in four regions of the containment. Each header contains a restriction orifice which balances the flow to each ring.

Technical specifications require the CT pumps and active valves to be operability tested quarterly. During the pump test, CT flow is recirculated back to the RWST via normally locked-closed test header isolation valve 1CT-050/049. Among the valves stroke tested are RWST suction isolation valve 1-HV-4758/4759, containment sump suction isolation valve 1-HV-4782/4783, and spray header isolation valve 1-HV-4776/4777. For the duration of the testing, the CT train remains inoperable. In addition, the CT train is disabled prior to quarterly Engineers Safety Features Actuation System (ESFAS) slave relay actuation testing in order to prevent pump damage.

Containment Fan Coolers

The fan coolers are part of the Containment Air Cooling and Recirculation System (CACRS). Fan cooler information is summarized in Table 4.1.2-1 and in Figures 4.1-20.1 and 20.2. The CACRS for each unit consists of four 33-1/3 percent capacity cooling units and fans. The cooling unit consists of eight cooling coils. During normal operation, three out of four cooling units and fans will operate. The CACRS is not required to operate following a Design Basis Accident (DBA). Following a LOCA, the "S" signal shuts the fans down and closes the fan discharge dampers. Following a loss-of-offsite power, the Blackout Signal (BOS) automatically starts the fans. The CACRS fans and dampers are each powered from two separate and independent electrical sources Train A and B of Class 1E AC and DC buses, respectively. The non-safety related chilled water system provides cooling to the CACRS cooling coils.

Fan cooler operation is not credited in the CPSES IPE. However, the benefits of fan coolers were evaluated in section 4.6.3 for potential use in accident management. The potential impact of fan coolers on the severe accident progression is twofold: (1) they can extend the RWST duration by preventing or delaying the containment pressure from reaching the spray set point; and (2) fan coolers can prevent containment failure due to overpressure as calculated in Section 4.6.3. These advantages notwithstanding, fan coolers were not credited because: (1) fans at CPSES are cooled by chilled water which is isolated on a containment isolation signal; (2) restarting the fans would require operator intervention which is not proceduralized for severe accident situations; and (3) the fans are not qualified for operation in a severe accident environment. Therefore, fans are assumed to operate only until an SI signal is generated, since this is the expected boundary condition for the accident sequence development. Operation for this short period has little bearing on the accident progression. Neglecting the fans for the balance of the sequence

is conservative because when fans are not credited, a higher containment pressure is calculated, resulting in a more severe challenge to the containment than if they are assumed to be in operation. This assumption allows bounding of the scenarios in which the fans operate with similar scenarios in which they do not. However, since it may be possible to restart fans, a sensitivity study is described in Section 4.6.3 demonstrating that under certain circumstances, fan operation alone, without additional ECCS or spray, can prevent containment failure. While credit for this capability is not taken in the risk assessment process as indicated above, the information was developed for incorporation into an accident management knowledge base.

Containment Isolation System (CZ)

The design objective of the CZ is to allow normal and emergency passage of fluids through the containment boundary while preserving the integrity of the boundary. The CZ logic is part of the Engineered Safety Features Actuation System. The CZ was modeled in the Front-End of the IPE (Ref. 6). For completeness it should be mentioned that the CZ includes the following subsystems:

- Steam Line Isolation - closes the main steam isolation valves (MSIV) and main steam drain pot isolation valve. Once steam line isolation is initiated, the ESFAS output relays are latched and must be manually reset. Resetting the steam line isolation signal does not cause the valves to re-open.

- Main Feedwater Line Isolation - closes all feedwater isolation valves. Once feedwater line isolation is initiated, the ESFAS output relays are latched and must be manually reset. Resetting the feedwater isolation signal does not cause the valves to re-open.

- Containment Isolation Phase A - closes all non-essential process lines penetrating the containment. Containment Isolation Phase A is initiated by the Safety Injection Signal or manual actuation of either of two control switches per train for Phase A Isolation on the control board. Once Containment Isolation Phase A is initiated, the ESFAS output relays are latched and must be manually reset. Resetting the Containment Isolation Phase A initiation signal does not cause the isolation valves to re-open.

- Containment Isolation Phase B - closes all remaining process lines, with the exception of those serving Engineered Safety Features functions penetrating the containment. Containment Isolation Phase B is initiated by a "P" signal derived from the containment spray actuation signal or by manual activation of both of the two control switches per train for Containment Spray Actuation on the control board. Once Containment Isolation Phase B is initiated, the ESFAS output relays are latched and must be manually reset. Resetting the Containment Isolation Phase B initiation signal does not cause the isolation valves to re-open.

- Containment Ventilation Isolation (CVI) - closes all ventilation lines connected directly to the containment atmosphere. CVI is initiated by automatic or manual initiation of Containment Isolation Phase A or manual initiation of Phase B to limit radioactive emissions during accident/post-accident operations. To limit radioactive emissions during normal operation, the CVI is also initiated by high containment airborne radiation. Once the CVI is initiated, the ESFAS output relays are latched and must be manually reset. Resetting the CVI does not cause the isolation valves to re-open.

Containment penetrations and their respective isolation schemes can be classified as:

- Type A - Lines that form part of the reactor coolant pressure boundary (RCPB). These penetrations are provided with one of the following isolation schemes:

  - One locked-closed isolation valve inside and one locked-closed valve outside the containment.
  - One automatic isolation valve inside and one locked-closed isolation valve outside the containment.
  - One locked-closed isolation valve inside and one automatic isolation valve outside the containment.
  - One automatic isolation valve inside and one automatic isolation valve outside the containment.

- Type B - Lines that connect directly to the containment atmosphere. These penetrations are provided with isolation schemes identical to those set forth for Type A penetrations as well as the following additional isolation schemes:

  - The redundancy requirement is satisfied by having two isolation barriers in series, one on each side of Type A and Type B penetrations.
  - One blind flange inside the containment and one locked-closed isolation valve outside the containment.
  - One blind flange inside the containment and one blind flange outside the containment.

- Type C - Lines that are part of a closed system, i.e., lines that are neither part of the RCPB nor connected to the containment atmosphere. These penetrations are provided with at least one containment isolation valve that is either automatic, locked-closed, or capable of remote-manual operation. These valves are located outside the containment and as close to it as practicable.

- Special Containment Isolation Provisions - Special provisions are provided for certain valves. Valves in lines required to operate post accident are designed to remain open or be opened following the accident, but consistent with containment isolation requirements, they can be closed by remote-manual operation from the control room.

There are four instrument lines that penetrate the containment that are required to remain functional following a LOCA or steam line break. Isolation is provided by means of sealed bellows that are connected to a fluid filled tube. The arrangement consists of a double isolation barrier. If the instrument line breaks outside the containment, leakage of the containment atmosphere is prevented by virtue of the sealed bellows. If the instrument line breaks inside the containment, leakage is prevented by a leak-tight diaphragm installed in the pressure instrument that is designed to withstand the full containment design pressure.

4.1.2.2 Containment Design and Structures

The CPSES containment is a large, dry, reinforced concrete structure with approximately 3 million cu. ft. volume and a 50 psig (64.7 psia) design pressure. This section contains an overview of the structure and a description of the reinforcements, liner, penetrations, reactor cavity area and leakage testing.

Overview of the CPSES Containment Structure

The Comanche Peak containment structure is a fully continuous, steel-lined reinforced concrete structure, consisting of a vertical right cylinder with a flat base and a hemispherical dome. It is supported on an essentially flat foundation with a reactor cavity pit. A welded steel liner is attached to the entire inside surface of the containment (walls, dome and mat) with anchors to ensure a high degree of leak-tightness. The design objective is to provide vapor containment and limit leakage of radioactive material which might be released from the core during a design basis accident. It also protects the RCS from extreme environmental conditions including tornados and external missiles.

The containment structure, as shown in Figures 4.1-18.1 through 18.3, consists of the following:

- A cylindrical wall (internal diameter of 135 ft 0 in.), measuring 195 ft from the top of the base to the springline of the dome with a thickness of 4 ft 6 in.

- A hemispherical dome with a thickness of 2 ft 6 in. The inside radius of the dome is equal to the inside radius of the cylinder, so that the discontinuity at the springline due to the change in the thickness is on the outside surface.

- A flat concrete foundation base mat with a thickness of 12 ft 0 in.

An additional overall view of the containment layout is provided in Figures 4.1-21.1 through 21.3. Containment sump piping and arrangement are shown in Figure 4.1-22.1 and 22.2.

Reinforcements

The principal reinforcement used in the containment shell (mat, walls, and dome) are No. 18 bars, made continuous at splices by the use of cadweld connections. Shell reinforcement is illustrated in Figure 4.1-

23.1. The reinforcing steel pattern in the cylindrical wall consists of vertical bars (inside and outside faces), horizontal hoop bars (also at each face) and 45 degree diagonal bars in each direction, near the outside face. The dome reinforcement consists of top and bottom meridional layers of rebars, extending from the cylindrical wall vertical bars. Circumferential hoop bars are provided in the top and bottom layers of the dome. The meridional reinforcement terminated at the apex of the dome is anchored by cadwelding the end of the rebar to a fabricated steel ring assembly.

At penetration openings, reinforcing steel is generally bent around the openings; supplementary bars are provided around the opening when required by design. At the major penetrations (i.e., the Personnel Lock and the Equipment Hatch) some of the wall reinforcement is terminated at the opening by cadwelding steel plates on the end of the bar. Additional reinforcing is provided around these openings to carry stress concentrations and make redistributions at these openings.

The foundation mat is reinforced with top and bottom layers of bars as shown in Figure 4.1-23.2.

Liner

The entire inside surface is lined with welded steel 3/8 inch thick at the wall, 1/2 inch in the dome. A 1/4 inch thick plate is used on top of the foundation mat and covered with a 2 ft 6 in. concrete slab, the top of which forms the floor of the containment. Typical steel liner details are provided in Figure 4.1-23.1 Liner chase channels are provided at liner seams which, after construction, are inaccessible for other means of leak tightness examination. The liner steel plates on the wall and dome are anchored into the concrete with 5/8 in. by 6 3/8 in. long headed, welded studs. The studs in the cylindrical wall and dome are spaced approximately 12 inches each way. The vertical wall liner is anchored at the foundation mat. The bottom liner is installed after foundation mat construction and is welded at seams to structural members embedded in the top of the mat. The embedded structural members are approximately 8 by 10 ft apart. Locally thickened liner plate sections are provided at penetrations, at major pipe and duct support attachments and at the bottom of the cylindrical wall's steel liner.

Containment Penetrations

From the perspective of severe accidents, the CPSES containment penetrations, as with most other large, dry PWR containment penetrations, can be divided into the four categories considered in Reference 11: (1) Large Opening Penetrations, (2) Purge and Vent System Isolation Valves, (3) Piping Penetrations and

(4) Electrical Penetration Assemblies, the most important of which are shown in Figures 4.1-23.4 through 23.7. The severe accident response of each of these types of penetrations is discussed in Section 4.4. Figure 4.1-23.3 shows the location of the various penetrations along the containment wall.

Reactor Cavity Area

The CPSES reactor cavity has very favorable severe accident features: (1) a thick basemat (12 ft) with a buried (unexposed) liner that delays basemat penetration for sequences in which core concrete interaction occurs; (2) a large area (812 ft.^{2}) that is conducive to the formation of a shallow bed, which is highly likely to be coolable in the aftermath of violent events such as steam explosions or high pressure melt ejection (HPME) or burns in the cavity; (3) an always open but tortuous path to the containment lower compartment, which makes direct containment heating (DCH) difficult because the obstacles would cause most of the debris to be de-entrained from the blowdown gases; and (4) the absence of a curb between the cavity and the lower compartment, allowing nearly all the water in the containment to drain into the cavity and delaying the onset of core concrete interactions until cavity dry out (unless the debris falls into a non-coolable configuration, which is unlikely due to the large cavity area).

The following drawings of the reactor cavity area illustrate these points:

Figure 4.1-15	Containment Water Level vs Containment Water Volume
Figure 4.1-16.1	Reactor Vessel Supports
Figure 4.1-16.2	Reactor Vessel Sepports Details
Figure 4.1-17	Containment Cavity

Containment Leakage Testing

Reliability is assured by conducting periodic tests to check the operability of the isolation valves, actuators, and controls. Containment leakage tests are performed periodically to verify that containment leakage is maintained below the limits stated in the technical specifications. The leakage testing program consists of the following types of leakage tests.

- Type A tests are those tests that are performed after the containment building has been completed, prior to operation, and at periodic interval thereafter, to determine the overall containment integrated leakage rate. Three Type A tests are performed at approximately equal intervals during each 10 year service interval. The third test is performed while

the plant is shut down for the 10 year plant inservice inspection. Type A tests are only conducted while the plant is in the shutdown condition.

- Type B tests are those tests that are performed periodically to determine leakage rates for individual mechanical and electrical penetrations, air locks, and hatches. Type B tests are performed during each reactor shutdown for refueling, or at another interval, but in no case at intervals greater than two years. The personnel airlock and emergency airlock are tested after each opening or at six month intervals if not opened for that period of time.

- Type C tests are those tests that are performed periodically to measure containment isolation valve leakage rates. Type C tests are performed during each reactor shutdown for refueling but in no case at intervals greater than 2 years.

Any major modification or replacement of a component that is part of the primary containment that is performed after the preoperational leakage-rate test will be followed by a Type A, Type B, or Type C test, as applicable. All other requirements for regularly scheduled leakage-rate tests apply.

Furthermore, a fail-safe feature is incorporated into air-operated and solenoid-operated isolation valve design, so that in the event of actuating power loss, the valve assumes the position that ensures safety. Each train of electrically activated valves is supplied from separate and independent Class 1E sources. The motor operated valves are powered from Class 1E 480V AC MCCs. Pilot solenoids for the air operated valves are powered from Class 1E 125V DC and 118V AC distribution panels.

Table 4.1.2-1: Safeguards Systems

Containment Sprays System	
Number of Operational Trains	2
Number of Operational Pumps per Train	2
Differential Pressure Across Nozzle, psig	40
Mass Flow Rate per Pump, gpm	2,896
Pressure Setpoint, psia	35
Fan Coolers (FC)	
Number of Operational FC	4
Volumetric Flow Rate per FC, cfm	65,000
Inlet Cooling Water Temperature, °F	51
Inlet Cooling Water Flow Rate per FC, gpm	320

Table 4.1.2-2: Containment Design and Structures

Total Free Volume, ft^3	2,985,126
Design Pressure, psig	56
Design Temperature, °F	280
Absolute Failure Pressure, psia	129
Concrete Composition	Limestone/Common Sand
Mass Fractions, %	
SiO_2	35.80
CaO	31.30
Al_2O_3	3.60
K_2O	1.22
Na_2O	0.08
MgO, MnO, TiO2	0.69
Fe_2O_3	1.44
Fe	0.00
Cr_2O_3	0.01
H2O	4.70
CO_2	21.15
O_2	0.00
Upper Compartment	
Outer Wall Type	Reinforced Concrete
Free Volume, ft^3	1,984,422
Metal Equipment Volume, ft^3	15,835
Metal Equipment Mass, lbm	7,759,150
Metal Equipment Heat Transfer Area, ft^2	22,208
Outer Wall Inside Surface Area, ft^2	68,821
Outer Wall Total Thickness, ft	3.6
Outer Wall Liner Thickness, ft	0.036
Internal Wall Surface Area ft^2	1,189
Internal Wall Thickness, ft	2.0
Internal Wall Liner Thickness, ft	0.0
Deck Area, ft^2	7,038
Deck Thickness, ft	1.5
Deck Liner Thickness, ft	0.0

Table 4.1.2-2: Containment Design and Structures (continued)

Lower Compartment	
Outer Wall Type	Reinforced Concrete
Free Volume, ft^3	836,282
Metal Equipment Mass, lbm	2,133,583
Metal Equipment Heat Transfer Area, ft^2	90,653
Outer Wall Inside Surface Area, ft^2	7,906
Outer Wall Thickness, ft	2.75
Outer Wall Liner Thickness, ft	0.0
Internal Wall Surface Area, ft^2	166,671
Internal Wall Overall Thickness, ft	1.0
Internal Wall Liner Thickness, ft	0.0
Floor Area, ft^2	7,530
Floor Thickness, ft	9.3
Floor Liner Thickness, ft	0.0
Annular Compartment	
Outer Wall Type	Reinforced Concrete
Free Volume, ft^3	151,146
Outer Wall Inside Surface Area, ft^2	41,457
Outer Wall Total Thickness, ft	4.5
Outer Wall Liner Thickness, ft	0.03
Floor Area, ft^2	1,546
Cavity Compartment	
Free Volume, ft^3	13,276
Area of Cavity Debris, ft^2	812
Height of Bottom of Reactor Vessel above Bottom of Cavity, ft	15
Outer Wall Inside Surface Area, ft^2	2,896
Outer Wall Thickness, ft	14.4
Outer Wall Liner Thickness, ft	0.0

Table 4.1.2-2: Containment Design and Structures (continued)

Containment Sumps	
Number of Operational Sumps	2
Area of Base per Sump, ft^2	81
Sump Depth, ft	6
Containment Operating Conditions	
Pressure (Normal Full Power), psia	15
Temperature (Normal Full Power), °F	117
Relative Humidity, %	100

4.1.3 Emergency Core Cooling System (ECCS)

The ECCS for each unit consists of two separate and independent trains. The key features of the major components are:

- The Centrifugal Charging Pumps (CCPs), shown in Figure 3.2.1.6, automatically align to the RWST upon receipt of an "S" or "BOS" signal. The CCPs discharge directly to all four RCS cold legs and continue to maintain seal injection to the Reactor Coolant Pumps (RCPs). Emergency boration is provided by redundant boric acid transfer trains. Suction during the cold and hot leg recirculation phase is aligned to the discharge of the RH pumps.

- The SI pumps, shown in Figure 3.2.1.8-1, start upon receipt of an "S" signal, and draw water from the RWST and discharge to all four RCS cold legs. The SI pump suction is realigned to the discharge of the RH pumps during the cold and hot leg recirculation phase.

- The RH pumps, shown in Figure 3.2.1.2, start upon receipt of an "S" signal, and draw water from the RWST. After RWST depletion, the RH pump suction shifts to the containment recirculation sumps, and water that is pumped is cooled by the RH heat exchangers and is delivered directly to the reactor vessel or to the suction of the CCP and SI pumps. A cross-tie is provided to ensure delivery of water to the CCP and SI pumps in the event that one train of RH system fails or the motor operated valves in the suction line to the pumps fail. The RH system for each unit consists of two separate, independent, and full capacity trains. Each train includes one RH pump and heat exchanger. The heat exchanger flow control valve (1-HCV-606/607) is provided to allow the operator to control the RCS cooldown rate. Heat is transferred from the RCS to the CC system. The RH pumps are powered from two separate and independent sets of Class 1E 6.9kV buses.

- Containment sumps provide suction for the RH and CT pumps. One sump is provided for each train.

- One RWST is provided for each unit. The RWST is shared between the CH and the CT systems.

- The CCPs, SI, and RH pumps are powered from separate Class 1E 6.9kV buses. The boric acid transfer pumps (BATP) are powered from separate Class 1E 480V MCCs.

- Figures 4.1-26.1 through 4.1-26.4 show the ECCS valve alignments for the standby, injection, cold leg recirculation, and hot leg recirculation phases.

The ECCS support requirements are:

- Each CCP, SI, and RH pump room is equipped with an associated room cooler unit. The room cooler units are powered by Class 1E 480V MCCs and are supplied chilled water by the CH system.

- The CCP and SI pump bearings are cooled by the SW system, and the pump seals are self-cooled.

- The Boric Acid Transfer Pumps (BATPs) are located in large open rooms, and the pump seals and bearings are self-cooled.

- Each RH pump room is equipped with an associated room cooler unit. The room cooler units are powered by Class 1E 480V MCCs and are supplied chilled water by the CH system.

- The RH pump seals are cooled by the CC system, and the pump bearings are self-cooled.

The ECCS testing requirements per Technical Specifications are:

- The CCPs and BATPs are tested quarterly. During testing of the CCPs, these pumps are unavailable because the normal pump discharge flowpath is isolated and the pumps operate in recirculation.

- The SI pumps are tested quarterly. During testing of the SI pumps, SI flow is recirculated back to the RWST via the miniflow lines. This configuration does not cause the pump to be inoperable. However, the pumps are inoperable during quarterly stroke testing of the miniflow valves 1-8814A,B and cross-connect isolation valves 1-8821A,B.

- The RH pumps are flow tested quarterly. Prior to the flow test, the pumps are disabled when the miniflow valves are stroke tested. During testing of the RH pumps, RH flow is recirculated back to the RWST via normally closed motor-operated test valve 1-8890A,B. The RH pumps remain operable during this test because the 3/4" test line does not divert enough flow to cause the pumps to be considered inoperable. Stroke testing of the RWST suction isolation valves 1-8812A,B are also completed quarterly.

Survivability concerns under conditions expected during a severe accident can be summarized as follows:

- The accident conditions are the accident and post-accident environmental conditions of temperature, pressure, relative humidity, radiation doses, chemical spray, and flooding. These environmental conditions are summarized for each equipment location, and the equipment is evaluated accordingly.

  The requirements delineated in IEEE 323-1974 include principles, procedures and methods of qualification which, when satisfied, confirm the adequacy of the performance of the equipment under these environments.

- The plant specific equipment performance requirements during normal and accident environmental conditions have been identified and documented accordingly. These

performance requirements are compared to the demonstrated performance characteristics to show satisfactory performance and qualification of equipment.

- All vital components and supports are located in buildings designed to Seismic Category I requirements. These buildings can withstand loadings due to tornado winds, depressurization, repressurization, and external missiles. In addition, they protect the components from the effects of flooding such that no flood protection of specific components is required. Missile barriers within these buildings separate the trains such that a missile will not affect both trains. Each train is protected from the dynamic effects from other piping associated with seismic or pipe break events.

The following qualification methodologies are used to qualify the electrical equipment:

- Type Tests - Generally used for qualification of equipment located in potentially harsh environments. This testing consists of using an identical item of equipment under similar conditions with supporting analysis to show that the equipment is qualified for its specific application and, therefore it demonstrates qualification of the installed equipment.

- Partial Tests - Generally used for large equipment. A justification for partial testing is provided through analysis.

Sections 3.2.1-3, 3.2.1-6, and 3.2.1-8 provide additional descriptions on the functions, design features, and success criteria of the RH, CS, and SI systems respectively. Tables 4.1.3-1 and 4.1.3-2 summarize ECCS system data. Figures 4.1-26.1 through 4.1-26.4 show the various ECCS alignments. The support systems mentioned in this section, e.g., Component Cooling Water, Station Service Water and Electrical Power System, are discussed in Section 3 (Volume I of the IPE submittal).

Table 4.1.3-1: Accumulator Tanks

Number of Operational Accumulator Tanks	4
Initial Water Mass per Tank, lbm	50,493
Initial Pressure, psia	603
Liquid Temperature, °F	130

Table 4.1.3-2: ECCS Pumps

Refueling Water Storage Tank	
Initial Water Mass, lbm	3,764,568
Liquid Temperature, °F	99
Number of Operational ECCS Trains	2
Number of Operational ECCS Pumps per Train	
Centrifugal Charging Pump	1
High Head Safety Injection Pump	1
Residual Heat Removal Pump	1
Centrifugal Charging Pumps	
Pressure Setpoint, psia	1835
RCS Pressure (psia) / Flow Rate (gpm)	
2655 / 0	
(0)	
2435 / 200+	
(138)	
2115 / 300+	
(220)	
1455 / 450+	
(325)	
15 / 660+	
(480)	
+, ( ) Data represents 2 pumps and 1 pump operating, respectively	

Table 4.1.3-2: ECCS Pumps (continued)

High Head Safety Injection Pumps Pressure Setpoint, psia RCS Pressure (psia) — Flow Rate (gpm) 1585 — 0 (0) 1465 — 175+ (125) 1215 — 375+ (275) 765 — 575+ (425) 15 — 800+ (625) +, ( ) Data represents 2 pumps and 1 pump operating, respectively	1535
Residual Heat Removal Pumps Pressure Setpoint, psia RCS Pressure (psia) — Flow Rate (gpm) 215 — 0 (0) 200 — 1250+ (750) 155 — 3000+ (2000) 105 — 4250+ (3000) 15 — 6000+ (4150) +, ( ) Data represents 2 pumps and 1 pump operating, respectively	210

Table 4.1.3-2: ECCS Pumps (continued)

Secondary Feedwater Sources	
Number of Operational Motor-Driven Auxiliary Feedwater Pumps (MDAFWP)	2
Number of Operational Turbine-Driven Auxiliary Feedwater Pumps (TDAFWP)	1
Condensate Storage Tank Water Mass, gals	282,540
MDAFWP (per pump) SG Pressure (psia) / Flow Rate (gpm) 1577 / 0 1200 / 568 1100 / 621 800 / 621 15 / 621 TDAFWP SG Pressure (psia) / Flow Rate (gpm) 1608 / 0 1200 / 874 900 / 1123 600 / 1316 15 / 1316	

4.1.4 Auxiliary Building

Figures 4.1-24.1 through 4.1-25.13 show the auxiliary building in relation to the control room, containment building, emergency diesel building, and turbine building. Since scrubbing in the auxiliary building is not credited in the CPSES IPE due to the low frequency of V-sequences, a detailed description of the internals of that building is not included.

For a Steam Generator Tube Rupture scenario, the release of radionuclides and non-condensible gases to the outside environment will be either via the spring-loaded safety valves or the atmospheric relief valves. Steam is conveyed from the steam generators to the main turbine by four steam lines. Upstream from the MSIV's, each line is provided with five spring-loaded safety valves and one atmospheric relief valve. These valves are located in the safeguards building with relief stacks located on the building roof.

Figure 4.1-1: General Plant Schematic

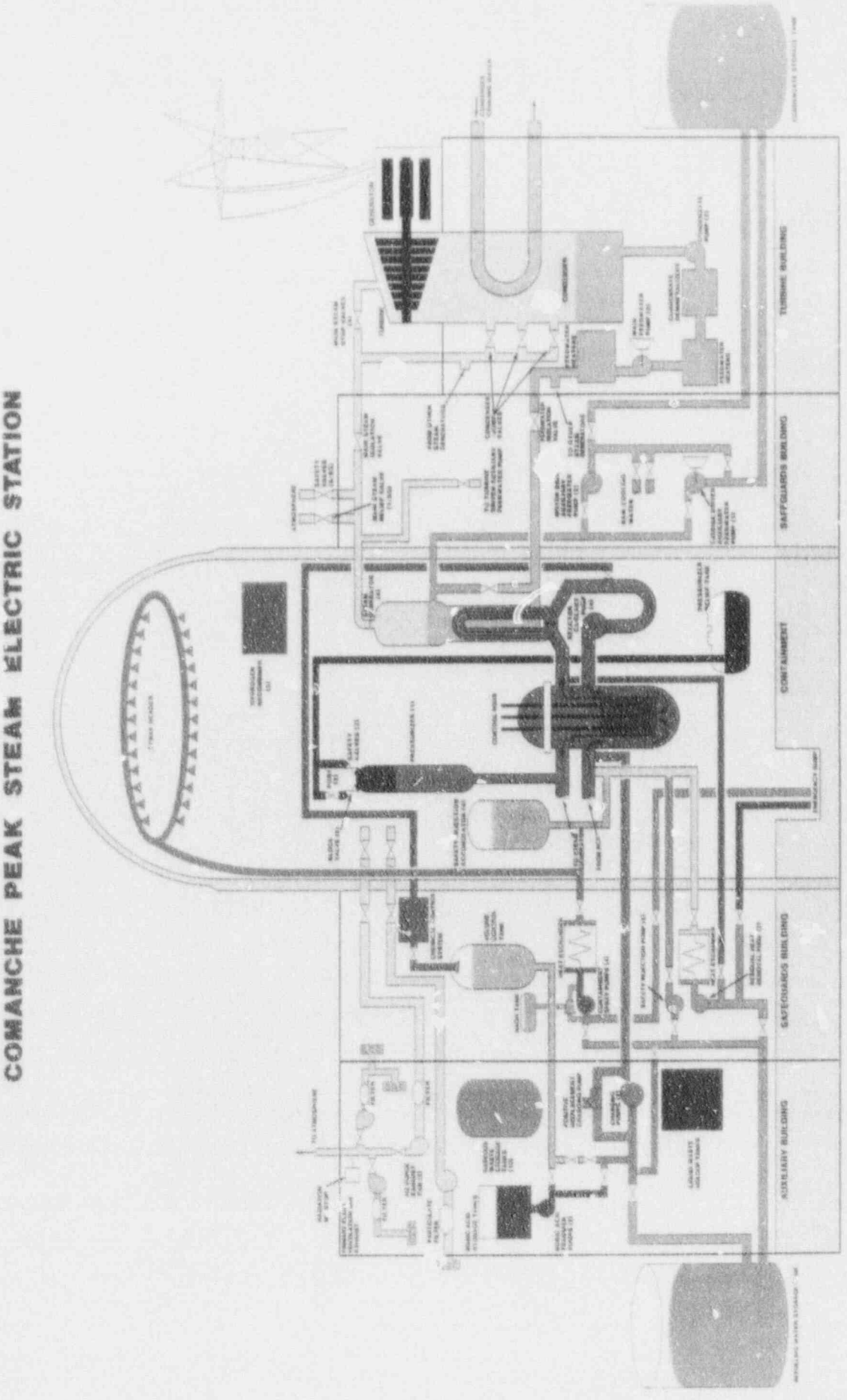

Figure 4.1-1: General Plant Schematic

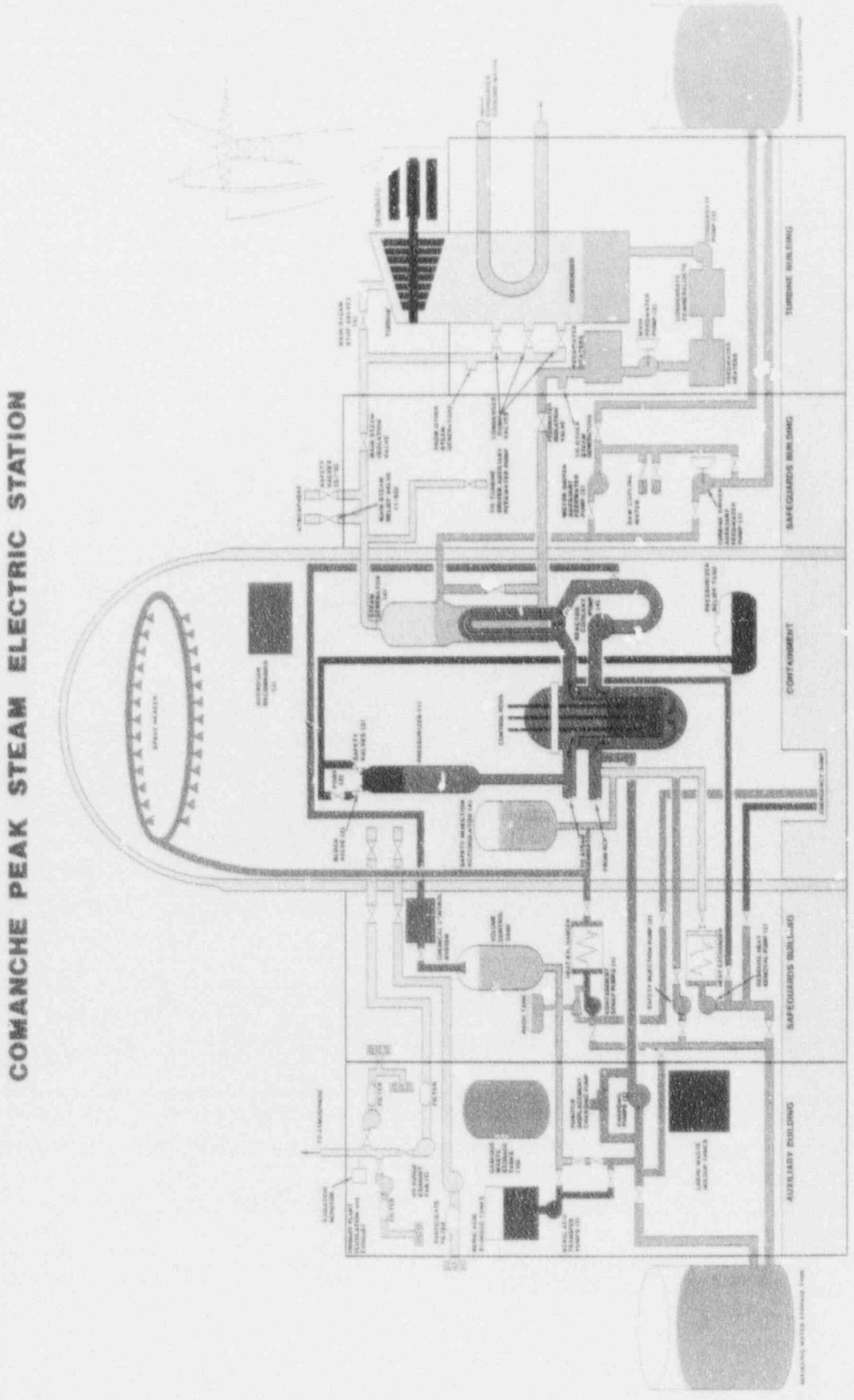

Figure 4.1-2: Simplified Process Flow Diagram of the RCS

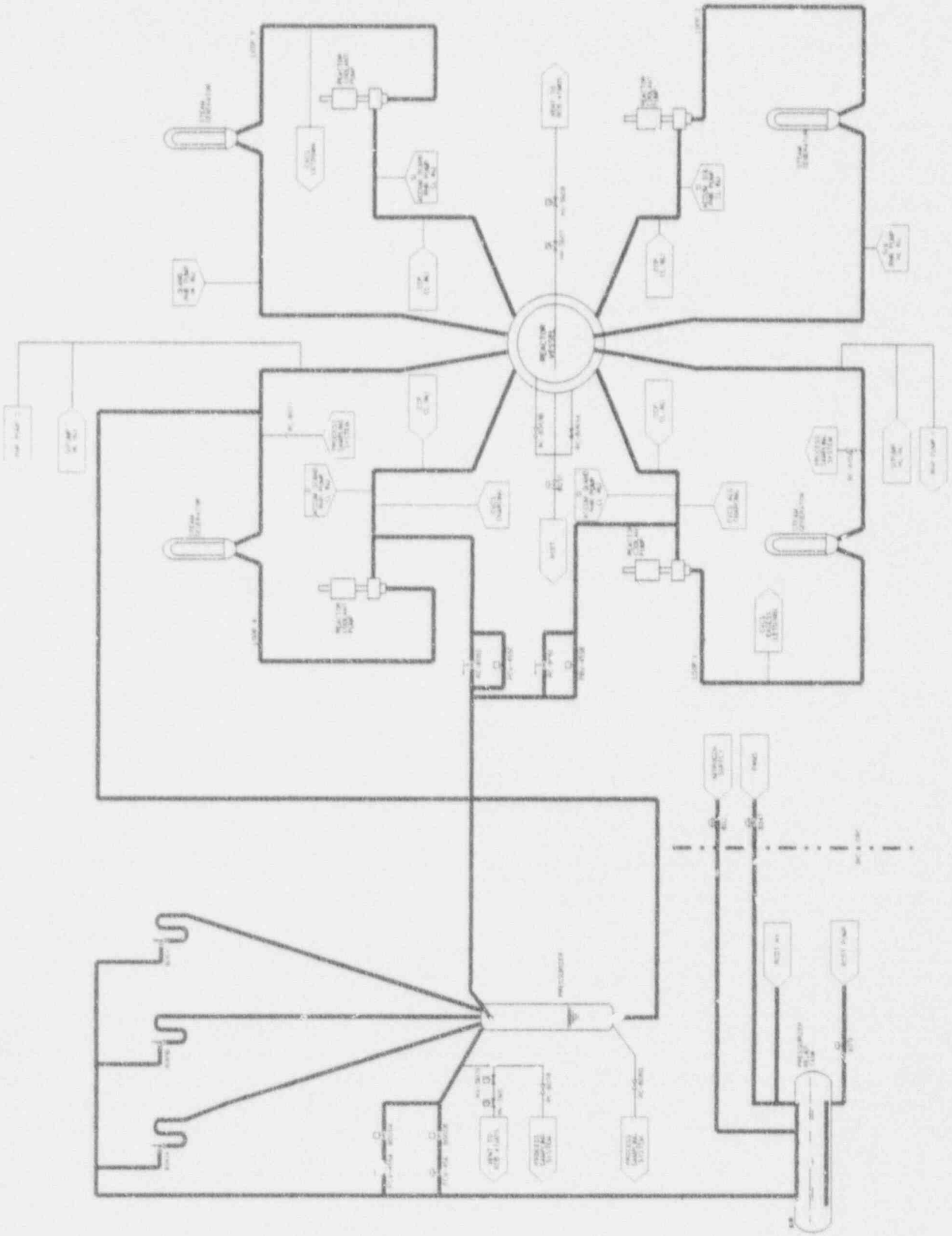

Figure 4.1-3: Main Components of the RCS

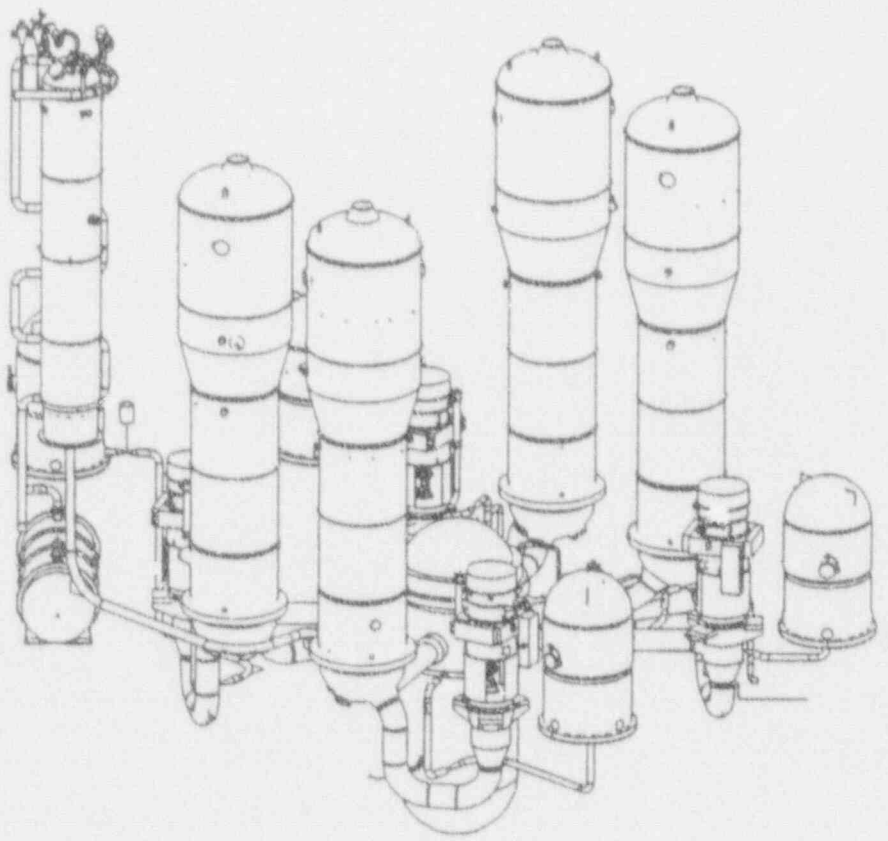

Figure 4.1-4: Primary Side Process Flow Diagram

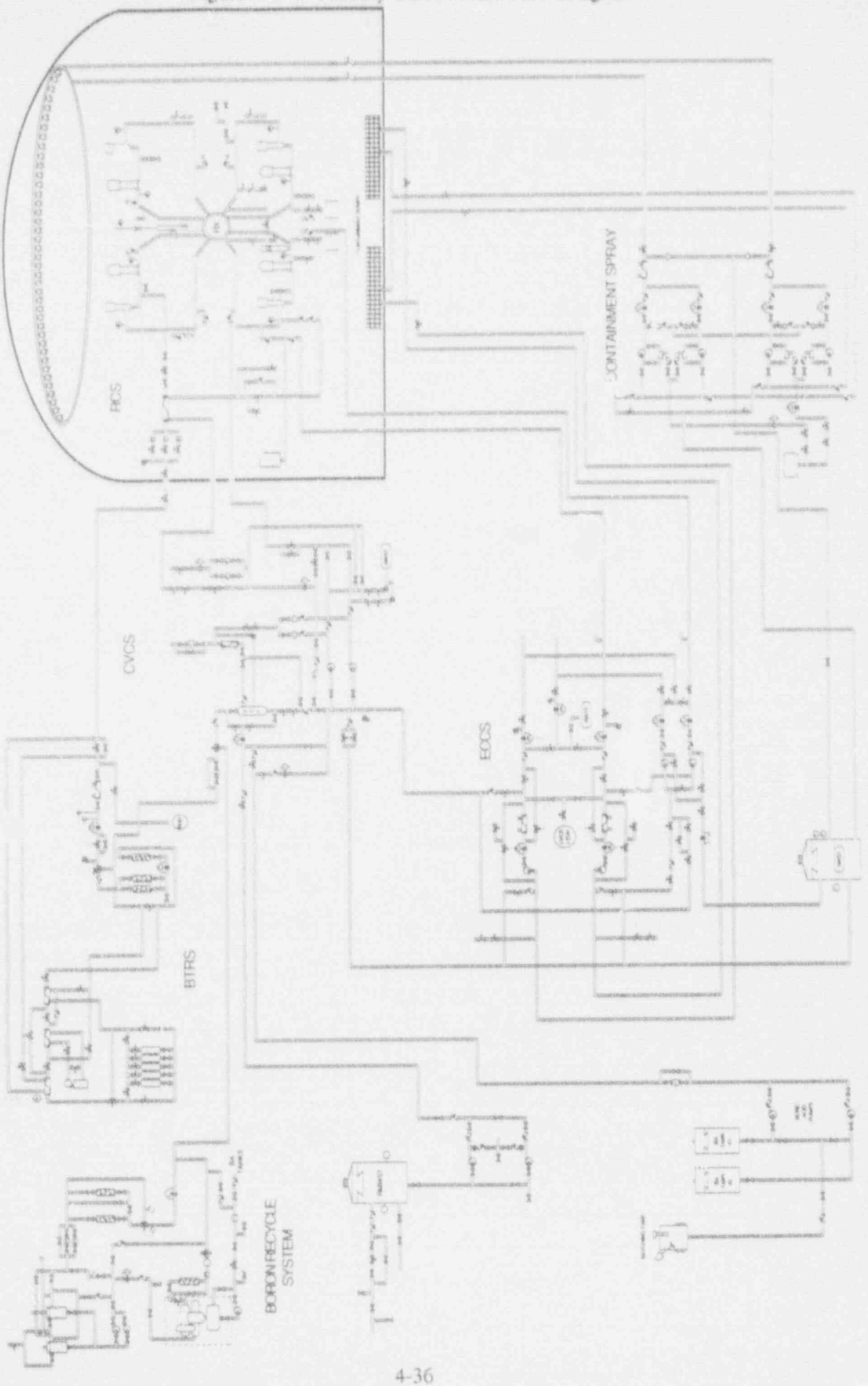

Figure 4.1-5: Secondary Side Process Flow Diagram

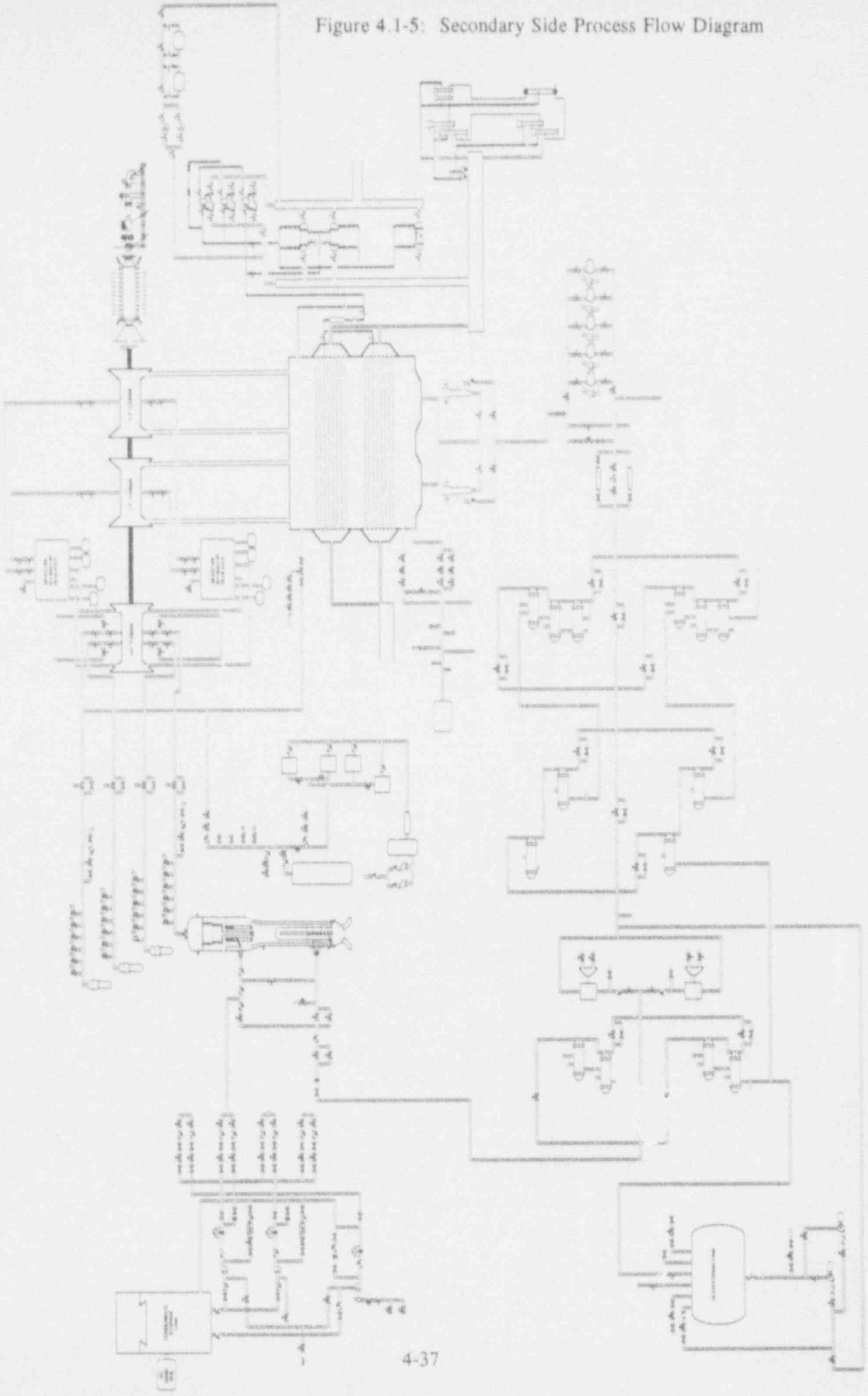

Figure 4.1-6: Structural Plant Arrangement

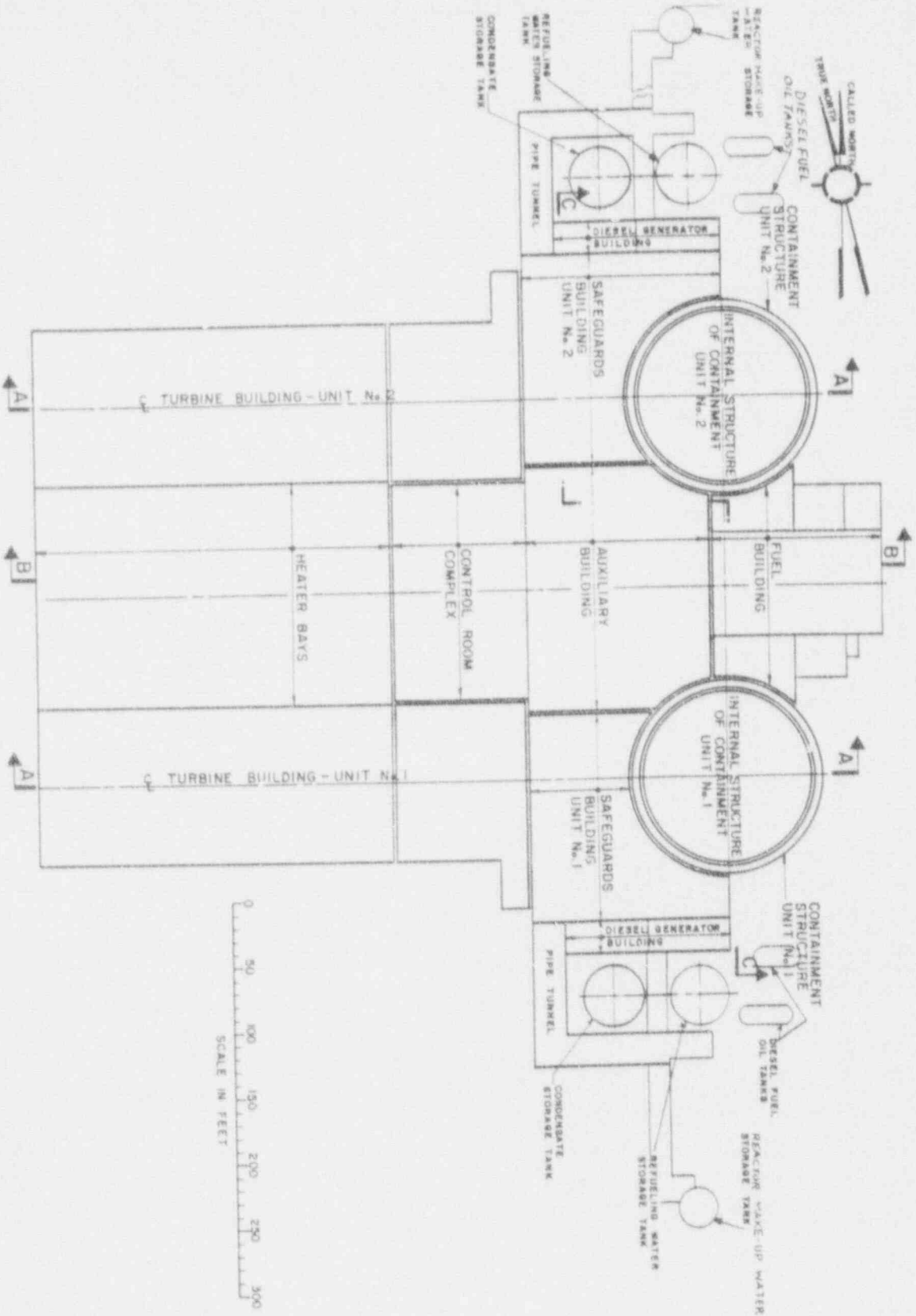

Figure 4.1-7: Containment Cut View with Main RCS Component

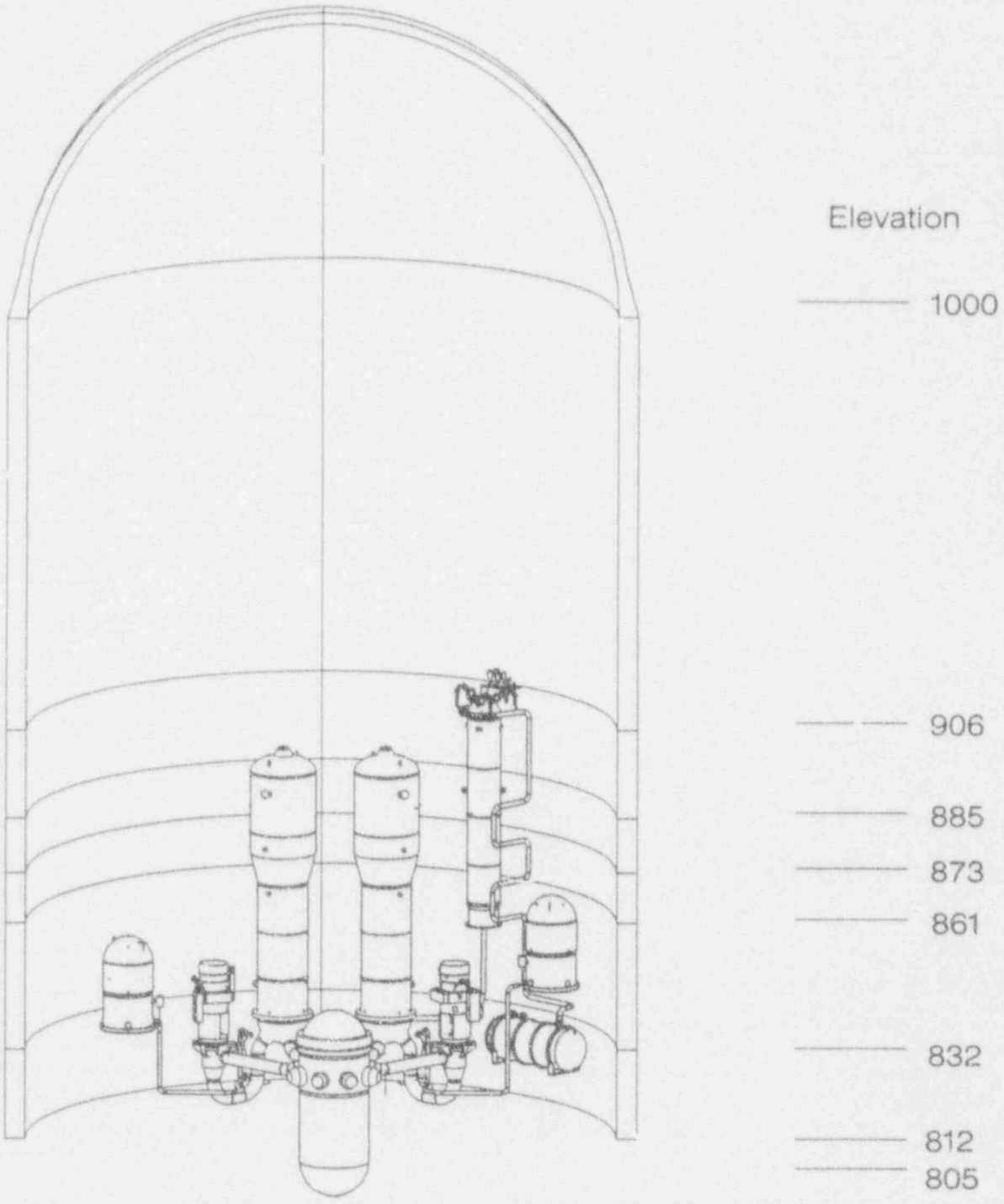

Figure 4.1-8: General Reactor Vessel Assembly

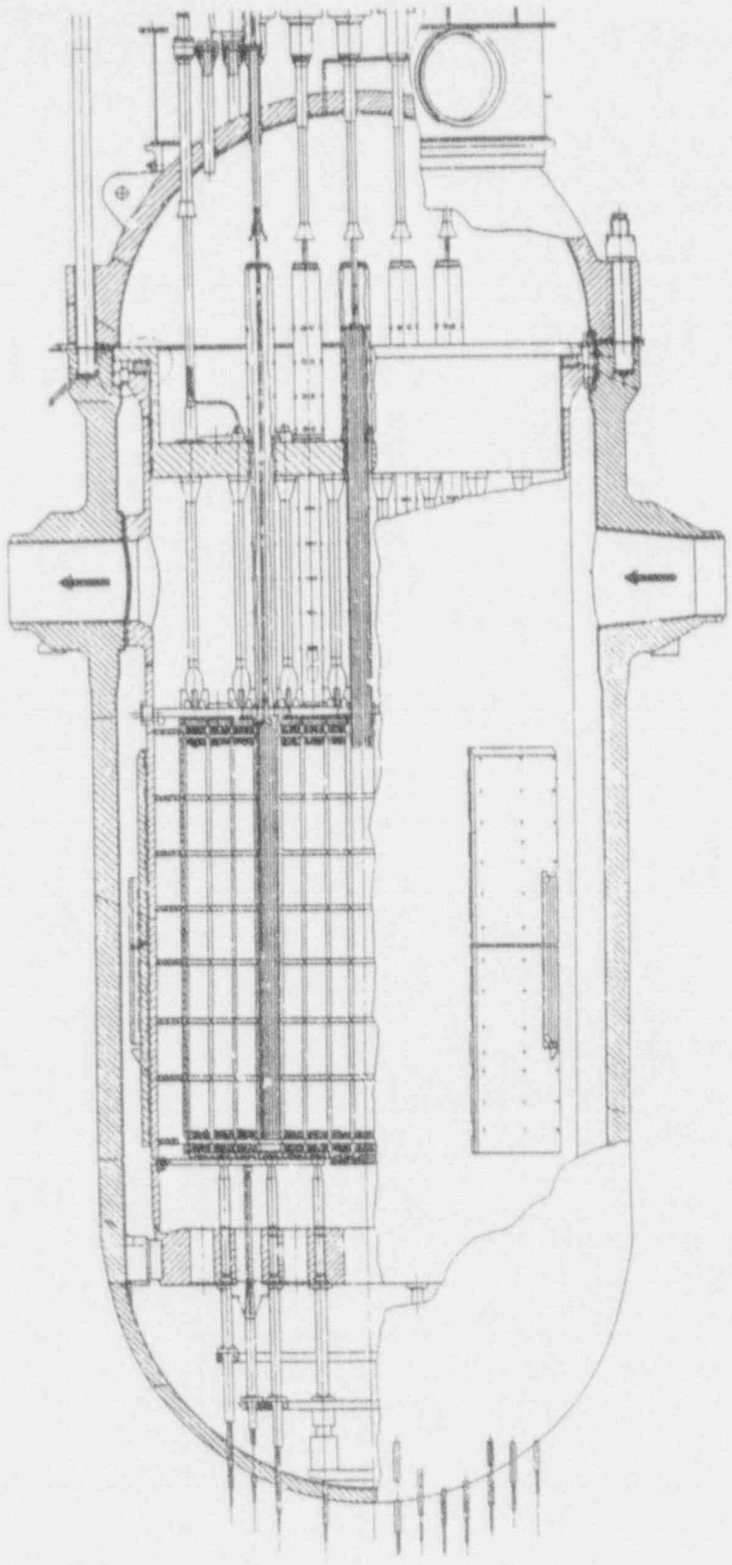

Figure 4.1-9.1: Reactor Vessel Lower Internals Assembly

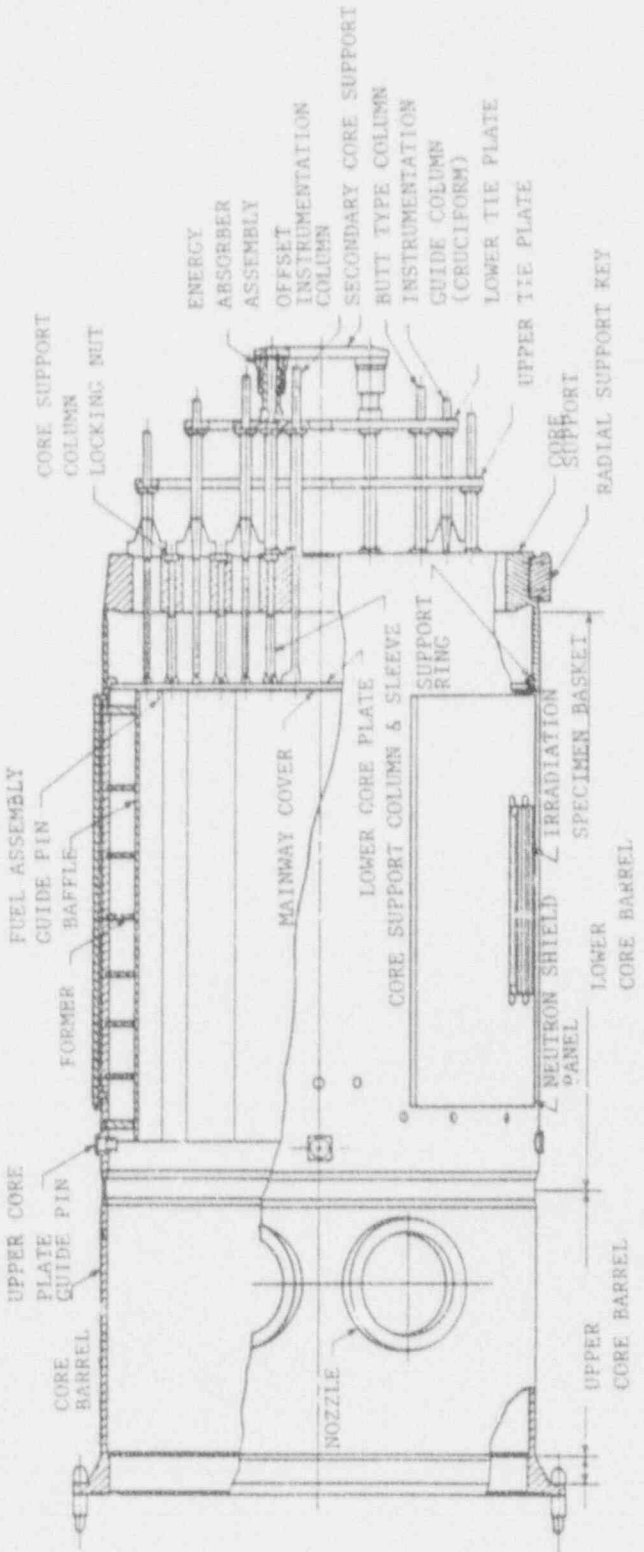

Figure 4.1-9.2: Lower Core Support Assembly

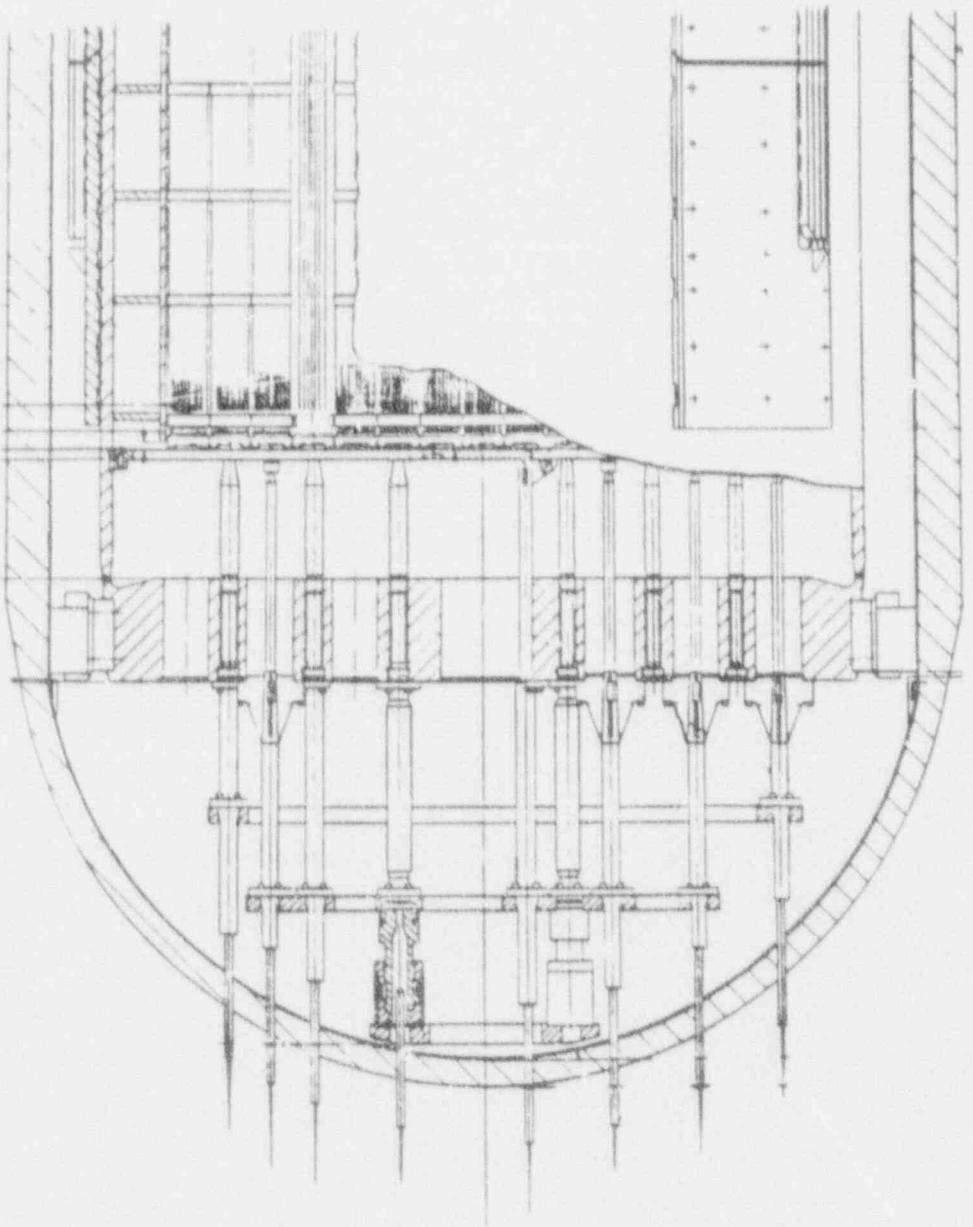

Figure 4.1-10: Bottom Mounted Reactor Vessel Instrumentation

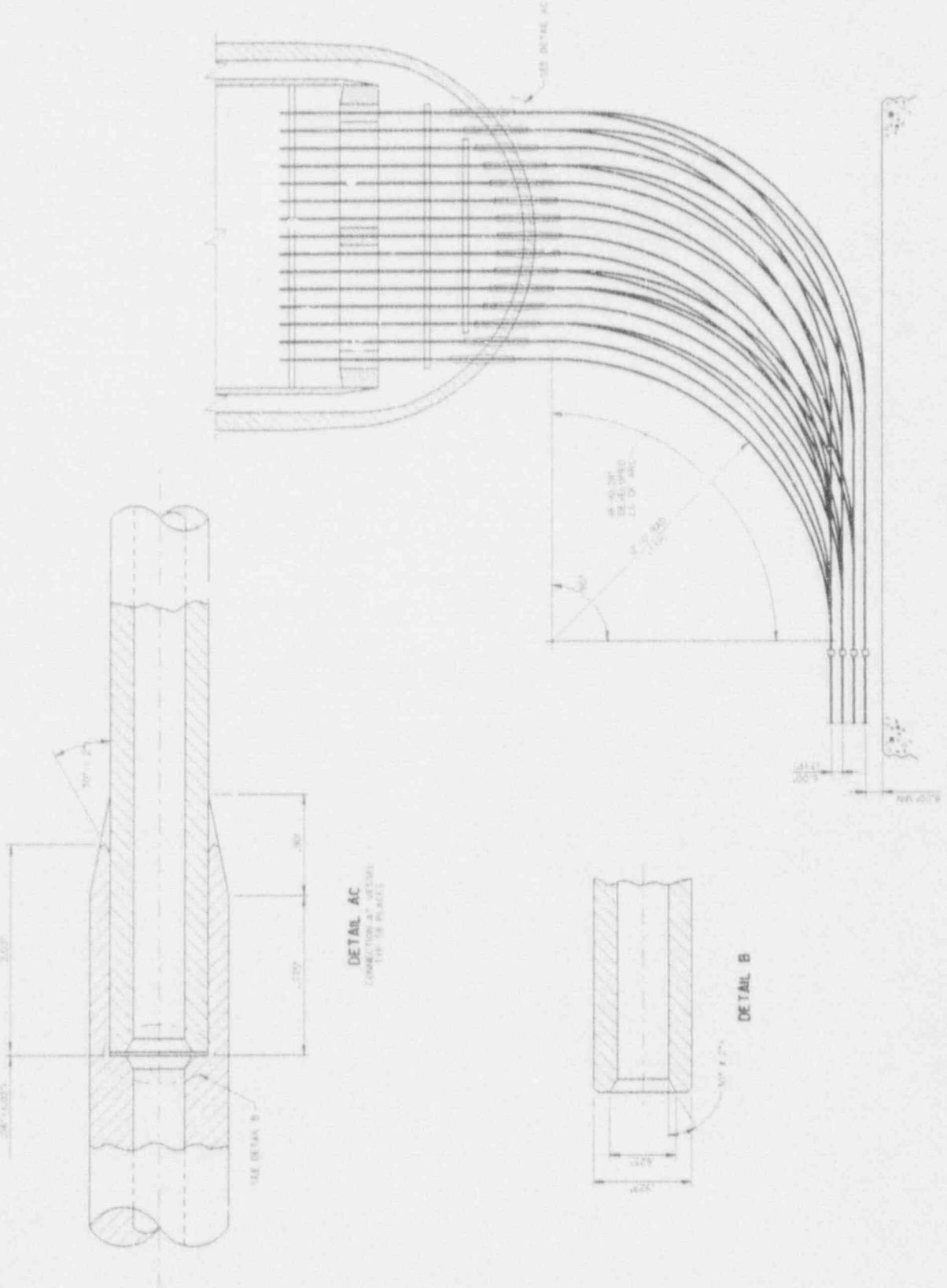

Figure 4.1-11.1: Pressurizer (Cutaway)

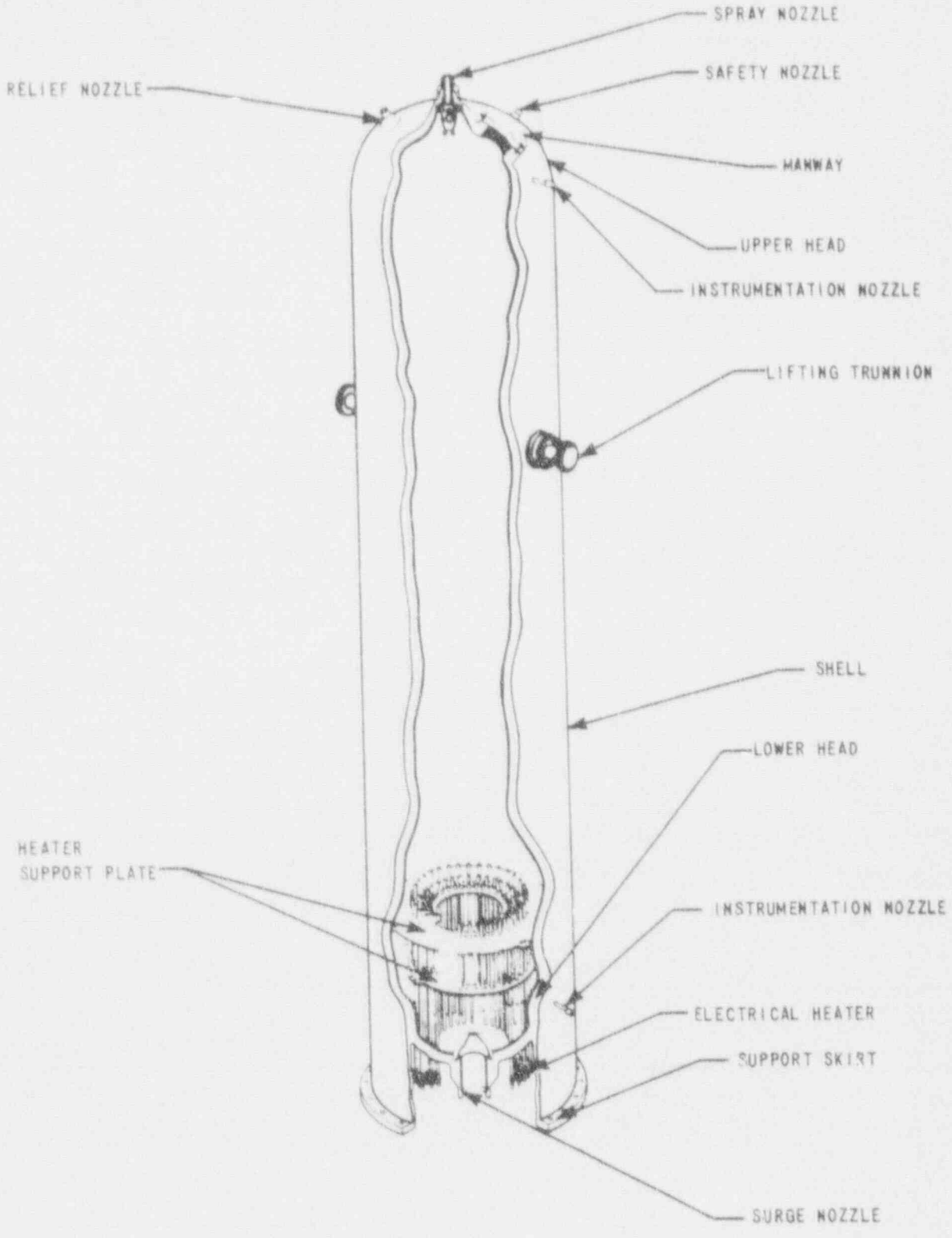

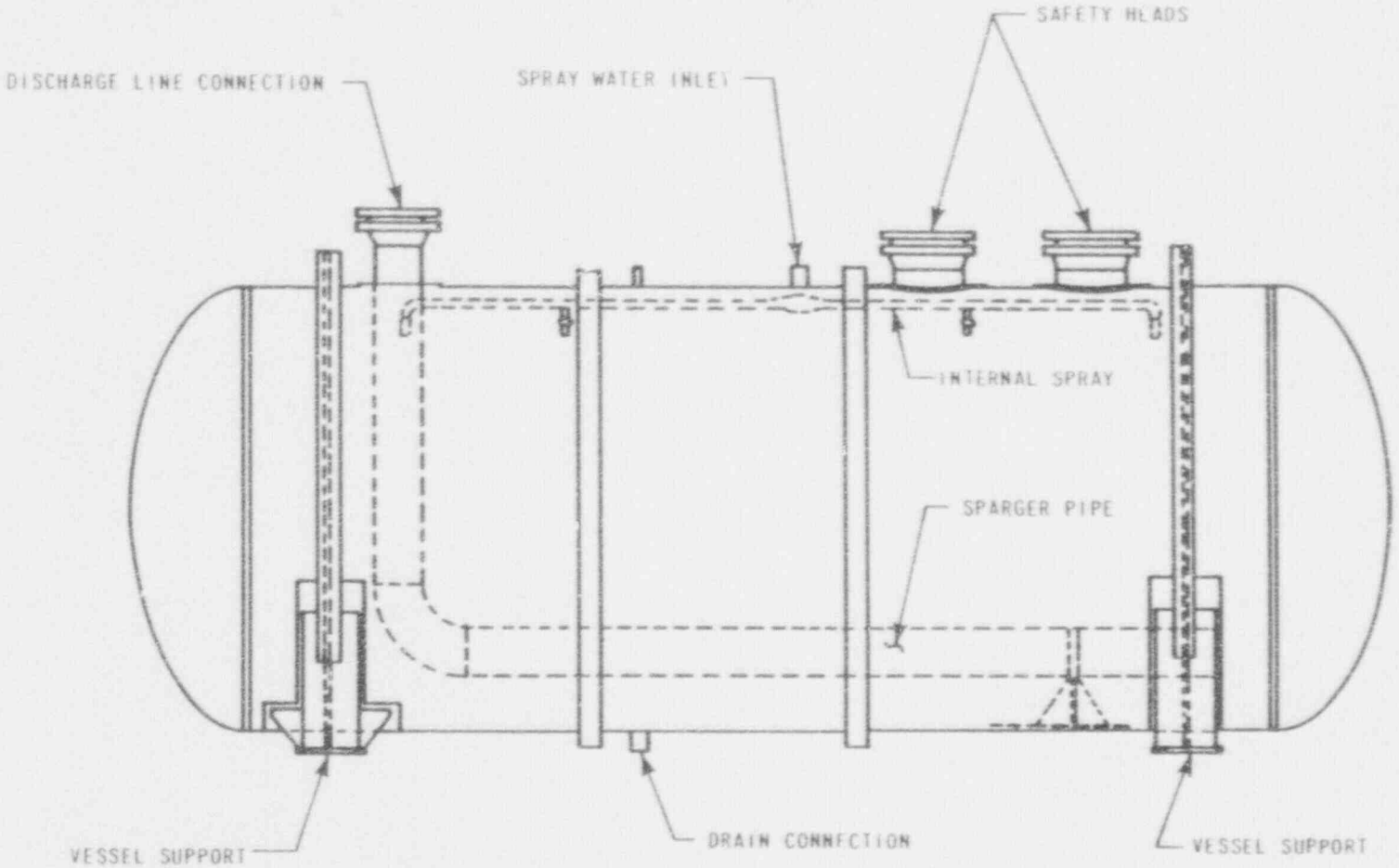

Figure 4.1-11.2: Pressurizer Relief Tank

Figure 4.1-12: Steam Generator (Cutaway)

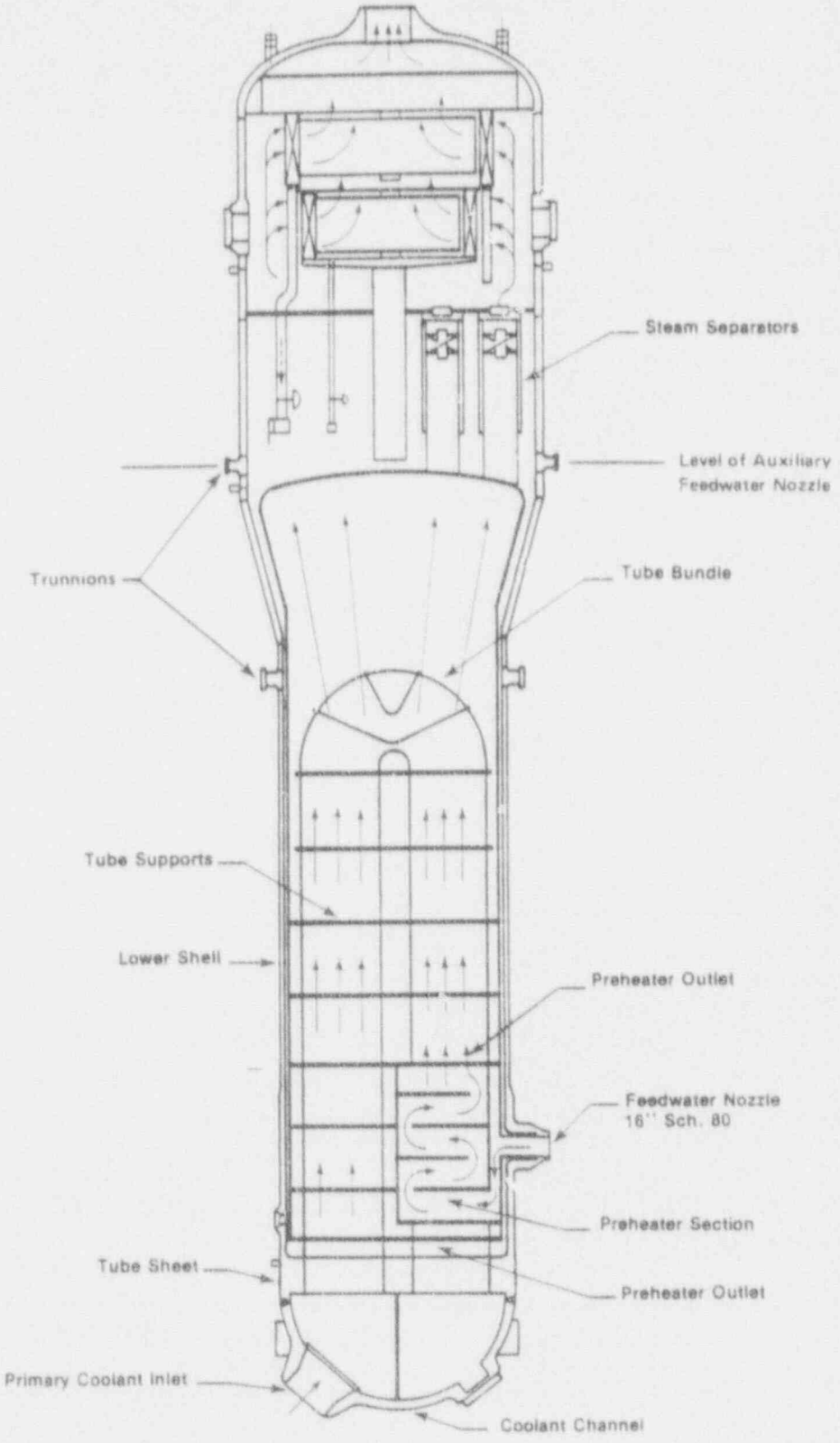

Figure 4.1-13: Reactor Coolant Pump (Cutaway)

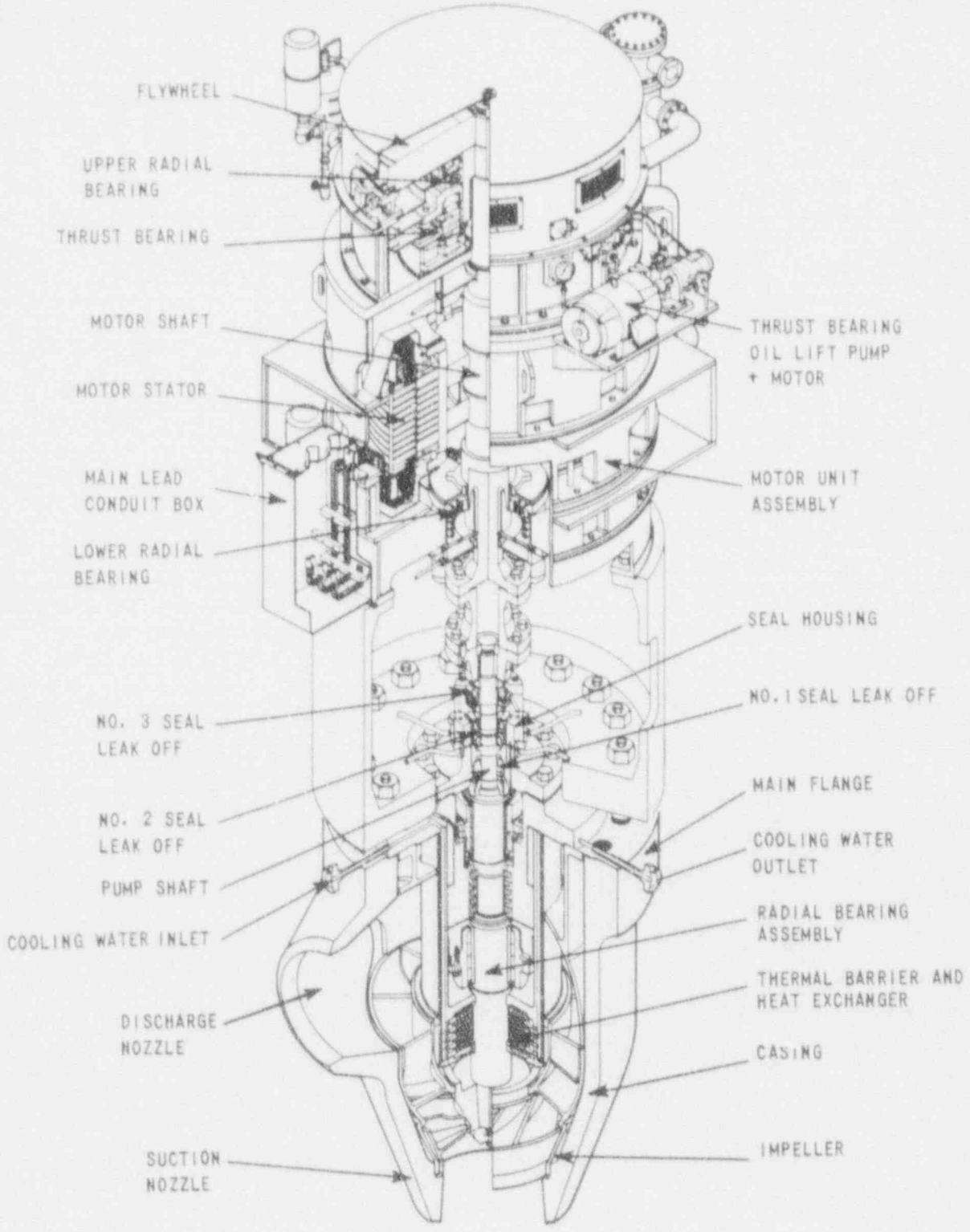

Figure 4.1-14: Accumulator Tank

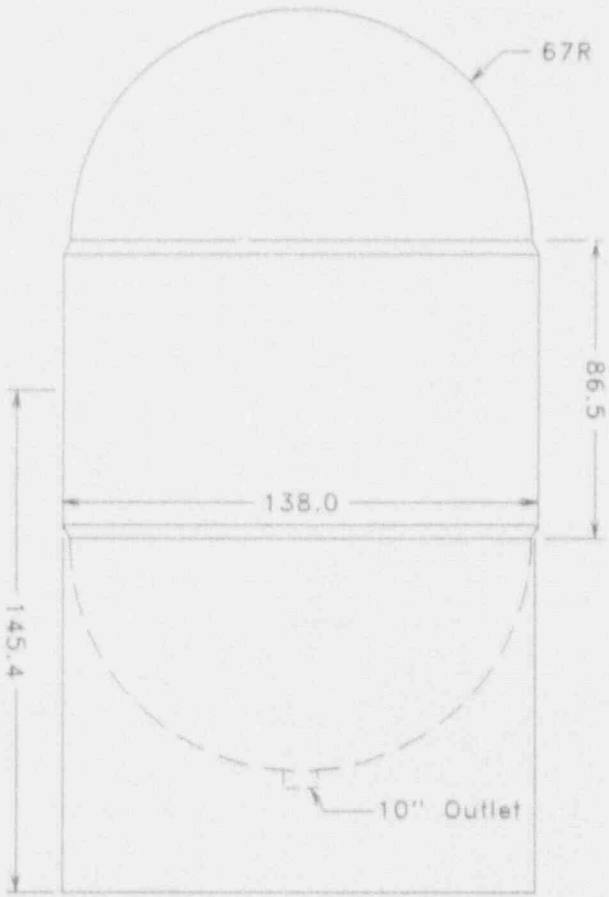

Figure 4.1-15: Containment Water Level vs Containment Water Volume

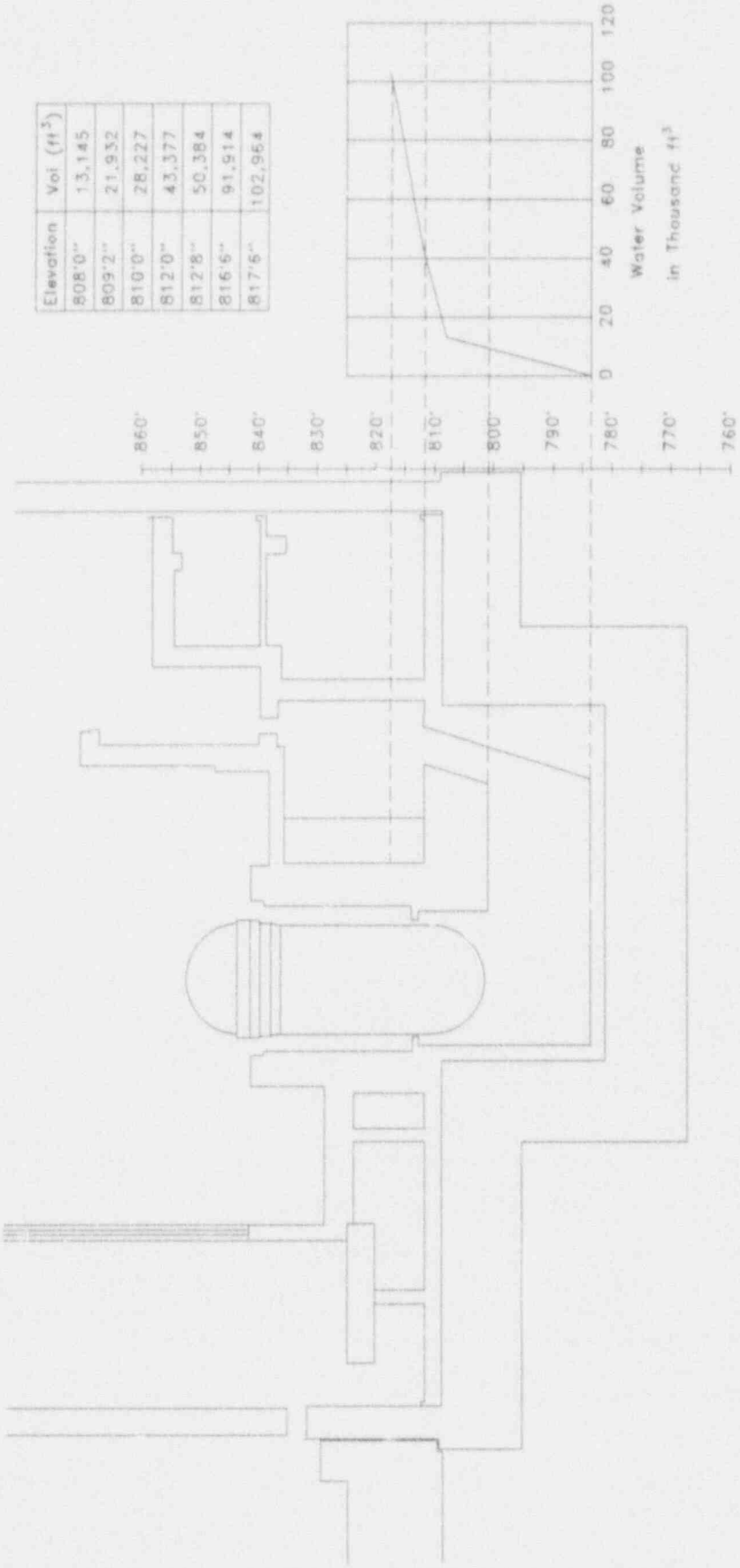

Figure 4.1-16.1: Reactor Vessel Supports

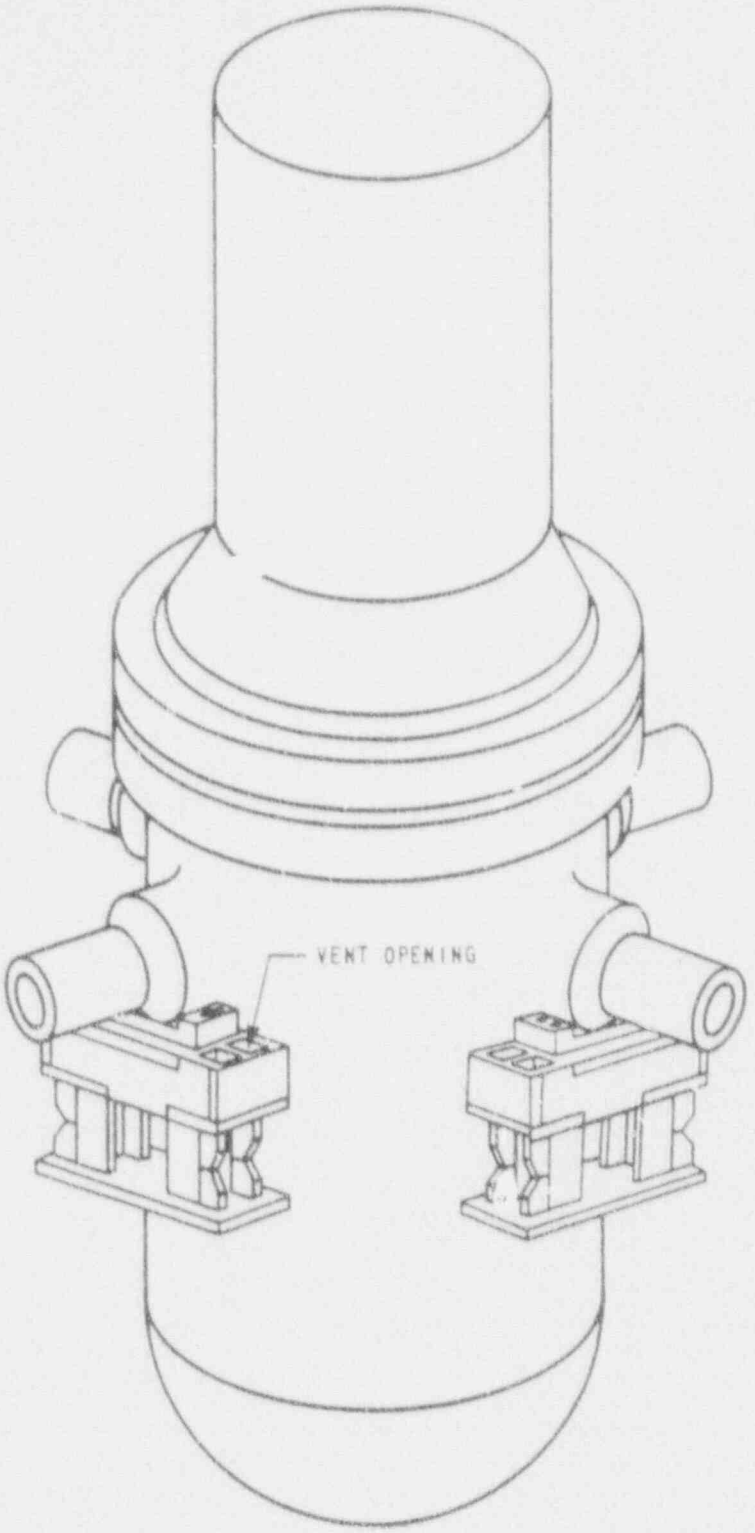

Figure 4.1-16.2: Reactor Vessel Supports Details

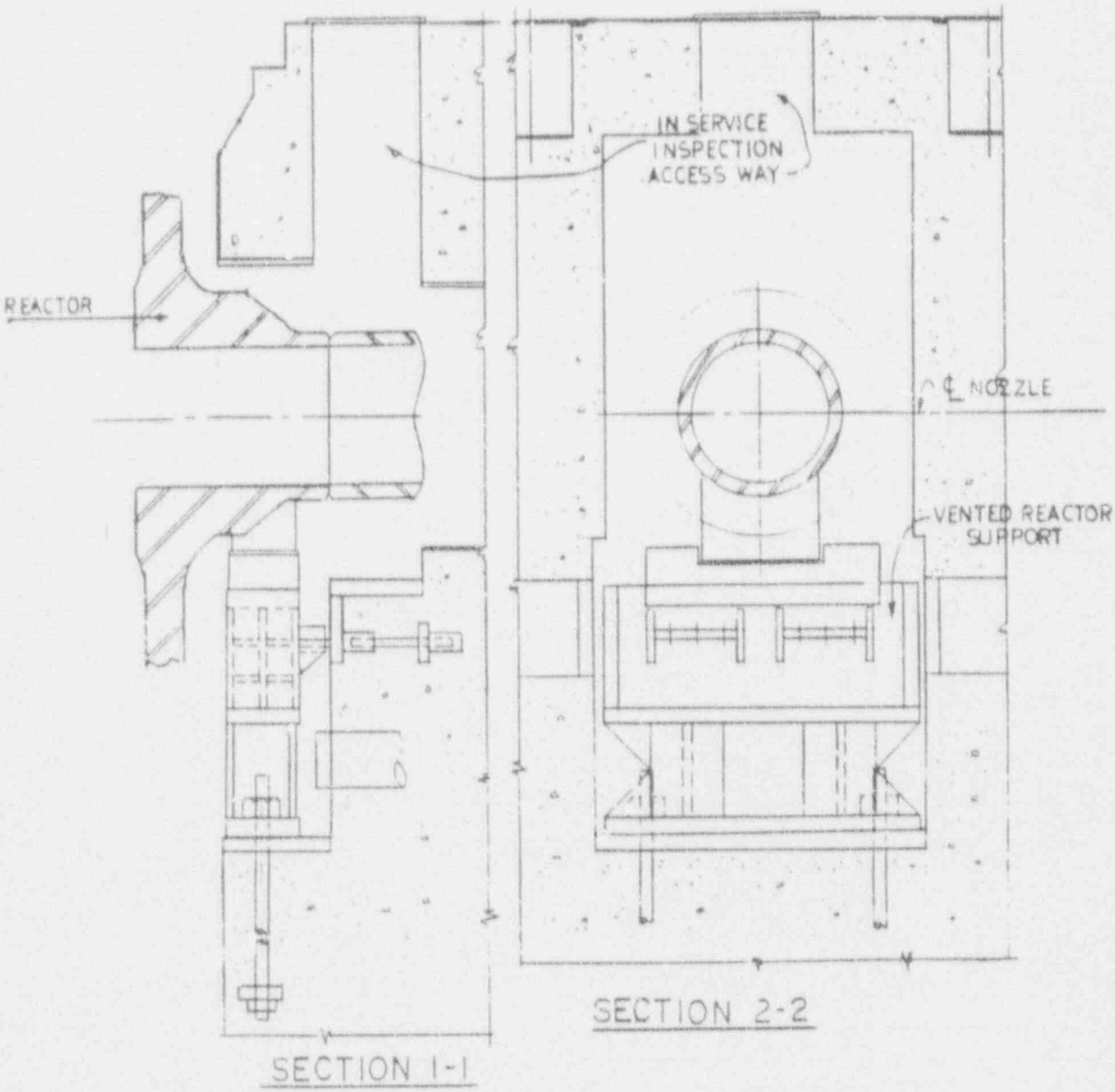

Figure 4.1-17: Containment Cavity

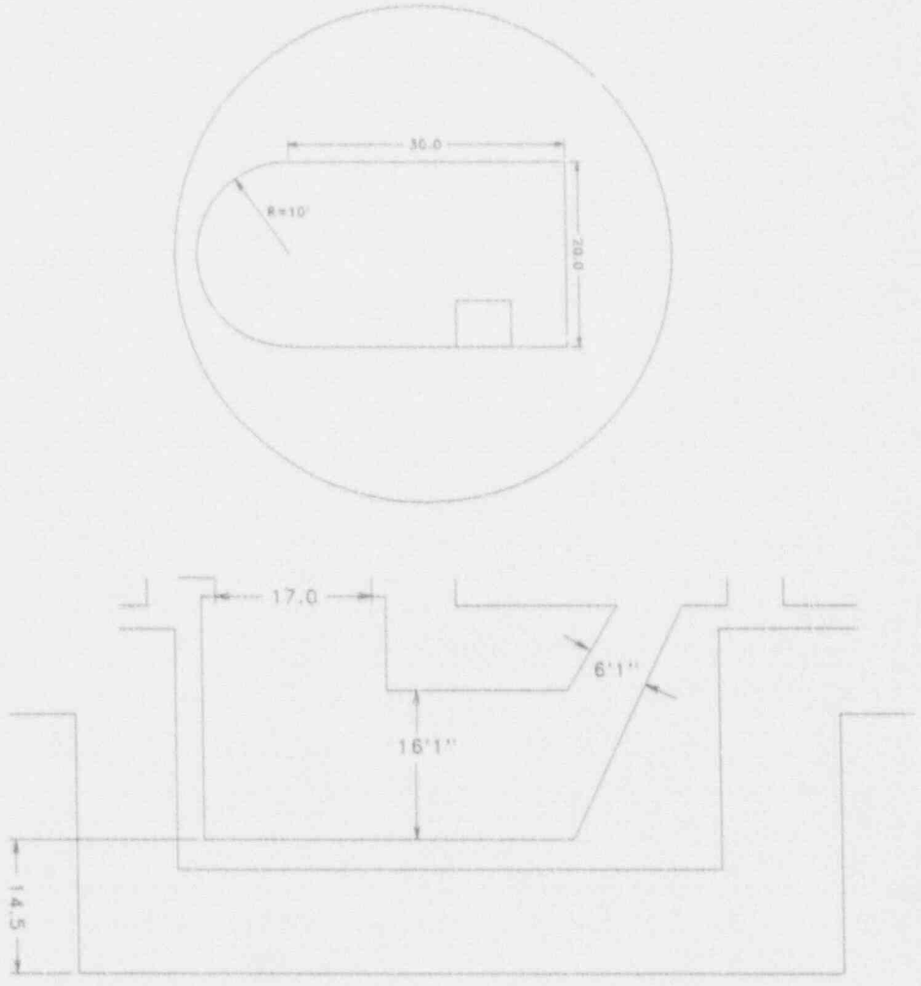

Figure 4.1-18.1: Containment and Safeguards Building Structure (East-West Sectional)

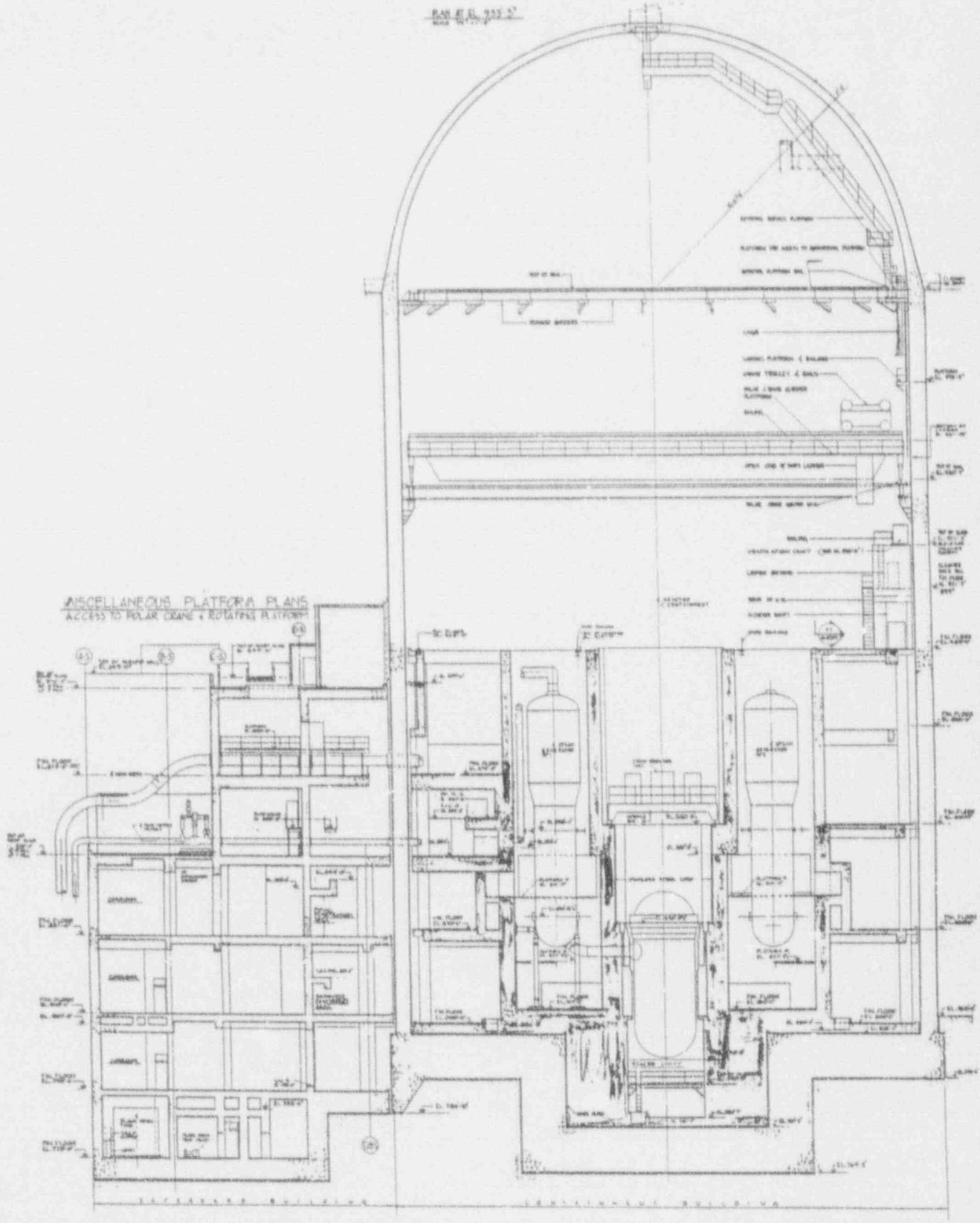

Figure 4.1-18.2: Containment Structure and Internal Arrangement (North-South Sectional)

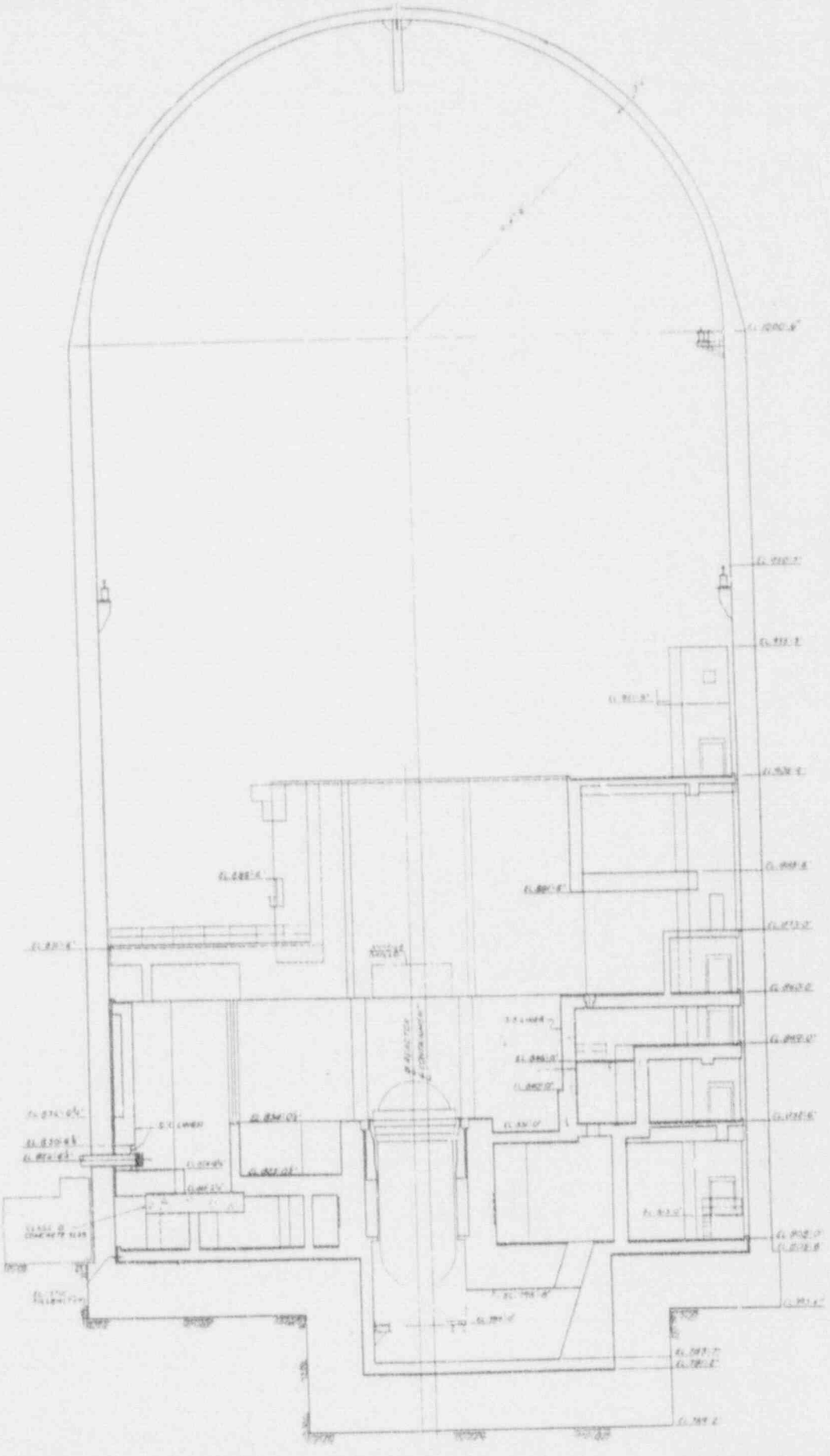

Figure 4.1-18.3: Containment Internal Structure

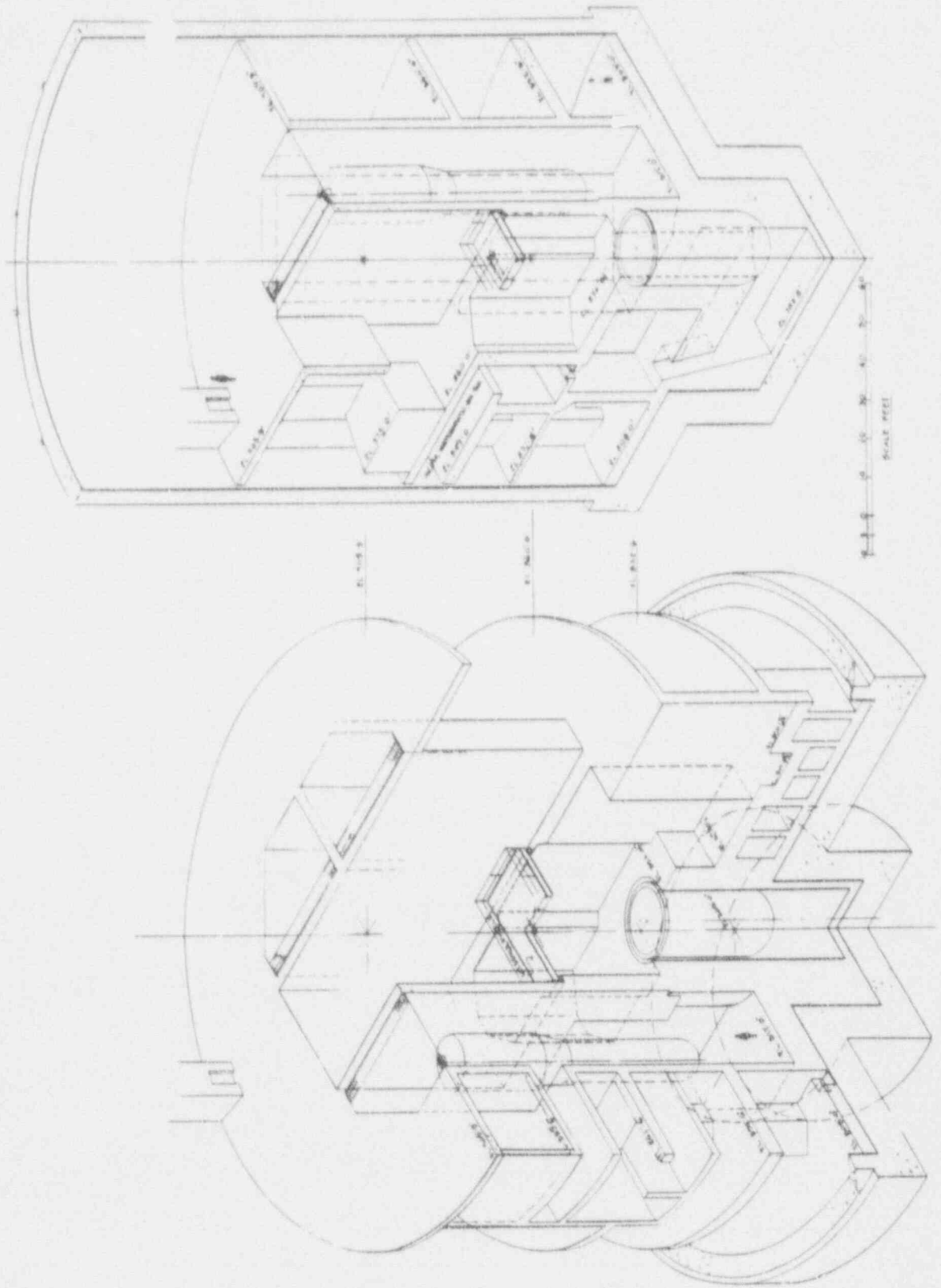

Figure 4.1-19: Containment Spray System Header Arrangement

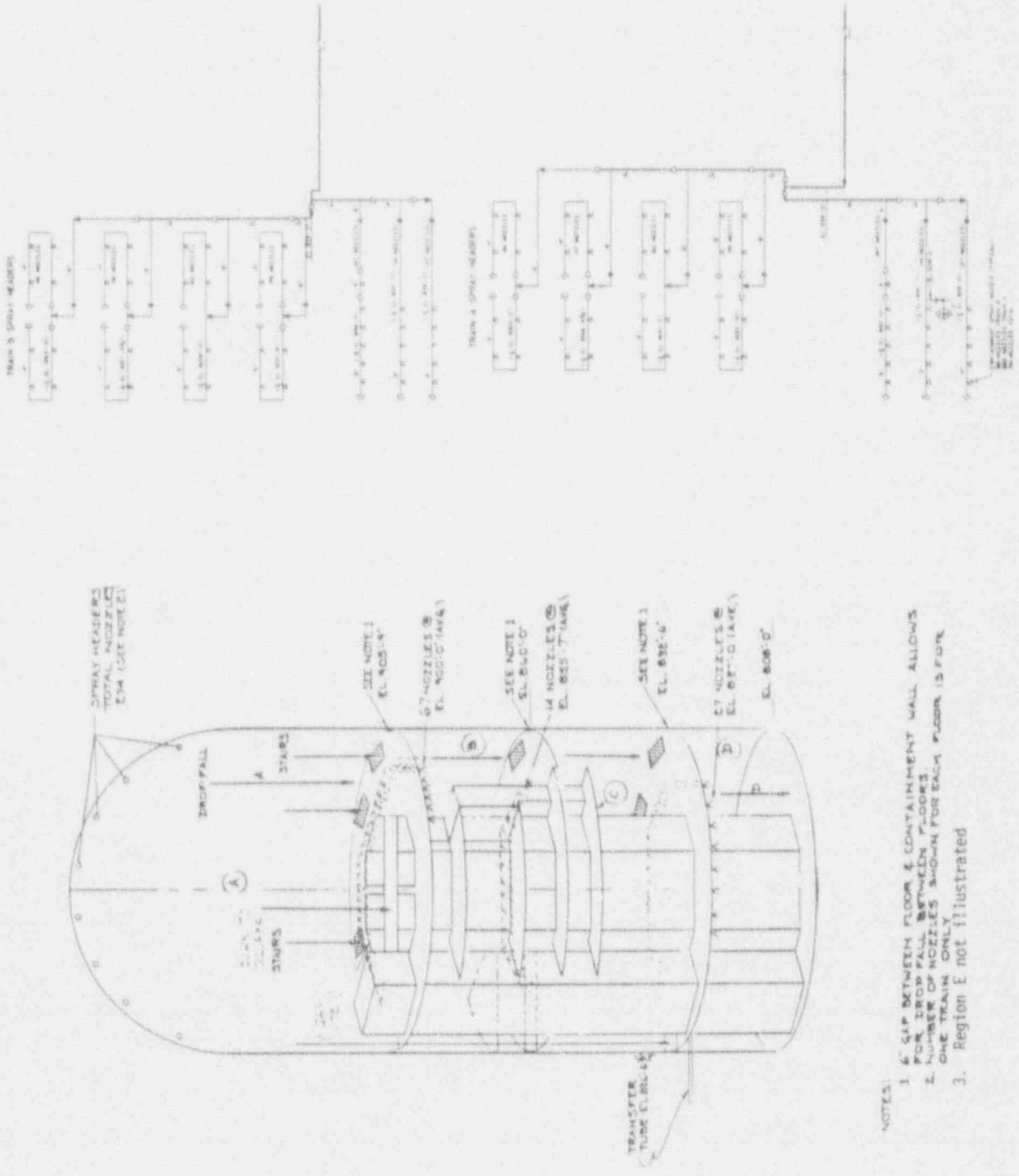

Figure 4.1-20.1: Simplified Flow Diagram Containment Air Cooling and Recirculation System (CACRS)

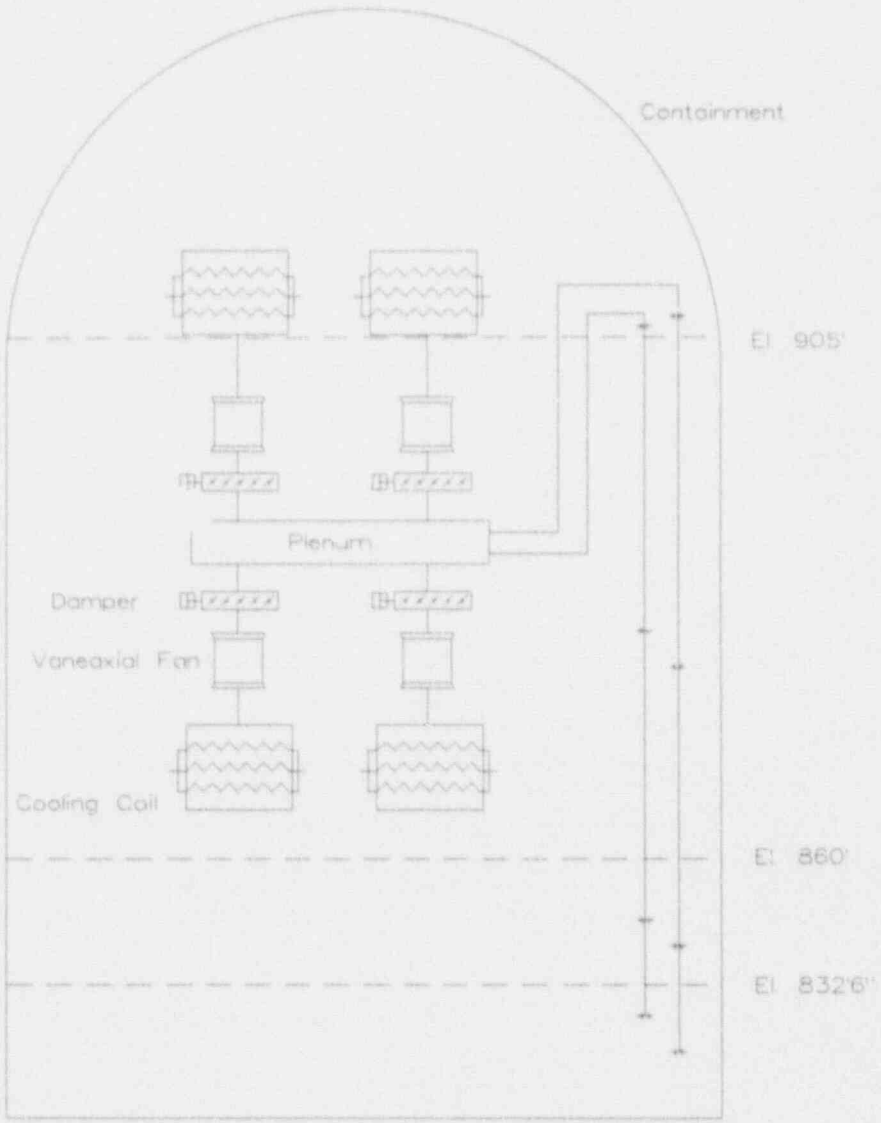

Figure 4.1-20.2: Ple. m and Duct Arrangement CACRS

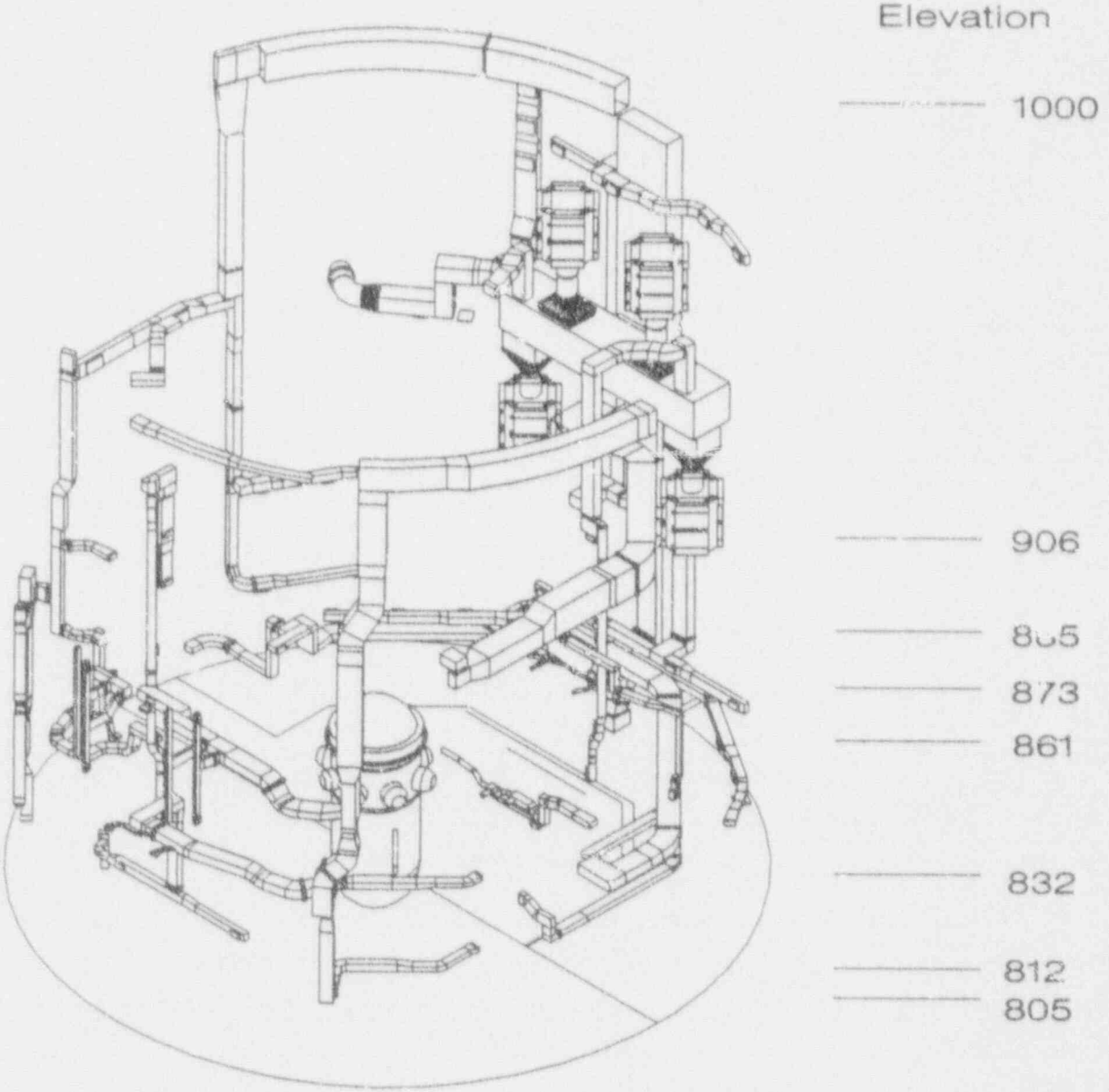

Figure 4.1-21.1: Containment Layout – RCS Components

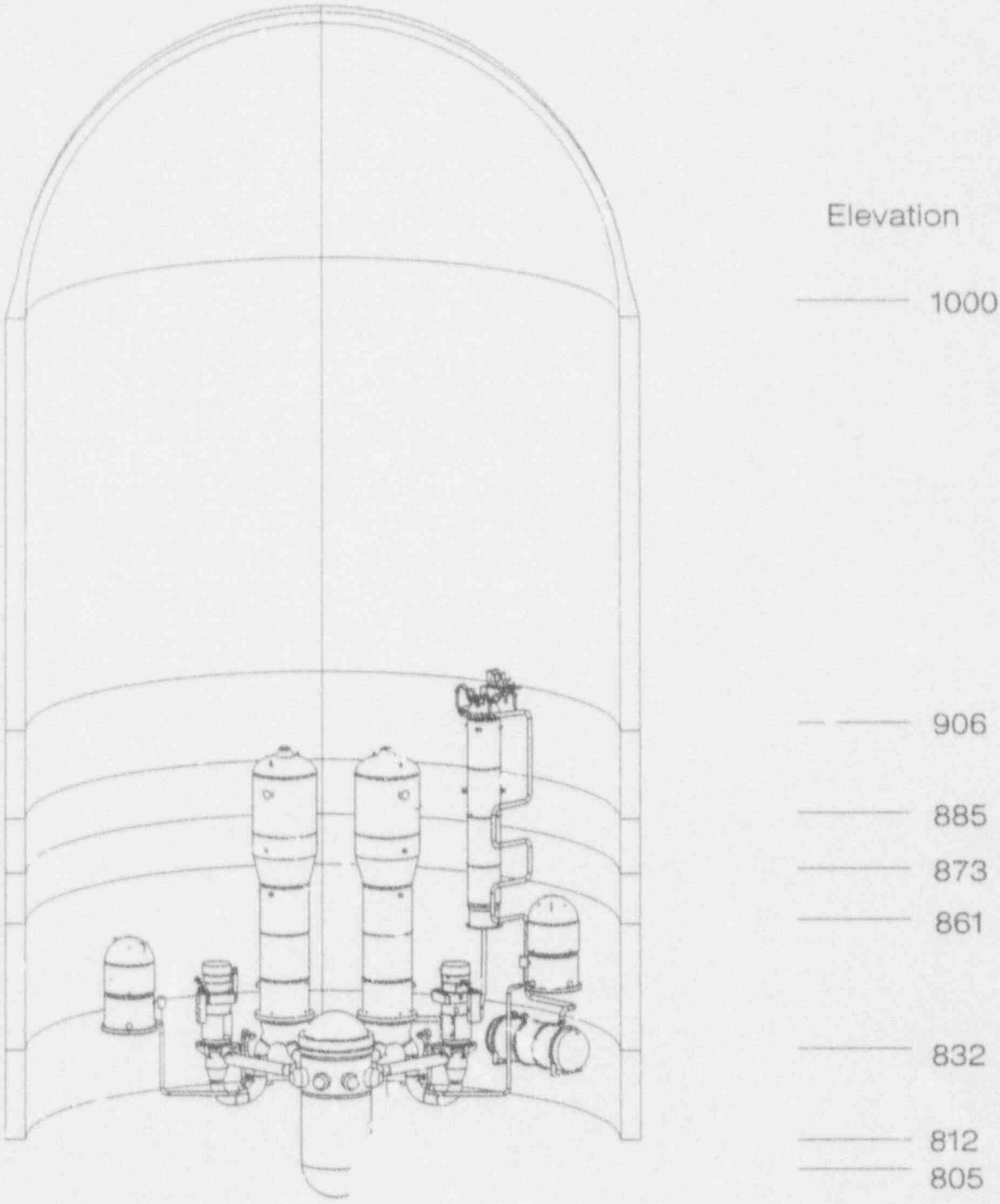

Figure 4.1-21.2: Containment Layout - Floors and Cranes

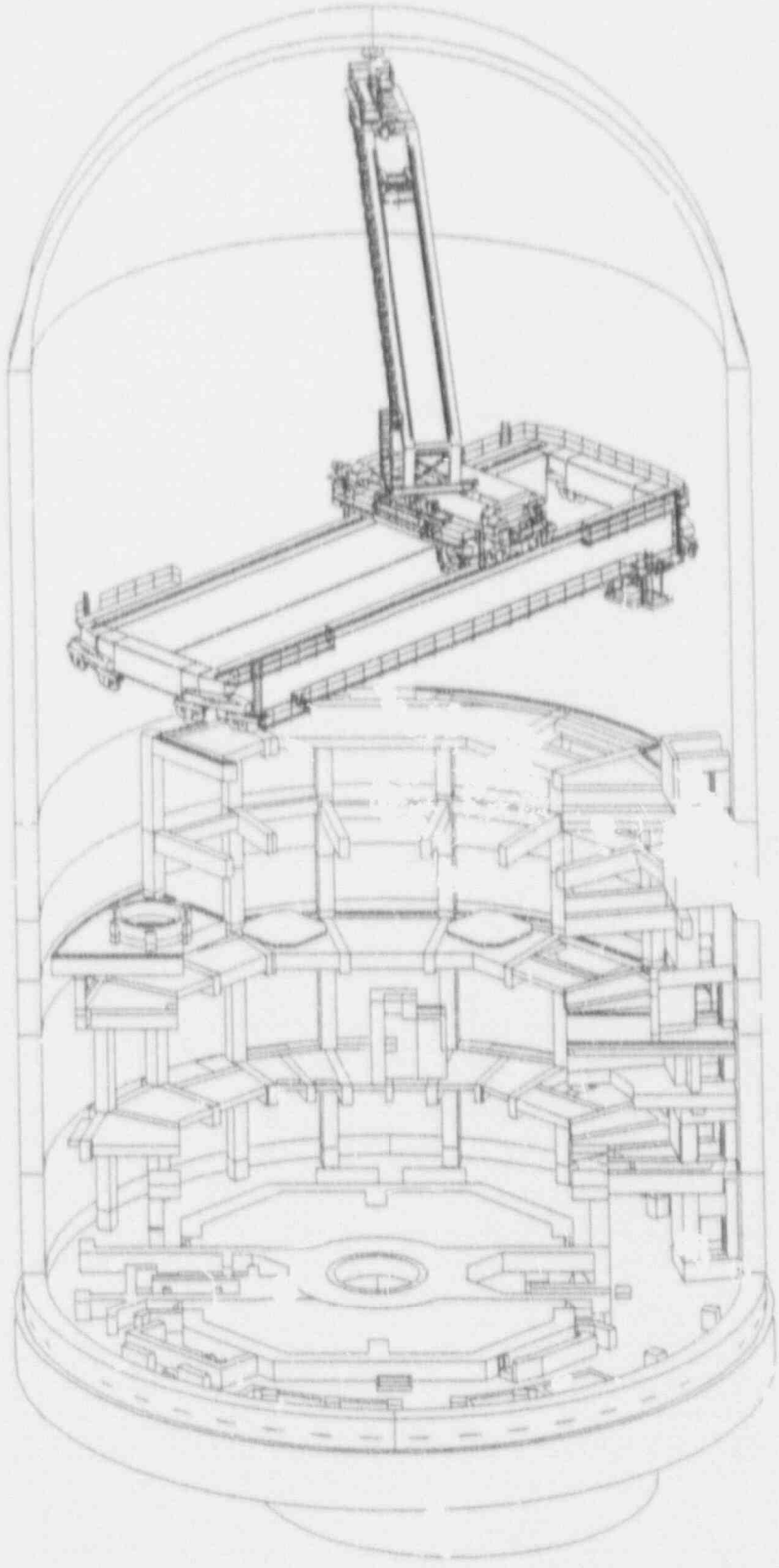

Figure 4.1-21.3: Containment Layout - Floors and Containment Spray Piping

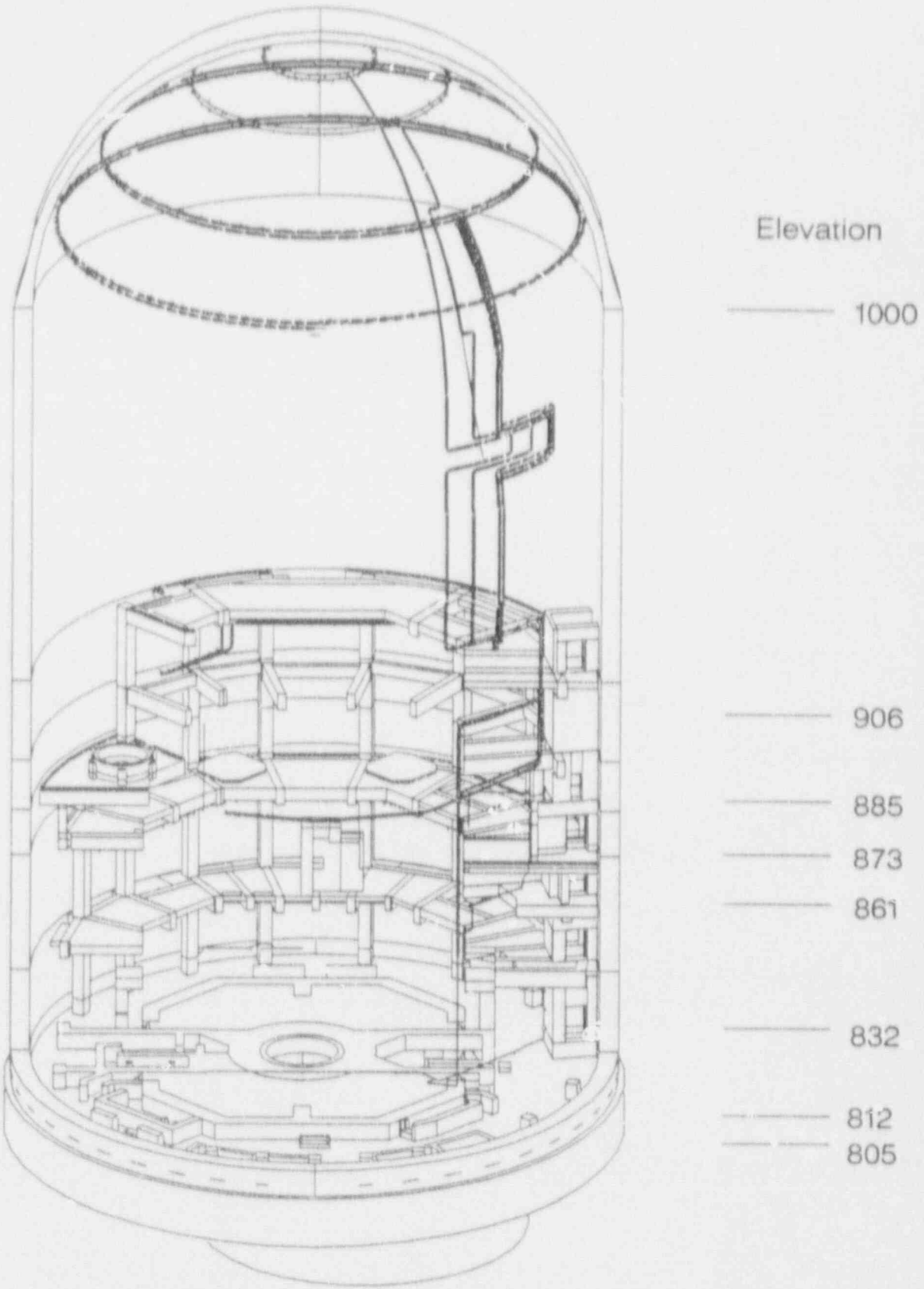

Figure 4.1-22.1: Containment Sump Piping and Arrangement (Structural View)

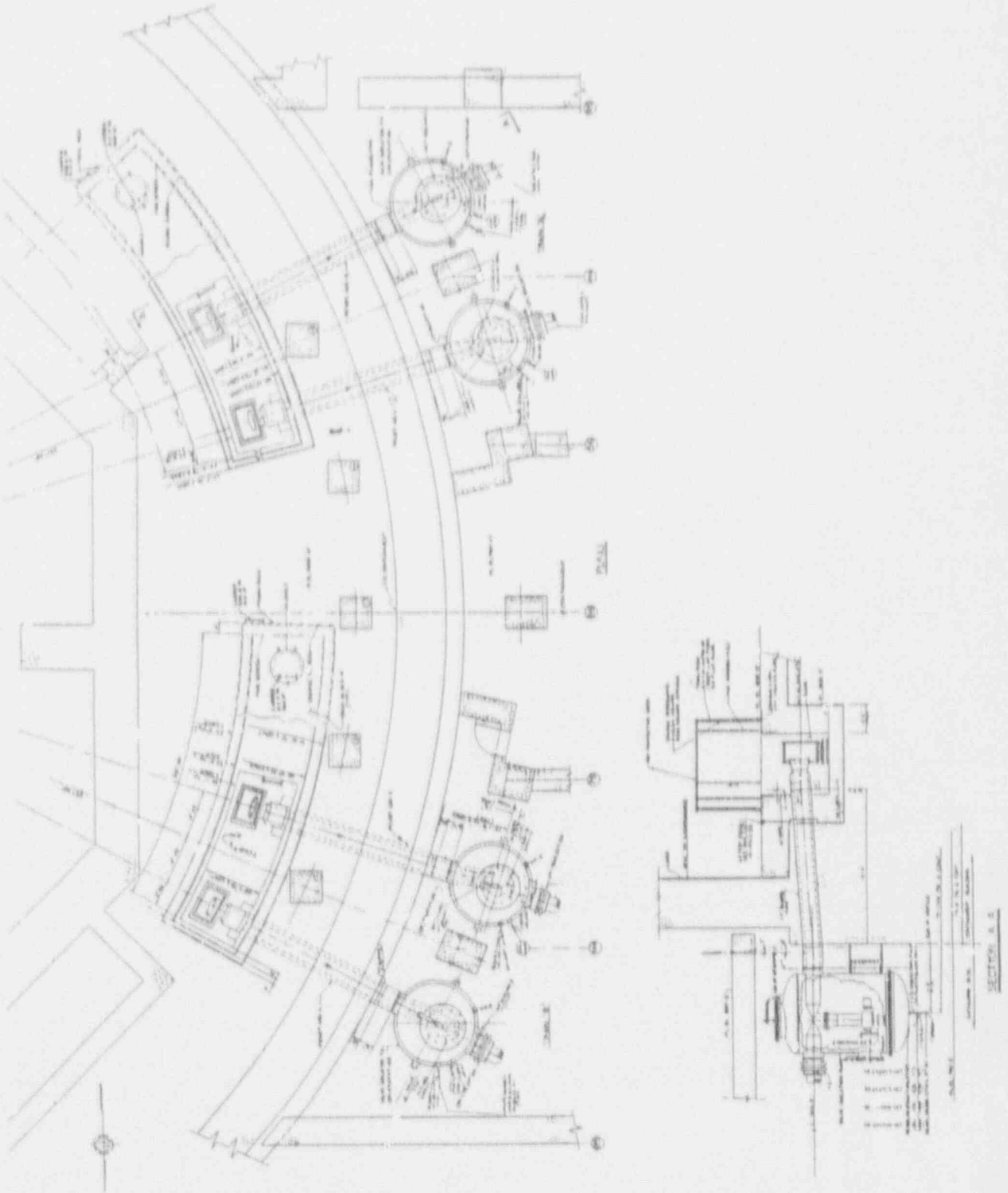

Figure 4.1-22.2: Containment Sump Piping Schematic

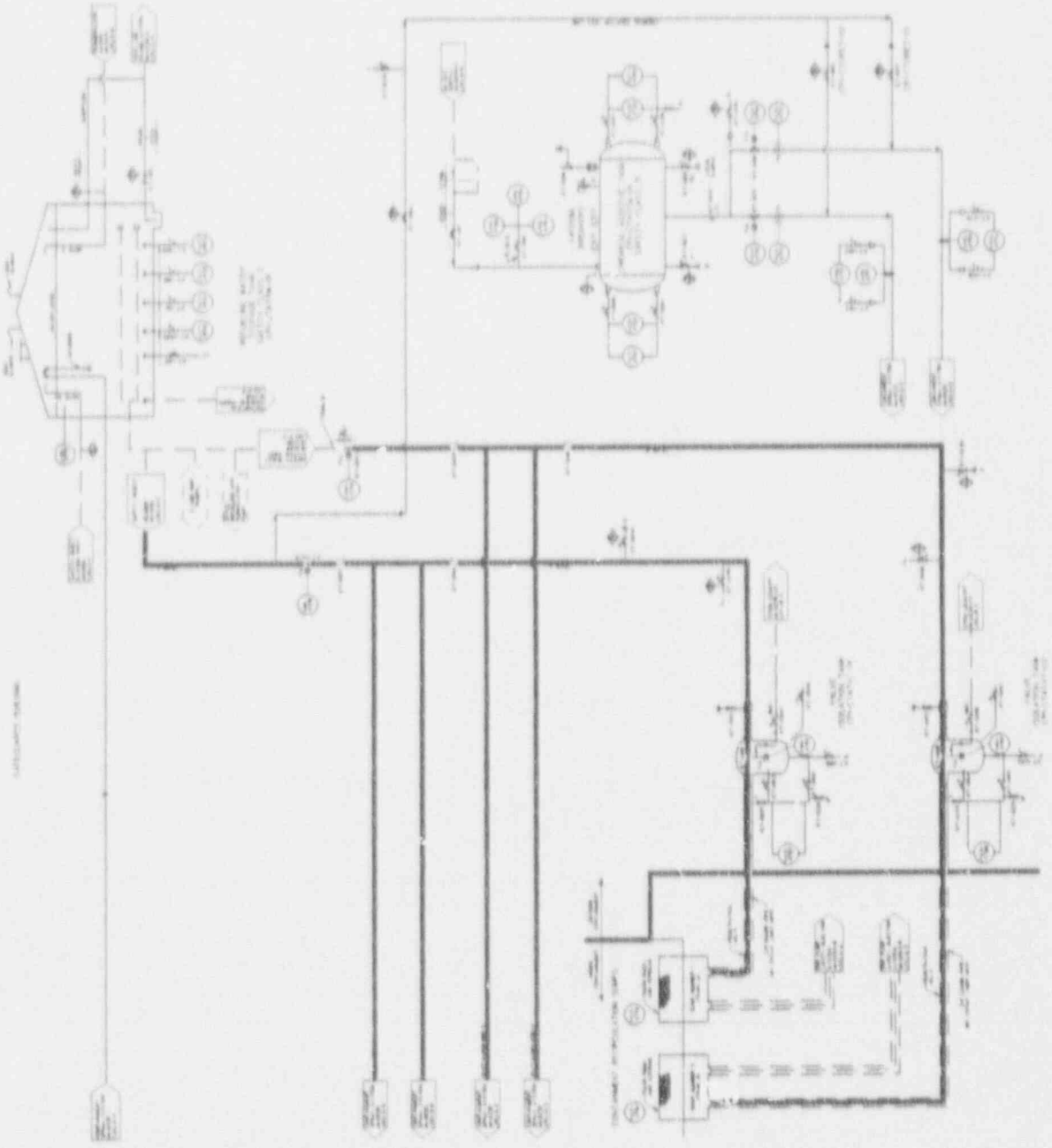

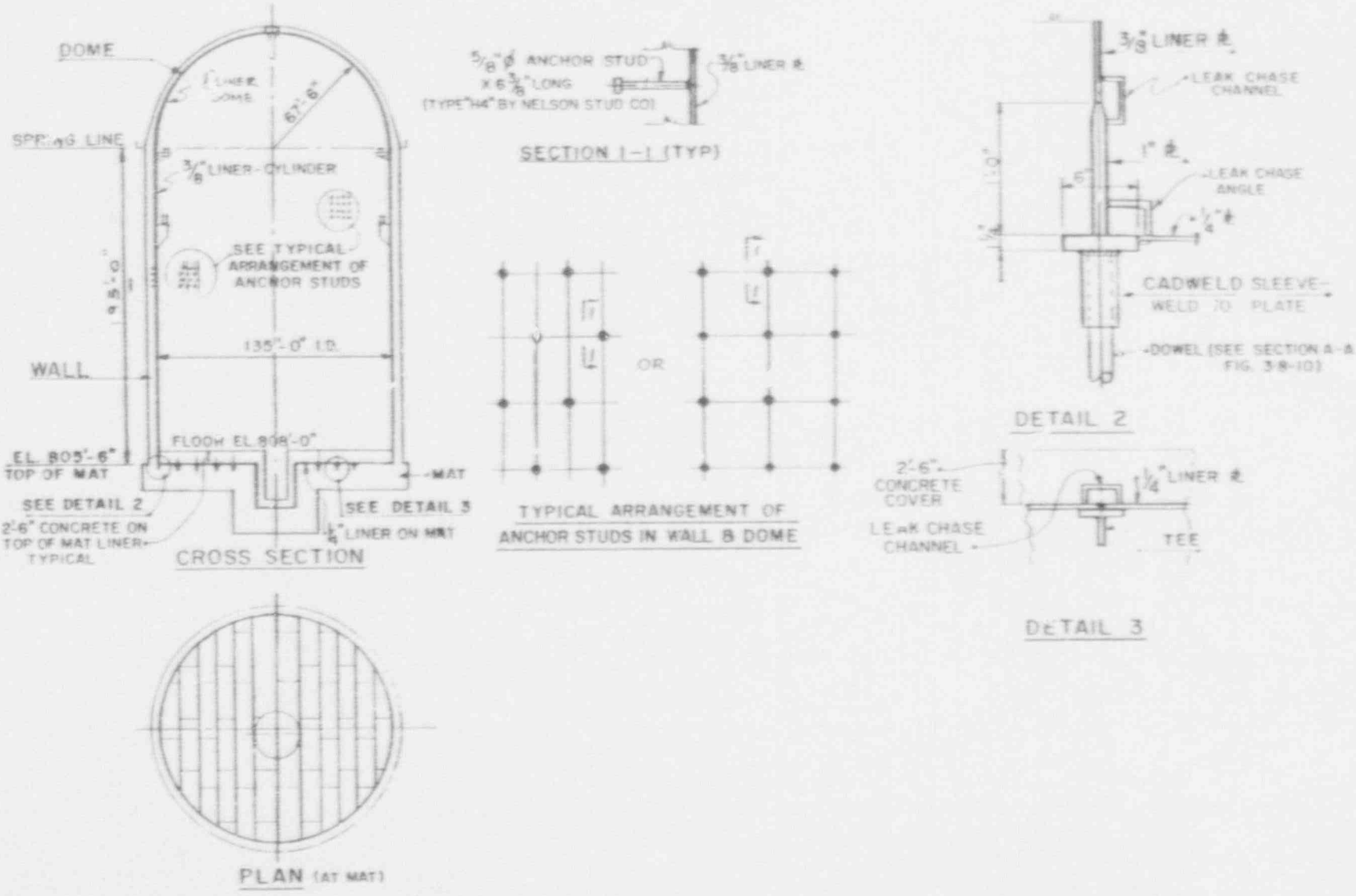

Figure 4.1-23.1: Containment Shell Reinforcement Detail

Figure 4.1-23.2: Foundation Mat Reinforcement

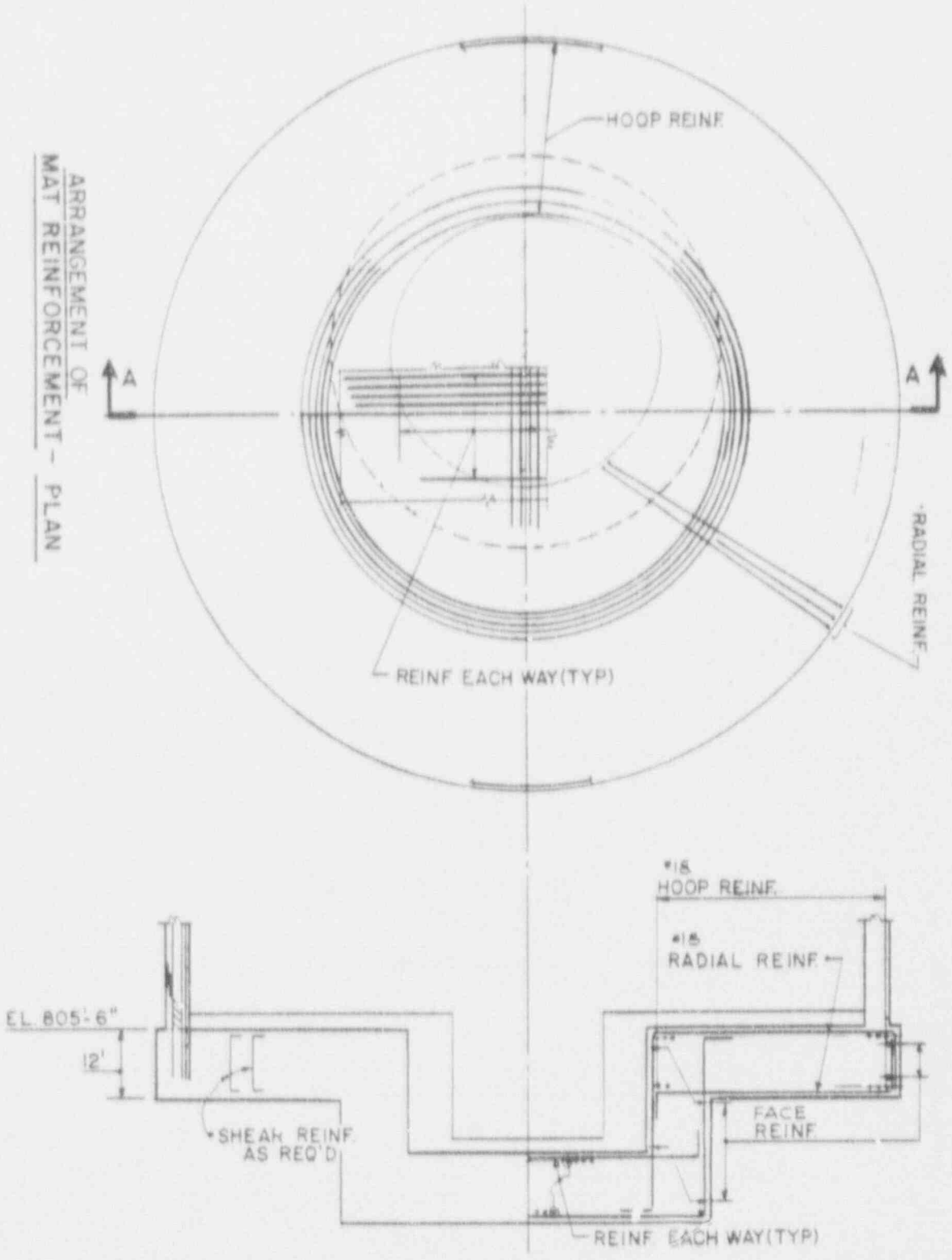

SECTION A-A

Figure 4.1-23.3: Containment Penetration Locations

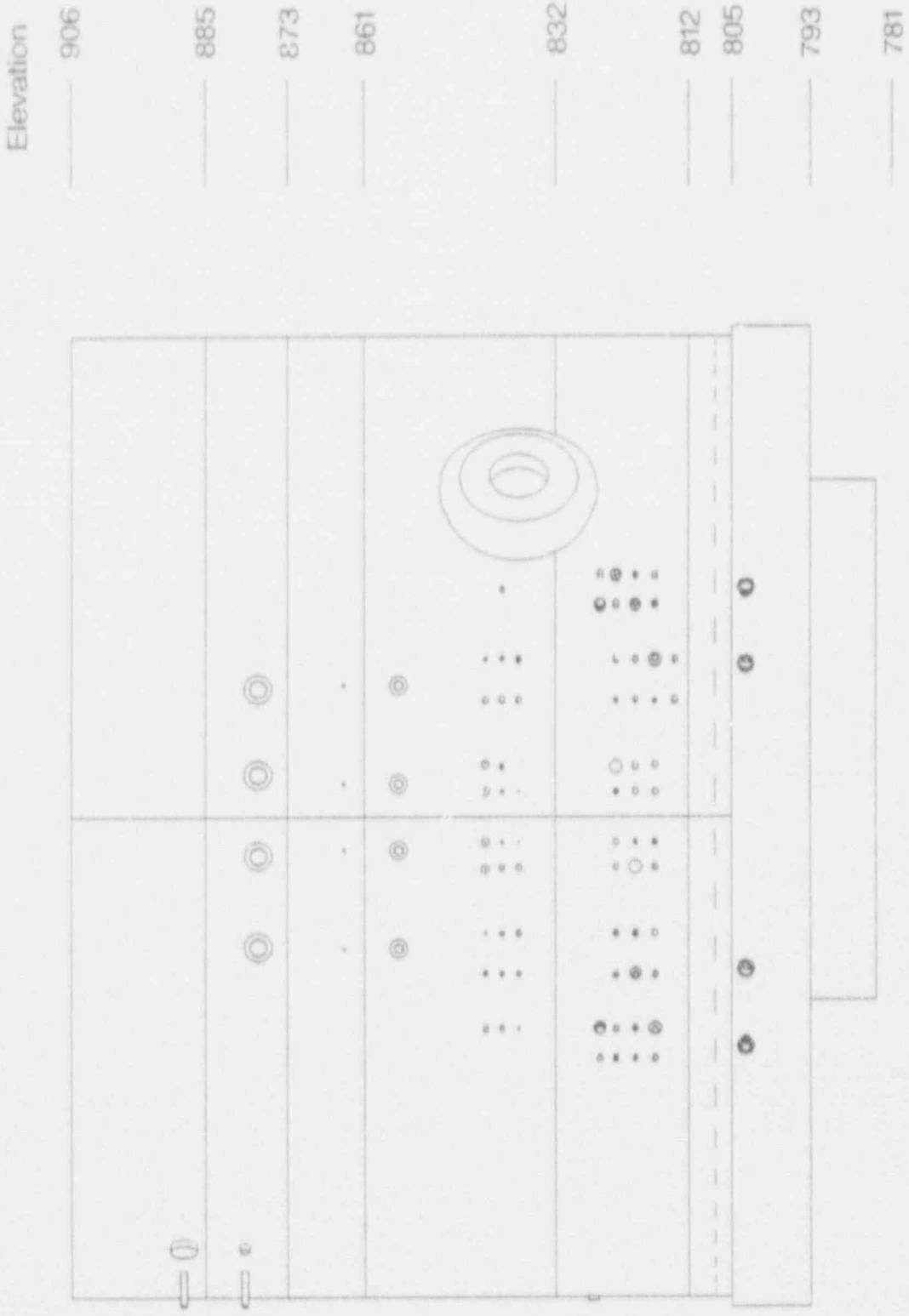

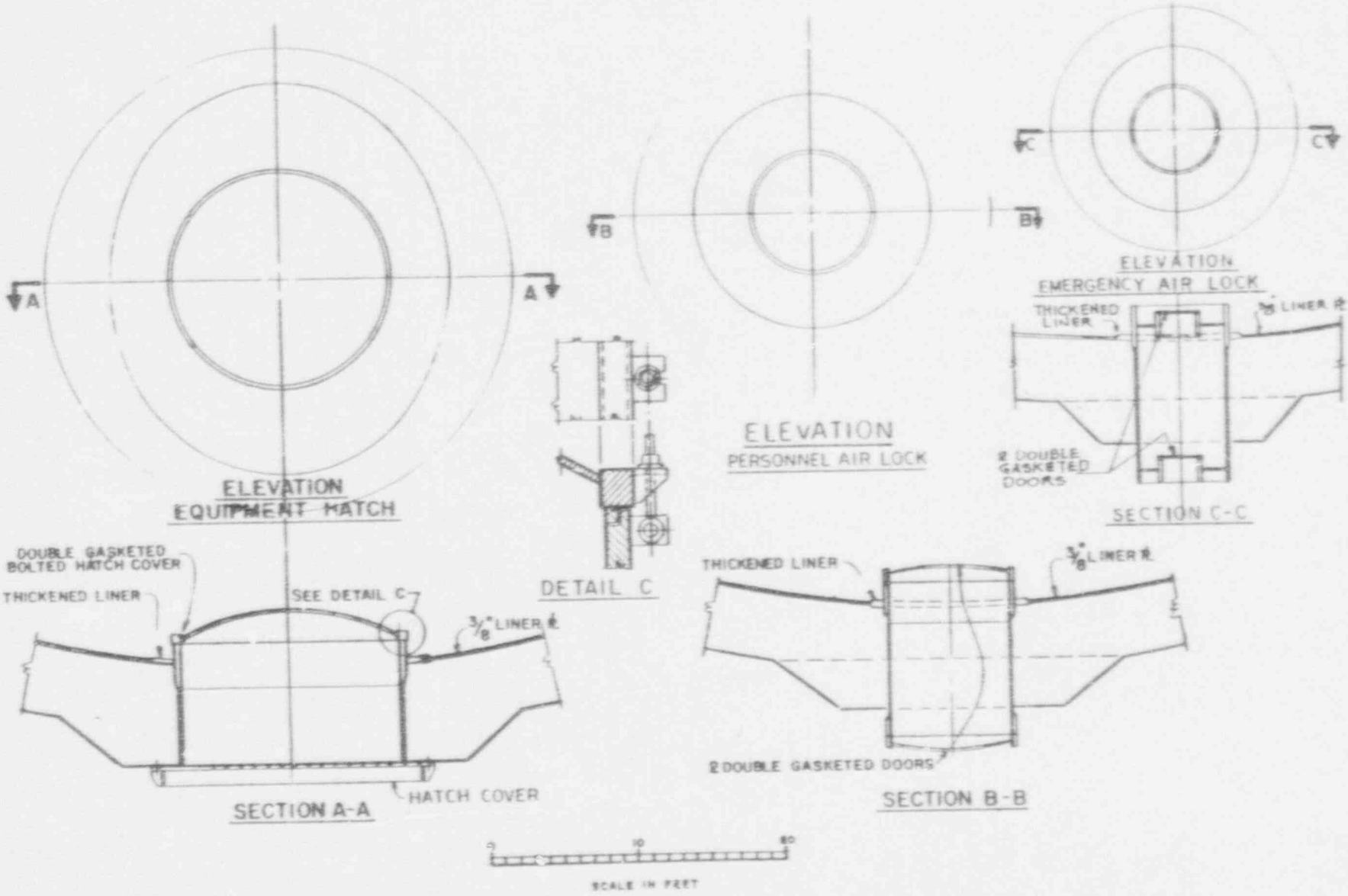

Figure 4.1-23.4. Containment Hatch Details

Figure 4.1-23.5: Personnel Airlock General Arrangement

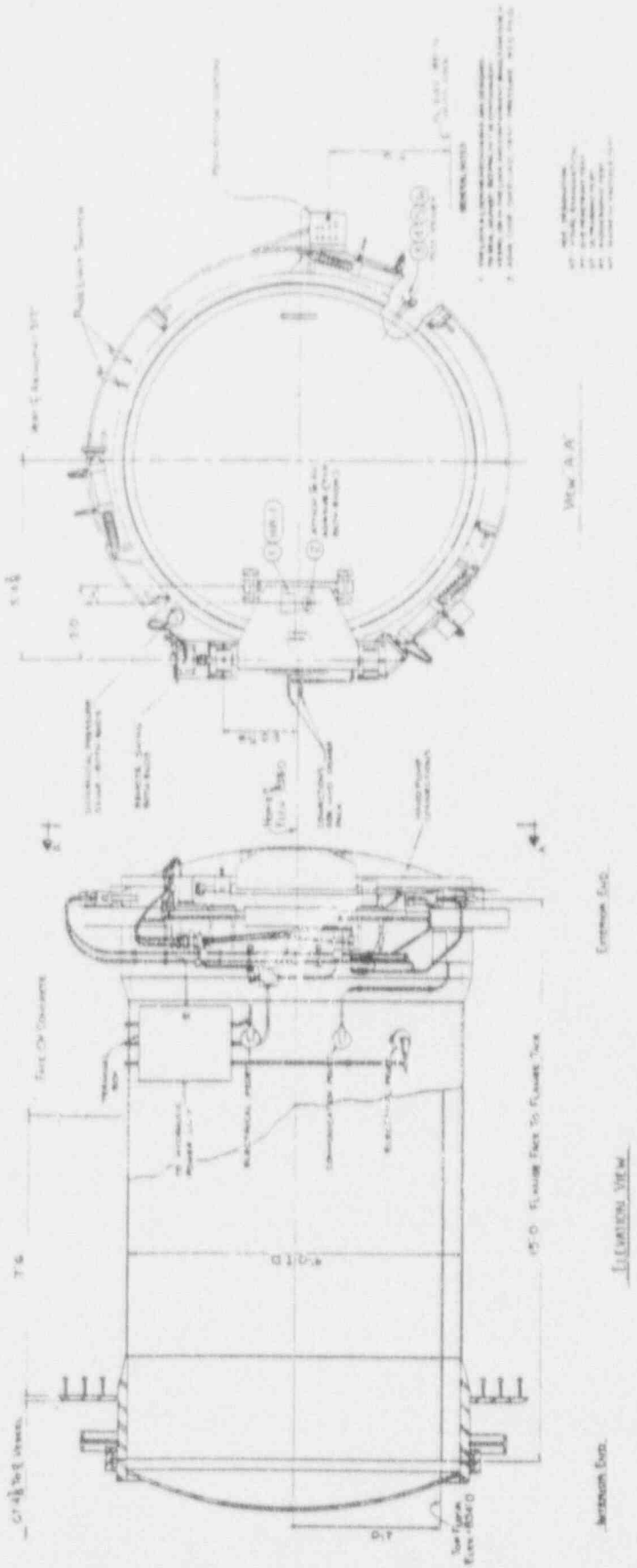

Figure 4.1-23.6: Fuel Transfer Tube Details

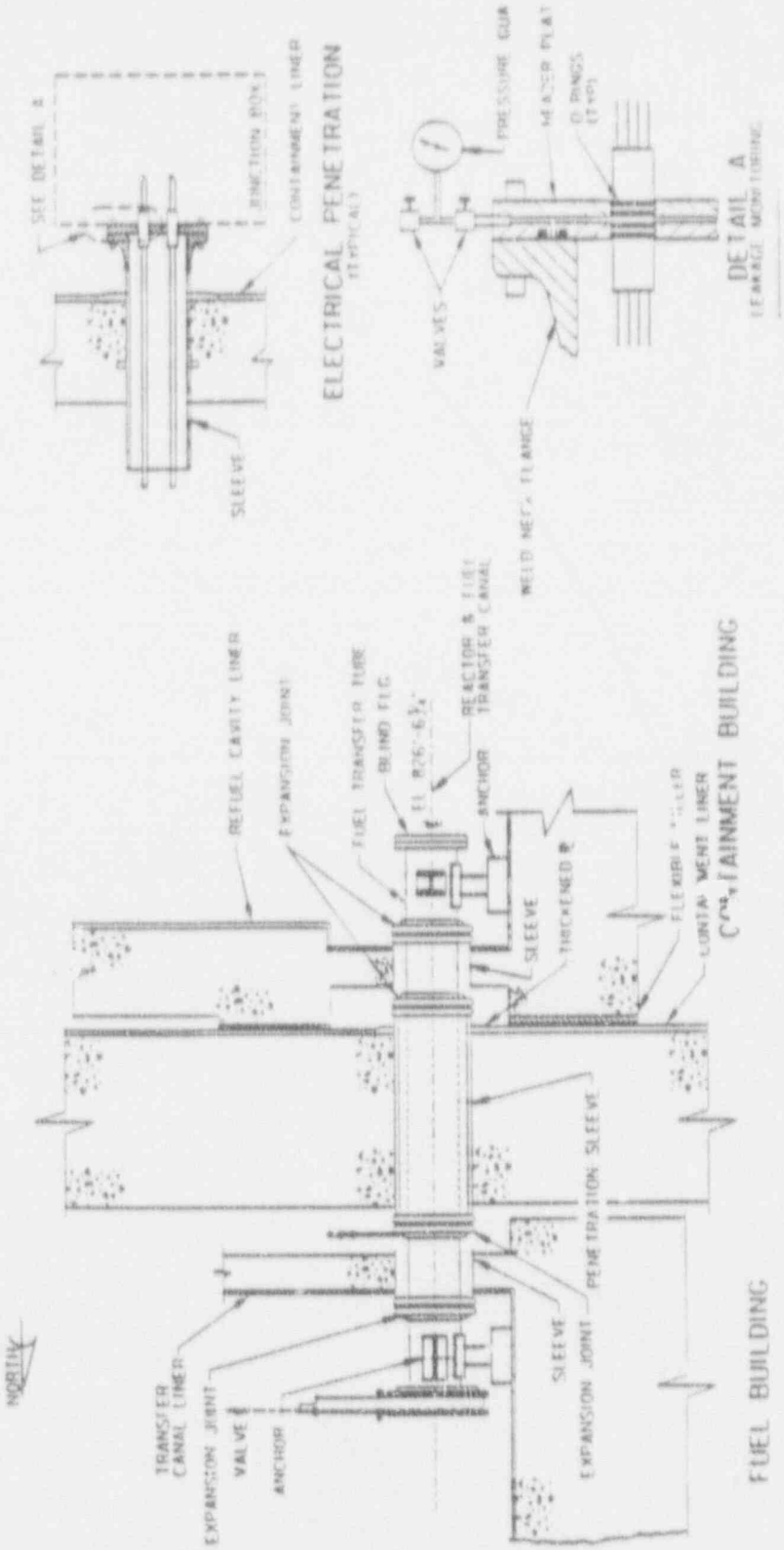

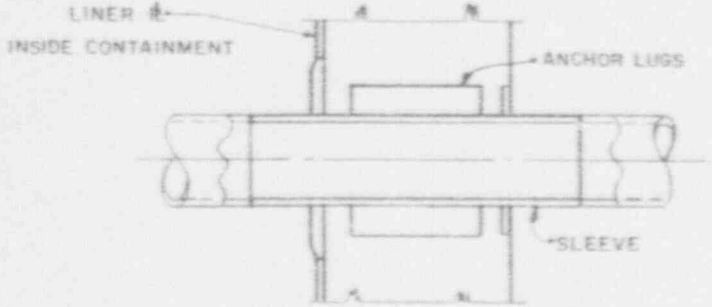

COLD PIPE PENETRATION
(CARBON STEEL)

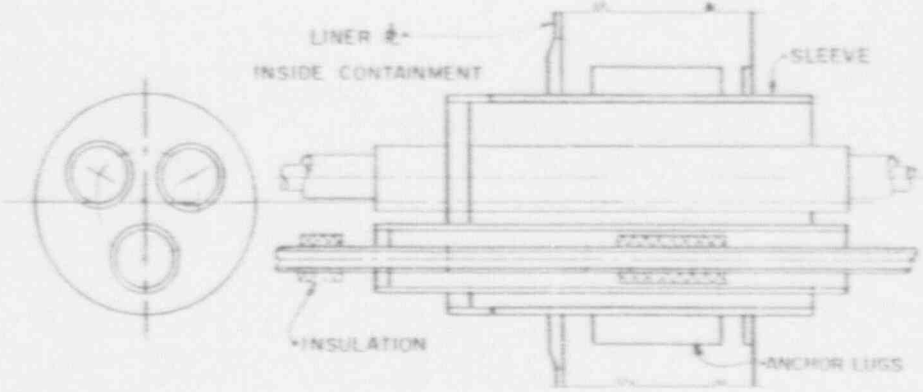

MULTIPLE PIPE PENETRATION

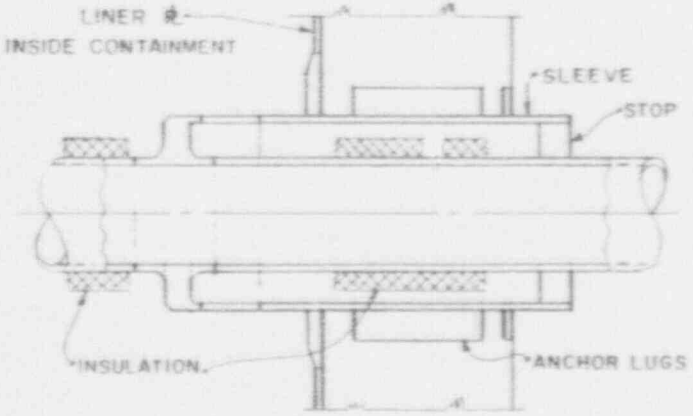

COLD PIPE PENETRATION
(STAINLESS STEEL)

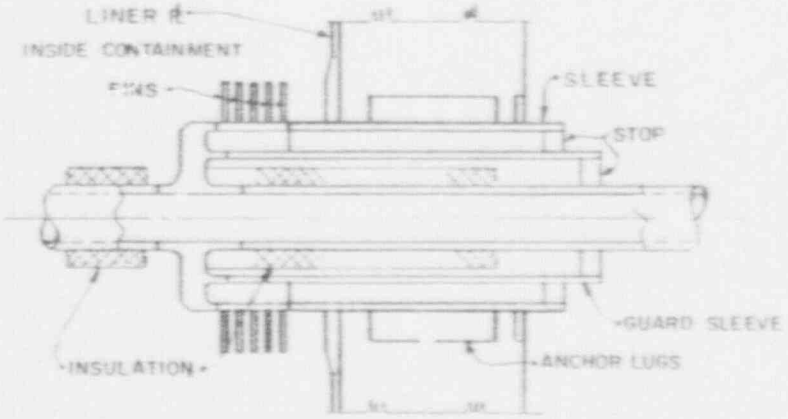

HOT PIPE PENETRATION

Figure 4.1-23.7: Containment Penetration Details

Figure 4.1-24.1: Structural Plant Arrangement

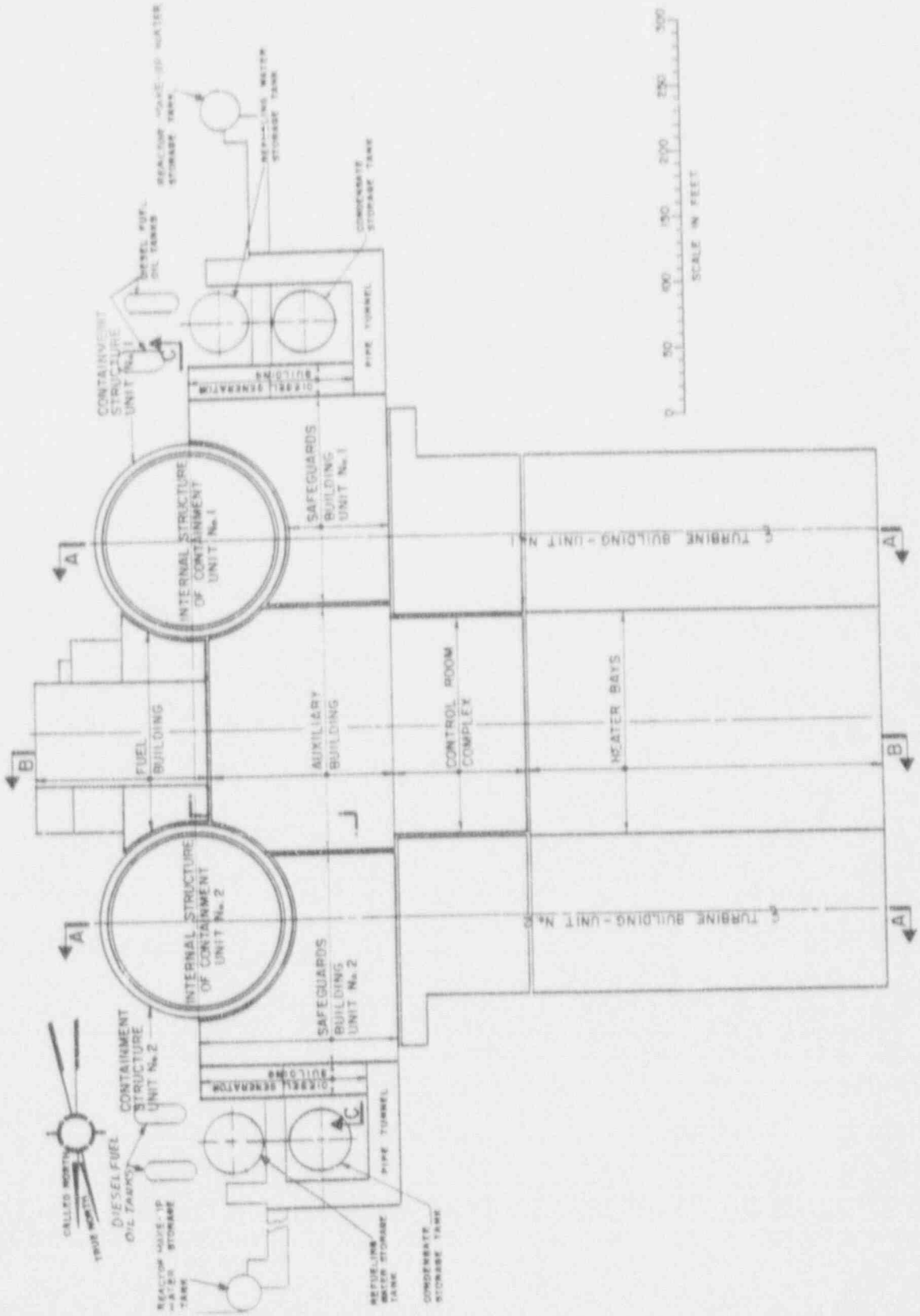

Figure 4.1-24.2: Structural Plant Arrangement (Section A-A)

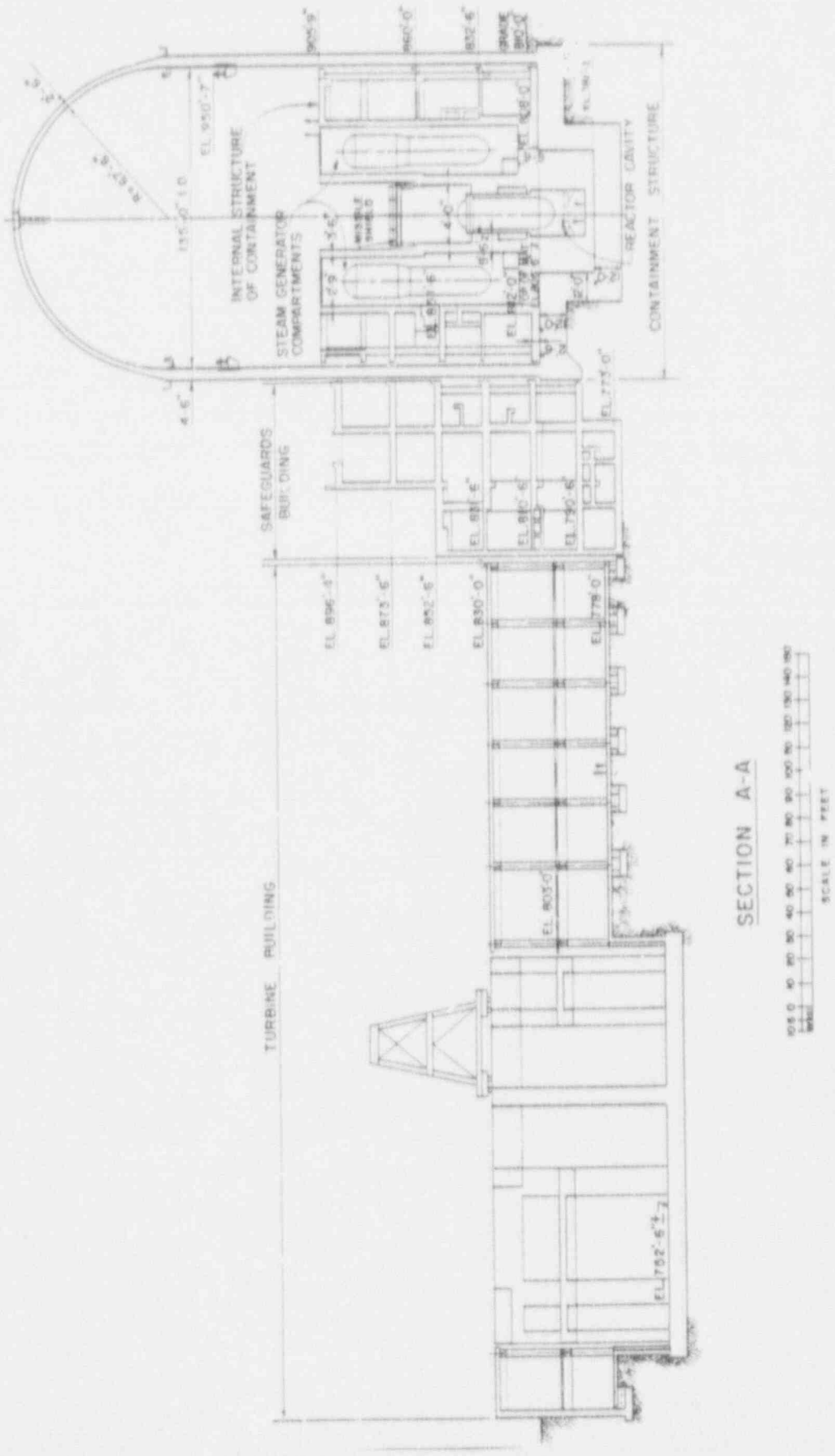

Figure 4.1-24.3: Structural Plant Arrangement (Section B-B)

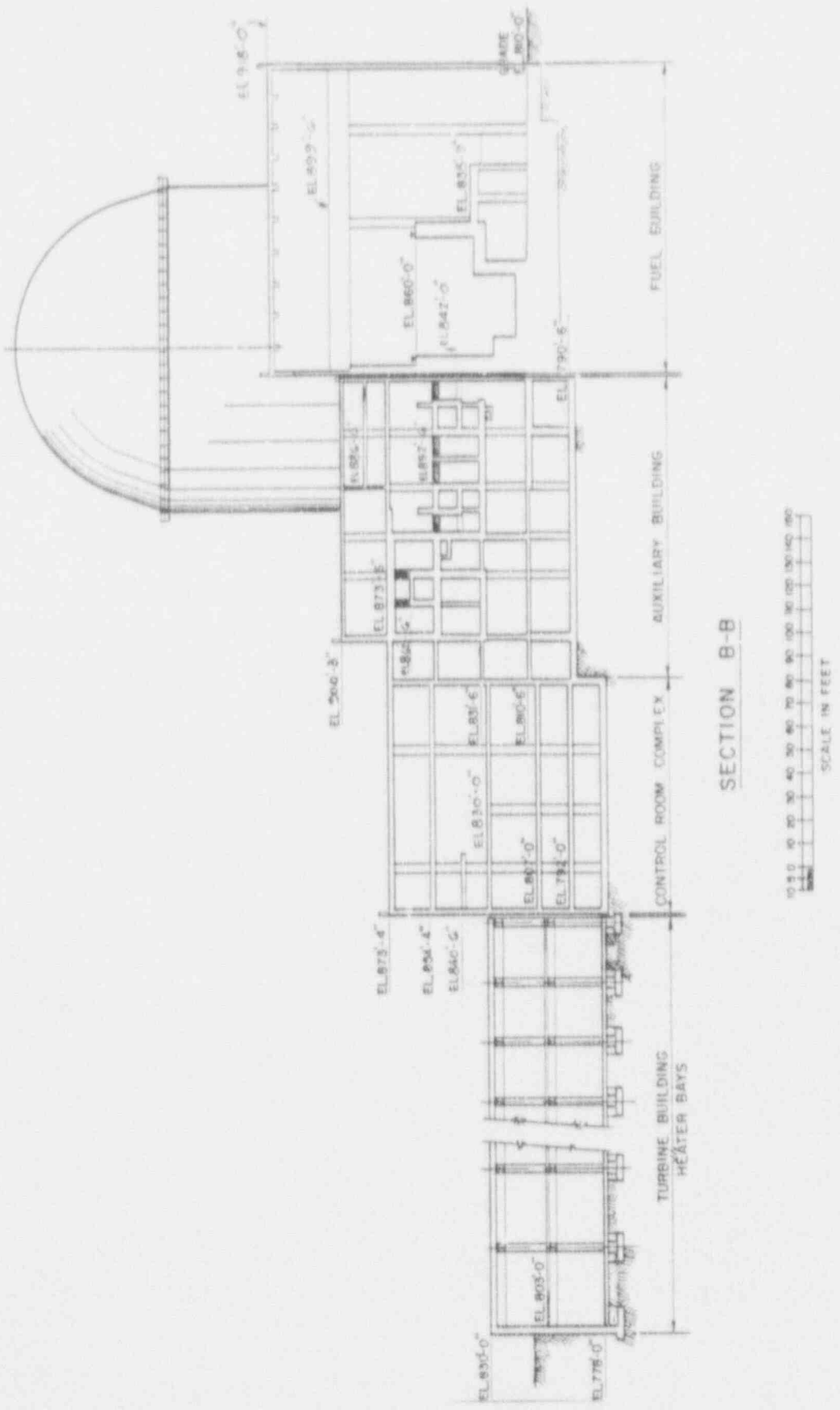

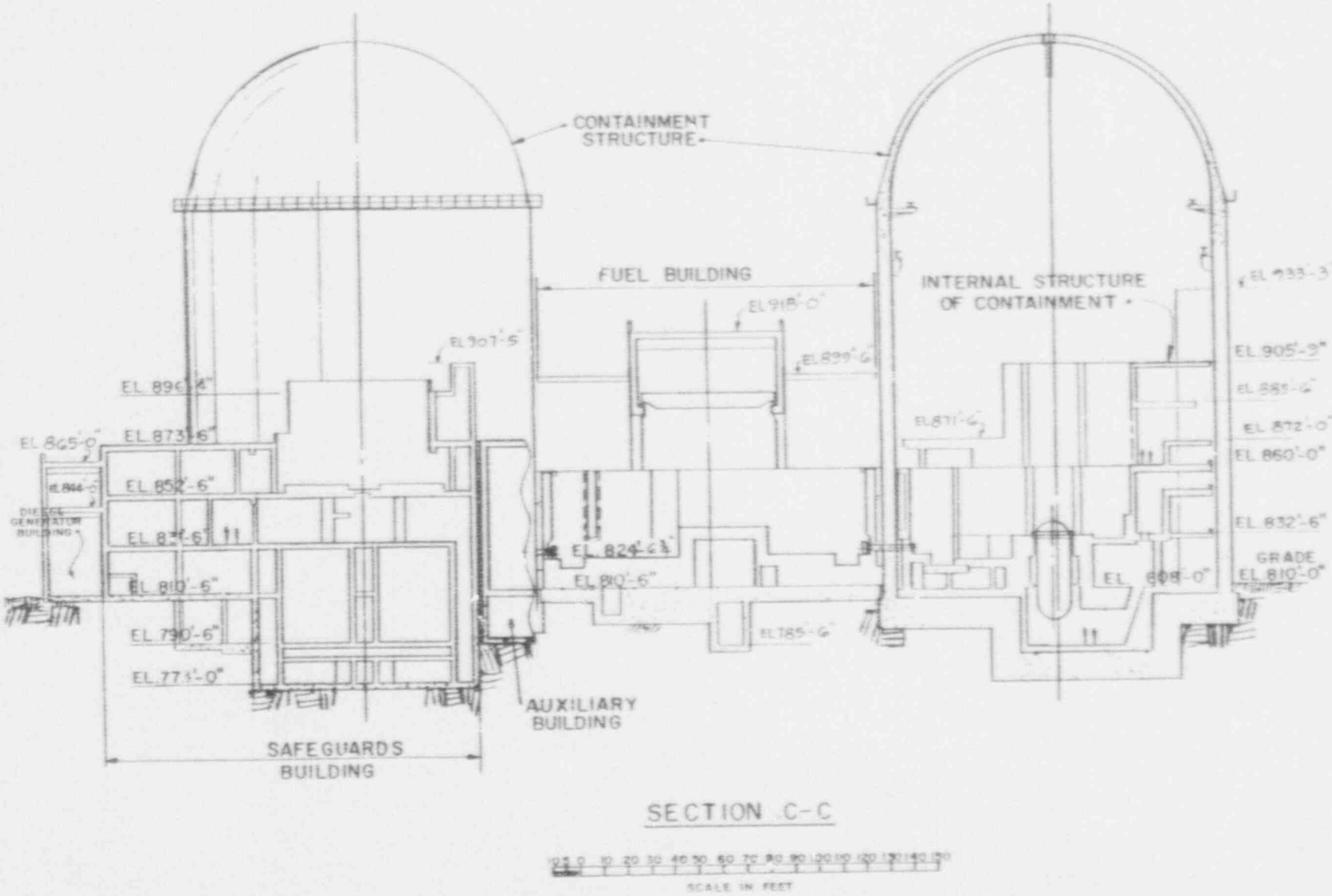

Figure 4.1-24.4: Structural Plant Arrangement (Section C-C)

Figure 4.1-25.1. Containment and Safeguards Building Plans (Els. 773,785,790)

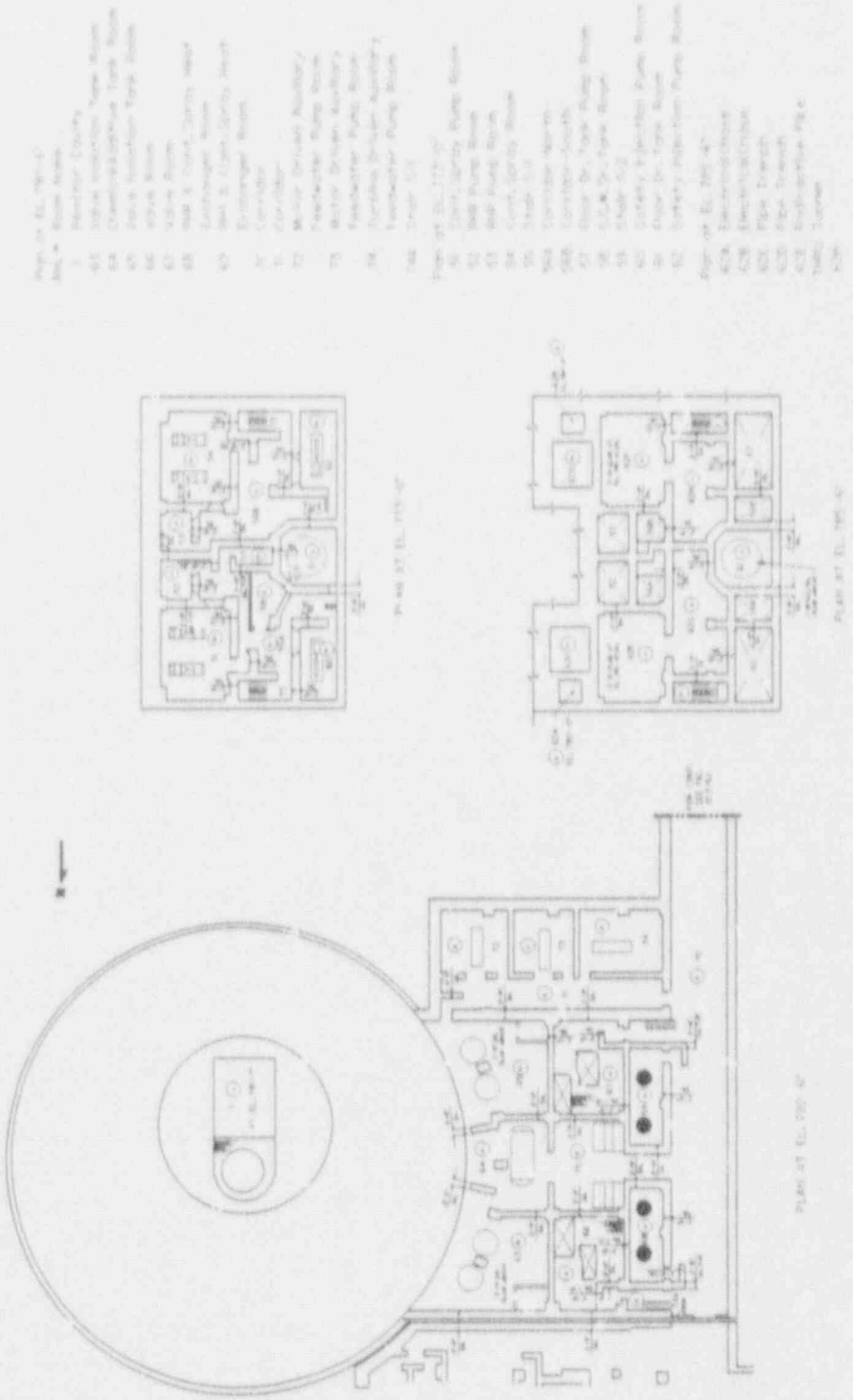

Figure 4.1-25.2: Safeguards Building Plan (El. 810)

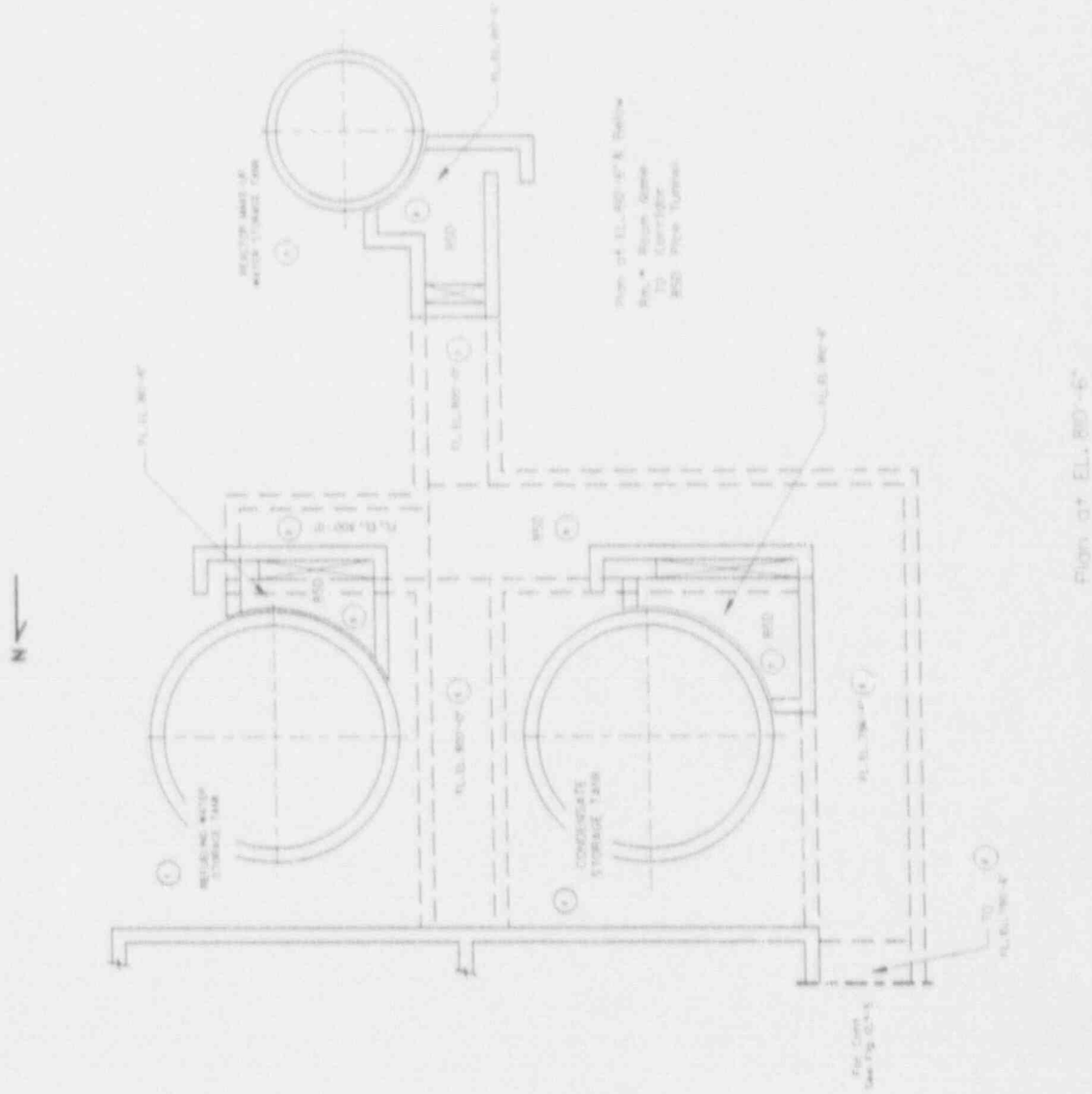

Figure 4.1-25.3: Containment and Safeguards Building Plans (El. 810)

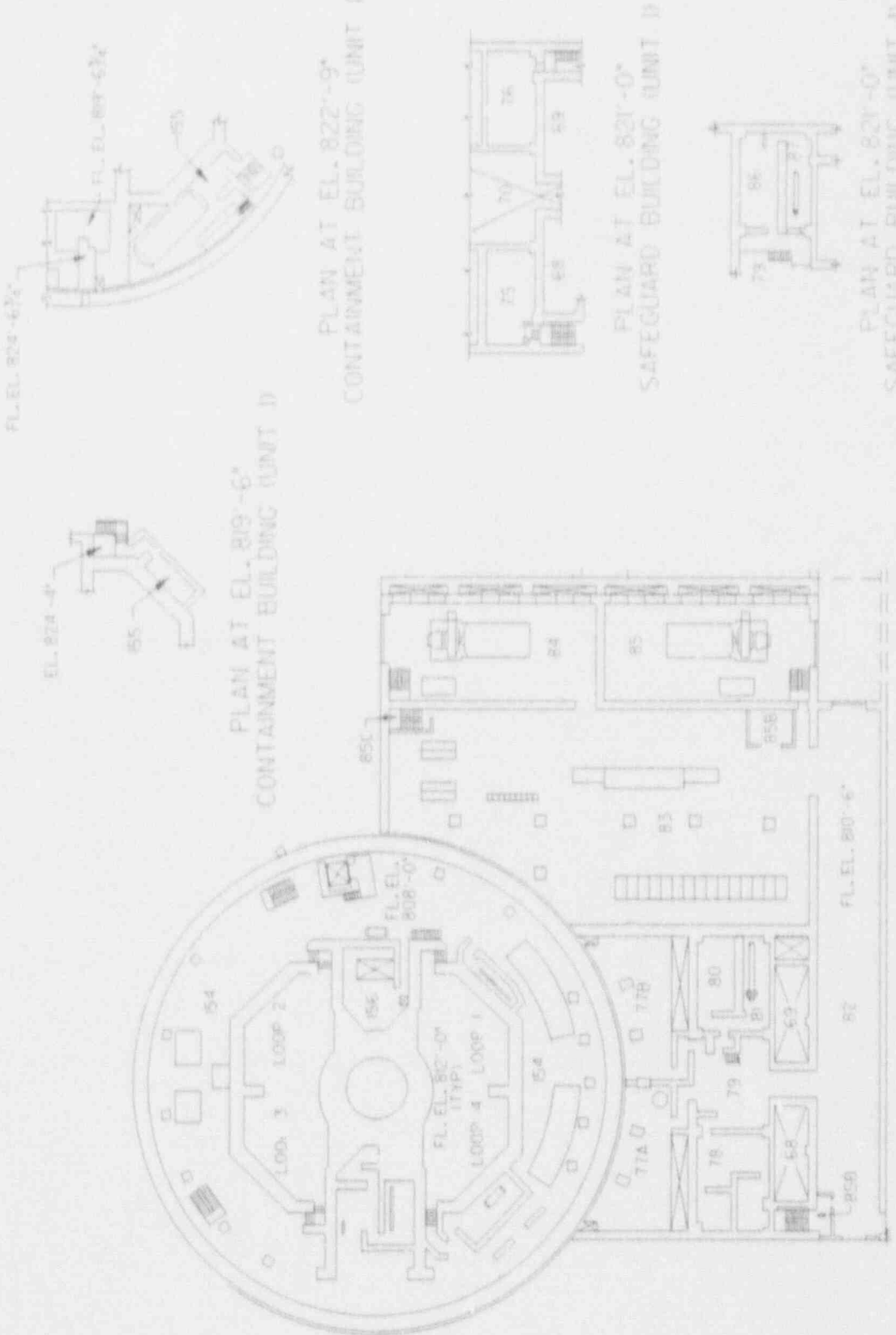

Figure 4.1-25.4: Containment and Safeguards Building Plans (El. 832)

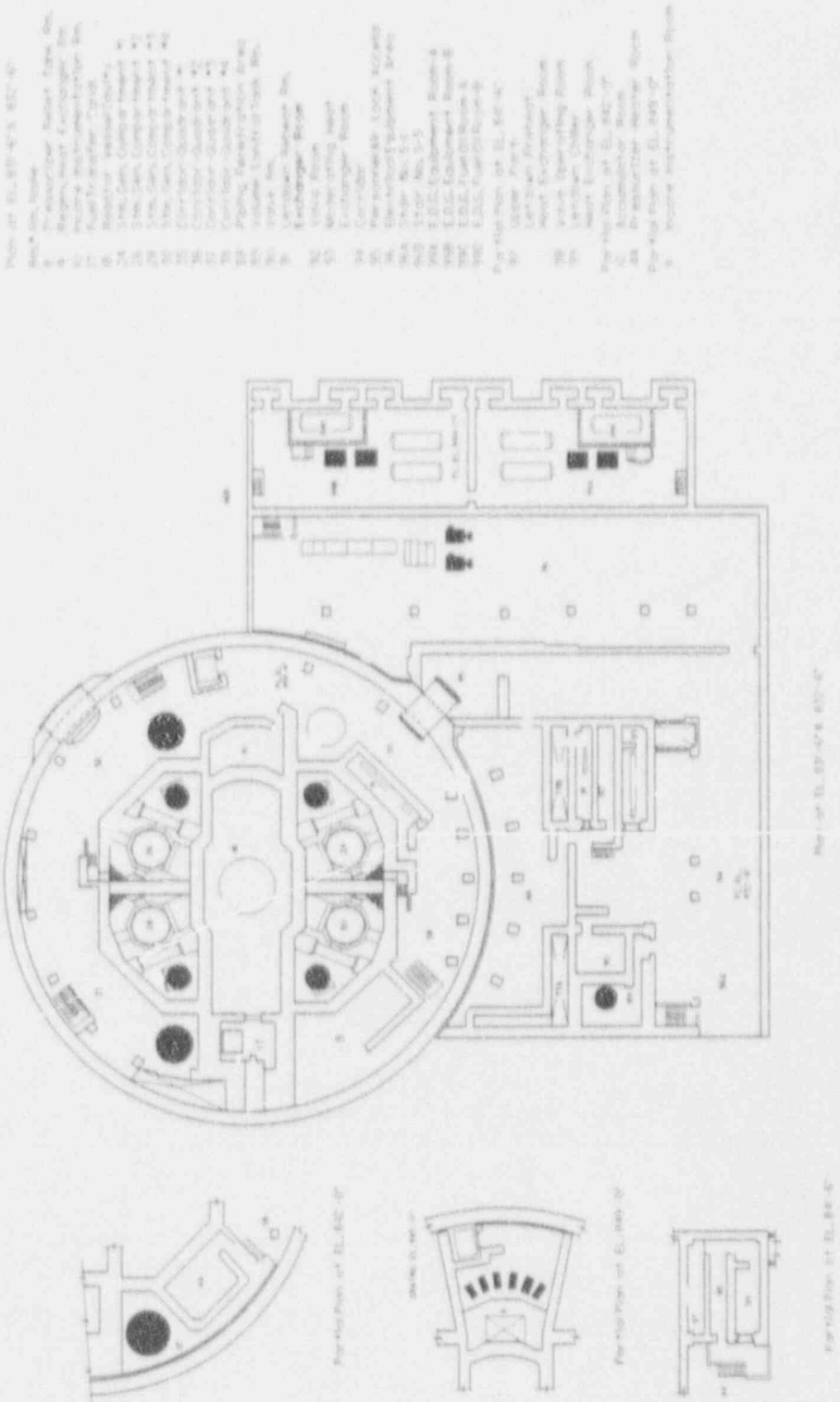

Figure 4.1-25.5: Containment and Safeguards Building Plans (El. 852)

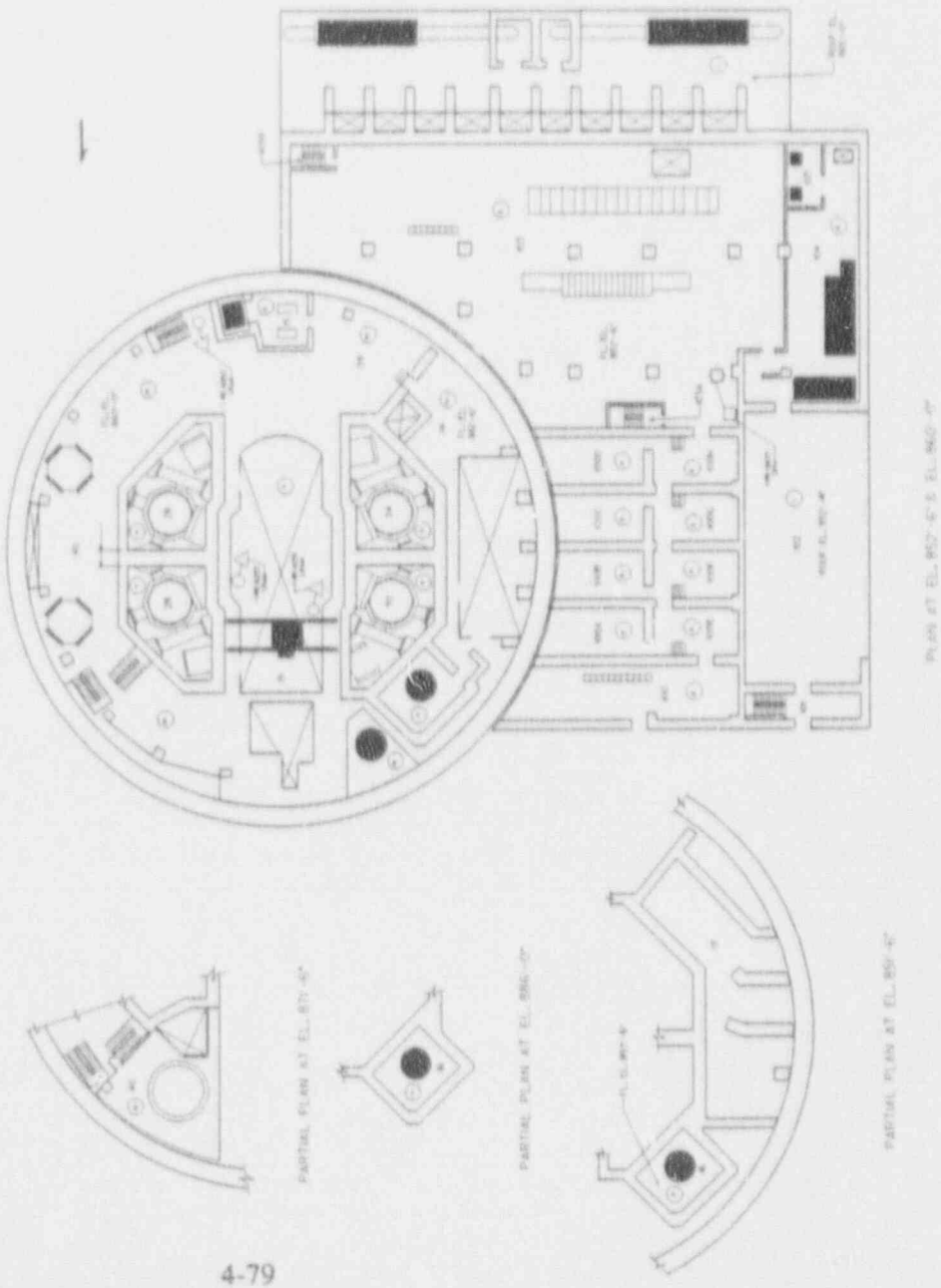

Figure 4.1-25.6: Containment and Safeguards Building Plans (Els. 873,880)

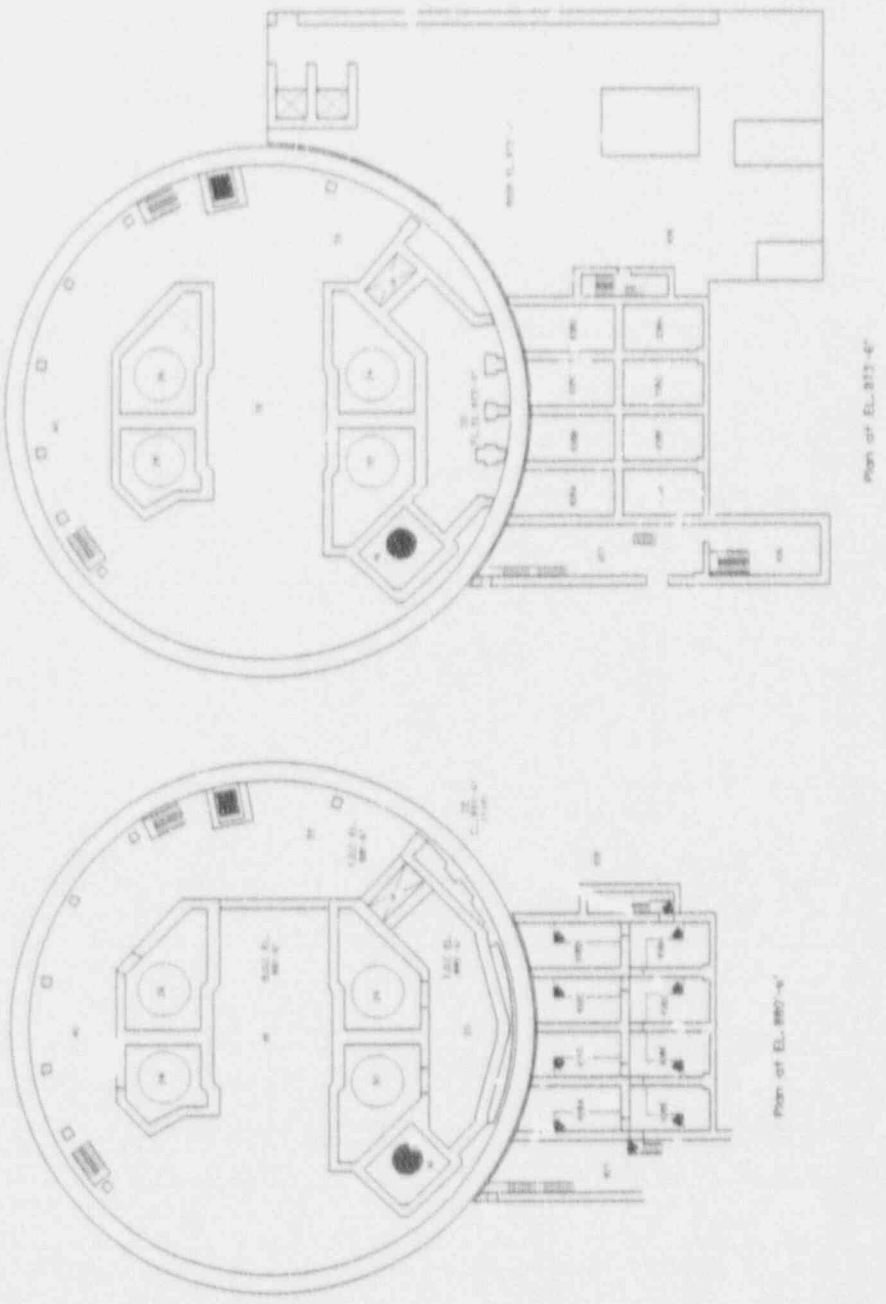

Figure 4.1-25.7: Containment and Safeguards Building Plans (El. 896,905)

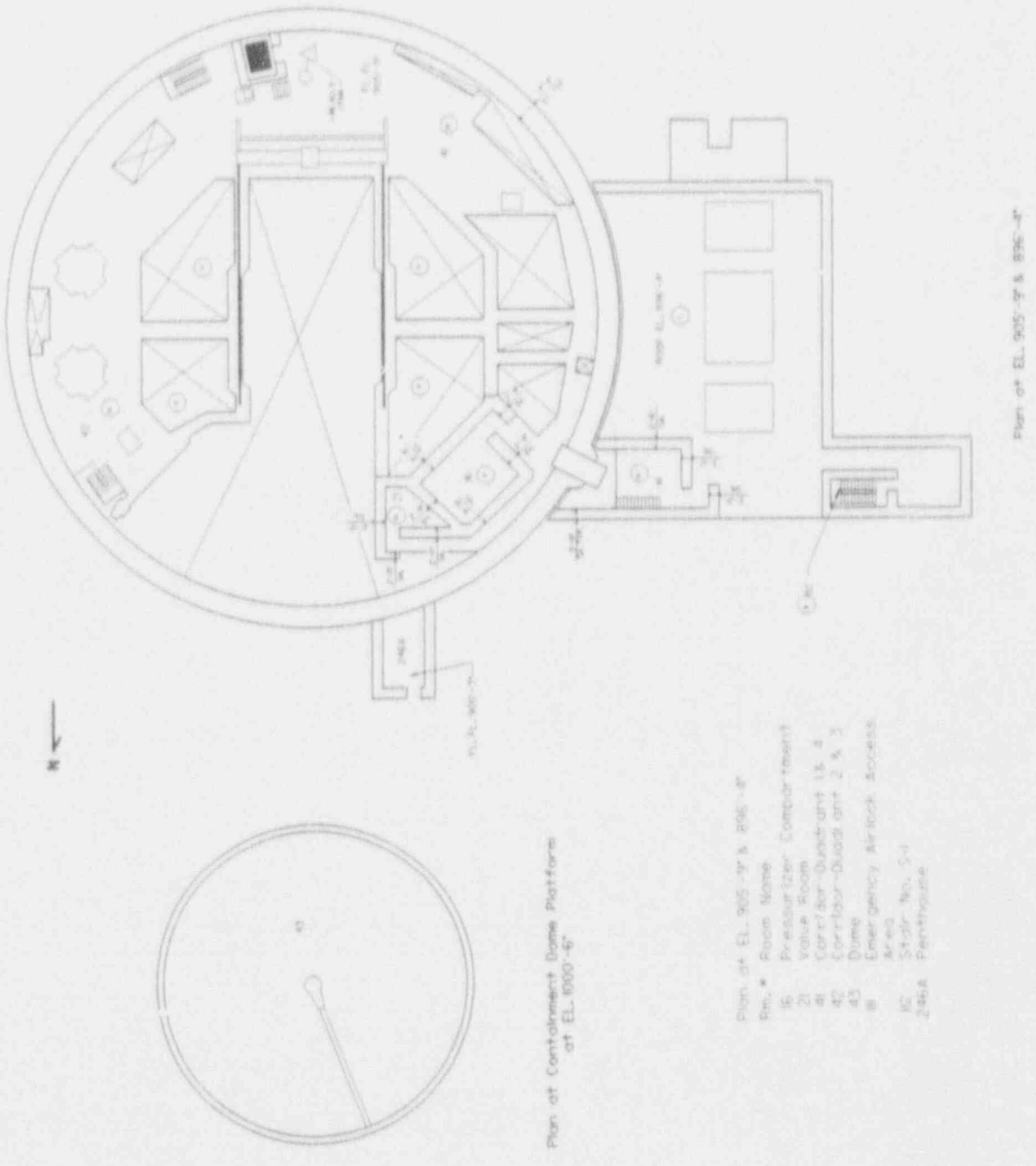

Figure 4.1-25.8: Containment and Safeguards Building Plans (El. 778,790)

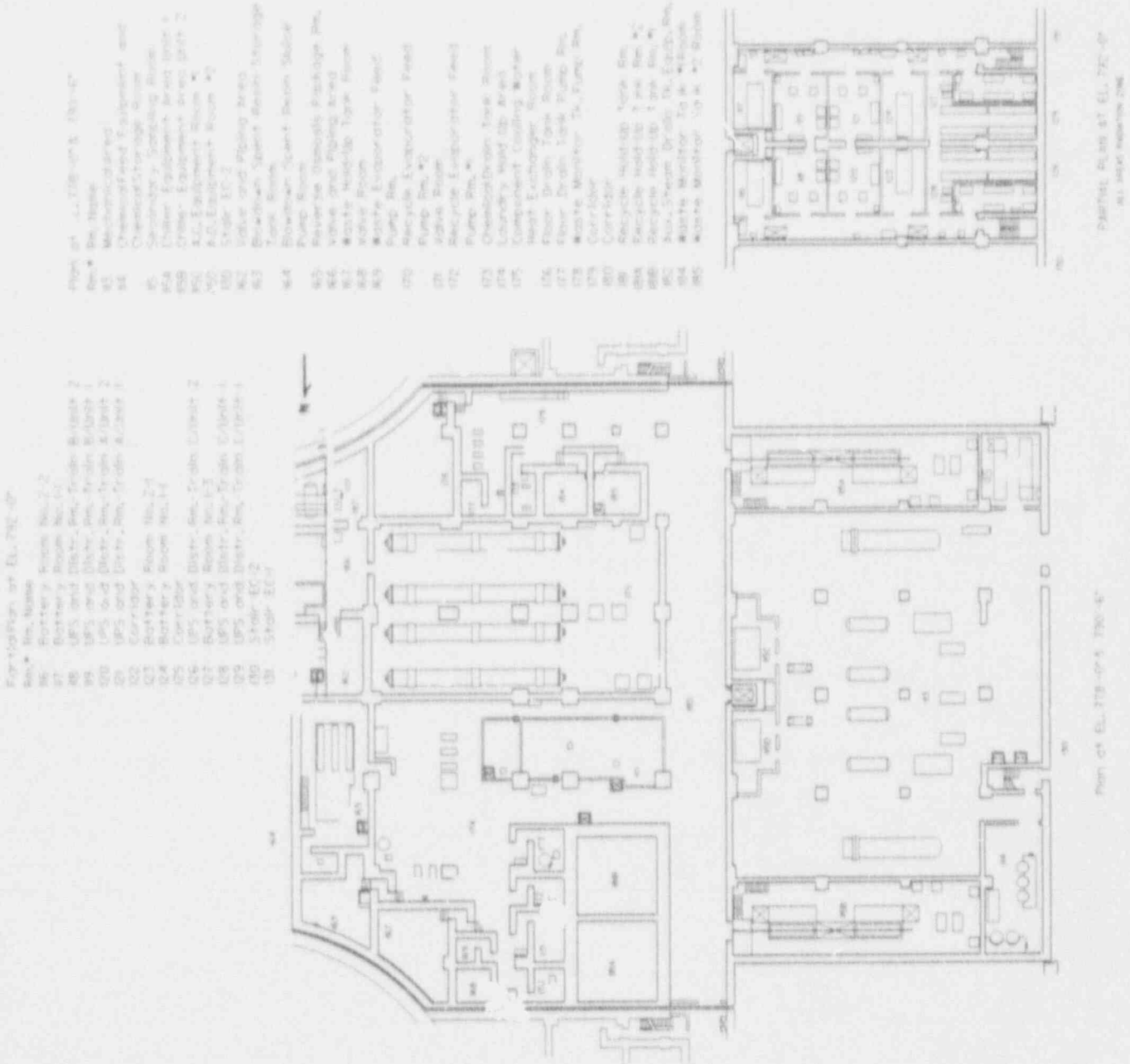

Figure 4.1-25.9: Auxiliary and Electrical Control Building Plans (Els. 807,810)

Figure 4.1-25.10. Auxiliary and Electrical Control Building Plans (El. 830)

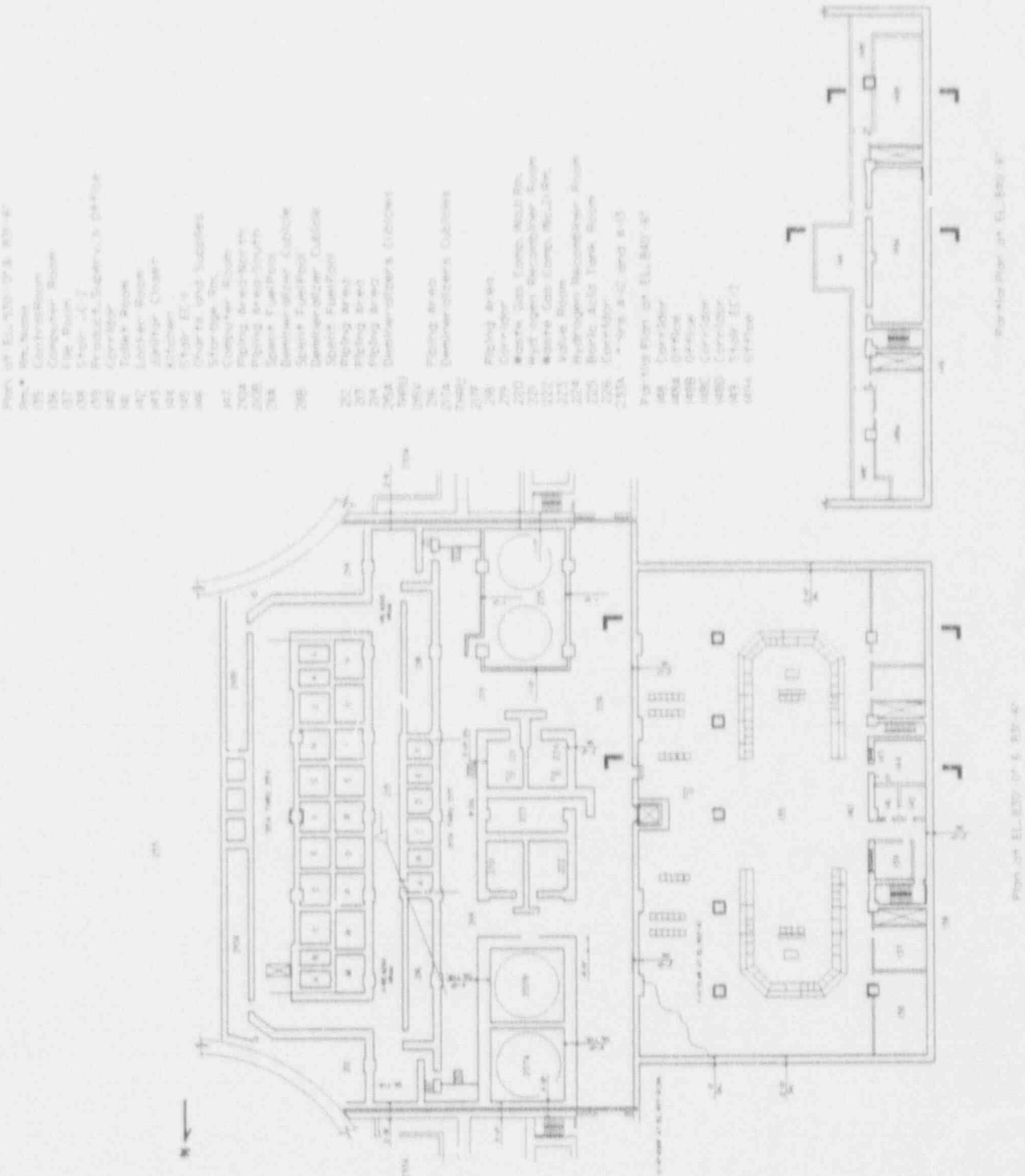

Figure 4.1-25.11: Auxiliary Building Plan (El. 842)

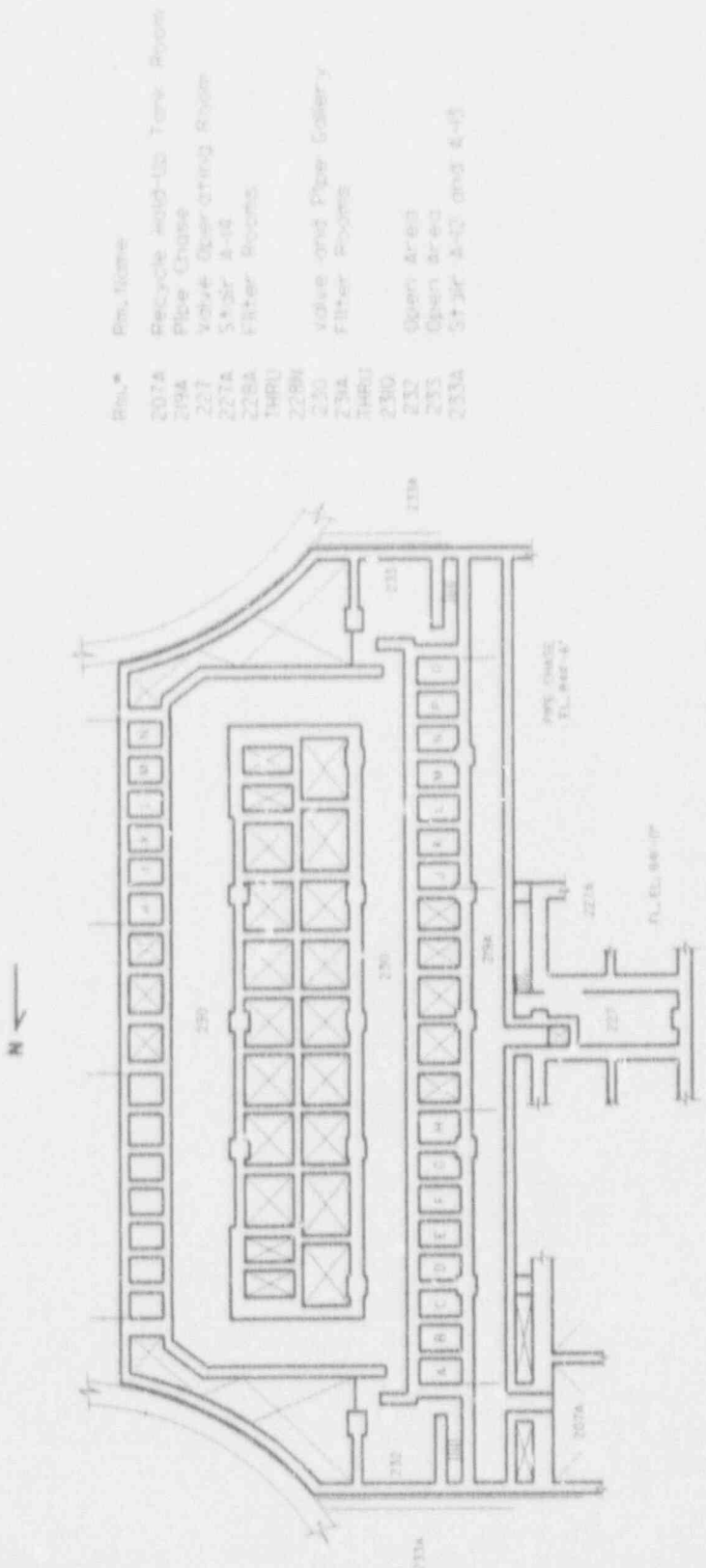

Figure 4.1-25.12: Auxiliary and Electrical Control Building Plans (El. 852)

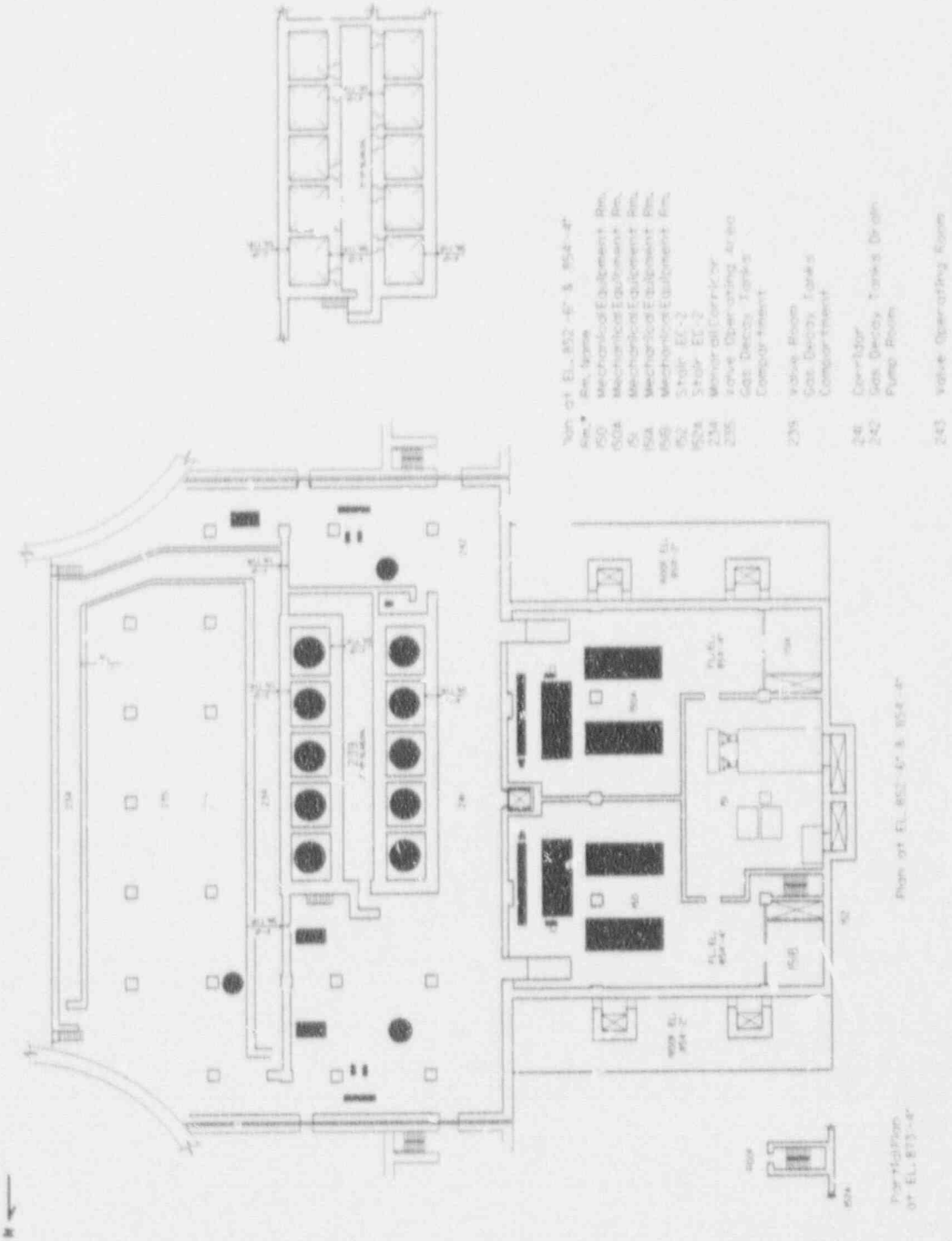

Figure 4.1-25.13: Auxiliary and Electrical Control Building Plans (Els. 873,886)

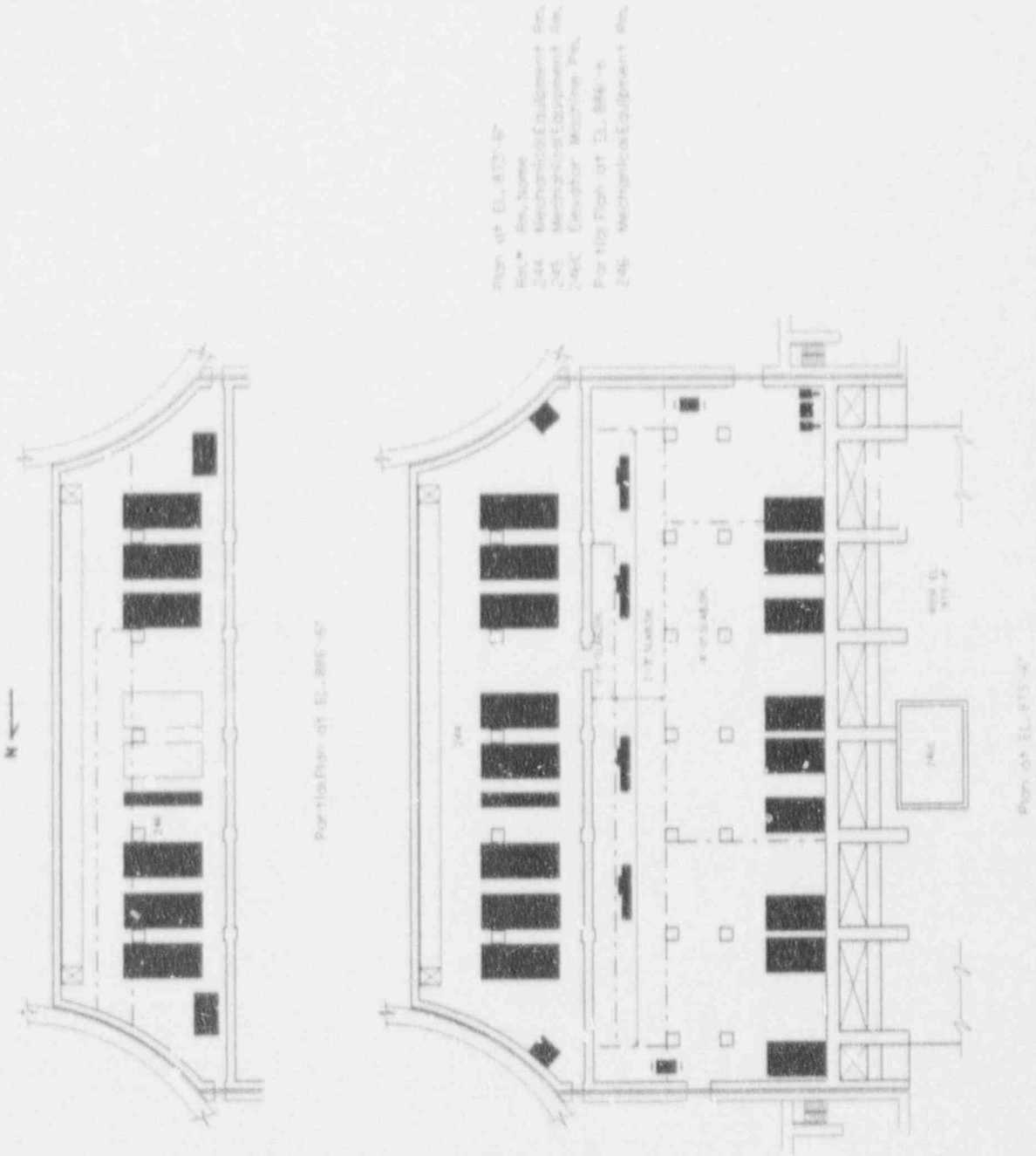

Figure 4.1-26.1: ECCS Valve Alignments (Standby)

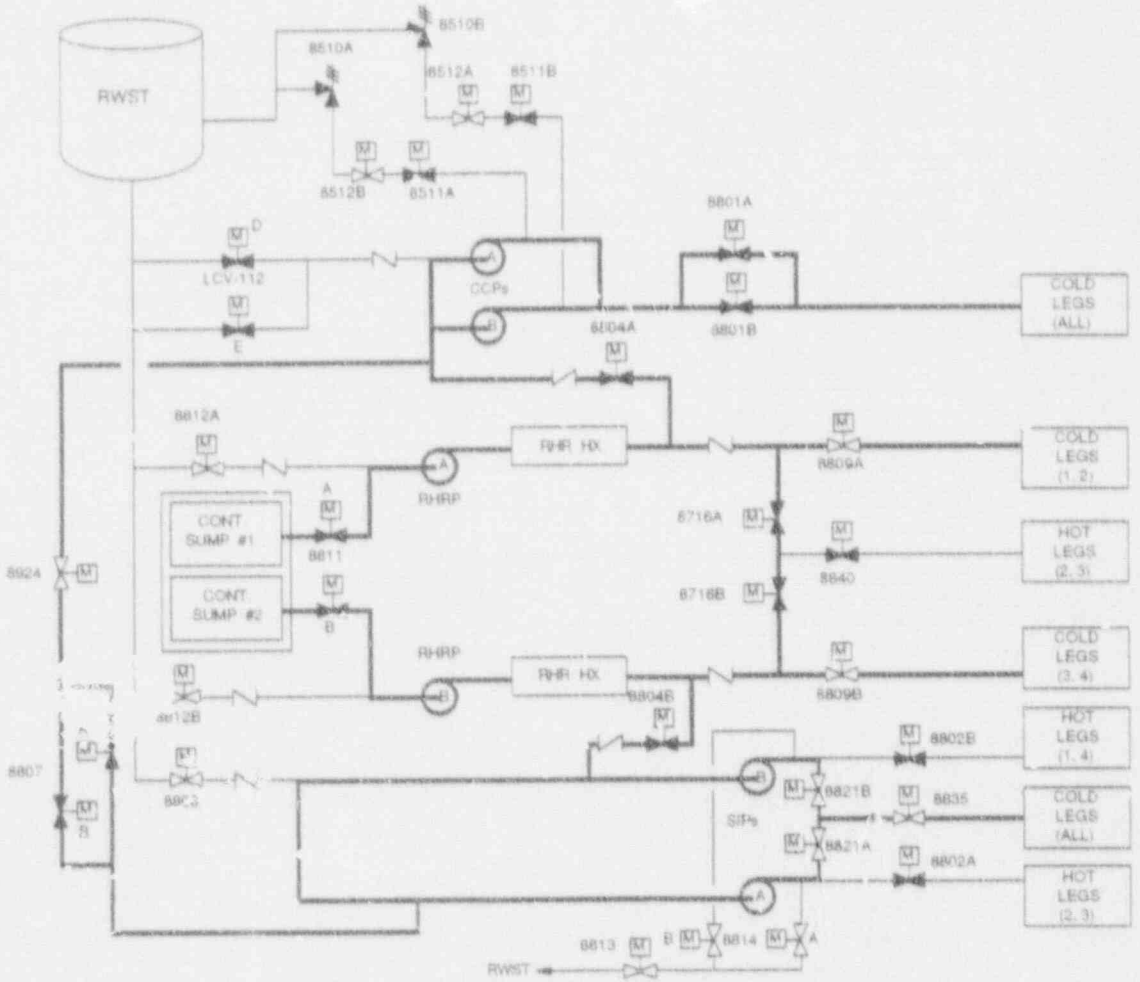

Figure 4.1-26.2: ECCS Valve Alignments (Injection)

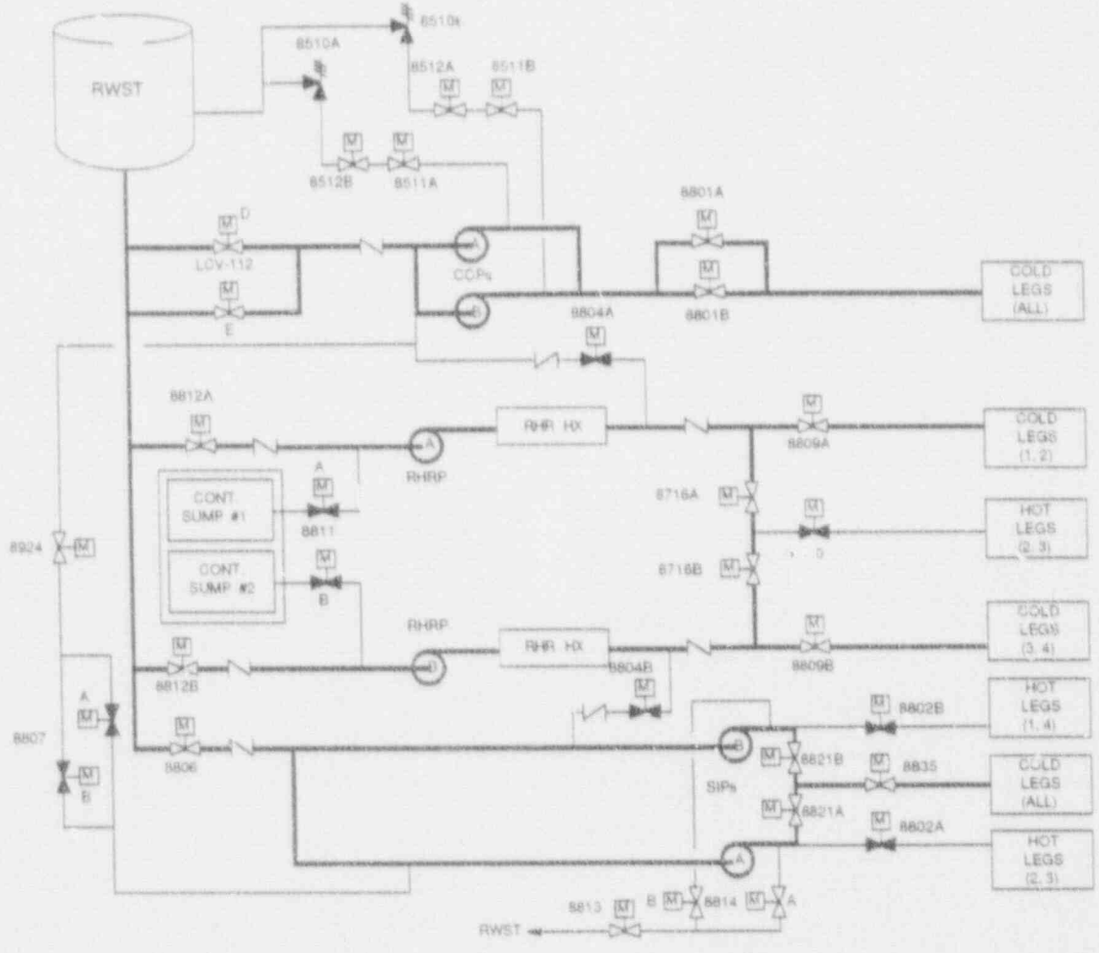

Figure 4.1-26.3: ECCS Valve Alignments (Cold Leg Recirculation)

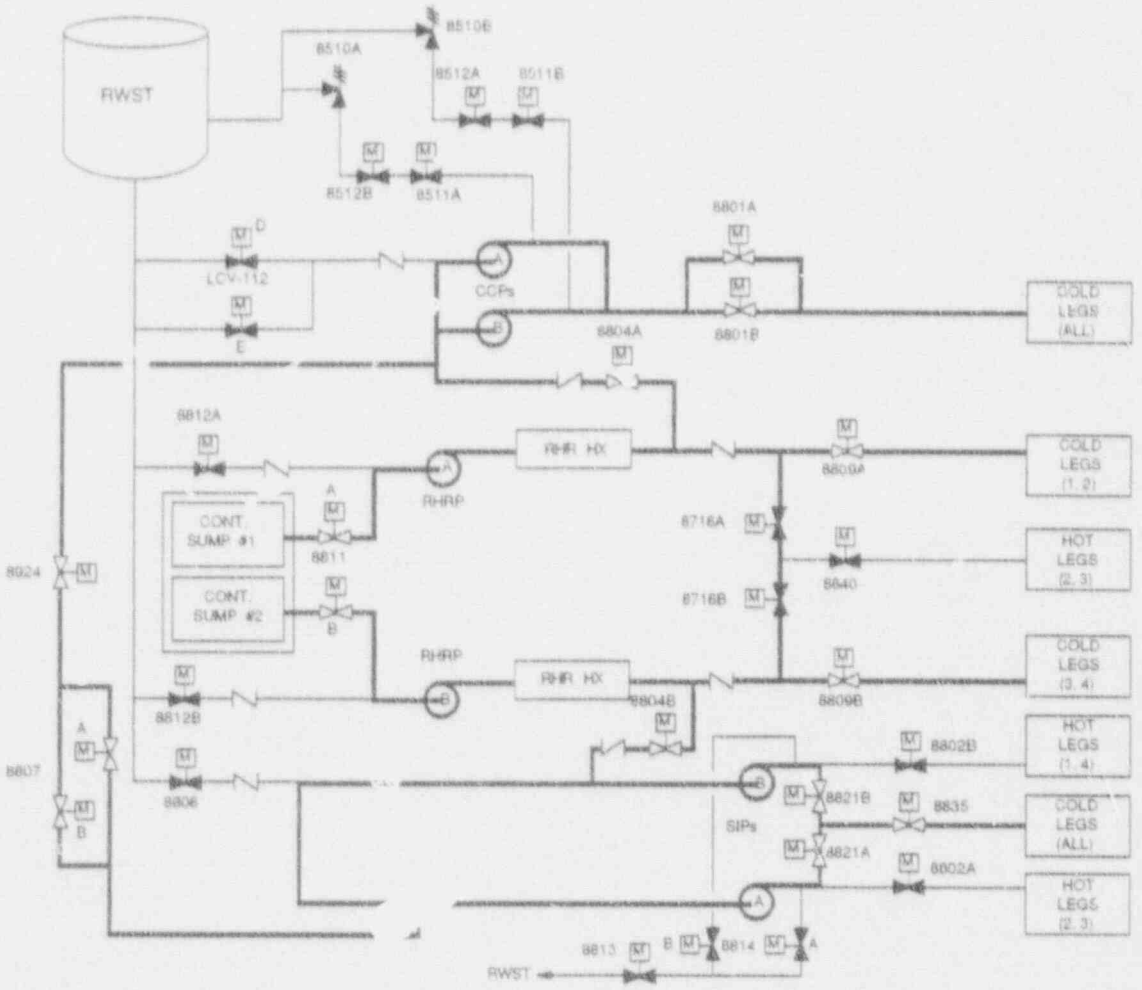

Figure 4.1-26.4: ECCS Valve Alignments (Hot Leg Recirculation)

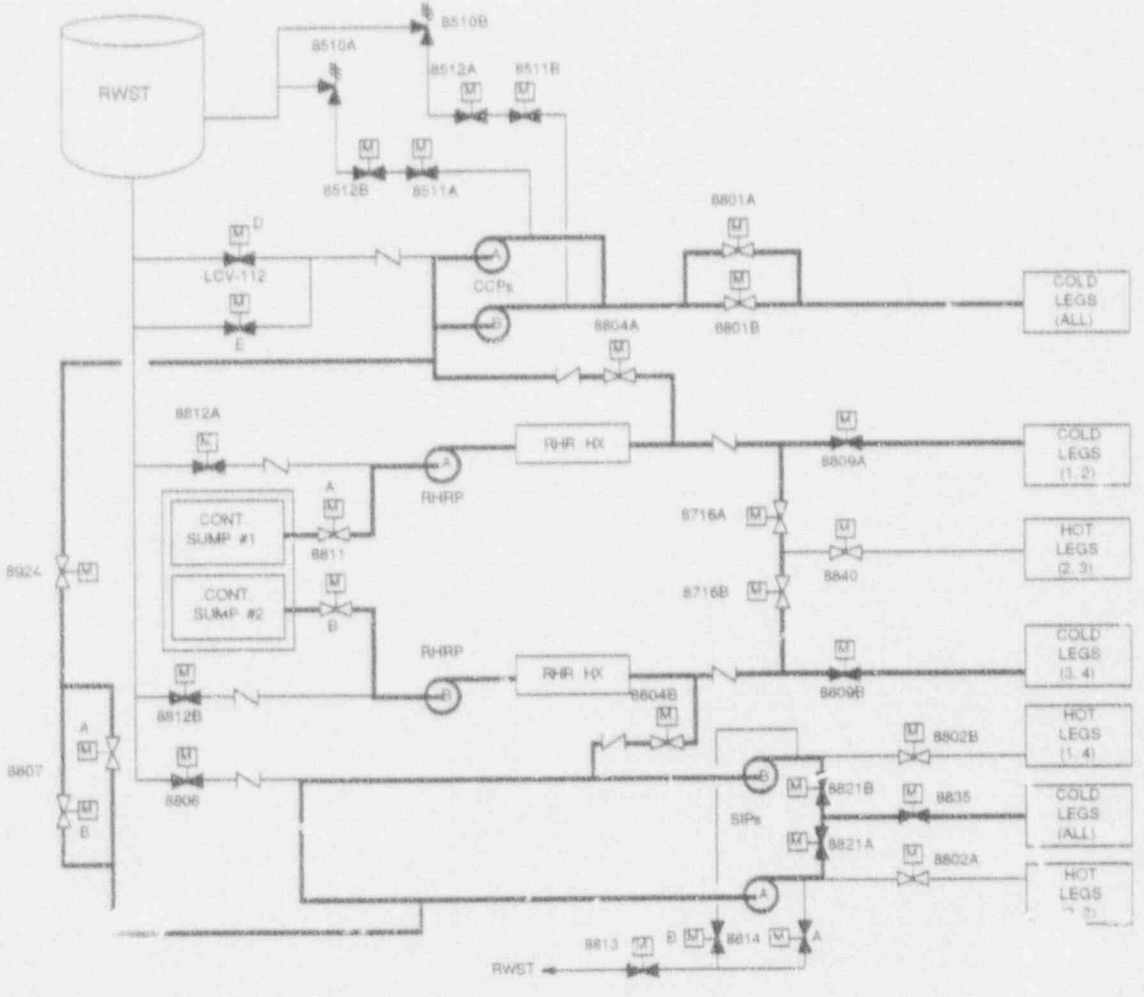

4.2 Plant Models and Methods for Physical Processes

The severe accident sequences relevant to the CPSES IPE were analyzed with the Modular Accident Analysis Program (MAAP 3.0B, Rev. 16). The MAAP code is an integrated analytical tool for the analysis of severe accidents. A detailed description of its methods for physical processes is available in Reference 10 and is not repeated here. The plant model utilized in MAAP for the CPSES IPE is an input to the code called a parameter file. The data used in the preparation of the parameter file is given in Section 4.1. The actual parameter file and the derivation of each value is provided in Reference 25.

Many complex physical processes are often modeled in MAAP with simple formulations. In addition, the code is capable of calculating the potential range of outcomes of these processes by varying certain parameter file constants. In cases where issue resolution has not been achieved pending further research, parameter values that lead to more severe consequences were selected. Furthermore, sensitivity studies were carried out as described in Section 4.6. These sensitivity studies address, among other things, the issues listed in Table A.5 of NUREG-1335 and take into consideration the EPRI (Ref. 33) guidelines for sensitivity studies for IPEs performed using MAAP.

MAAP calculations were used to quantify outcomes, but were never used to limit the number of possible outcomes. For example, with a cavity area of 70 m^2 and an overlying water pool, the debris bed is coolable using base-case MAAP parameters. In the present study, however, the issue of crust formation was recognized, and the non-coolable debris bed case was also calculated.

4.3 Bins and Plant Damage States

This Section summarizes the process and the results of the binning of the Level 1 functional sequences leading to core damage into Plant Damage States (PDS). A detailed description of the CPSES PDS formulation process is provided in Reference 27. Results of the binning processes are discussed in detail in Reference 7.

A PDS is defined as a group of core damage sequences that have similar characteristics with respect to the severe accident progression and containment response. The CPSES PDS result from combining core damage state attributes with containment safeguards systems status. The core damage states attributes and the containment safeguards status are described below:

CORE DAMAGE STATES:

Core Melt Timing

The time of core damage determines the decay power level and directly affects the rate of core damage and energy loads to the containment. It also affects the consequence assessment, i.e., the time of release of fission products to the environment. For the purpose of characterizing the time of release and potential off-site consequences, two time periods were considered:

Early: Within 3 hours from the time of shutdown. Results from unavailability of ECCS at injection and/or of AF, depending on the type of accident.

Late: Later than 3 hours. Usually occurs when ECCS fails in the recirculation stage following successful injection at the required flow rate.

RCS Pressure

The pressure of the RCS at the time of core damage affects the phenomenological events that can lead to containment challenges.

Low: These are pressures less than 200 psia. Direct Containment Heating (DCH) is assumed not to occur at these pressure levels. On the other hand, this is the situation where steam explosions leading to the alpha failure mode are given the highest probabilities.

High: These are pressure levels near the RCS operating pressure (defined here as more than 2000 psia) where HPME provides the highest loads to the containment and is examined closely. It is also the situation that can result in hot leg failure, pressurizer surge line failure, or induced steam generator tube ruptures. All of these are considered in the CET.

Medium: These are pressures in the 200 to 2000 psia range, where HPME loads to containment at vessel failure are reduced in comparison with the high pressure situation but still require investigation. All failure modes mentioned above are considered possible in this mode but have lower probabilities. Although this is a wide range, Level I results show that the range is populated almost exclusively by induced seal LOCAs of approximately 250 GPM/PMP (1" diameter-equivalent) leading to RCS pressures at vessel failure around 1000 psi.

CONTAINMENT STATES:

Containment Pressure Boundary Status

The containment status at the time of core damage affects the fission product release timing. The three cases considered are:

Intact: Normal containment leakage (0.1% volume/day)

Un-isolated: An air-to-air penetration is open.

Bypassed: The core damage release bypasses the containment as in a Steam Generator Tube Rupture sequence resulting in core damage or a V-sequence.

Containment Safeguards System Status

Containment Sprays

These provide substantial fission product mitigation and can preclude containment failure if operating in the recirculation mode. The conditions considered are:

- sprays operate in the injection mode,
- sprays inject successfully but fail during recirculation, and
- sprays are failed.

Fan-Coolers

Credit was not taken for fan coolers because they are normally shed on a safety injection signal and require an operator action that is not proceduralized to restore them. The potential benefits of the fan coolers are discussed in Section 4.1.2.1 and in Section 4.6.3.

PLANT DAMAGE STATES:

The CPSES PDS result from combining the core damage state attributes described earlier with the containment safeguards and/or isolation status. The PDS labeling is implemented by combining the Core Damage Bin number given in Table 4.3-1 with the Containment Safeguard Bin letter given in Table 4.3-2. Thus, each of the Core Damage Bins 1 through 6 results in three PDS when combined with Containment Safeguard Bins, e.g.: 1E, 1F, 1H. The station blackout (3SBO and 4SBO), the containment bypass (1CB and 2CB), and isolation failure (1CI) Core Damage Bins are not combined with Containment Safeguard Bins because those are implied by the core damage state.

The actual binning of Level I sequences is implemented in a two-step process. First, the accident sequence event trees for all the initiating events will eventually lead to a defined end-state, which is either a stable plant condition or one of the Core Damage Bins defined above. This is seen in Figures 3.1.2-1 through 3.1.3-6. Then, after all cutsets are binned into each sequence and Core Damage Bin (Table 4.3-1), they are further segregated according to their Containment Safeguard Bins (Table 4.3-2). The frequency result of the binning is shown in Table 4.3-3, where the columns are the PDS bins, with the first character defining the Core Damage Bin and the second the Containment Safeguard Bin. The selection of representative sequences for each bin is discussed in Section 4.6.

Table 4.3-1: Sequence Characteristics of Core Damage Bins

CORE DAMAGE BINS	SEQUENCE CHARACTERISTICS
1	Reactor Coolant System (RCS) breach with pressure and leakage rates associated with LOCAs of 0.6 to 2 inches in diameter (includes stuck open PORVs and larger seal LOCAs), with early melting of the core.
2	RCS breach with pressure and leakage rates associated with LOCAs of 0.6 to 2 inches in diameter, (includes stuck open PORVs and larger seal LOCAs), with late melting of the core.
3	High RCS pressure. Leakage rates associated with boil-off of the reactor coolant through cycling pressurizer relief valves (not stuck open) or small seal LOCAs up to 60 GPM/PM (0.6 inch diameter), with early melting of the core.
4	High RCS pressure and leakage rates associated with boiloff of the coolant through cycling relief valves (not stuck open) or small seal LOCAs up to 60 GPM/PM (0.6 inch diameter), with late melting of the core.
5	Large rates of leakage from the RCS and low pressures associated with LOCAs greater than 2 inches in diameter and failure of coolant injection, resulting in early melting of the core.
6	LOCA greater than 2 inches in diameter conditions, with failure of coolant recirculation and delayed melting.
$\underline{x}$CB	Bypass sequences ($\underline{x}$=1 interfacing LOCA, $\underline{x}$=2 SGTR) with failure of coolant make up.
1CI	Any core melt sequence where the containment is also unisolated.
$\underline{y}$SBO	Station Blackout sequences (or equivalent equipment failures), (y=3 early melt, y=4 late melt).

Table 4.3-2: Sequence Characteristics of Containment Safeguards Bins

CONTAINMENT SAFEGUARD BIN	FAN COOLERS	CONTAINMENT SPRAY
E	Failed	Injection only
F	Failed	Injection and recirculation
H	Failed	Failed

Table 4.3-3: Binning of Level I Functional Sequences into PDS

	1H	1E	1F	2H	2E	2F	3H	3E	3F	4H	4E	4F	5H	5E	5F	6H	6E	6F	7SBO	8SB	SGTR	CI Failure	V-Seq	Total
#ATCM1																1.1E-8		2.0E-6				5.0E-10	3.7E-9	2.05E-6
#ATCM2													2.1E-7		5.9E-7							2.0E-10	5.0E-9	8.08E-7
#ATCM1							4.2E-9		2.5E-8													7.3E-12		2.97E-8
#ATCM2									1.3E-8													3.6E-12		1.49E-8
#ATCM3									1.4E-6													3.5E-10		1.44E-6
#ATCM4																								
#ATCM5																								
#ATCM6									2.9E-6													7.2E-10		2.95E-6
#ATCM7																								
#ATCM8																								
#CVCM1												1.1E-8										2.7E-12		1.11E-8
#CVCM2							2.2E-7		5.3E-8													6.7E-11		2.74E-7
#MCM1													1.1E-7		2.3E-8							3.4E-11		1.38E-7
#MCM2																8.9E-7		4.7E-8				2.3E-10		9.36E-7
#SCM1				1.4E-7		2.1E-7																8.7E-11		3.55E-7
#SCM2	1.2E-5		2.4E-6																			3.6E-9		1.49E-5
#SCM2C3																								
#SCM2ER																								
#VSCM1										1.3E-8		1.0E-8										5.6E-12		2.28E-8
#VSCM2																								
#VSCM3							1.3E-7															3.8E-11		1.54E-7
#VSCM4										1.0E-6		4.1E-7										3.6E-10		1.46E-6
#VSCM5																				5.0E-7		1.2E-10		5.02E-7
#VSCM6																			1.8E-7			4.5E-11		1.85E-7
#MCM1																		9.4E-7				2.3E-10		9.39E-7
#MCM2															8.2E-8							2.0E-11	1.1E-8	9.32E-8
#RCM1																					3.4E-6			3.38E-6
#RCM2																								
#RCM3																					5.9E-9			5.88E-9
#RCM4																					9.6E-8			9.64E-8
#RCM5																								
#SCM1						1.5E-6																3.6E-10	9.9E-8	1.59E-6
#SCM2	2.6E-8		7E-7																			4.8E-11		1.97E-7
#T1CM1												3.9E-8										9.4E-12		3.85E-8
#T1CM2							2.2E-6																	2.19E-6
#T3CM1																								
#T3CM2																								
#T4CM1																								
#T4CM2							4.6E-8															1.1E-11		4.56E-8
#T6CM1												1.1E-8										2.8E-12		1.14E-8
#T6CM2							8.9E-7		1.8E-7													2.6E-10		1.06E-6
#VSCM1										3.2E-9		3.3E-6										8.0E-10		3.27E-6
#VSCM2																								
#VSCM3																								
#VSCM4										5.2E-8		4.2E-7										1.2E-10		4.74E-7
#VSCM5																								
#VSCM6																								
#X1CM1												1.0E-9										2.5E-13		1.01E-9
#X1CM2							4.4E-7		3.6E-7													2.0E-10		8.01E-7
#X2CM1												2.0E-7										5.0E-11		2.02E-7
#X2CM2							7.4E-9		3.1E-8													9.5E-12		3.89E-8
#X3CM1												2.8E-8										6.8E-12		2.78E-8
#X3CM2							1.9E-6		5.0E-9													4.7E-10		1.92E-6
#X4CM1												1.1E-8										2.8E-12		1.14E-8
#X4CM2							2.1E-8															5.2E-12		2.14E-8
#X5CM1																								
#X5CM2							2.2E-8															5.3E-12		2.17E-8
#X6CM1																								
#X6CM2							8.6E-7															2.1E-10		8.61E-7
#X7CM1																								
#X7CM2							2.9E-7															7.1E-11		2.92E-7
#X8CM1																								
#X8CM2																								
#XLCM1																		2.7E-7				6.5E-11		2.66E-7
#XLCM2																								
Total	1.3E-5		2.6E-6	1.4E-7		1.7E-6	7.1E-6		5.1E-6	1.1E-6		4.4E-6	3.3E-7		7.0E-7	9.0E-7		3.3E-6	1.8E-7	5.0E-7	3.5E-6	9.9E-9	1.2E-7	4.41E-5

4.4 Containment Failure Characterization

The first step in this task was to identify the possible CPSES containment failure modes from the point of view of the challenges. These are listed in Table 4.4-1. Each Plant Damage State (PDS) can lead to more than one outcome and, conversely, a failure mode can be due to various PDS, as indicated in Table 4.4-1. Although the unconditional probabilities for the various failure modes are listed in Table 4.4-1, they were actually determined in Section 4.6.

The second step in this task was to examine and summarize the possible ways by which the CPSES containment might fail to perform its function. The examination consisted of an analysis of penetrations and an evaluation of containment strength from the perspective of liner tear at discontinuities and from the perspective of ultimate strength.

Section 4.4.1 of this work provides an analysis of penetrations. These penetrations were grouped into four categories and compared to the penetrations that were examined in detail in an NRC-sponsored generic study (Ref. 11). This was done to check the structural stability and failure and leakage potential of the penetrations. The objective of this analysis was to demonstrate that the CPSES penetrations are similar to those that are used throughout the industry and that the conclusion of the generic study, that failure at penetrations is not expected, also holds for CPSES.

Section 4.4.2 examines the containment strength from the point of view of rupture. That is, it attempts to estimate the pressure at which gross failure is most likely to occur. This was done using the rupture to design pressure scaling method of Reference 17. The result was compared to existing finite element analysis results for similar containments and was shown to be conservative.

Section 4.4.3 examines containment failure from the point of view of liner tear. An approximate methodology developed by EPRI was used to determine leakage onset due to liner tear at penetrations. The approximate methodology (Ref. 13) makes use of experimental test results of peak strains applicable for steel-lined concrete containments. It also requires an assessment of the global strains imposed on the containment. This was done using results obtained from detailed structural analyses of a containment of similar design.

In Section 4.4.4, a containment fragility curve was developed by assuming a normal distribution for the failure pressure, a 7% coefficient of variation and a mean equal to the lowest of the failure pressures determined above.

4.4.1 Penetrations

As with any other large dry PWR containment, the CPSES containment penetrations were divided into the four categories considered in Reference 11: (1) Large Opening Penetrations, (2) Purge and Vent System Isolation Valves, (3) Piping Penetrations and (4) Electrical Penetration Assemblies.

4.4.1.1 Large Opening Penetrations

There are four of these in the CPSES containment structure: (1) personnel airlock, (2) emergency airlock (3) equipment hatch and (4) fuel transfer tube. All are shown in Figures 4.1-23.4 through 23.6.

Personnel Airlock

The personnel airlock is a double door assembly approximately 9 feet in diameter located at the 832' elevation of the containment. Each door is hinged and double-gasketed, with the leakage test pressure applied to the annulus between the gasket sealing surfaces. Both doors are interlocked such that if one door is open, the other cannot be activated. The doors are designed to maintain their functional capability during testing with no additional requirements for locking beyond the normal locking procedure. The double lock mechanism minimizes the potential for isolation failure during normal operation. The personnel airlock, which is shown in detail in Figure 4.1-23.5, is essentially the same as that shown in Figure 9 of Reference 11 and is similar to that of the Surry plant. The analysis of Appendix C of Reference 11 is appropriate for obtaining an upper bound on the flange separation under internal pressurization for this airlock. Based on the relative similarity between the example airlock and the CPSES airlock and the similar sizes of the containment, it was assumed that these separations are also representative for CPSES. The leak area corresponding to this separation was calculated for the CPSES 9 ft diameter airlock and is given below as a function of pressure.

CONTAINMENT PRESSURE (psig)	FLANGE SEPARATION (in.)	LEAK AREA (in.2)
30	0.00017	0.06
44	0.00024	0.08
100	0.00049	0.17
119	0.00057	0.19

It should be noted that this analysis assumes that the inner door is open or failed and the full containment pressure is placed on the outer door. It does not credit the seal which is fully compressed when the door is locked, nor does it credit the pressure-seating of the inner door or the equipment hatch described below. Elastometer seal tests discussed in Appendix A of Reference 11 revealed that flange separation resulting from extremes of severe accident related pressures is not likely to be the source of significant containment leakage. In fact, for all materials and configurations tested, no leakage was observed for flange separations up to 0.06in. and temperatures up to 420°F, which corresponds to the highest temperatures expected at CPSES for dry sequences. This is a bulky structure with a large thermal inertia. Therefore, it is not expected that non-uniform thermal environments or sudden temperature spikes, such as those associated with burns, would challenge its integrity.

Therefore, given the small leakage area associated with these penetrations, even when improbable assumptions are made for their maximization, leaks from these penetrations were not credited in the analyses of containment failure times, nor were they assumed to fail at pressures lower than those discussed in Sections 4.4.2 and 4.4.3.

Emergency Airlock

The emergency airlock is a 5 ft 9 in. diameter double door assembly, with 2 ft 6 in. diameter doors. It has operating features similar to the personnel airlock. The interlocking mechanism prevents both doors in either personnel or emergency airlocks from being opened simultaneously and ensures that one door is completely closed before the opposite door can be opened. Since both doors are pressure-seating, the discussion of equipment hatches below applies.

Equipment Hatch

The equipment hatch is shown in Figure 4.1-23.4. It is a 16 feet internal diameter single closure penetration. The bolted hatch cover is mounted on the inside of the containment and is double-gasketed with a leakage test tap between gaskets. It is essentially the same as the pressure-seating design shown in Figure 6 of Reference 11. The discussion on analysis methods for pressure-seating closures in Section 2.2.2 of Reference 11 is primarily a verification for buckling stability beyond the ultimate pressure capacity of the containment, since it is felt that otherwise these hatches will not leak. An extensive non-linear analysis of Sequoya's equipment hatch was performed by Ames Laboratory to evaluate all pressure seating aspects of that pressure-seating hatch. The results of that analysis were judged in Reference 11 to indicate that leakage is not likely for this type of closure, nor is buckling of the hatch below containment ultimate pressure capacity likely to occur. Hand calculations were performed to check the structural stability for Sequoya's hatch which is similar to that of CPSES, and the buckling limit is felt to be applicable to CPSES. This hand calculation method in Appendix F of Reference 11 showed the probable actual minimum buckling to be around 150 psig for the Sequoya hatch, which is well above gross containment failure pressure (for CPSES - 136 psig, Section 4.4.2).

Fuel Transfer Tube

As shown in Figure 4.1-23.6, the fuel transfer tube is a 20 in. diameter stainless steel pipe inside a carbon steel sleeve extending from the reactor refueling cavity through the reactor cavity wall, containment wall and fuel building wall. The fuel transfer tube (FTT) is sealed on the containment side by a blind flange and on the fuel building side by a closure valve. The FTT is supported by anchors on the refueling cavity floor and the fuel building pool floor. For a leak to occur between the FTT and its penetration sleeve, the leak must penetrate a belows on the containment side, the seal plate and a belows on the outside of the containment. The CPSES FTT is similar to that analyzed in Appendix F of Reference 11. That analysis has found that the FTT and closure assembly should not leak for the following reasons:

- Rising containment pressure increases sealing force
- Hydrostatic pressure increases sealing force
- Volumetric swell of o-rings from fluid environment increases sealing effectiveness

4.4.1.2 Purge and Vent System Isolation Valves

Four penetrations are in this category: (1) hydrogen purge supply and (2) exhaust, and (3) containment purge air supply and (4) exhaust. These are the only penetrations vented to the containment atmosphere, although the containment purge air line is opened once a week for three hours during normal operation as a part of the normal ventilation program.

The containment purge air lines are 48 in. diameter butterfly valves and the hydrogen purge lines are 12 in. diameter butterfly valves.

Reference 11 considers these butterfly valves associated with large diameter pipes as having the greatest potential for containment leakage. This is because these valves use non-metallic seals, whereas other isolation valves, such as gate, globe and check valves, use a metal-to-metal seals. Since these valves are designed to the ASME Code, they are capable of maintaining their structural integrity under severe accident conditions. The main concern is that the non-metallic seals between the body and disc might become degraded when subjected to the high pressures and temperatures associated with severe accident conditions.

Figure 4.4-5 shows seal life as a function of time for various materials and temperatures. The materials used for pressure seals at CPSES are all silicone based (Ref. 14). It is evident from the figure that significant purge leakage is not expected for CPSES because silicone based seals show excellent temperature resistance (over 1000 hrs at 400°F). The maximum calculated temperatures for dry sequences (Refs. 2,7) are of that order (420°F).

4.4.1.3 Piping Penetrations

Eight different types of penetrations were analyzed for the six reference plants of Reference 10. The CPSES penetrations are of three types, all of which are similar to the types analyzed in Reference 11.

The first type is an embedded pipe penetration that is used at CPSES for cold pipes. It is shown in Figure 4.1-23.7 and is essentially the same as that shown in Figure 18 of Reference 11. At CPSES there is a sleeve around the process pipe, with an inner diameter slightly greater than the process pipe's outer

diameter. Gusset plates or lugs are welded to the sleeve for improved load transfer to the concrete wall. The pipe is connected to the containment liner through a plate of greater thickness than the liner.

The second type used at CPSES for hot piping is the flued head type of penetration, also shown in Figure 4.1-23.7 and in Figure 20 of Reference 11. The term flued head designates the manner in which the process pipe is attached to the sleeve. This is essentially a forged piece with integral welding attachment points for sleeve and process piping.

The third type of penetration used at CPSES for hot and cold piping penetrations running close to one another is the flanged penetration shown in Figure 4.1-23.7 and in Figure 19 of Reference 11. The term also refers to the attachment between the sleeve and the process pipe. The sleeve is also embedded in the concrete with anchor lugs attached to the sleeve.

Two types of loading should be considered for all the types of piping penetrations. The first is the effect of differential pressure across the penetration. This is the same type of loading considered for the large opening penetrations. The second type is unique to piping penetrations. Deflections of the containment wall occur during severe accidents because of the internal pressure and because the containment experiences thermal expansion due to accident temperatures. Piping that passes through the containment is typically attached to structures both interior and exterior to the containment as well as to those of the containment itself. The resulting differential support displacement induces loads in the piping and the penetration.

Both types of loading were evaluated in Reference 11 and the findings were judged to apply to CPSES, based on the similarity of pipe types, layouts and materials used for Westinghouse PWRs in large dry containments. The effect of differential pressure was evaluated using hand calculations. The evaluation of the displacement loading in Reference 11 was complex and very detailed. Nevertheless, the findings were that for all types of piping penetrations examined for all plants, a failure in the piping penetrations was not likely before the containment approached instability, which is past the gross failure point defined as 1% strain (for CPSES 136 psig, Section 4.4.2).

On the basis of the results of these studies, it was concluded that the piping penetrations and associated piping were not likely to contribute to leakage before reaching the containment rupture limit discussed in Section 4.4.2 of this work.

4.4.1.4 Electric Penetration Assemblies

A typical electrical penetration consists of a metal pipe passing through the containment wall. Inside this pipe is a stainless steel canister containing electrical cables, as shown in Figure 4.1-23.6. The canister is welded on the inside and outside ends to the pipe. The welds form an hermetic barrier. The cables are passed through the stainless steel header plates located on both sides of the canister. The electrical conductors passing through these plates are sealed. These seals form critical elements of the penetration. Only one side of the penetration would be exposed to high temperatures and harsh environment. The projecting portion of the pipe could pick up a significant amount of thermal energy by radiation and convection and its temperature could rise significantly. However, Reference 11 concludes that even if the inboard seals fail on the inboard side of the penetration, the outboard seals will protect the penetration from leakage. As discussed in Reference 15, thermal energy transfer through the canister is low and outboard seals will never reach high temperature.

4.4.2 Containment Rupture (Gross Failure) Limit

The containment rupture limit is the pressure at which gross failure of the containment structure leading to a puff release is most likely. The Comanche Peak containment is designed to be essentially leak-tight under design pressure conditions. It is a steel-lined, reinforced concrete vessel with a design pressure of 50 psig. The ultimate pressure capacity of the cylindrical wall, rounded dome and thick basemat configuration of typical containment structures has been extensively studied (Refs. 16,17,18,19,20). Similar containments have demonstrated structural failure limits in the range of 2.1 to 3.5 times the design pressure for reinforced concrete, as illustrated in Table 4.4-2. This is a CPSES equivalent of 105 to 175 psig.

Since the radius to thickness ratio (67.5:4.6) is compatible with thin shell theory, primary internal stresses due to pressure consist of membrane meridional and hoop stresses. The meridional and hoop forces generated by the internal pressure load may be calculated as a statically determinate problem (Refs. 17,19) in which the hoop stress in the cylinder is equal to the product of the pressure and the radius divided by thickness. The results of these calculations have been compared with refined finite element analyses of the containment structure and found to be in good agreement (Refs. 16,17).

Therefore, based on the analysis of a similar structure (Ref. 17) using the containment analysis techniques of References 19 and 21 the pressure ratios at yield (Ref. 17) can be estimated by:

$$\frac{P}{P_d} = \frac{f_{ry}\ A_r}{R_i\ P_d} + \frac{f_{ly}\ A_l}{R_i\ P_d}$$

where:

P = Internal pressure

P_d = Design pressure

R_i = Containment inside radius

f_{ry} = Rebar yield strength at 1% strain

A_l = Liner steel areas per unit of wall thickness

A_r = Rebar steel area per unit of wall thickness

f_{ly} = Liner yield strength at 1% strain

Note that the above expression implies the failure pressure is assumed as that corresponding to a global stress state at the 1% strain level at the cylindrical wall and the dome. WASH-1400 used this conservative definition of failure criterion for reactor containments, and it remains an important measure of strength that can be related to the design pressure.

For the Comanche Peak containment:

P_d = 50 psig = 7.2ksf

R_i = 67.5 ft.

f_{ry} = 60 ksi

f_{ly} = 60 ksi

For the cylindrical wall, the following areas are used:

A_r = 17.46 in^2/ft.

A_l = 4.5 in^2/ft.

Similarly, for the dome,

A_r = 17.46 in^2/ft.

A_l = 6 in^2/ft.

Substituting the most conservative of these numerical values yields:

$$\frac{P}{P_d} = \frac{60.0\ (17.46)}{67.5\ (7.2)} + \frac{60.0\ (4.5)}{67.5\ (7.2)}$$

$$\frac{P}{P_d} = 2.71$$

$$P = (50)(2.71) = 136 \text{ psig}$$

The sources of each value are:

f_{ry} Yield strength value taken from the specifications under the jurisdiction of ASTM Committee A-1 on Steel, Stainless Steel and Related Alloys (Annual Book of ASTM Standards, Vol. 01.03). The containment reinforcing steel is ASTM A 516-72 grade 60.

f_{ly} Yield strength taken from the ASTM specification SA-537/SA-537M-86 for pressure vessel plates, heat treated carbon manganese silicon steel ASME SA 573-74 Class 2.

A_l The area for the containment liner is based on a 3/8 inch thick plate in the wall and 1/2 inch thick plate in the dome.

A_r The reinforcing steel area for the vertical rebars is based on three layers of #18 bars at 10 5/8 inches, and for the horizontal (hoop) rebars, on four layers of #18 bars at 11 inches. Two layers of diagonal rebars are also #18 bars at an angle of 45 degrees. These represent the minimum specifications contained in Drawings 2323-S1-501 through 509. Variations in the spacing of the vertical and horizontal reinforcements with elevation are indicated in the drawings. The values selected above represent the minimum areas at elevation 856'.

The calculated structural failure limit pressure, assuming 1% uniform strain limit in the cylindrical wall, falls within the range of 105 to 175 psig (2.1 - 3.5 times the design pressure). Specifically, the value of 136 psig is 2.71 times the design pressure and is comparable to other large, dry, reinforced concrete containments with steel liner as indicated in Table 4.4-2.

4.4.3 Containment Liner Ductile Failure Limit

Recent experiments indicate that the dominant mode of failure for steel-lined, reinforced concrete domed structures is steel liner tearing and leakage. The onset of localized liner tearing has been shown to occur at pressure levels greater than the design pressure but lower than those needed to reach the ultimate strength of the containment.

Methods for determining the onset of liner tearing, and the subsequent formation of leak pathways, have been developed in Reference 13. The correlation of test data and analysis results presented in that document are the result of a five-year research program for developing a test-validated methodology for predicting the overpressure behavior of concrete containments.

Tests on individual containment segments and a 1:6 scale concrete containment were conducted by Construction Technology Laboratory (CTL) under contract to EPRI and by Sandia National Laboratory under contract to USNRC. The former simulate local conditions in various parts of the containment under overpressure loading. The latter involved internal pressures up to 145 psig, at which point the leakage rate became excessive and the test was terminated. Both segment tests and reduced model test demonstrated the leakage mode of failure. Analysis results were correlated with the tests, and methods were developed to determine the liner strain state at local discontinuities from global strain levels obtained from a basic 2-D axisymetric finite element analysis of the containment (Ref. 13). Peak strain magnification factors for each "type" of discontinuity were determined for the pressure range of interest and combined with the associated global strains to yield a peak liner strain versus pressure curve around each discontinuity type considered. Uniaxial ductility tests of liner materials commonly used in reactor containment construction were conducted to determine the ductile failure strain level of the materials.

4.4.3.1 Description of the Method

The criteria and guidelines set forth in Reference 13 are applicable to either prestressed or reinforced concrete containments. These guidelines provide an experimentally verified methodology for obtaining peak strains at typical steel containment liner stiffness discontinuities. These regions are subject to ductile liner failure and are identified as typical leak sites. The regions are:

- Cylinder wall-skirt juncture;
- Main steam/medium sized penetration (24 to 60 in. diameter);
- Equipment and personnel hatches (> 60 in. diameter);
- Springline (dome-cylinder juncture); and
- General liner embedments (at cylinder base, midheight and springline regions).

These are also the regions that were considered in the analysis of the Comanche Peak containment.

Figure 4.4-1 illustrates how the method is used to determine the onset of liner tear. Liner tear (initiation of leakage) is predicted to occur at the pressure and location where the peak strain in the liner meets or exceeds the uniaxial failure strain level. The criteria assumes that liner tear, once initiated, will progress in a stable, incremental manner until an equilibrium leakage rate is permitted. While it is recognized that additional pressure is required to propagate the initial tearing, leakage failure pressure is defined in this analysis to be the pressure at which onset of tearing is predicted. Therefore, it is conservative to assume that once tearing is initiated, failure of the containment occurs.

The peak strains in the containment liner that occur adjacent to discontinuities are the product of a calculated global strain value at the specific discontinuity and the corresponding strain magnification factors. These are:

Alpha Factor - Experimental work and very detailed calculations through the years have shown that, even with closely spaced strain measurements or relatively fine computational grids, localized liner strain concentrations next to stiffness discontinuities are sharper, more localized, and have higher peaks than what are measured or calculated. This magnification factor has been named the strain localization factor or gage length factor (alpha). Not enough experimental data is available to develop a functional

dependence for alpha. Consequently, an alpha is introduced in the guidelines for predicting containment, leakage as a constant magnification factor with an experimentally determined average value of 4.0.

K Factor - K produces peak effective plastic strain following global liner yielding and is defined as the peak effective strain to global strain ratio at a specific location. K factors have been derived from test and analytical data for each of the discontinuity types and are provided as curves of K vs. normalized strain. These are illustrated for reinforced and prestressed containments in Reference 13 for each of the types discontinuity of interest.

Beta Factor - Beta is a stress biaxiality factor applied to represent the effect on ductility of the liner stress state. Over most of the cylinder wall, the hoop stress to meridional stress ratio is approximately 2 to 1 in the elastic stress range. The ratio decreases after the onset of plasticity and the biaxiality effect becomes stronger and more variable. The biaxiality conditions have been determined for all of the discontinuity types of interest and are provided in Reference 13 as curves of beta vs. normalized pressure. Since biaxiality effects are typically characterized as a reduction in ductility, the strain magnification approach in the criteria requires that the reciprocal of the ductility ratio be used to represent beta:

$$\text{beta} = 1/\text{ductility ratio} \quad (1.0 \leq \text{beta} \leq 2.0)$$

Beta is determined from the curves in the reference document and is multiplied, along with alpha and K by the calculated global strains to obtain the peak local strains for comparison to the uniaxial failure strain for each discontinuity type at each pressure level, as illustrated in Figure 4.4-1.
The global strains are defined for each discontinuity type as follows:

Discontinuity	Global Strain
Wall-Basement Juncture	Meridional strain at one wall thickness above wall-base juncture
Main Steam/Medium Penetration	Hoop strain at the penetration elevation
Equipment/Personnel Hatch	Hoop strain at the penetration elevation
Springline	Meridional strain at one wall thickness below springline

The results are expressed as two failure pressures for the containment liner. Where the adjusted peak uniaxial liner strain intercepts epsilon$_{bcd}$, the pressure level is the lowest credible pressure at which leakage could develop for the specific location plotted; and where it intercepts epsilon$_{bcd}$, the pressure level is the pressure at which the liner has a high probability of developing leakage.

4.4.3.2 Application of the Method

The example (Ref. 13) of a reinforced concrete containment is a typical PWR with a design pressure of 40 psig. The example containment was compared to CPSES (Figure 4.4-2) and it was verified that they are indeed similar. The global strains from the finite element analysis of this containment (Table 4.4-3) were scaled by the design pressure ratios to obtain the CPSES global strains. This is justified by the similarity of the containments and by the small sensitivity of results to perturbations in these strains as stated in Reference 1. The uniaxial failure strains were obtained as described in step 4 below. The method was applied according to the following 9 steps originally outlined in Reference 13.

Step 1: Confirm that the containment is within the range of applicability of the method. The range of applicability for containment parameters specified in the reference document is listed as follows:

Parameter	Range of Applicability	CPSES
Containment Diameter	120 to 160 feet	135
Concrete Wall Thickness	3.5 to 4.5 feet	3.5
Steel Liner Thickness	0.2 to 0.4 inches	1/4-1/2
Design Pressure	30 to 60 psig	50

The Comanche Peak containment is a reinforced concrete structure, with a design pressure (50 psig) that is within the range of applicability indicated above. Other CPSES dimensions are also noted to be within the range of radius and wall and cylinder liner thickness.

Step 2: Analyze the containment with the 2-D axisymetric finite element analysis as described in Reference 1.

This step was substituted by the analysis performed in Reference 13. That analysis was of a typical PWR containment with a design pressure of 40 psig. That containment is quite similar to the CPSES containment as evidenced in Figure 4.4-2. The global strains computed for that plant, which are listed in Table 4.4-3 for each discontinuity type, were scaled by the ratio of design pressures (multiplied by 40/50) as an estimate for the CPSES containment global strains.

Step 3: Plot the global strains for each discontinuity type (see list in Section 4.4.3.1) as a function of internal pressure. This is done in Table 4.4-3. Strains and pressures correspond to those of the reference plant as given in Reference 22. The listed strains include the strain localization factor (alpha=4). The CPSES strains at these pressures were obtained by adjusting the values in Table 4.4-3 by the ratio of design pressures (multiply by 4/5), since the same strain levels are expected at the design pressure due to the similarity in the design of the containments.

Step 4: Determine the upper and lower levels of the uniaxial failure strain. These were obtained for CPSES from the actual line material specification SA 537-74 Class 2 steel and are:

$$\text{epsilon}_{ksi} = 20\%$$

$$\text{epsilon}_{bsi} = 22\%$$

Step 5: Perform steps 6 through 8 for each type of discontinuity.

Step 6: Determine k and beta for the pressure range of interest. (Since alpha is a constant, it is already included in the global strains given in Table 4.4-3.) The k and beta factors are given as a function of normalized global strain (normalization factor epsilon = 0.002) in Figures 4.4-3.1 through 3.8. These values are from Reference 22 and correspond to updated values originally given in Reference 13.

Step 7: Calculate the peak strains. The peak strains were calculated for each discontinuity type as a function of internal pressure using:

$$\text{epsilon}_{peak} = (K)\ (beta)\ (\text{epsilon}_{global})$$

Step 8: Plot the peak strains together with the uniaxial failure strain. This is shown in Figure 4.4-4.

Step 9: Determine the onset of liner tearing and leakage.

Peak strain for each pressure increment calculated is shown in Figure 4.4-4. The peak strain curves were plotted together with the highest and lowest credible ductility values, epsilon_{hcd} and epsilon_{lcd}. Liner tearing and leakage is predicted to occur between the pressures where epsilon_{peak} intercepts the uniaxial failure lines of lowest credible ductility and highest credible ductility. The upper and lower failure pressure confidence levels were determined by calculating the two points of intersection on the uniaxial failure strain vs. pressure curve representing each of the discontinuity types. The pressure levels at the intersections were calculated and presented as predicted values for containment leakage.

The results indicate onset of leakage to occur first at the main steam line penetration at a pressure of 114 psig. Leakage was then predicted to follow, successively, at the large penetrations and wall-skirt juncture.

The findings are as follows:

Medium Penetration:

P_{lcd} = 114.1 psig (P_{lcd}/P_{design} = 2.281)
P_{hcd} = 114.2 psig (P_{hcd}/P_{design} = 2.284)

Large Penetration (equipment and personnel hatches):

P_{lcd} = 117.0 psig (P_{lcd}/P_{design} = 2.30)
P_{hcd} = 117.2 psig (P_{hcd}/P_{design} = 2.34)

Wall-Skirt Juncture:

P_{lcd} = 119.9 psig (P_{lcd}/P_{design} = 2.39)
P_{hcd} = 120.3 psig (P_{hcd}/P_{design} = 2.41)

Springline:

P_{lcd} = 125.0 psig (P_{lcd}/P_{design} = 2.50)
P_{hcd} = 125.4 psig (P_{hcd}/P_{design} = 2.51)

4.4.4 Containment Fragility Curve

In order to estimate the probability of containment failure due to spiked pressure loadings such as those associated with high pressure melt ejection phenomena or steam spikes associated with vessel failure or hydrogen burns, it is necessary to know the containment failure probability as a function of the internal pressure loading.

The accuracy of the failure pressure predictions of the analysis results depends, to a large extent, on the accuracy of the material nonlinearities exhibited by the reinforced concrete and reinforcing steel. The containment failure is considered to occur because of a global stress on the containment structure due to static pressure load. Localized failure due to potential construction defects or variations in the assumed strength of materials, or local stresses, is considered by assigning a range of containment failure probabilities at various containment pressures.

Since failure of structures is probabilistic in nature, the actual failure level is represented by a statistical distribution about the predicted failure level as the mean. Typically these distributions are normal (Gaussian) (Ref. 23) and the probability density function (pdf) is:

$$f(t;\ \mu,\sigma) = \frac{1}{\sigma\sqrt{2\pi}} \quad \exp-\left[\frac{t-\mu)}{2\sigma^2}\right]$$

where: μ is the mean (also the median in this case) failure value;

σ is the standard deviation; and

t is the independent variable (pressure failure level).

such that: $-\infty < t < \infty$;

$-\infty < \mu < \infty$; and

$\sigma > 0$.

If only one failure location is considered, the probability, P, that the containment has failed at a given pressure $\geq$ t is the cumulative normal distribution:

$$P(t;\mu,\sigma) = \int_{o}^{t} \frac{1}{\sigma\sqrt{2\pi}} \quad \exp-\left[\frac{(x-\mu^2)}{2\sigma^2}\right]dx$$

A convenient measure of variability is the coefficient of variation which is the ratio of the standard deviation of the strength (or failure pressure) to the mean value (σ/μ). According to Reference 24, the coefficient of variation for reinforced concrete of typical containment structures is 7%, based on the yield strength of the reinforcing bar.

Based upon the previous liner tear analysis, medium penetrations such as the steam line showed the lowest failure pressure (114 psig). For these types of failures, the complementary cumulative containment failure pressure distributions (or the probability of surviving a load) are shown in Table 4.4-4. These probabilities assume a mean value of 114 psig and 7% coefficient of variation as discussed above.

It is felt that these failure pressures are conservative for the following reasons:

- The liner tear pressures used as the basis are low because the global strains used in their determination were taken from a 40 psig design pressure containment, whereas, CPSES has a design pressure of 50 psig. Although the global strains were scaled, it is felt that the resulting values are still too high for CPSES. For example, if one took the 40 psig plant's global strains (Table 4.4-3) as a function of $P_{Rupture}/P_{Design}$ for that plant, instead of renormalizing by the CPSES design pressure of 50 psig, the liner tear limits would be:

  Medium Penetration:

  P_{lcd} = 141.55 psig (P_{lcd}/P_{design} = 2.83)

  P_{hcd} = 141.79 psig (P_{hcd}/P_{design} = 2.84)

  Large Penetration (equipment and personnel hatches):

  P_{lcd} = 144.59 psig (P_{lcd}/P_{design} = 2.89)

  P_{hcd} = 145.24 psig (P_{hcd}/P_{design} = 2.90)

  Wall-Skirt Juncture:

  P_{lcd} = 148.48 psig (P_{lcd}/P_{design} = 2.97)

  P_{hcd} = 149.25 psig (P_{hcd}/P_{design} = 2.99)

  Springline:

  P_{lcd} = 153.20 psig (P_{lcd}/P_{design} = 3.06)

  P_{hcd} = 154.20 psig (P_{hcd}/P_{design} = 3.08)

  (Here it is noted that the approach described above was not used in order to preserve an element of conservatism.)

- The second reason why the present failure pressure probabilities are conservative is that the rupture pressure determined in Section 3 is also too low. A more realistic failure limit could be obtained by using actual reinforcing steel and liner plate tests. For example, actual material properties provided in Reference 18 indicate that the yield strength of reinforcing bars (#18) can range from 67.3 to 74.6 ksi, with a mean value of 69 ksi. The same reference provides a

specification value of 60 ksi. Similarly, the liner plate yield strength provided in the document indicates a mean value of 37 ksi, with a range of 31.3 to 48.1. The specification value is 24 ksi. Using the mean value of 69 ksi as a more realistic characterization of the yield strength in the above equation, the failure pressure limit obtained would be 155.8 psig.

4.4.5 Conclusion

The failure pressures and failure pressure probabilities of Table 4.4-4 are conservative estimates that may be upgraded following a plant specific calculation of global strains.

The following ways in which the CPSES containment might fail to perform its function have been examined:

- Four categories of penetrations were examined, the same as those considered in Reference 11. These are: (a) Large Opening Penetrations, including personnel and emergency airlock, equipment hatch and fuel transfer tube, verified to be pressure seating and their structural stability (buckling) checked where appropriate; (b) Purge and Vent System Isolation Valves, examined from the stand point of temperature resistance of the seal materials; (c) Piping Penetrations, examined for resistance to pressure differentials and to loads resulting from differential support displacements; (d) Electrical Penetration Assemblies, examined from the seal exposure perspective. The examinations consisted of comparison of CPSES penetrations type by type with those examined in great detail in the study of Reference 11. All CPSES penetration types have equivalents in that study and it is concluded, as in that report, that the CPSES penetrations are not likely to fail before the ultimate capacity of the containment is reached.

- The ultimate capacity of the containment including liner, rebar and concrete was determined to be P = 136 psig utilizing the scaling methodology developed in Reference 17. The failure criteria was conservatively set at 0.01 strain in the rebar. This definition of the structural failure limit is consistent with yielding of the containment pressure boundary that might result in rupture failure of the containment under very rapid pressurization.

- The leakage or liner tear limit of the containment was examined at four key discontinuities: (a) the wall-skirt juncture, (b) the springline, (c) the equipment hatch and (d)large pipe penetrations such as the steam line. The method used was recently developed by EPRI (Refs. 1,13). The result of the application of this method to the CPSES containment is that ductile failure of the liner is expected around the steam line penetration at 114 psig, around large penetrations at 115 psig, at the wall-skirt juncture at 120 psig and at the springline at 125 psig.

A containment fragility curve was developed by assuming a normal distribution for the failure pressure with a mean of 114 psig and a 7% coefficient of variation.

Also for the purposes of containment performance evaluations, it should be noted that releases from liner tear and/or gross failure of the containment were assumed to go directly to the environment. This is conservative because the onset of leakage is predicted to occur at a liner discontinuity near a steam line penetration; and therefore, it might be argued that leakage would take place into the turbine building and, consequently, be subject to some retention which could be quantified and credited.

Table 4.4-1: CPSES Containment Failure Modes

FAILURE MODE	PDS[2] LABEL	UNCONDITIONAL PROBABILITY	HOW THE FAILURE MODE IS ANALYZED
CONTAINMENT BYPASS			
1. Interfacing Systems LOCA (V-Sequence or ISLOCA)	1CB	1.5E-07	Fault tree [5] for probability. MAAP for releases [7].
2. Steam Generator Tube Rupture (SGTR and ISGTR[3])	2CB	3.5E-06	same as above except ref. is [4] and ISGTR probabilities come from the CETs.
3. Isolation failures	1CI	9.9E-09	same as above except ref. is [6].
EARLY CONTAINMENT FAILURES			
4. Pressure load due to steam explosion (AFCdm).	4H,1H,3H,3F,4F,6F, 1F,4SBO,6H,5F,2F,5 H,3SBO	2.9E-07	CONTAINMENT EVENT TREE (CET)
5. Direct Containment Heating (DCH) / combustion processes.	same as above	2.2E-07	CET
6. Vessel thrust force (Rocket)	same as above	< 1E-09	CET
LATE CONTAINMENT FAILURES			
7. Overpressurization due to noncondensibles (NC)	1H,3H,4SBO,3F,5H,4 F,6F,1F,3SBO,2F,6H ,4H,5F	2.16E-05	CET
8. Overpressurization due to steam generation (SG)	6H, 4H, 2H	9.16E-07	CET
9. Basemat melt-through (BM)	same as NC overpressure	1E-06 (included in 7 above)	CET
10. Late combustion	same as NC overpressure	2.2E-09 (included in 7 above)	CET
TOTAL:	========== >	2.67E-05 (60.5% CMF)	

[2]Plant Damage State, see Section 4.3

[3] Induced Steam Generator Tube Rupture.

Table 4.4-2: Summary of Various Containment Strengths

Plant	Type of Containment	Free Volume	I.D.	Design Pressure	Analysis	Failure Pressure	$\frac{P_{fail}}{P_{design}}$	Dominant Failure
Zion	Large Dry: concrete cylinder w/steel liner (pre-stressed)	2.86E6 ft^3	141 ft.	47 psig	NUREG-1150 IDCOR 10.1	108-180 psig 149 psig	2.3-3.8 3.17	Leak/rupture in cylinder wall or basemat/wall intersection Hoop/tendon strain
Surry	Sub-atmospheric: concrete with steel liner (reinforced)	1.3E6 ft^3	126 ft.	45 psig	NUREG-1150	95-155 psig	2.1-3.5	Leak/rupture near dome/wall intersection
Indian Point	Large Dry: concrete cylinder with steel liner (reinforced)	2.61E6 ft^3	135 ft.	47 psig	IDCOR 10.1	126 psig	2.7	Hoop rebar yield/cylinder shell near spring line
Seabrook	Large Dry: concrete cylinder with steel liner (pre-stressed)	2.76E6 ft^3	140 ft.	60 psig	Seabrook Risk Management Study 1985	211 psig (wet seq.) 190 psig (dry seq.)	3.5 3.1	Feedwater penetration
Oconee Unit 3	Large Dry: concrete cylinder with steel liner (pre-stressed)	1.91E6 ft^3	116 ft.	59 psig	Oconee PRA (NSAC-60)	162.5 psig	2.7	2.5 x design pressure, rupture of pre-stress tendons and liner failure

Table 4.4-3: Reference Plant Global Strains at Discontinuities

WALL-BASEMAT		SPRINGLINE		EQUIPMENT HATCH		MAIN STEAM LINE	
Pressure (psig)	Global Strain	Pressure (psig)	Global Strain	Pressure (psig)	Global Strain	Pressure (psig)	Global Strain
10	1.20E-06	5	1.20E-06	5	9.00E-07	5	9.00E-07
58	1.84E-04	20	1.32E-05	10	3.22E-05	10	3.22E-05
60	3.40E-04	25	2.04E-05	15	4.64E-05	15	4.64E-05
62	4.03E-04	30	2.03E-05	20	6.06E-05	20	6.06E-05
64	4.45E-04	32	2.25E-05	25	1.15E-04	25	1.15E-04
66	4.46E-04	34	1.69E-05	30	4.07E-04	30	4.07E-04
68	4.74E-04	36	2.68E-05	32	4.45E-04	32	4.45E-04
70	4.95E-04	38	2.71E-05	34	4.71E-04	34	4.71E-04
72	5.21E-04	40	3.10E-05	36	4.99E-04	36	4.99E-04
74	5.58E-04	43	3.53E-05	38	5.25E-04	38	5.25E-04
76	5.80E-04	47	4.09E-05	40	5.50E-04	40	5.50E-04
78	6.15E-04	50	4.96E-05	43	5.90E-04	43	5.90E-04
80	6.50E-04	54	6.33E-05	47	6.43E-04	47	6.43E-04
82	7.00E-04	58	7.90E-05	50	6.83E-04	50	6.83E-04
84	7.74E-04	60	1.11E-04	54	7.36E-04	54	7.36E-04
86	8.15E-04	62	2.55E-04	58	7.89E-04	58	7.89E-04
88	8.50E-04	64	4.48E-04	60	8.16E-04	60	8.16E-04
90	8.65E-04	66	5.15E-04	62	8.43E-04	62	8.43E-04
92	8.79E-04	68	5.60E-04	64	8.71E-04	64	8.71E-04
94	9.31E-04	70	6.61E-04	66	9.05E-04	66	9.05E-04
96	9.41E-04	72	7.30E-04	68	9.38E-04	68	9.38E-04
98	9.66E-04	74	7.91E-04	70	9.72E-04	70	9.72E-04
100	1.09E-03	76	8.54E-04	72	1.01E-03	72	1.01E-03
102	1.16E-03	78	8.97E-04	74	1.04E-03	74	1.04E-03
104	1.18E-03	80	9.49E-04	76	1.07E-03	76	1.07E-03
106	1.17E-03	82	9.97E-04	78	1.12E-03	78	1.12E-03
108	1.20E-03	84	1.05E-03	80	1.15E-03	80	1.15E-03
110	1.25E-03	86	1.10E-03	82	1.19E-03	82	1.19E-03
110.5	1.27E-03	88	1.15E-03	84	1.24E-03	84	1.24E-03
111	1.29E-03	90	1.20E-03	86	1.26E-03	86	1.26E-03
111.5	1.31E-03	92	1.25E-03	88	1.29E-03	88	1.29E-03
112	1.33E-03	94	1.30E-03	90	1.33E-03	90	1.33E-03
114	1.57E-03	96	1.35E-03	92	1.36E-03	92	1.36E-03
114.5	1.70E-03	98	1.41E-03	94	1.40E-03	94	1.40E-03
115	1.80E-03	100	1.47E-03	96	1.44E-03	96	1.44E-03
115.5	1.90E-03	102	1.52E-03	98	1.47E-03	98	1.47E-03
116	2.01E-03	104	1.58E-03	100	1.51E-03	100	1.51E-03
116.5	2.08E-03	106	1.64E-03	102	1.54E-03	102	1.54E-03

Table 4.4-3: Reference Plant Global Strains at Discontinuities (continued)

WALL-BASEMAT		SPRINGLINE		EQUIPMENT HATCH		MAIN STEAM LINE	
Pressure (psig)	Global Strain	Pressure (psig)	Global Strain	Pressure (psig)	Global Strain	Pressure (psig)	Global Strain
117	2.16E-03	108	1.74E-03	104	1.58E-03	104	1.58E-03
117.5	2.24E-03	110	1.89E-03	106	1.63E-03	106	1.63E-03
118	2.33E-03	112	2.18E-03	108	1.85E-03	108	1.85E-03
119	3.00E-03	115	2.70E-03	110	2.28E-03	110	2.28E-03
120	3.71E-03	118	3.20E-03	112	3.33E-03	112	3.33E-03
121	4.90E-03	120	3.60E-03	112.5	3.90E-03	112.5	3.90E-03
122	6.50E-03	120	4.02E-03	113	4.50E-03	113	4.50E-03
124	8.50E-03	125	7.00E-03	113.5	5.10E-03	113.5	5.10E-03
126	9.53E-03	130	1.50E-02	114	5.78E-03	114	5.78E-03
130	1.36E-02	135	3.00E-02	114.5	6.98E-03	114.5	6.98E-03
135	2.79E-02	140	5.00E-02	115	8.17E-03	115	8.17E-03
140	4.10E-02	150	1.00E-01	115.5	9.38E-03	115.5	9.38E-03
150	8.63E-02	160	2.00E-01	116	1.06E-02	116	1.06E-02
160	2.32E-01			116.5	1.20E-02	116.5	1.20E-02
				117	1.35E-02	117	1.35E-02
				117.5	1.46E-02	117.5	1.46E-02
				118	1.64E-02	118	1.64E-02
				118.5	1.81E-02	118.5	1.81E-02
				119	2.00E-02	119	2.00E-02
				119.5	2.17E-02	119.5	2.17E-02
				120	2.35E-02	120	2.35E-02
				122	3.19E-02	122	3.19E-02
				124	4.02E-02	124	4.02E-02
				126	4.92E-02	126	4.92E-02
				128	5.79E-02	128	5.79E-02

Table 4.4-4: Complementary Cumulative Probability Distribution for CPSES Containment Failure Pressures Based on Liner Tear at Medium Penetrations at 114 psig Assumed as the Mean and a Normal Distribution with a 7% Coefficient of Variation

PROBABILITY OF SURVIVING LOAD	LOAD (PSIA)
.9986	105
.9772	113
.8410	121
.5000	129
.1590	137
.0228	145
.0014	153

Figure 4.4-1: Uniaxial Strains vs Normalized Containment Pressure (Example Plant)

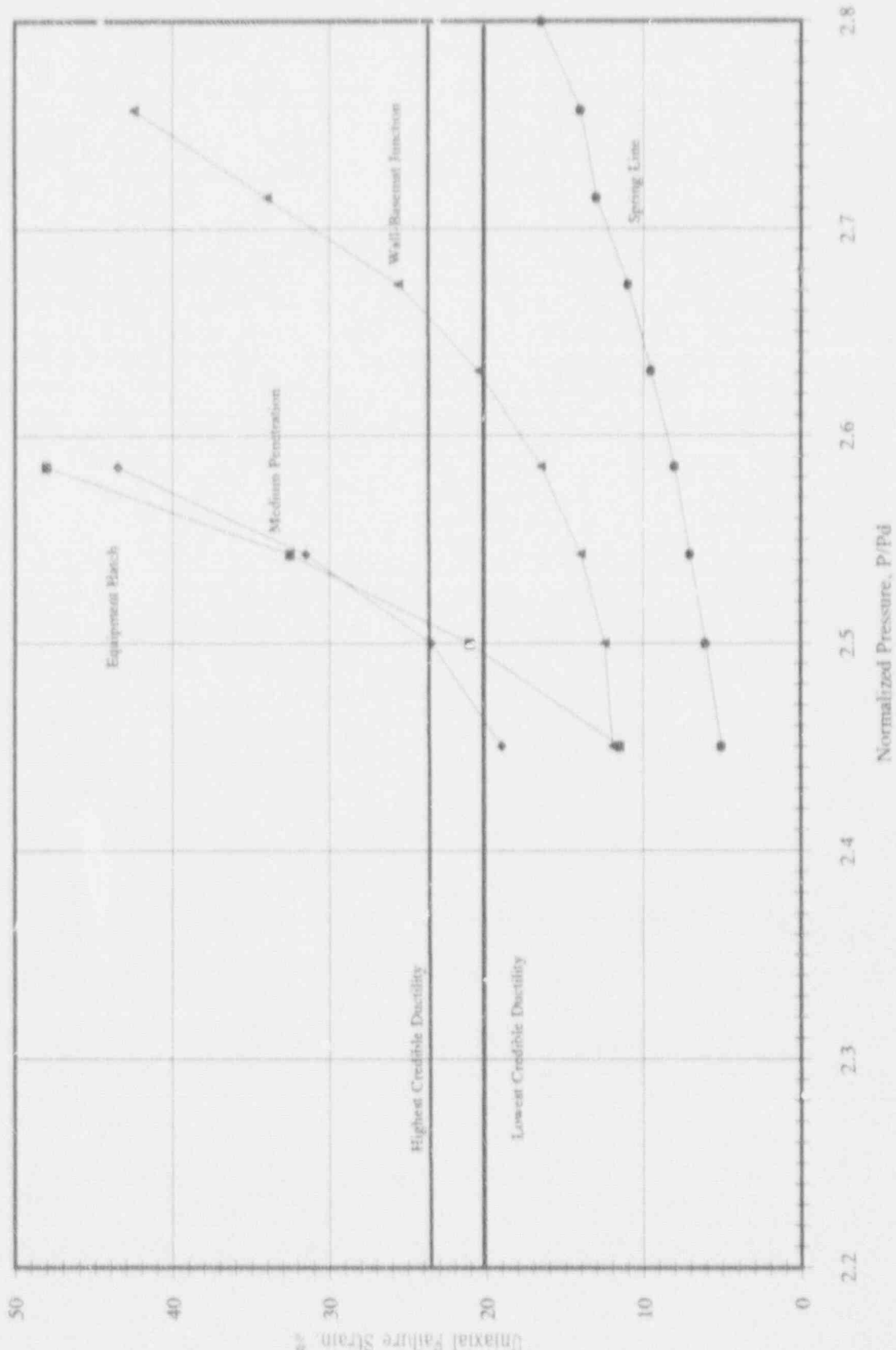

Figure 4.4-2: Comparison of CPSES Containment to Prototype

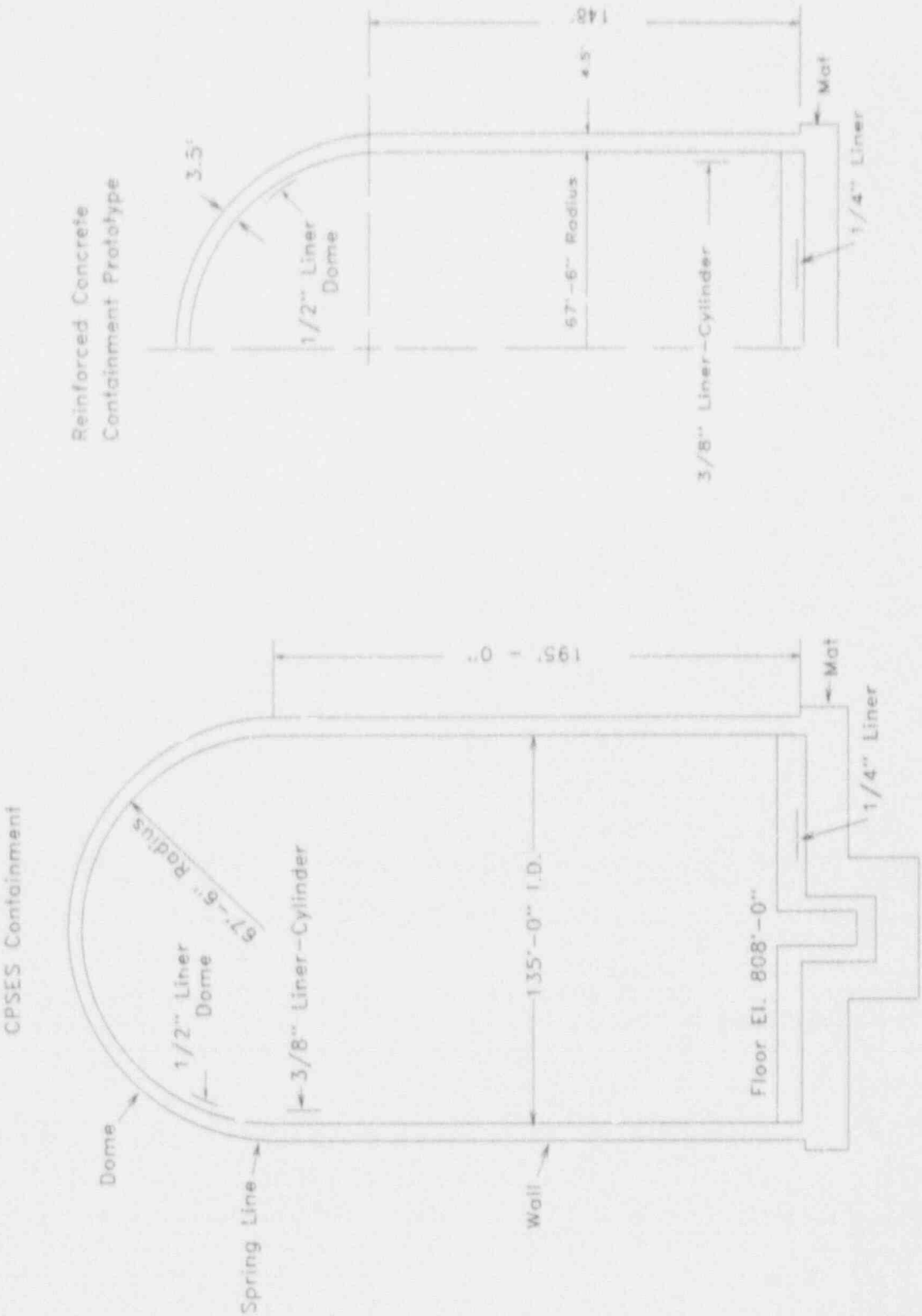

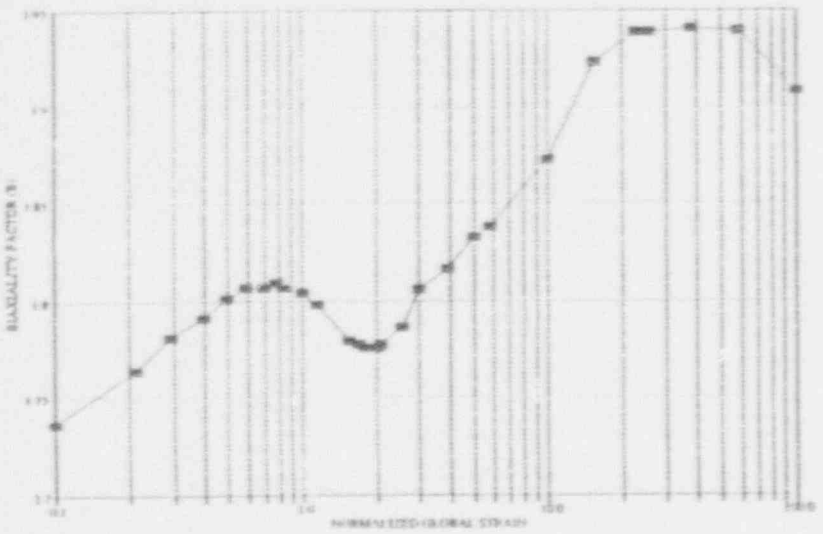

Figure 4.4-3.1: Biaxiality Factor for Typical Springline Geometry Reinforced Concrete Containments

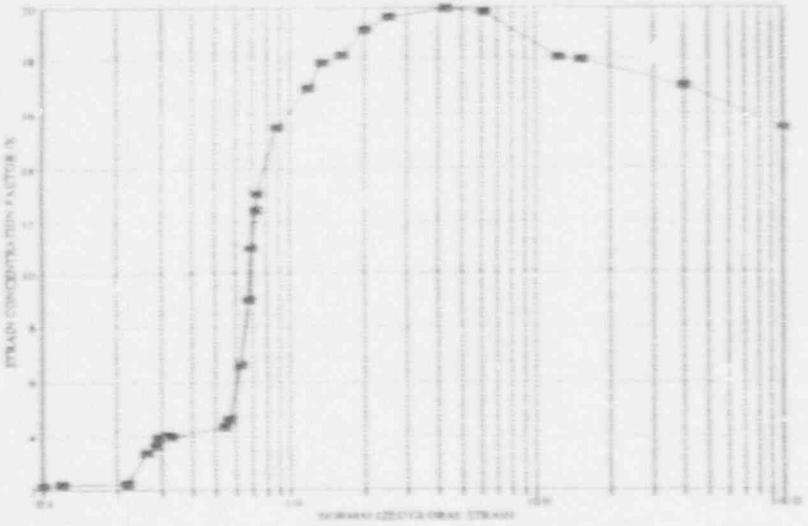

Figure 4.4-3.2: Strain Concentration Factor for Typical Springline Geometry Reinforced Concrete Containments

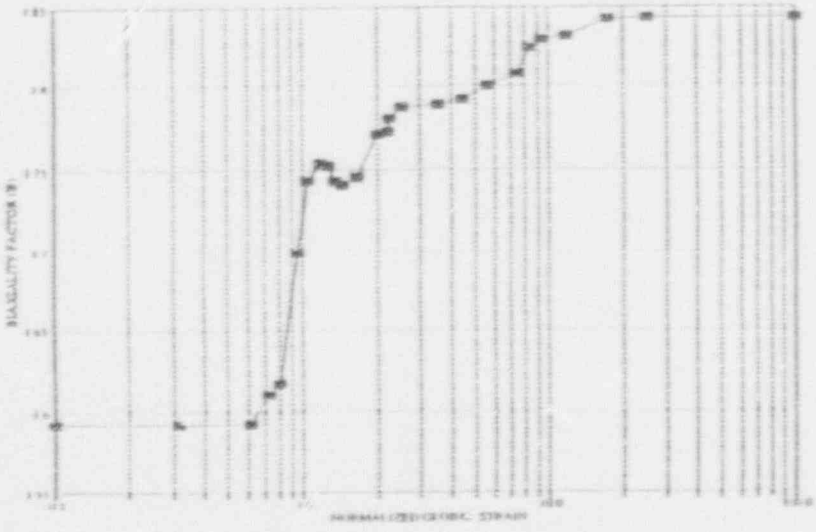

Figure 4.4-3.3: Biaxiality Factor for Typical Equipment and Personnel Hatches Reinforced Concrete Containments

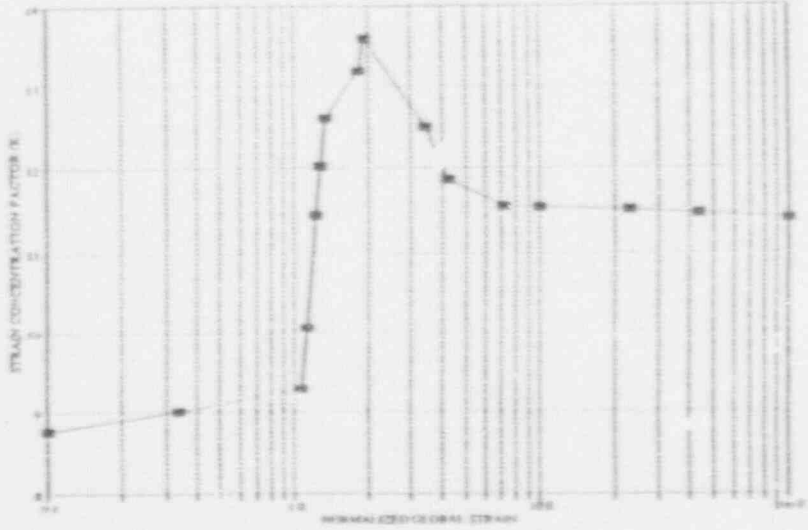

Figure 4.4-3.4: Strain Concentration Factor for Typical Equipment and Personnel Hatches Reinforced Concrete Containments

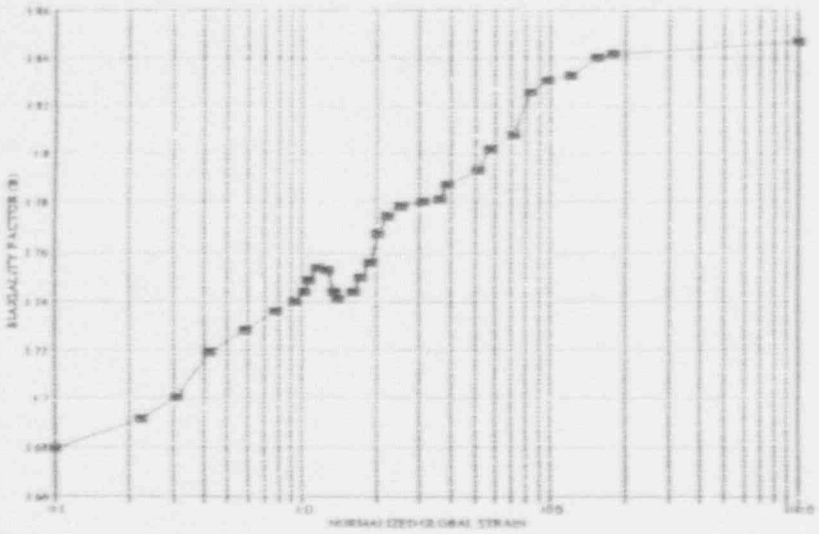

Figure 4.4-3.5: Biaxiality Factor for Typical Steam Line and Other Penetrations Reinforced Concrete Containments

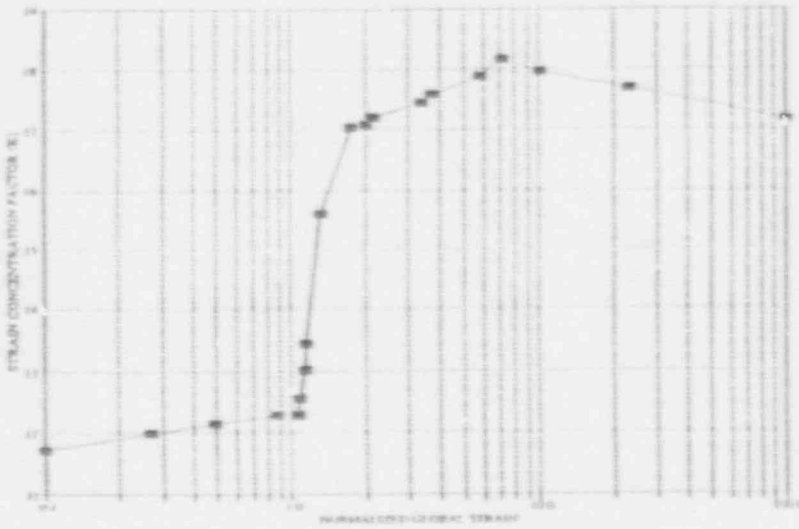

Figure 4.4-3.6: Strain Concentration Factor for Typical Steam Line and Other Penetrations Reinforced Concrete Containments

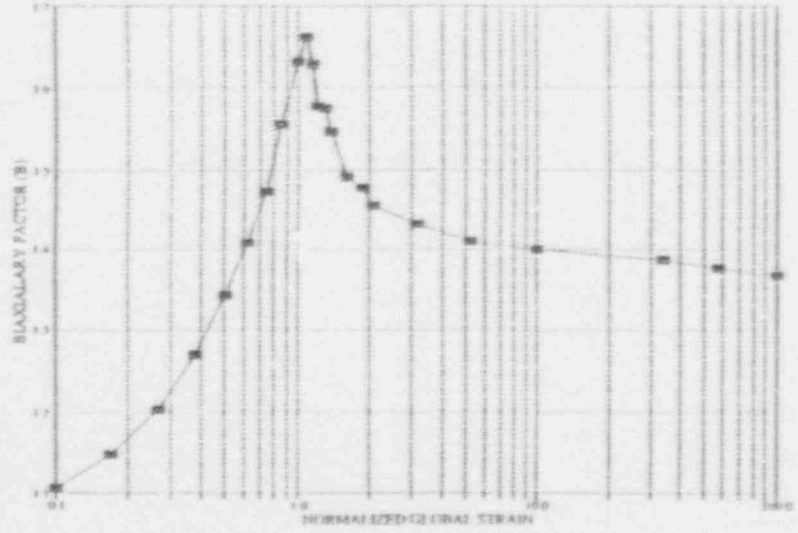

Figure 4.4-3.7: Biaxiality Factor for Typical Wall-Basemat Juncture Reinforced Concrete Containments

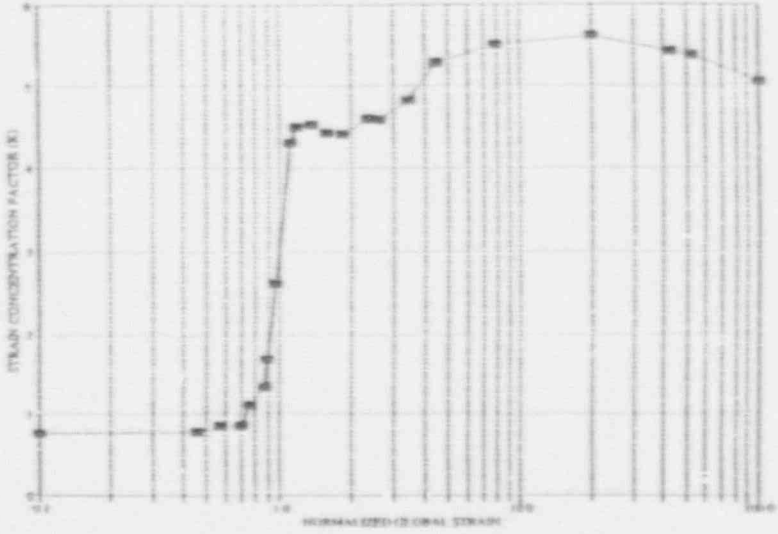

Figure 4.4-3.8: Strain Concentration Factor for Typical Wall-Basemat Juncture-Reinforced Concrete Containments

Figure 4.4-4: Containment Peak Strains Compared to Uniaxial Failure Strain (Comanche Peak)

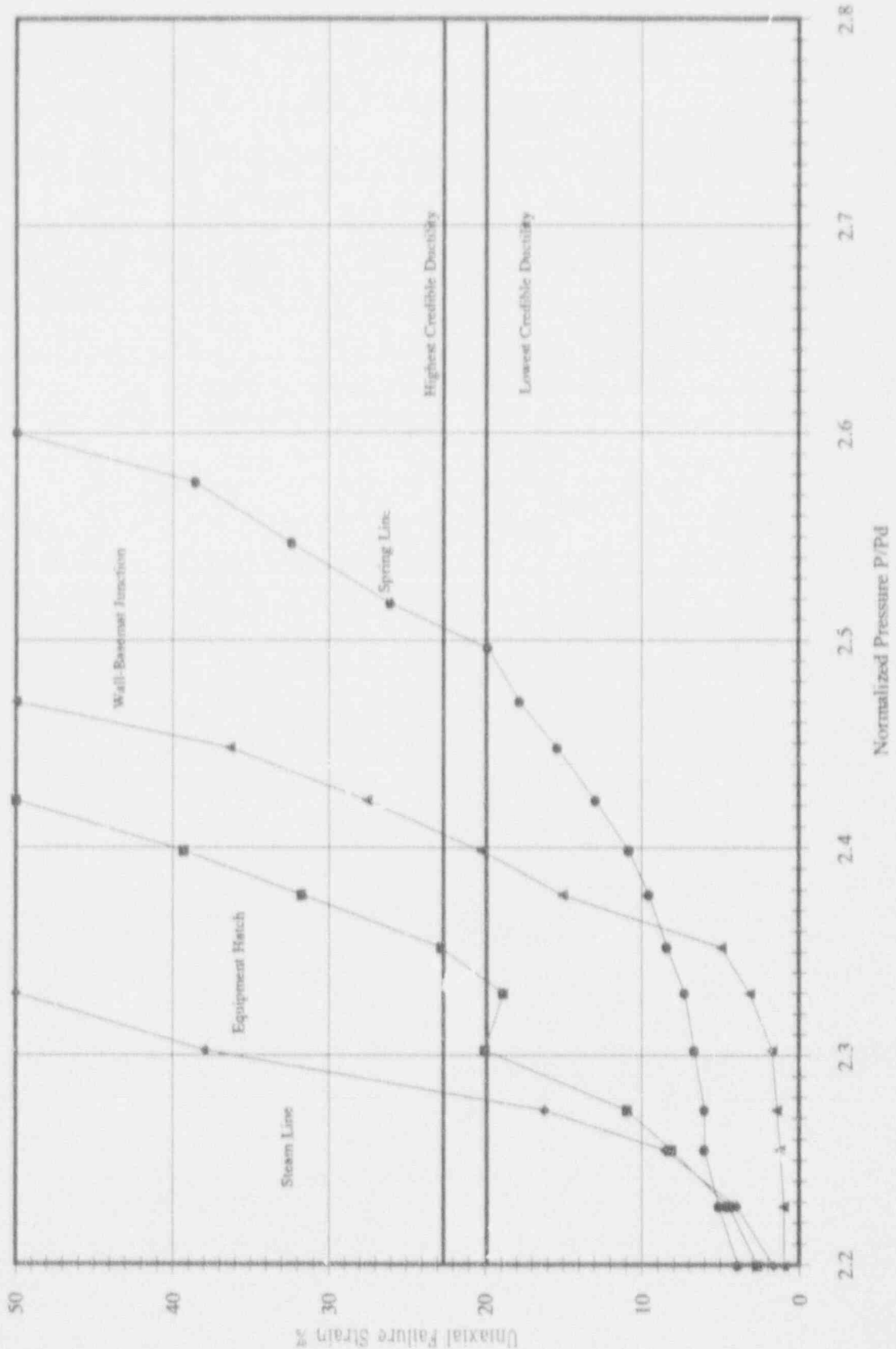

Figure 4.4-5: Seal Life as a Function of Time at Temperature (Ref. 26)

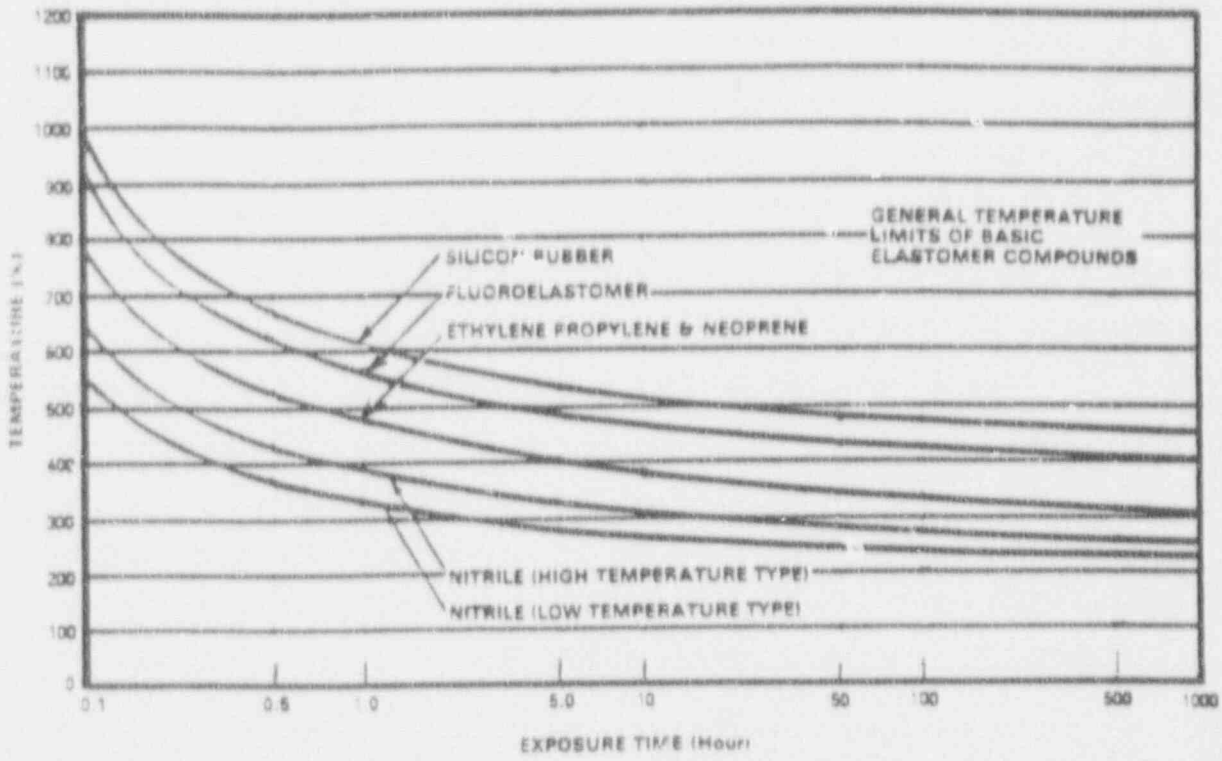

4.5 Containment Event Trees

The CPSES IPE treats containment bypass and isolation failure cases separately from cases in which the containment is available. Bypass and isolation failures are discussed in Section 4.5.1, and the intact containment cases and the Containment Event Trees (CETs) are discussed in Section 4.5.2.

4.5.1 Containment Bypass and Isolation Failures

The Level I analyses identify sequences and determine probabilities of occurrence of containment bypasses (Refs. 4,5) and containment isolation failures (Ref. 6) for sequences leading to core damage. MAAP analyses are used to determine the release fractions and timing for the associated release categories (Ref. 7).

4.5.1.1 Containment Bypass

Two types of bypass situations are identified: (1) Steam Generator Tube Ruptures, both induced (Ref. 7) (ISGTR, 1.7E-7) and as initiators (Ref. 4) (SGTR, 3.5 E-6) which are binned into PDS 2CB and, (2) interfacing systems LOCAs (Ref. 5) (ISLOCAs or V-Sequences) which are binned into PDS 1CB.

SGTR & ISGTR

The SGTR core damage frequency (3.5 E-6) was determined in the Level I analysis (Ref. 4). The ISGTR frequency was determined (Refs. 7,8) from the fraction of the non-depressurized high pressure PDS frequencies for which the SG tubes fail prior to the hot leg or the pressurizer surge line. MAAP analyses (Ref. 7) were used to establish the associated release category release fractions and timing. The path for the releases is out the SG safeties or the atmospheric relief valves as described in Section 4.1. The SGTR accident progression is discussed in Section 4.6. The SGTR event tree is shown in Figure 3.1.2-18 and discussed in Section 3.1.2 (Volume I of this submittal).

ISLOCA

The ISLOCA or V-sequence (PDS 1CB) core melt frequency (1.5E-7) was calculated (Ref. 5) based on NUREG/CR-5102 (Ref. 8). MAAP analyses (Ref. 7) were used to establish the associated release category, release fractions and timing. The path for the releases is through the Safeguards Building as described in Reference 5. Approximately 70% (8.7E-08) of the total ISLOCA frequency results in releases via pump seals, which would be submerged and scrubbed. However, credit is not taken for fission product scrubbing in that building since the total ISLOCA frequency is low.

Four classes of ISLOCA events are defined for CPSES:

Class i: Small LOCA inside containment - In these scenarios, the leak through the pressure isolation valves (PIV) is within the capacity of the relief valves and they relieve to a tank inside containment.

Class ii: Small LOCA outside containment - In these scenarios, the relief valves discharge to a tank outside containment.

Class iii: Overpressurization/LOCA inside containment - In these scenarios, either the leak through the PIVs is beyond the capacity of the relief valves or the relief valves fail to open. This results in overpressurization of the low pressure piping and a potential break in the low pressure system.

Class iv: Overpressurization/LOCA outside containment - In these scenarios, either the leak through the PIVs is beyond the capacity of the relief valves or the relief valves fail to open. This results in overpressurization of the low pressure piping and a potential break in the low pressure system. The break occurs outside the containment.

The interfacing lines where ISLOCAs in any of the above categories can occur are:

- Letdown Line
- Excess Letdown Line
- RH Suction Line

- Low Pressure Injection to the Cold Legs
- Low Pressure Injection to the Hot Legs
- Intermediate Pressure Injection to Cold Legs
- Intermediate Pressure Injection to Hot Legs
- Accumulator Injection to the Cold Legs

Each of these interfacing system lines was reviewed for its functional requirements, for potential small LOCA and overpressurization scenarios, and for plant parameters and/or alarms that provide indication of the event. Small LOCAs result from pressure isolation valves (PIV) leaking and lifting of the relief valves, whereas, overpressurization results from PIV rupture (or failing open) or PIV gross leakage and failure of the relief valve to lift.

The determination of the initiator frequencies of ISLOCAs through the various pathways identified earlier was accomplished by adapting the generic system failure models found in NUREG/CR-5102, "Interfacing Systems LOCA: Pressurized Water Reactors", to the specific valve arrangements found at CPSES.

At CPSES, as with the majority of PWRs, the low pressure injection (LPI) lines and the accumulator outlet lines have a common inlet header to the RCS. This inlet header is also shared with the intermediate pressure injection (IPI) lines. Therefore, based upon the result of NUREG/CR-5102, the analysis of ISLOCAs involving common inlet pathways has taken into account the proneness of the accumulator outlet check valve to fail to reseat on demand due to the lack of a differential pressure across its disc.

Each of the eight interfacing lines was examined for two conditions: a) Small LOCA and b) Overpressurization. The Small LOCA represents the case of the low pressure piping of the interfacing system reaching pressures up to the relief valve setpoint leading to a Small LOCA, including pipe ruptures and failure of the RH pump seals. The Overpressurization represents the case of pressures exceeding the relief valve capability, with pressure potentially reaching those seen on the RCS.

The initiating event frequency, the affected ESF equipment and the event classifications are provided in Table 4.5-1 and are applicable to the Small, Medium and Large break LOCA scenarios defined in Table 4.5-2. That information was then applied to the representative LOCA sequence to ascertain the potential for core damage and its probability. The result of that step is shown in Table 4.5-3.

The initiating events of Table 4.5-2 were evaluated to determine if the initiating event would lead to core damage directly (no further quantification required) or if additional equipment failures would be necessary to lead to core damage (additional quantification required). It was determined that event 5 would lead directly to core damage due to failure of both trains of RH during a Large break LOCA scenario (also events 1, 4, 7 and 8 have sufficiently small initiating frequencies that further evaluation was deemed unnecessary and core melt was also assumed). Thus, any possible recovery actions were not credited for these cases.

The remaining initiating events (2, 3, 6, 9 and 10) were quantified using the methodology and models defined in the front-end analysis (Volume I of the submittal), with equipment affected by the ISLOCA redefined as failed. These results include some feasible mitigation actions for recovering failed equipment or systems, but do not take credit for existing procedures for mitigating the ISLOCA initiating event prior to core uncovery (Ref. 5).

4.5.1.2 Containment Isolation Failures

A fault tree model was developed for the Containment Isolation System (Ref. 6). This fault tree model includes: (1) the pathways that could significantly contribute to containment isolation failure, (2) the signals required to automatically isolate the penetrations, (3) the potential for generating the signals for each initiating event, (4) the examination of the testing and maintenance procedures and (5) the quantification of each containment isolation failure mode (including common-cause failure). The fault tree model for the containment isolation system was quantified independent of the accident sequence analysis task. Then the cutsets were combined to determine for what fraction of each sequence the containment failed to isolate. As a practical matter, containment isolation failures were found to be independent of the support systems whose failures were present in the core melt sequences. As a result, the failure probability of the containment to isolate in those core melt sequences is low.

The Containment Isolation System (CZ) consists of sleeves, pipes, valves, instrumentation and controls for piping penetrations. The system isolation valves, piping design and location ensure containment integrity is maintained for any postulated single failure. Double isolation barriers ensure that no single failure of any active or passive component renders the CZ either partially or wholly inoperable. All system paths penetrating the containment wall were evaluated on the basis of their function at the time

of the accident and classified as either essential or non-essential. Essential paths are those required to mitigate an accident or whose unavailability could increase the magnitude of an accident and, as such, may contain remote-manual isolation valves. Non-essential systems are automatically isolated by the containment isolation signal or normally closed isolation valves.

Instrumentation and controls for the CZ includes the control and indicating devices for the power operated valves. The containment isolation system logic is part of the ESFAS logic and includes the following subsystems:

- Steam Line Isolation
- Main Feedwater Line Isolation
- Containment Isolation Phase A
- Containment Isolation Phase B
- Containment Ventilation Isolation

Each CZ power operated valve, with the exception of those that serve or support ESF systems, are provided with two methods of actuation: an automatic closure from the ESFAS and a remote-manual control switch. Each power operated valve in the CZ is also provided with a position indicating light. Provisions have been made at each containment penetration to facilitate leak rate testing (Types A, B, and C) in accordance with 10CFR Part 50, Appendix J.

The fault tree model (Ref. 6) developed for the containment isolation system was based on the criterion that a penetration required evaluation if it did not fall within one of the following categories:

- Locked closed manual valves
- Valves used for ESF systems
- Valves that are closed Prior to an accident and remain closed
- High pressure/Closed systems

Spare and maintenance/test penetrations are normally closed and/or isolated and were not considered due to their small contribution to CZ failure.

The remaining penetrations were quantified, independently of the accident sequence quantification effort, for each potential failure mode, including common cause failures. A subset comparison of the CZ quantification cutsets with each of the accident sequence quantification cutsets was completed to determine for what fraction of each sequence the containment failed to isolate.

4.5.2 Containment Not-Bypassed and Successfully Isolated, Containment Event Trees (CETs)

A CET was developed for each PDS for which the containment is not bypassed and successfully isolated during core melt. The CETs used in the CPSES IPE were based upon the approach developed by the Electric Power Research Institute (EPRI) (Ref. 1). Specific characteristics of CPSES were incorporated through adaptation of the EPRI trees, definition of the Basic Event (BE) probabilities (Section 4.6) and in the implementation of the CET quantification process (Section 4.6). BE probabilities were determined by PDS definitions, by systems performance for core damage sequences determined from the Level I analysis (Ref. 4), and by a substantial number of plant-specific MAAP analyses (Ref. 2).

The CET structure for a PDS for which the containment is initially intact is illustrated in Figure 4.5-1. A single CET structure is shown since the top events are the same for all these PDS. The difference between CETs for different PDS lies in the mechanisms that could challenge containment integrity and potential recovery measures associated with the RCS condition. The CETs were further developed for each PDS using logic trees to break down the top events into phenomenological, systems, or operator human response issues. Thus, a limited number of CET event nodes were defined that convey the full spectrum of the accident progression outcomes in a single event tree. The basic events (BE) affecting the CET top event nodes are: (1) decomposed severe accident phenomena, (2) systems availability and performance and (3) recovery measures. The logical relationship of these BE was modeled by a fault tree framework. The fault trees are also referred to as logic trees (LT).

Figure 4.5-1 shows the CET top events. The rationale and basis for each of these events is described in this section.

Top Event DP: RCS Not Depressurized Before Vessel Breach

The question asked in this top event node is related to depressurization of the RCS prior to vessel breach. Success in this branch implies that RCS pressure is low (less than 200 psia) at the time of vessel failure, reduced either through the capability of the operator to depressurize the reactor or through a phenomenological condition that could induce RCS depressurization, or because the initiating event is a break large enough (2 inches, Ref. 2) to lead to a low pressure condition at vessel failure. This event node is relevant for high pressure PDS to indicate a potential mitigating condition during core melt prior to vessel breach. For accident sequences leading to core melt with the RCS at high pressure, depressurization means that the high RCS pressure that could exacerbate containment challenges at vessel breach (such as direct containment heating) is removed.

The DP event node impacts subsequent CET event nodes related to in-vessel recovery and early containment challenge. Figure 4.5-2 displays the logic tree developed for this event node. The issues considered are:

- Initial RCS state as determined by initiating event (e.g., LOCA vs. Transients).
- Active operator action to depressurize the RCS before vessel breach.
- Severe accident induced LOCA due to high RCS piping temperature.

Top Event REC: Coolant Not Recovered In-Vessel Before Breach

Recovery in the back-end analysis, i.e., after core damage, is not credited in the CPSES IPE with the exception of Station Blackout PDS.

The question asked in this top event node is related to recovery of coolant injection and electric power after core degradation, prior to vessel breach. The recovery is only considered possible if RCS depressurization was successful, i.e., the question is only asked along the success path for event DP as can be seen in Figure 4.5-1. The logic tree for event REC is illustrated in Figure 4.5-3. The issues considered include the following:

- Availability of coolant injection upon depressurization.
- Recovery of electric power.

Top Event VF: Vessel Failure Occurs

The question raised by this event node addresses the actual arrest of core degradation within the vessel, which prevents lower vessel head thermal attack. Vessel failure is prevented only if coolant make up recovery was successful in the previous event node. Therefore, this event is also not relevant in the CPSES IPE for PDS other than those corresponding to Station Blackout.

Success at the Vessel Failure event requires that core cooling be recovered prior to core blocking (MAAP model) or relocation of molten debris to the lower plenum and thermal attack of vessel head (MARCH model). Therefore, the primary consideration for successful in-vessel recovery is the time available from incipient core degradation to the point of non-recovery. Core recovery in-vessel is modeled as unsuccessful once molten debris starts to relocate to the lower plenum and thermal attack of the vessel penetration weldments occur. MAAP calculations performed for the Zion plant indicate that this could occur when approximately 25% to 50% of the core is predicted to be molten. The NRC Source Term Code Package (STCP) calculations in BMI 2104, NUREG/CR-4624, and NUREG/CR-4587 show higher melt fractions (a user-specified criterion) are required before core slumping occurs. In either case, the time to vessel head attack can occur within 60 minutes (or longer) following core uncovery depending upon the sequence, based on published MARCH or MAAP calculations. More mechanistic MELPROG 2-D calculations (discussed in NUREG-1265) indicate that progressive relocation of lower-melting-point materials into the lower plenum tend to insulate the lower head penetration weldments from the higher-melting-point core materials. This might support the position that the time to vessel failure could extend even longer.

This event physically signifies that the core degradation process leading to vessel failure is successfully terminated, thus arresting core melt and precluding significant fission product release to the environment.

Figure 4.5-4 illustrates the issues considered for this event node. For purposes of this assessment, core debris cooling and termination of core degradation prior to vessel head attack is a probabilistically weighted average in the plant- and sequence-specific time windows of core uncovery to core melt and core melt to core slump. In the tree, the potential for terminating melt progression prior to vessel breach is either by debris cooling from within the vessel, or vessel bottom head cooling from outside the vessel, thus terminating head attack. The former depends on the success of the previous event node, REC and phenomenological considerations of coolable debris bed information, implemented by the weighted average approach mentioned above. The latter might be achieved by filling the cavity with water above

the vessel bottom head, allowing heat transfer to be established through the vessel walls. For some vessel head (no instrument tube penetrations) and containment configurations, this option might be plausible. However, this external cooling was not credited for CPSES and the corresponding BE probability was assigned the value of 0.0. This is felt to be a conservative assumption and some reviewers have suggested a value of 0.5. However, a more detailed discussion of the rationale for probability assignments is available elsewhere (Ref. 8).

Success of event VF is determined by the physical processes controlling core melting and material relocation to the lower plenum. A good understanding is very important in order to determine possibilities of arresting vessel head attack once significant core degradation has occurred. Exact modeling is not always possible; therefore, simplifying assumptions are made to approximate the analytic treatment of the physical process involved. There is considerable uncertainty in determining the formation of a coolable configuration once significant core geometry deformation and melting has occurred. There are recognized limitations in the existing analytical models (MAAP and MARCH) in predicting coolable debris bed formation within the vessel. The limiting factor, therefore, is the time available between core vulnerability (i.e., conservatively defined as core uncovery, the end-state of a core damage sequence) and core melting (i.e., peak temperatures exceeding core material eutectic temperature of 4130°F).

MAAP calculations conducted by IDCOR indicate that the time period between core uncovery and onset of core melting is typically one half hour to several hours (TSR, Task 23 Technical Reports) depending on the accident sequence. MAAP calculations also indicate that core degradation cannot be arrested once fuel melting has started and core reflood (as determined by the success branch of event REC) would not preclude support plate failure and vessel breach. MARCH (STCH) calculations, on the other hand, indicate that vessel breach can be arrested provided that coolant injection is recovered before significant core melting has occurred. Because of the phenomenological uncertainty associated with this event, the limiting factor used for the conditional probability of success is the time period between core uncovery and core melting compared with the time period between core uncovery and core collapse.

The logic tree for this top event is shown in Figure 4.5-4. Worthy of mention in this tree is event CAV-DRY where SECCS-INJ is ANDed with SNOSPRAY1. This accounts for the fact that the cavity will not be dry if the RWST water has previously been injected into the containment, regardless of whether sprays have operated or not. The CAV-DRY event appears in other logic trees as well.

Top Event CFE: Early Containment Failure Occurs

This functional event was included in the CET to signify that the containment integrity is maintained during the early phases of core degradation and release of fission products from the fuel up to vessel breach. The fission products released from the fuel are contained within the primary containment system so that natural removal mechanisms can effectively act to deplete airborne concentrations in the containment.

Failure at event CFE is defined as loss of containment integrity early in the accident sequence. Several failure mechanisms were postulated for this top event node as shown in the logic tree of Figures 4.5-5 and 4.5-6. These include containment challenges resulting from:

- Pressure spikes occurring due to blowdown at reactor pressure vessel (RPV) failure with the RCS at high pressure.

- Fuel-coolant interaction resulting in rapid steam generation within the vessel at core slump or in the reactor cavity at vessel breach.

- High pressure melt ejection loads such as combustion of hydrogen released prior to and at vessel breach and direct containment heating.

The failure mechanisms identified above that, individually or in combination, result in loss of containment integrity early in the accident were considered in the CFE logic trees.

Uncertainties in containment loads at vessel breach arise from the non-stochastic nature of some of these events (e.g., hydrogen burns), as well as a poor understanding of the phenomena governing others (e.g., direct containment heating). Although more experimental and analytical information regarding direct containment heating has been generated, substantial uncertainties persist and the phenomenon continues to generate controversy. Pressure loads from high pressure melt ejection and fuel-coolant interaction are further discussed below.

High Pressure Melt Ejection (HPME) Loads: The potential for pressure rise as a result of the high pressure melt ejection of molten debris from the vessel to the containment atmosphere is considered in this issue. Direct Containment Heating (DCH) is used to define the physical process when the vessel fails

at high pressure and large fraction of the molten core debris is dispersed into the containment as fine particles and a substantial portion of the core material sensible heat is directly transferred to the atmosphere. The containment pressure rise depends strongly on the reactor cavity geometry and the mass of material dispersed. The pressure rise can also be augmented by the hypergolic burn (a forced and complete burn not limited by flammability considerations) because of the very high temperatures caused by direct heating of the containment atmosphere. The containment pressure rise accompanying direct containment heating depends on reactor cavity geometry, the mass of material dispersed by reactor vessel blowdown, and several other parameters described in the quantification (Section 4.6) and in Reference 8.

There are several parameters included in the logic tree to model the dependencies of the containment challenge resulting form DCH:

- Provided the reactor pressure prior to vessel breach is sufficiently high to transport molten material and hot gases to the upper regions of the containment, the pressure rise is probably insensitive to reactor pressure. The reactor pressure threshold below which DCH does not occur is still not clear-cut based on Sandia experiments of debris dispersal. In this assessment, DCH is regarded as possible if the pressure is above 200 psi (NUREG-1150). MAAP calculations were performed to provide insights into the determination of the extent of debris dispersal.

- The fraction of core melt ejected from the vessel at the time of vessel breach determines the amount of material that can participate in DCH. This is governed by the model used to represent core melting and, to some extent, the accident sequence definition.

- The size of the vessel failure, since it affects the blowdown time and debris dispersal.

- The availability of water in the reactor cavity at the time of vessel breach is considered, because it can influence DCH. The water can interrupt the pathway for debris dispersal following vessel breach as it is displaced only after a fraction of the debris is injected to the cavity, or the water can be co-dispersed, in which case the droplets can continue to quench the debris.

DCH resulting from the dispersal of molten core debris can induce hazards that challenge containment in the short term. An additional simultaneous hypergolic burn of hydrogen can generate chemical energy

that can increase the pressure and temperature of the containment. If the amount of debris involved in this process is significant, extremely high pressure and thermal loads can indeed fail the containment.

In a HPME, combustion of sufficient hydrogen to generate a substantial pressure rise is subject to physical requirements regarding minimum hydrogen concentrations, oxygen availability, but not inerting gas concentrations. Hydrogen concentrations in containment prior to vessel breach depend upon in-vessel core melt progression (primarily the fraction of the core Zircaloy oxidized before vessel breach), and the type of accident scenario being considered.

Hydrogen burning alone, i.e., not in combination with DCH, can for some plants also induce over-pressure failure. While such burns are possible at CPSES, they lead to post-burn, worst-case containment pressures on the order of 80 psia if only Zircaloy oxidation-generated hydrogen is considered at 100% clad reacted. Therefore, the probability that they will fail the CPSES containment is negligible, since it has a design pressure (tested) of 65 psia and has a failure pressure of 129 psia as shown in Section 4.4. However, the possibility of these burns is included in basic events (BE) PRWCP-PULT and PRDCP-PULT (Figure 4.5-6) as a feature of the HPME challenge pressure probability distribution developed for Zion in NUREG/CR-4551, which is adjusted for each CPSES PDS as described in Section 4.6. That distribution includes the loads from blowdown, to burns alone, to DCH alone, to DCH in combination with burns, and the probability of occurrence.

Fuel-Coolant Interaction (FCI): The consequences associated with the rapid transfer of thermal energy from fuel-coolant interaction in the vessel or ex-vessel can be risk-significant as it poses a plausible threat to containment integrity. There is a possibility that in certain accident sequences, molten material can flow into a pool of water in-vessel (reactor vessel lower plenum) or ex-vessel (reactor cavity) leading to steam explosion failing the containment. It is also noted that ex-vessel steam explosion may result not only in an impulse load, but also in a quasi-static pressure load on the containment structures (NUREG-1150).

In-vessel steam explosion was first assessed in the Reactor Safety Study, WASH 1400. Since then, numerous simulant tests and related analytical models have been developed. However, some uncertainty still exists regarding this issue, much of which is related to the applicability of the small and intermediate-scale tests to reactor scales and geometries. In this assessment, the likelihood of in-vessel steam

explosion is dependent on the RCS pressure. The draft NUREG-1150 assessments also indicate a low likelihood of containment failure due to steam explosions relative to other failure modes.

Ex-vessel steam explosions for the Zion and Surry containments were assessed as unlikely to threaten containment integrity (NUREG-1150). The cavity walls are heavily reinforced concrete to support the reactor core and the primary shield wall and even more so for CPSES. The cavity configuration (if filled with water), not unlike that of Zion or Surry, would not allow water to represent a vulnerability to containment structures from impulse loads generated during ex-vessel steam explosion. Although potential ex-vessel interactions between core debris and water are of concern only for accidents scenarios during which the water covers the reactor cavity floor prior to vessel breach, that is always the case at CPSES. Nevertheless, the effect of pressure spikes resulting from high pressure blowdown and rapid steam production, although subject to some uncertainty, are bound by conservative assumptions regarding the probability that such events would occur and fail containment.

The logic trees (Figures 4.5-5 and 4.5-6) developed for this event consider the time-dependency of the various phenomenological events that contribute to early containment challenges during a severe accident, in the manner discussed above. Note that there are two logic trees, CFE1 (Figure 4.5-5) and CFE2 (Figure 4.5-6). The difference is that CFE1 is along the high pressure path, and therefore includes HPME phenomena, while CFE2 is along the low pressure path of the CET (Figure 4.5-1). In both cases, induced containment isolation failure is considered, (which might occur given the combustible gas control procedures requiring purging the H_2 in containment by opening the purge valves, although this issue was found negligible at CPSES) in addition to the phenomena discussed. These induced isolation failures are separate from the cases of containment isolation failures per se, which are treated in the way discussed in Section 4.5.1. Many of the phenomenological issues are developed in the determination of the probabilities for basic events PRWCP-PULT and PRDCP-PULT so they cannot be seen explicitly on the trees. However, the analysis is summarized in the quantification (Section 4.6) and described in detail in Reference 8.

Top Event DC: Debris Bed Not Coolable

This event is included in the CET to signify the termination of the core melt progression subsequent to vessel breach. The success branch at this CET node means that a coolable debris bed is formed, precluding concrete attack, and thus precluding ex-vessel fission product releases from core-concrete interaction. Following the success branch also implies that containment overpressure challenges from

non-condensible gas generation and from basemat melt-through are precluded. Success in this branch requires two things: (a) that there is water over the debris and (b) that the debris is in a coolable configuration, i.e., that it can be cooled even with water over it because it is not insulated by an impervious crust. At CPSES the debris will not be coolable when the RWST water is not injected into the containment because in those cases the debris dries out prior to vessel failure, even if it was at first in a coolable configuration. The coolable configuration cases are coolable when the RWST water has been injected into the containment, or for PDS where the low pressure injection systems were previously unable to inject due to high RCS pressure, these systems would start to deliver coolant when the vessel is breached. Coolant injection will quench the debris if it is in a coolable configuration. This last condition can also establish a heat transfer cycle from the debris to the environment in the subsequent event node if switchover to recirculation is successful. In practice, these automatic LPI injections are not probabilistically significant at CPSES for the reasons discussed below in this section.

Failure at this branch implies that concrete attack occurs in the cavity, the core debris remains hot and sparging of the concrete decomposition products through the melt releases the less volatile fission products to the containment atmosphere. This condition is considered more likely if a deep core debris bed is formed in the cavity and, absent coolant addition, the debris is not able to effectively dissipate the decay heat to the surroundings. Should an impervious crust form, coolant addition would not likely terminate concrete attack, although the released fission product aerosols are scrubbed by the overlying water pool.

MAAP calculations for Zion (Ref. 33) indicate that dispersal and entrainment of molten core material outside the cavity region into the lower containment region occurs in most accident sequences where the vessel fails with the RCS at high pressure. The extent of debris dispersal could vary depending on the amount of core debris molten at the time of vessel failure. The CPSES cavity and instrument tunnel configuration is such that the flow path is more restrained than the sloped configuration of Zion. However, the STCP model used for the NUREG-1150 supporting calculations for the Surry plant does not model dispersal following vessel breach at high pressure. Separate effects calculation of DCH using CONTAIN (NUREG/CR-4896) indicate dispersal is likely to occur even with the restrictive design of the Surry cavity. Should debris dispersal occur, formation of a coherent, uncoolable debris bed is not likely. Conversely, formation of a more coherent debris bed is considered more likely for accident sequences with the RCS depressurized prior to vessel breach. The phenomenological uncertainty

associated with debris bed coolability given water injection is the formation of an impervious crust that precludes water ingress into the debris.

This event considers the formation of an uncoolable debris geometry and/or the absence of water in the cavity implying significant core-concrete attack that could challenge containment integrity. The ability to cool the debris after vessel breach is determined by the possibility of water ingress and the formation of a coolable corium geometry. The important issues include:

- Phenomenological considerations of crust formation.
- Sequence dependencies related to corium dispersion at vessel breach (i.e., high RCS pressure).
- Geometric configuration dependencies allowing formation of a shallow bed (cavity configuration).
- Systems-oriented considerations related to water availability (e.g., ECCS injection prior to or post vessel breach and/or sprays actuation).

An examination of the cut-sets indicates the availability of ECCS injection following vessel breach. The PDS definitions (whether high or low pressure) determine debris dispersal and, whether injection or recirculation failure occurred, determine the availability of water beyond the potential LPI injection at vessel breach. The CPSES cavity has a large spreading area ($70m^2$) so a shallow bed is likely. This is illustrated in Table 4.5-4. Considering that the core barrel and upper plenum internals are likely to stay in place, the debris depth is expected to be 2[illegible] cm (or 30 cm if an average corium density of 7000 Kg/m^3 is used). In any case, the possibility that the debris is not coolable cannot be neglected, particularly if the vessel fails at low pressure although, it is highly likely that it will be coolable for high pressure sequences where it is spread over the cavity $70m^2$ floor with some fraction even being expelled from the cavity. The stability is at issue if an impervious crust is formed. It is recognized that there is some disagreement in this area among experts in severe accident phenomena. However, experimental information and calculations are available in the literature and are used to provide the quantification of the likelihood of crust formation for this event node. The boundary conditions are obtained from the plant-specific assessments, e.g., depth of debris and coolant injection availability.

Injection of coolant through the breached vessel provides the most effective way of preventing concrete attack (absent crust formation) and of scrubbing vaporized fission product aerosols, if the debris is not in a coolable configuration. The systems-related events that contribute to the success branch depend: (a) on the PDS so the water availability prerequisite is satisfied, if core damage resulted from ECCS recirculation failure but not for an injection failure; and (b) passive actuation of the low pressure injection systems following RPV breach for high pressure PDS involving injection failure because, if the low pressure systems are initially available, as in some PDSs involving high RCS pressure, coolant addition to the debris is possible. As a practical matter, an examination of the PDS for which this would be possible has revealed this probability to be negligible (2E-05 for PDS 1H and 6E-4 for PDS 3H). Therefore, SNOLPI basic event, which is its complement, is assumed to have a 1.0 probability, and thus it is deleted from the CFE2 and CFE3 trees which are discussed below. The reason for the low values for automatic LPI injection probability at vessel failure is that CPSES Level I analysis considers the possibility of feed and bleed for success in those PDS and failure at that step occurs almost always due to failure of LPI to inject. In other words, failure of the LPI is mostly included in the PDS already.

The logic trees for this event are shown in Figures 4.5-9 for DC1, 4.5-10 for DC2 and 4.5-11 for DC3. DC1 and DC2 are essentially identical. Both are along the path of successful depressurization so they involve a higher likelihood that a coolable debris bed does not form than for DC3, which is along the path of a high pressure failure. The difference between DC1 and DC2 is that since DC1 is along the path of successful recovery, the SNOLPI event has a low probability in that tree. Conversely, it is assumed to have a 1.0 probability under the DC2 and DC3 trees for the reasons discussed in the previous paragraph. Again, two main issues are addressed in the DC logic tree. One is the physical configuration of the debris, whether it will be coolable or not coolable, regardless of whether there is an overlying pool. In the low pressure cases, this probability is dependent on whether a steam explosion occurs, hence the two events GDC1 and GDC2. If it does, the debris is much more likely to be dispersed and thus coolable. In the high pressure cases, the debris is likely to be dispersed, hence GDC3. The other aspect of debris coolability involves the presence of an overlying pool. It is assumed that if there is no overlying pool in the cavity (WTRPOOL and WTRPOOL2), then the debris is also not coolable. It should be noted that this constitutes a conservative simplification for PDS 1H, 3H and 5H where in the actual development, a pool would exist initially but would dry out prior to containment failure, at which point CCI would begin. The main difference between this situation and the situation where the debris is in a non-coolable configuration is that here, the debris would be coolable if water were re-introduced,

whereas in the other situation, it would not be. By lumping both cases, a higher number of late containment failures for these PDS is estimated. This conservatism exists for PDS 1H, 3H and 5H.

There is one noteworthy feature of the CET regarding the DC event. Along the early failure paths the question is not asked and the debris is assumed to be coolable. The reason is that the only possible causes for the early containment failure along those CET branches at CPSES would be either: (1) an alpha event or (2) HPME. If either one happens, it is further virtually certain that the debris would be so finely distributed in the containment that it would not get hot enough to cause core concrete attack, even if it were not covered by water. This is particularly obvious for CPSES when the Table 4.5-4 is taken into account and noting that the upper internals and core barrel should remain solid and have no associated decay heat.

Top Event CFL: Late Containment Failure Occurs

This event addresses the potential loss of containment integrity in the long term, after vessel breach and Core-Concrete Interaction (CCI) in the cavity if the debris is not coolable, or steam overpressurization if the debris is coolable. Potential failure modes considered at this stage of the core damage sequence include overpressure failure of the containment pressure boundary or basemat concrete attack. The conditions that contribute to containment overpressurization include boil-off of steam from the reactor cavity, given loss of heat removal function, and pressure and thermal challenges from hydrogen burning resulting from the long-term combustible gas formation in containment or non-condensible gas generation.

This event is included in the CET to characterize the long term behavior of the containment after core melt and vessel breach. Event CFL includes such events as overpressure failure of the primary containment, or basemat penetration. The success path here depends either on the recovery of systems that establish a complete heat transfer cycle from the core debris to the environment or on the availability of sprays as designated by containment safeguards bin "F" (see PDS definitions Section 4.3). One of the most important considerations is related to the time taken for gradual pressure build-up in the containment following vessel breach and ultimate disposition of the molten corium in the cavity and the containment floor.

The long-term containment pressurization is strongly influenced by the availability of decay heat removal systems (DHR), and this is included in the logic trees for event CFL. This event is related directly to the long-term reliability or recovery of the containment heat rejection function of the low pressure

systems, given that the core is recovered in-vessel or the debris is quenched ex-vessel. This event implies that a direct heat transfer cycle is established from the core to the environment, such that containment pressure rise is controlled. The implication of failure at this event node is that the containment pressure would increase and reach the ultimate capacity of the containment, challenging containment integrity.

The logic tree for this event node is shown in Figures 4.5-15 through 4.5-19. Trees CFL1, CFL3 and CFL5 apply to coolable debris situations where CCI does not occur and overpressure due to steam generation is likely unless sprays are operational. Trees CFL2, CFL4 and CFL6 apply where the debris is not coolable. In these trees, CCI occurs and basemat penetration is possible. Non-condensible gas overpressurization is most likely and hydrogen burns, with the additional amount generated from CCI, can fail the containment.

CFL1 is along the path of successful recovery in-vessel so it does not include containment failure mechanisms associated with CCI. In addition, the fact that recovery did occur is reflected in the probability of an early burn by setting SACSPREC to 1.0. Although BE QNOFAN allows for the possibility of fan cooler operation, these are not credited in the CPSES IPE and the BE is effectively flagged out in the quantification process. The benefits of fan coolers are addressed as a sensitivity issue for purposes of use in future accident strategies. The impact of fan coolers on the severe accident progression is twofold: (1) by preventing or delaying the containment pressure from reaching the spray set point, they extend the RWST duration; and (2) fan coolers can prevent containment failure due to overpressure, if all injection has failed as calculated in Section 5 of Reference 2. These advantages notwithstanding, fan coolers were not credited for risk abatement purposes in the base case of the CPSES IPE for the reasons discussed in Section 4.3.

CFL2 is along the path of a non-coolable debris so that only the CCI-related failure mechanisms are used with SACSPREC also set to 1.0, since recovery occurred in this path as well.

CFL3 is similar to CFL1 except that recovery did not occur prior to vessel failure so its probability of occurrence, SACSPREC3, must be considered for the purpose of evaluating early burn probabilities.

CFL4 is similar to CFL2 except that recovery did not occur prior to vessel failure so its probability of occurrence, SACSPREC3, must be considered for the purpose of evaluating early burn probabilities.

CFL5 is similar to CFL3 except that the time window for recovery of sprays and power is different. This translates into different recovery probabilities which are SACSPREC in CFL5 and SACSPREC3 in CFL3.

CFL6 is similar to CFL4 except that the time window for recovery of sprays and power is different. This translates into different recovery probabilities which are SACSPREC in CFL6 and SACSPREC3 in CFL4.

Top Event FPR: Fission Product Removal Fails

This event is included in the CET in order to characterize releases from the fuel (in-vessel and ex-vessel) into the containment, the fission product retention processes, and the potential release magnitudes to the environment should the containment fail. The question raised in this event node is related to the airborne fission product removal mechanisms within the containment system. Success implies reduction of the fission product release magnitudes to the environment. Failure implies that most of the fission products are ultimately released to the environment from the fuel and the containment without mitigation. The release magnitudes are likely to be relatively high should the containment fail early.

The issues considered in determining the success branch of this event node include mitigating the release mechanisms from the fuel (in-vessel or ex-vessel recovery) or ensuring in-containment removal processes. The capability of the containment to reduce release magnitudes is measured through availability of active systems (e.g., containment sprays), passive capabilities for natural depletion as a result of the long time period from release to containment failure, or scrubbing afforded by an overlying water pool. Success or failure of this event depends on previous event nodes in the CET and PDS boundary conditions defined by the accident sequence cut sets. The containment design mitigating features are examined to determine if fission products released from the fuel are contained within, if not permanently removed from, the containment atmosphere. These features include the containment sprays and a high ultimate pressure capacity.

This event node models the in-containment fission product removal process that might occur prior to containment failure. Both active and passive removal mechanisms were considered. The active systems include scrubbing of radioactive aerosols from the containment atmosphere by the sprays. Passive removal includes natural processes (e.g., gravitational settling, thermospheresis, or diffusiopheresis) that act on the radioactive airborne materials. The effectiveness of these natural removal processes in

reducing the fission product concentrations depends on the length of time that the containment integrity is maintained after release of fission products from the fuel.

The logic tree for fission product removal translates into four trees when the path dependencies are considered, as seen in Figure 4.5-1. FPR0, Figure 4.5-10, considers that only RCS retention mechanisms and containment sprays are available since recovery took place in this path. FPR1, Figure 4.5-11, considers the possibility of containment revolatization, which could potentially be mitigated by late spray action and the possibility of scrubbing by an overlying pool. FPR3, Figure 4.5-13, is similar to FPR1 except that an overlying pool always exists since in-vessel recovery occurred, followed by vessel failure. FPR2, Figure 4.5-12, is similar to FPR3 except that the probability that the containment sprays operate after vessel breach is different in the two cases: SNOSPRAY2 in FPR2 and SNOSPRAY21 in FPR3. This is because in FPR2 there was no recovery of power prior to vessel failure while in FPR3 there was. FPR4, Figure 4.5-14, is similar to FPR2 except that in FPR2 an overlying water pool always exists since this branch is along the path of a coolable debris; whereas in FPR4, which is in the non-coolable debris path, an overlying pool may or may not exist and this probability is incorporated into the tree.

Top Event CFM: Containment Failure Modes

This event is included in the CET to characterize the impact of containment failure modes as they affect the duration and mitigation of the fission product source terms.

This tree is specialized into three path-dependent trees: CFM1, Figure 4.5-21; CFM2, Figure 4.5-22; and CFM3, Figure 4.5-23. CFM1 is simply the probability that the containment will fail by rupture rather than by leakage, given that it fails late. As previously discussed, late failures are highly likely to be by leakage so this event probability has a low value as discussed in the quantification Section 4.5.6. CFM2 is the probability that it will fail by rupture given: (1) an early failure and (2) the RCS failed at low pressure. CFM3 is the probability that it will fail by rupture given an early failure with the RCS having failed at high pressure.

CET End-States or Release Modes

The various progression paths in the CETs lead to unique release end-states. These are shown as "A", "B", "C", and "D" release modes in the CET in Figures 4.5-1. These release mode labels are the following:

- "A" end-states are recovered in-vessel (vessel breach is precluded)

- "B" end-states are such that the vessel fails, but core concrete interaction is precluded and steam overpressure fails the containment.

- "C" end-states include late containment failures due to CCI.

- "D" end-states include early containment failures without ex-vessel vaporization release (CCI is precluded). As discussed under CFE above, this is the most likely release for early failure.

Table 4.5-5 summarizes the possible end-states of the CET for the spectrum of core melt accident sequences.

The probabilities of each of the 44 end-states shown in Figure 4.5-1 were determined for each PDS. However, the 44 end-states were later (Section 4.7) binned into 13 release categories and the release fractions were calculated for the 13 release categories in order to make the source term calculations more tractable.

Table 4.5-1: ISLOCA Initiator Frequencies for Various Pathways

ISLOCA INITIATOR	ISLOCA Frequency Small (Relief Valve) LOCA	ISLOCA Event Classification	Overpressurization: piping failure/ pump seal failure	ISLOCA Event Classification
Accumulator	9.78E-03	Class i	2.71E-05/NA	Class iii
RH Suction Line	9.32E-05	Class i	1.47E-07/7.08E-06	Class iv
Excess Letdown Line	1.30E-05	Class i	1.19E-10/NA	Class iv
Normal Letdown Line	2.27E-03	Class i	4.77E-10/NA	Class iv
Low Pressure Injection Cold Legs	1.44E-05	Class ii	2.22E-08/1.47E-07	Class iv
Low Pressure Injection Hot Legs	2.22E-07	Class ii	6.70E-11/8.07E-09	Class iv
Intermediate Pressure Injection Cold Legs	1.44E-05	Class ii	1.23E-09/1.47E-07	Class iv
Intermediate Pressure Injection Hot Legs	4.44E-07	Class ii	7.57E-12/8.07E-09	Class iv

Table 4.5-2: ISLOCA Initiator Frequencies for CPSES

Event No.	LOCA Type / Line Break Size	ESF Equipment Unavailable	ISLOCA Initiating Frequency	ISLOCA Event Classification
1	Small Break Less Than Or Equal To 2"	N/A	5.96E-10	Class iv
2	Small Break Less Than Or Equal To 2"	One Train SI	1.48E-05	Class ii
3	Small Break Less Than Or Equal To 2"	One Train RH	1.46E-05	Class ii
4	Medium Break Greater Than 2", But Less Than 6"	Both Trains SI	1.24E-09	Class iv
5	Large Break Greater Than Or Equal 6"	Both Trains RH	3.70E-08	Class iv
6	Large Break Greater Than Or Equal 6"	One Train RH	1.32E-07	Class iv
7	Medium Break Greater Than 2", But Less Than 6"	RWST	9.94E-09	Class iv
8	Large Break Greater Than Or Equal 6"	RWST	4.21E-09	Class iv
9	Small Break (pump seals) Less Than Or Equal to 2"	Both Trains RH	7.24E-6	Class iv
10	Small Break (pump seals) Less Than Or Equal to 2"	Both Trains SI	1.55E-07	Class iv

Table 4.5-3: Core Damage Frequencies and Their Functional Sequences

Event No.	ESF Equipment Unavailable	ISLOCA Core Damage Frequency	ISLOCA Functional Sequence
1	N/A	5.96E-10	SCM1
2	One Train SI	7.15E-10	SCM1
3	One Train RH	1.06E-08	SCM1
4	Both Trains SI	1.24E-09	MCM2
5	Both Trains RH	3.70E-08	ACM2
6	One Train RH	3.71E-09 7.35E-10	ACM1 ACM2
7	RWST	9.94E-09	MCM2
8	RWST	4.21E-09	ACM2
9	Both Trains RH	8.69E-08	SCM1
10	Both Trains SI	4.94E-10	SCM1

Table 4.5-4: Estimate of Debris Bed Thickness

Component	Mass (kg)	Density (kg/m^3)	Volume (m^3)	Contribution to Debris Bed Thickness (m)
UO_2	100,990	10,400	9.70	0.14
Zr	21,316	6560	3.25	0.05
Support Plate	23,415	7,888	2.97	0.04
Core Barrel I	51,756	7,888	6.56	0.09
Core Barrel II	14,939	7,888	1.89	0.03
Upper Pl. Intern	38,630	7,888	4.89	0.07
TOTAL				0.42

Table 4.5-5: Description of CET End-States

CET END-STATES	DESCRIPTION
A1	Recovered in-vessel, late containment failure, in-vessel fission product release not mitigated
A2	Recovered in-vessel, late containment failure, in-vessel fission product release not mitigated
B1	Recovered ex-vessel, late containment failure, in-vessel fission product release mitigated
B2	Recovered ex-vessel, late containment failure, in-vessel fission product release not mitigated
B3	No CCI, late containment failure, in-vessel fission product release mitigated by sprays
B4	No CCI, late containment failure, in-vessel fission product release not mitigated
B5	No CCI, late containment failure, in-vessel and late fission product release mitigated by sprays
B6	No CCI, late containment failure, in-vessel and late fission product release not mitigated
C1	CCI occurs, late containment failure, ex-vessel fission product release mitigated by overlying pool, in-vessel release mitigated by sprays
C2	CCI occurs, late containment failure, ex-vessel fission product release mitigated by overlying pool, in-vessel release not mitigated
C3	Significant CCI occurs, late containment failure, in and ex-vessel fission product release mitigated by sprays
C4	Significant CCI occurs, late containment failure, in- and ex-vessel fission product release not mitigated.
C5	Moderate CCI occurs, late containment failure, in- and ex-vessel fission product release mitigated
C6	Moderate CCI occurs, late containment failure, in- and ex-vessel fission product release not mitigated
D1	No CCI, early containment failure, in-vessel fission product release not mitigated
D2	No CCI, early containment failure, in-vessel fission product release not mitigated
D3-D5	No CCI, early containment failure, in-vessel and late fission product release mitigated
D4-D6	No CCI, early containment failure, in- and ex-vessel fission product release not mitigated

NOTE: The end-states are further characterized as Leakage (L) or Rupture (R) to indicate the duration of fission product releases to the environment. NCF stands for No Containment Failure (Figure 4.5-1)

Figure 4.5-1: Containment Event Tree

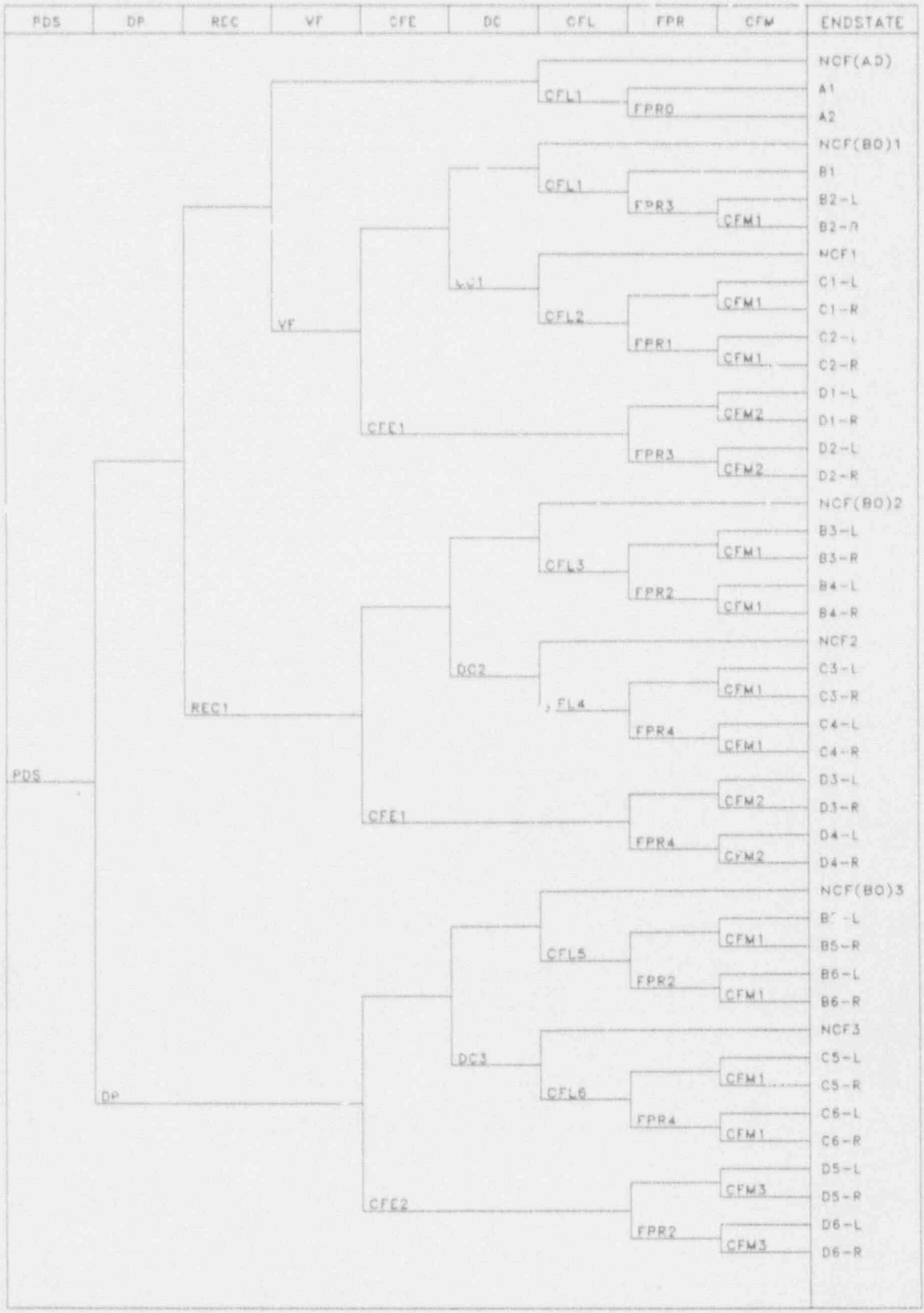

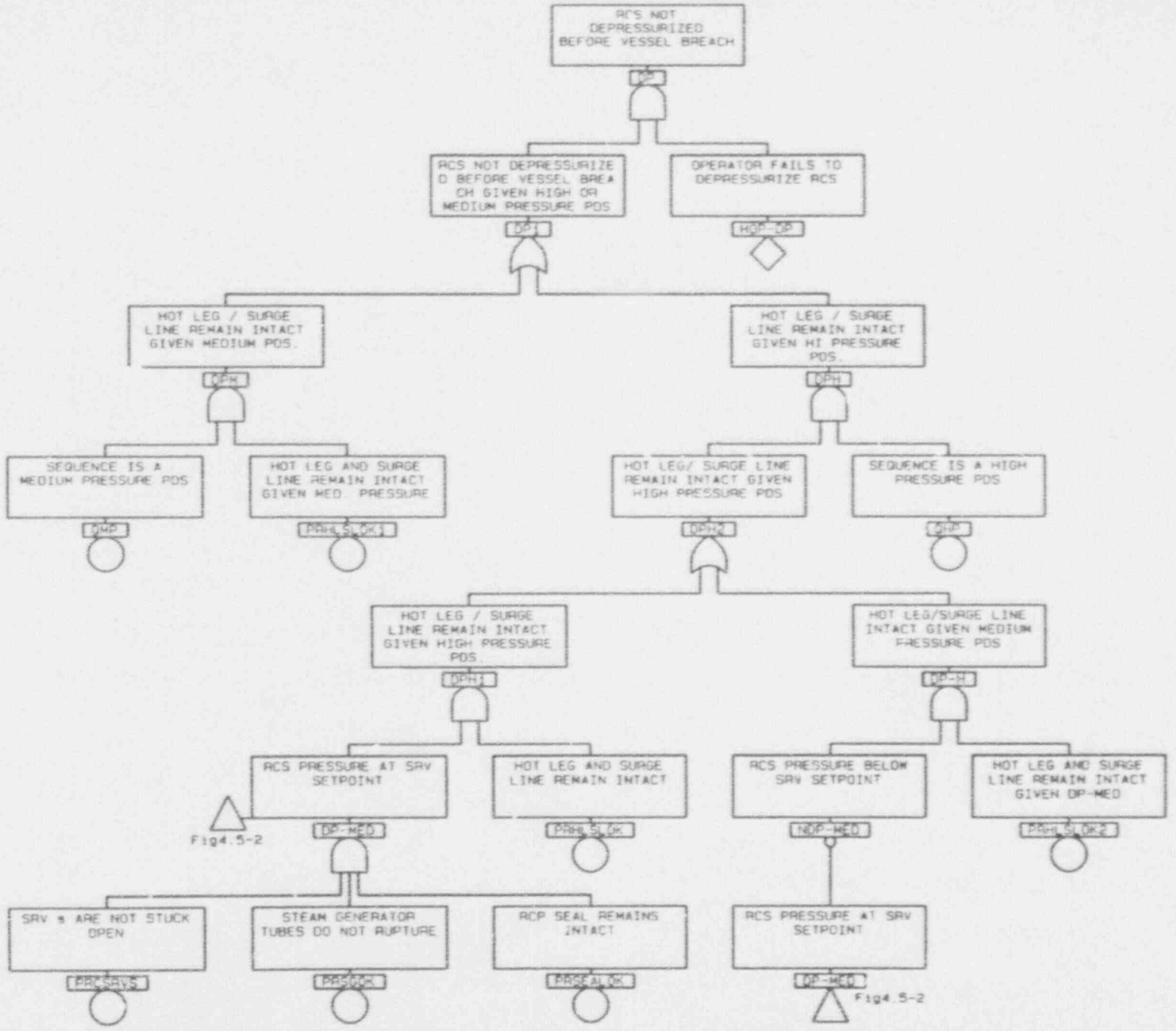

MASTER CONTAINMENT FAULT TREE	CP3.CAF	10-23-92	Fig4.5-2

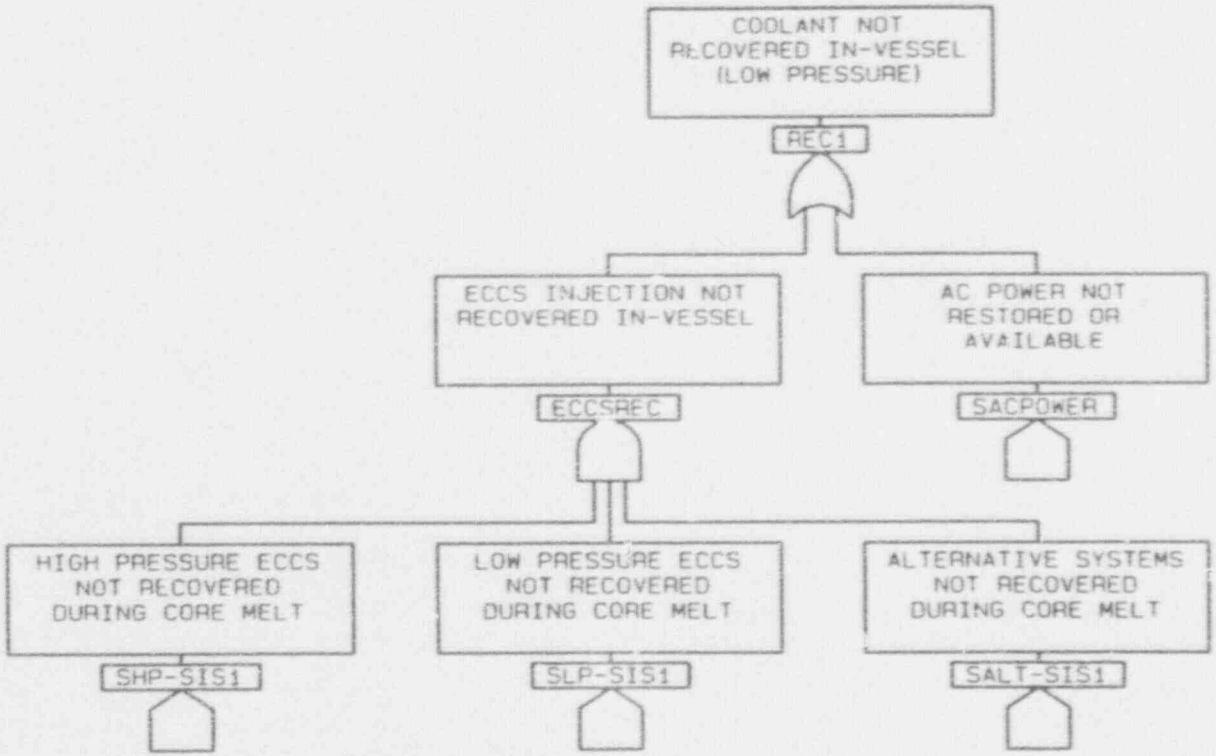

MASTER CONTAINMENT FAULT TREE | CP3.CAF | 10-23-92 | Fig4.5-3

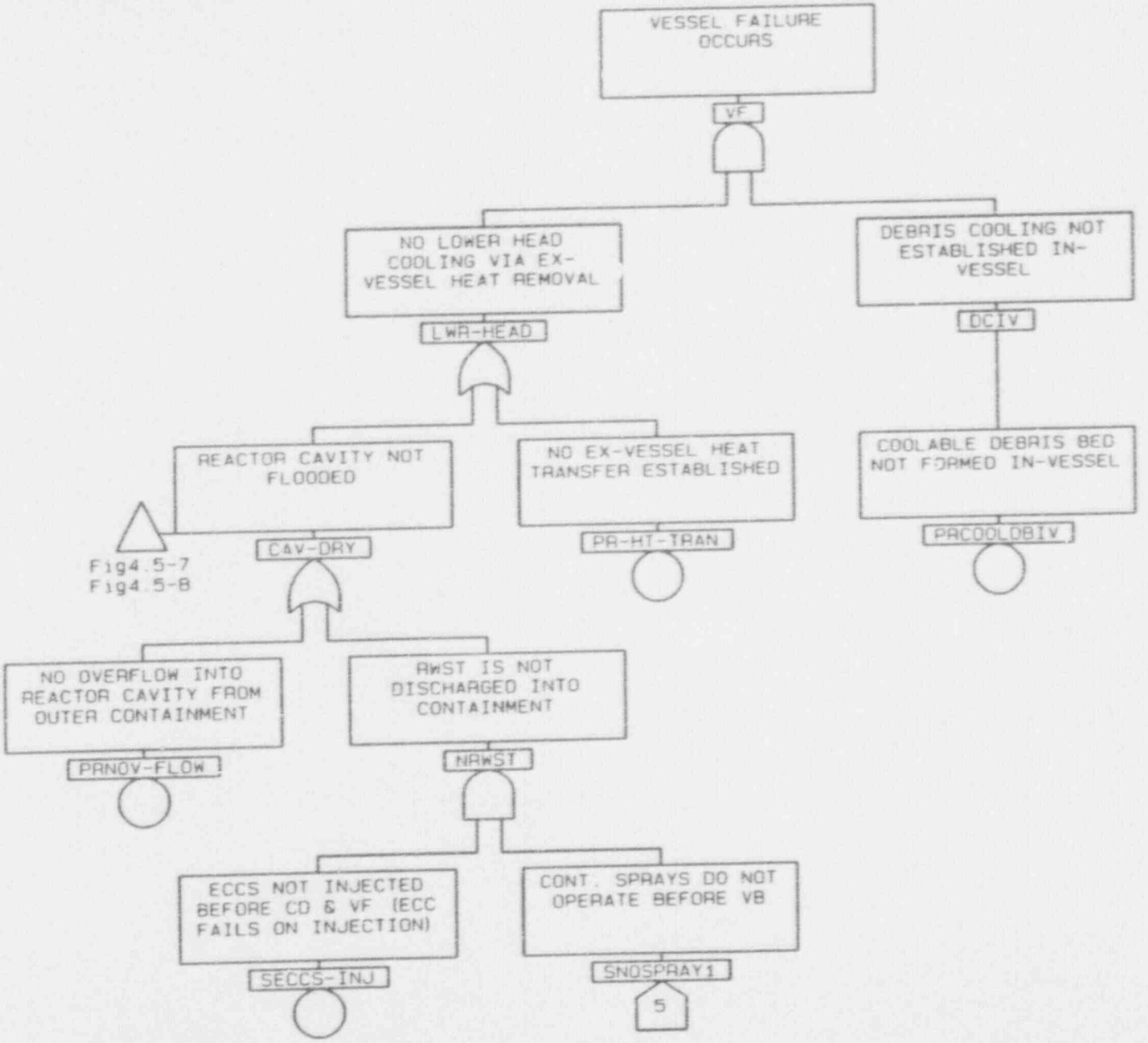

MASTER CONTAINMENT FAULT TREE | CP3.CAF | 10-23-92 | Fig4.5-4

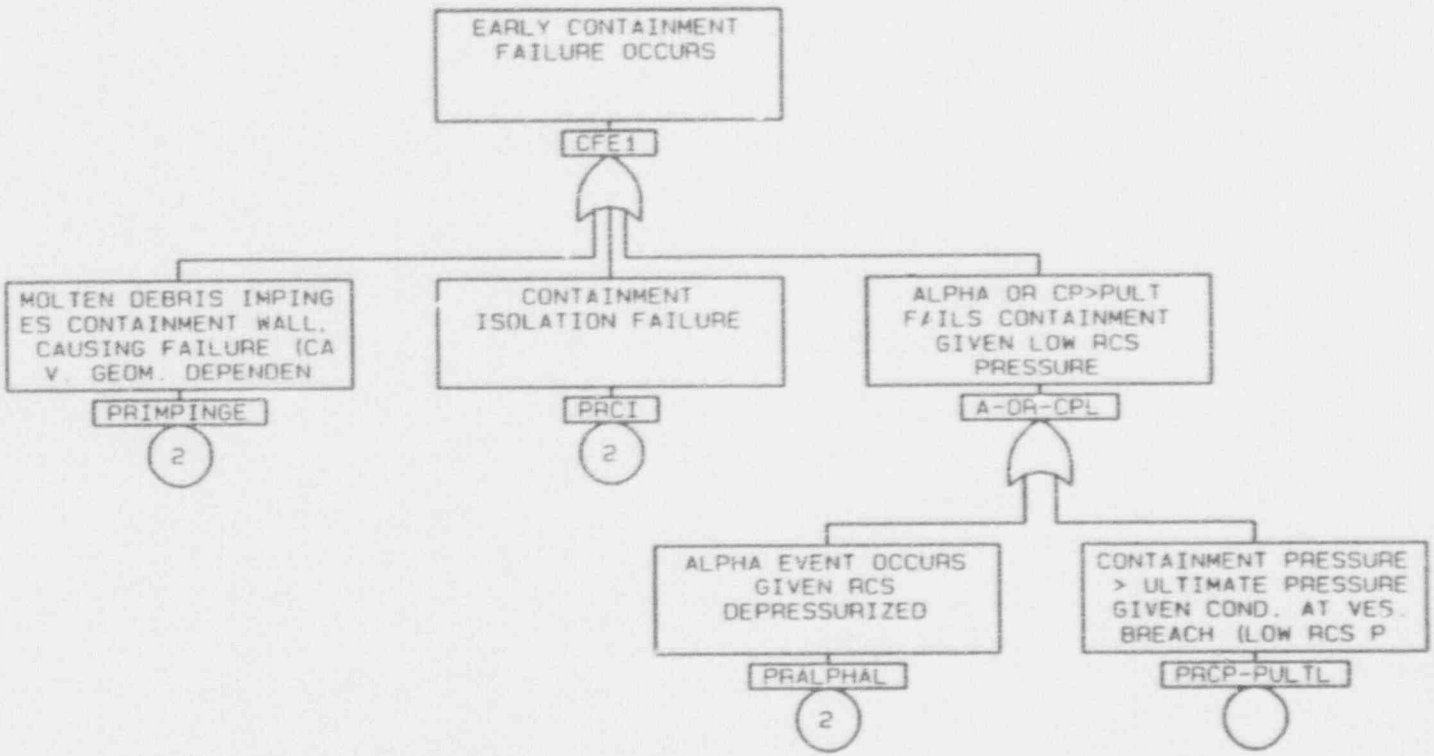

MASTER CONTAINMENT FAULT TREE | CP3.CAF | 10-23-92 | Fig4.5-5

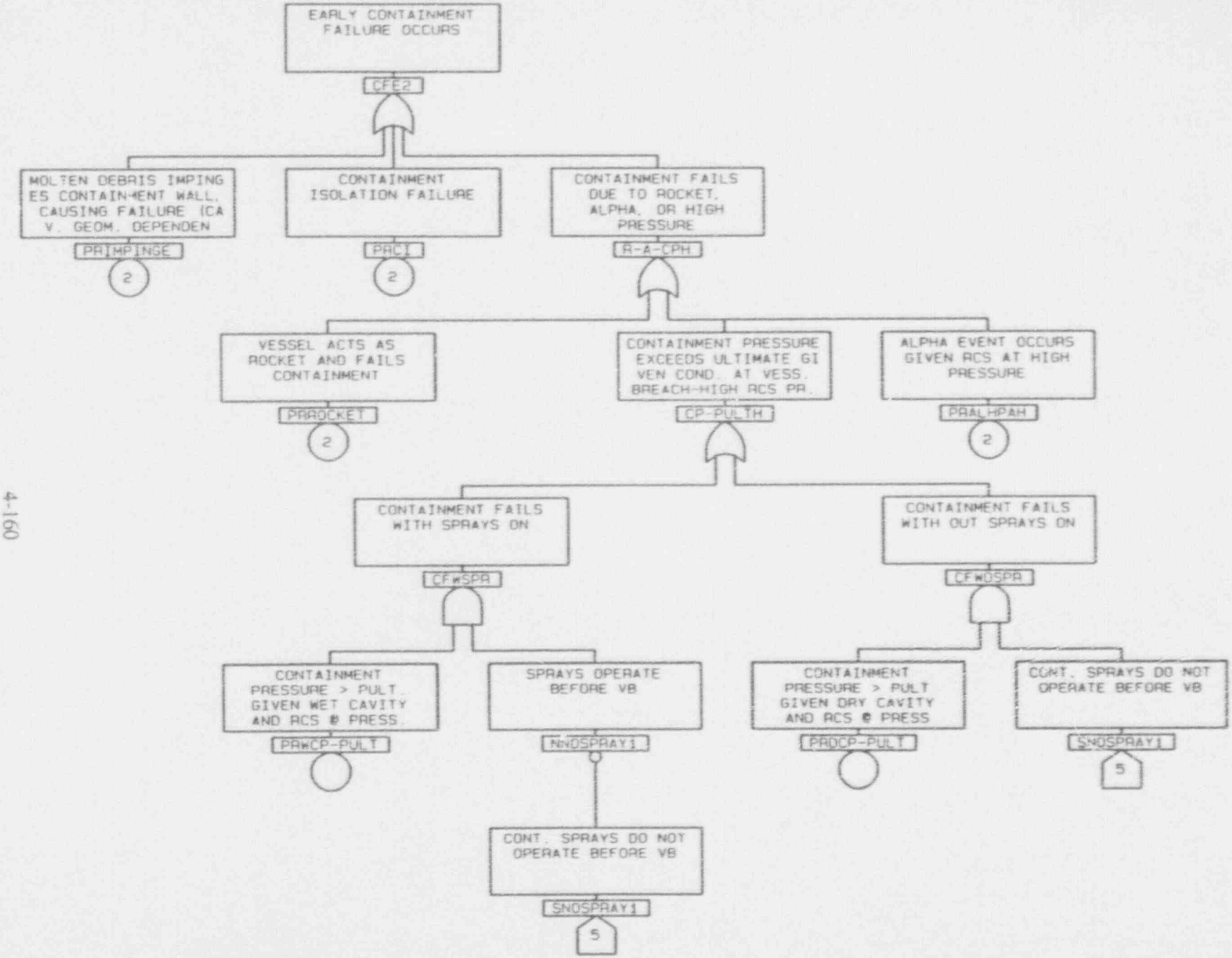

MASTER CONTAINMENT FAULT TREE	CP3.CAF	10-23-92	Fig4.5-6

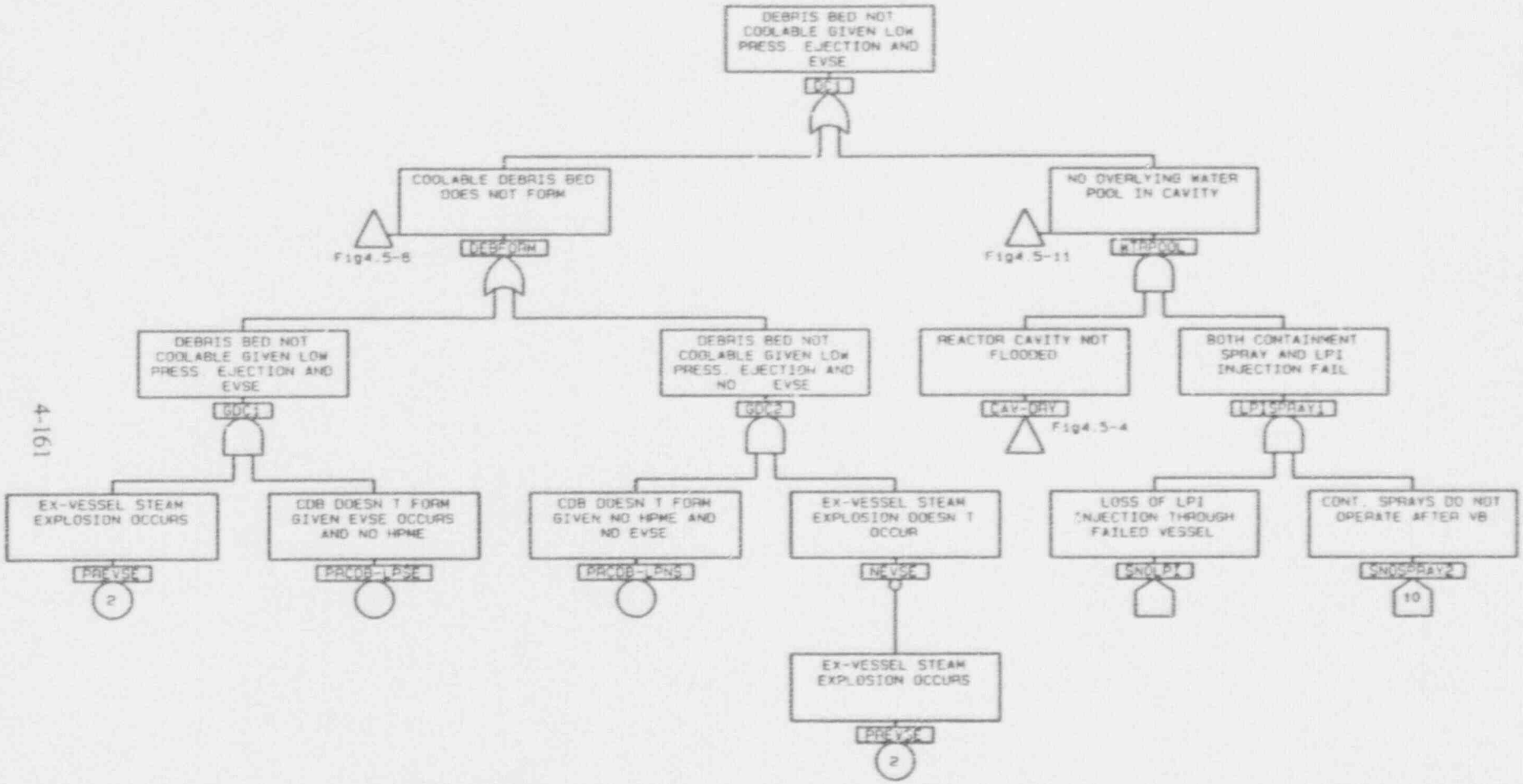

MASTER CONTAINMENT FAULT TREE	CP3.CAF	10-23-92	Fig4.5-7

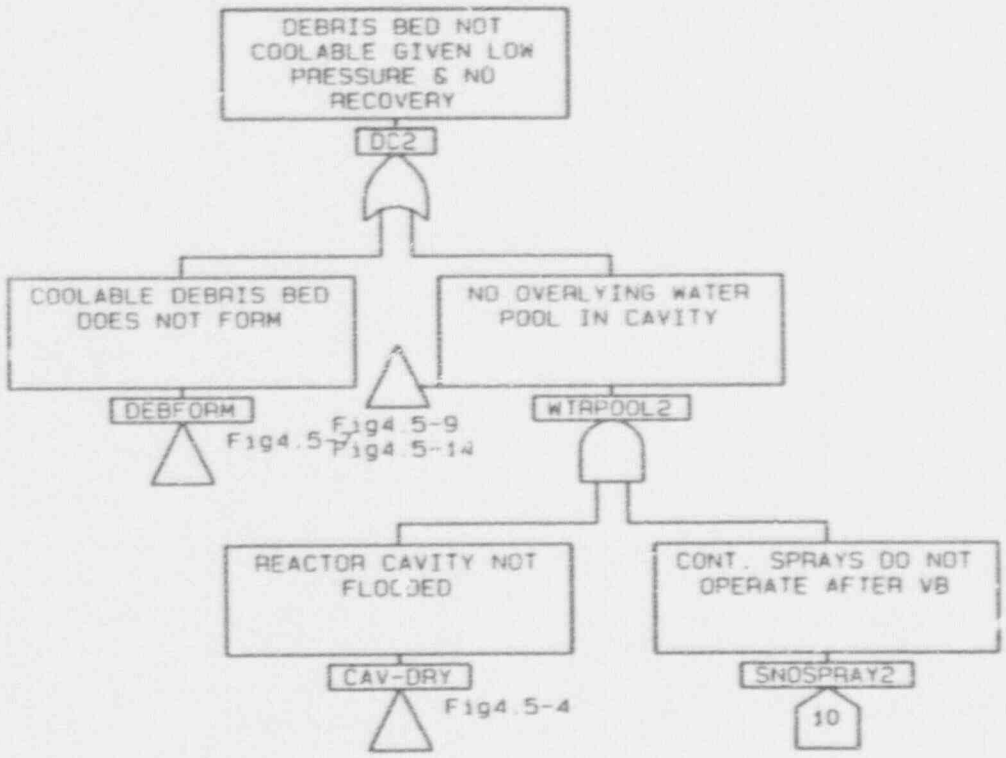

MASTER CONTAINMENT FAULT TREE	CP3.CAF	10-23-92	Fig4.5-8

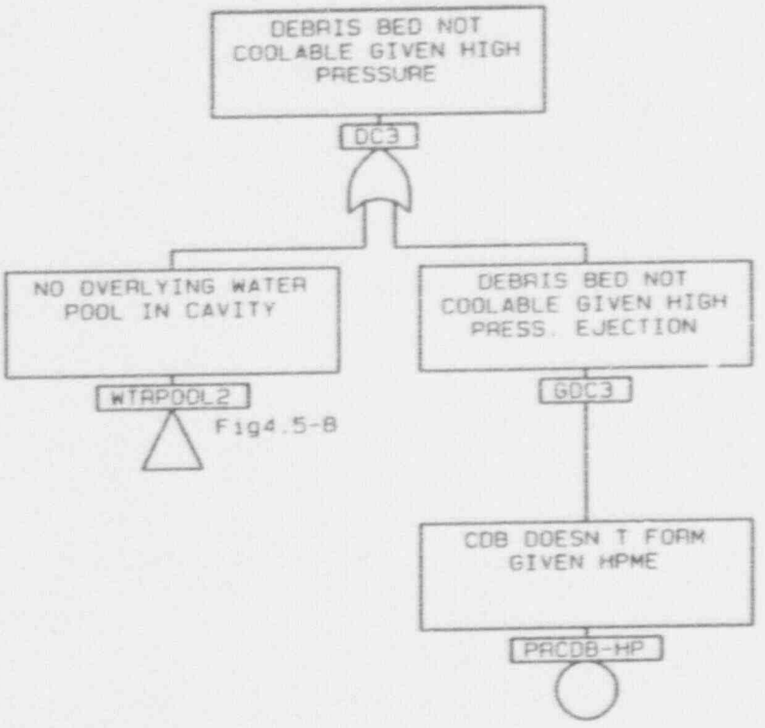

MASTER CONTAINMENT FAULT TREE	CP3.CAF	10-23-92	Fig4.5-9

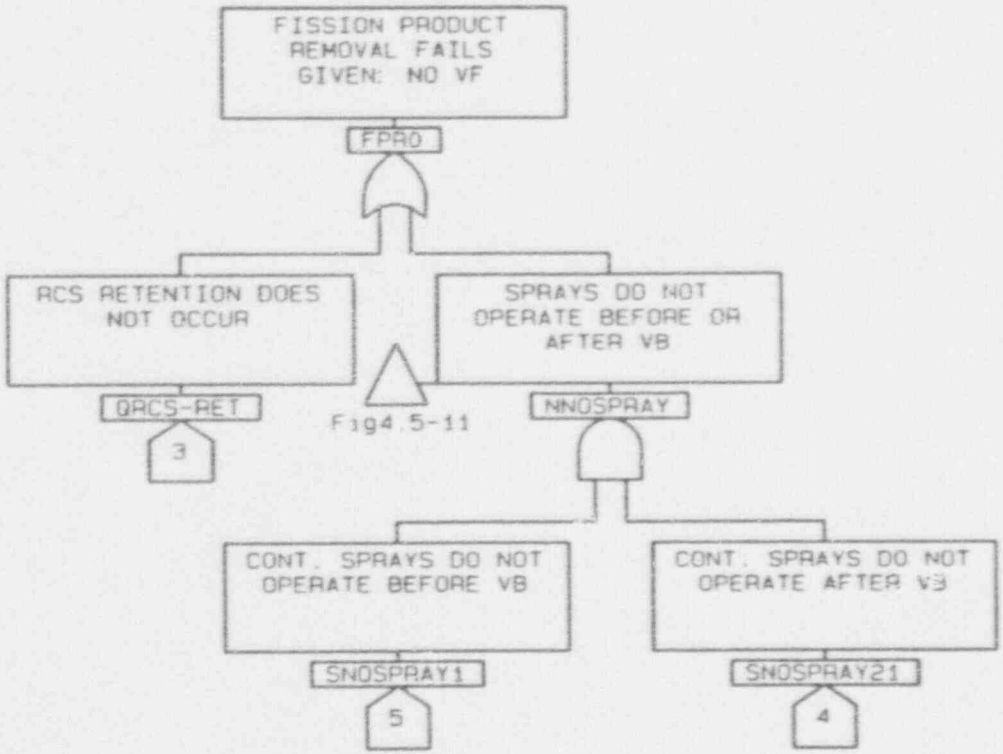

Fig4.5-11

MASTER CONTAINMENT FAULT TREE	CP3.CAF	10-23-92	Fig4.5-10

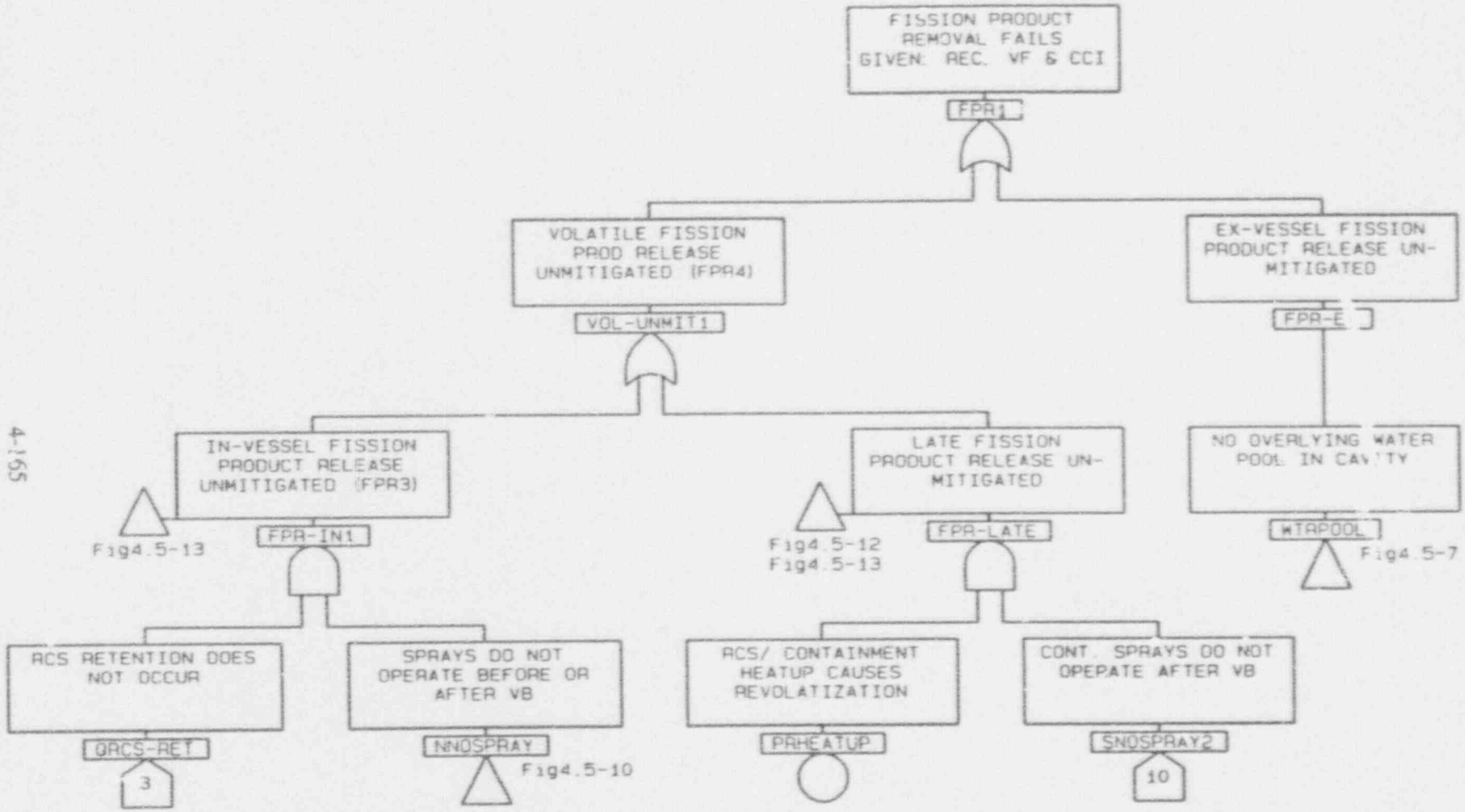

MASTER CONTAINMENT FAULT TREE	CP3.CAF	10-23-92	Fig4.5-11

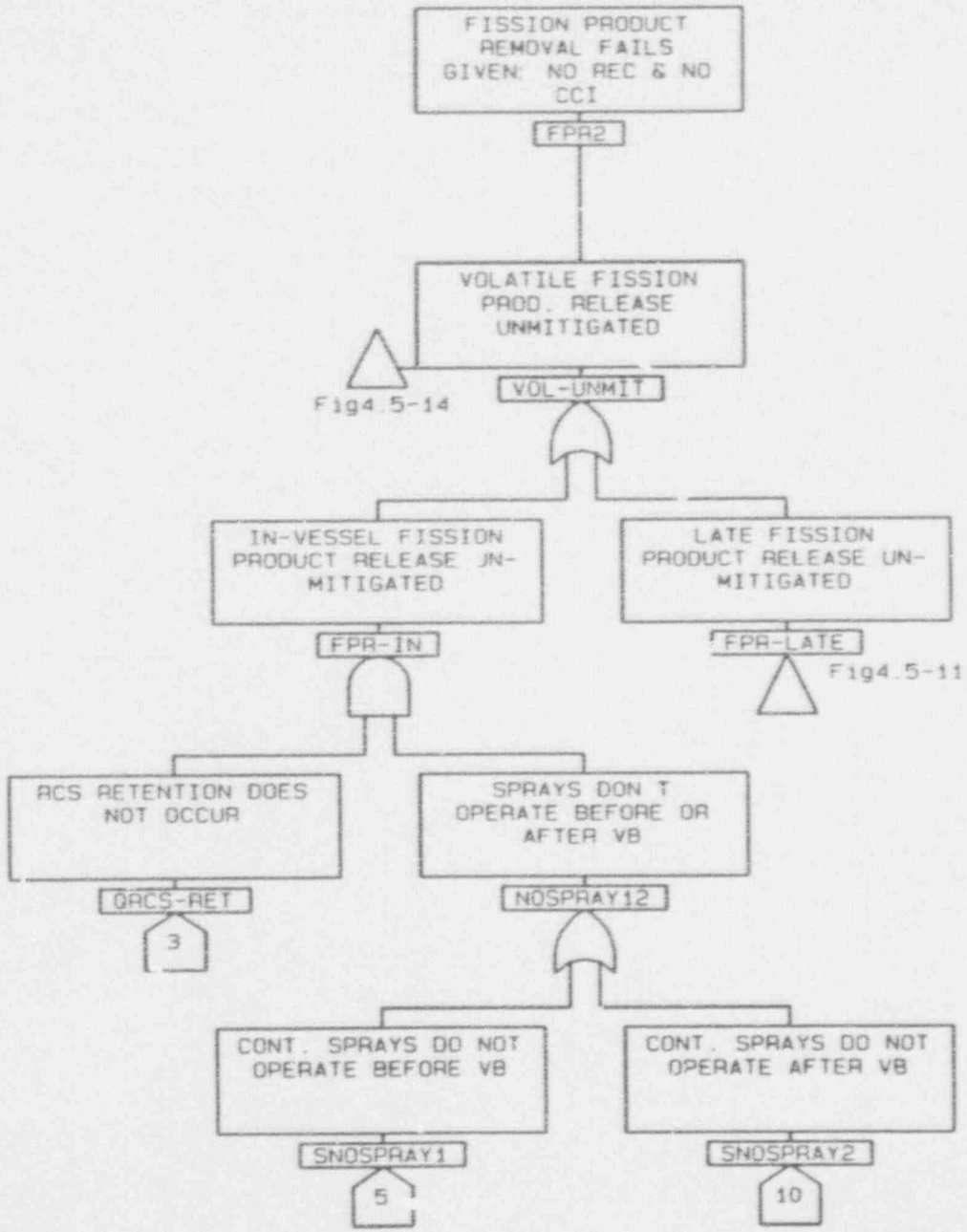

MASTER CONTAINMENT FAULT TREE	CP3.CAF	10-23-92	Fig4.5-12

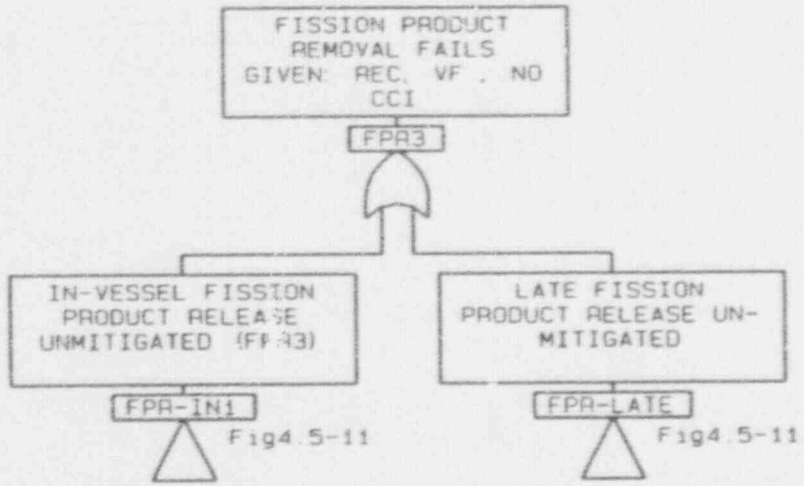

MASTER CONTAINMENT FAULT TREE	CP3.CAF	10-23-92	Fig4.5-13

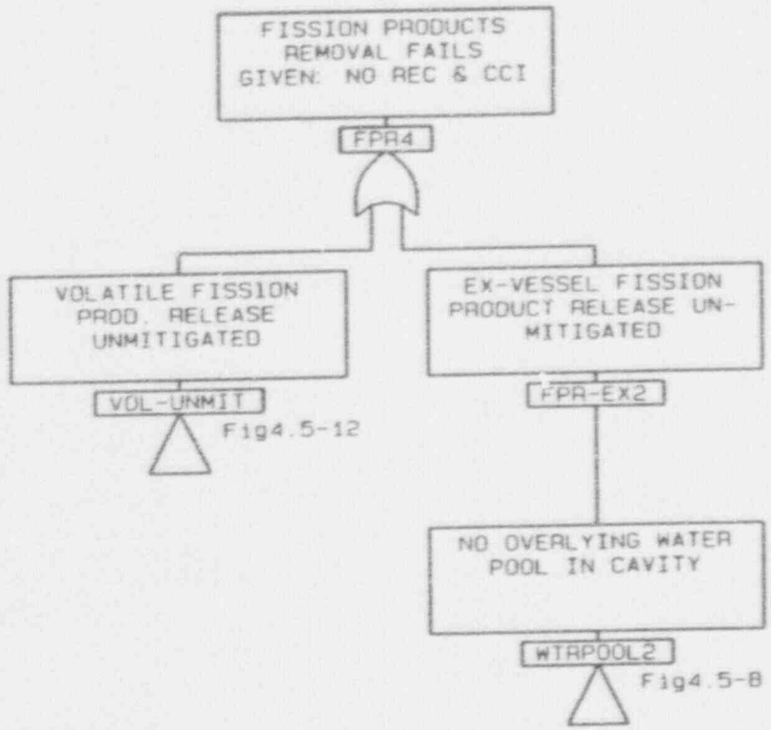

MASTER CONTAINMENT FAULT TREE	CP3.CAF	10-23-92	Fig4.5-14

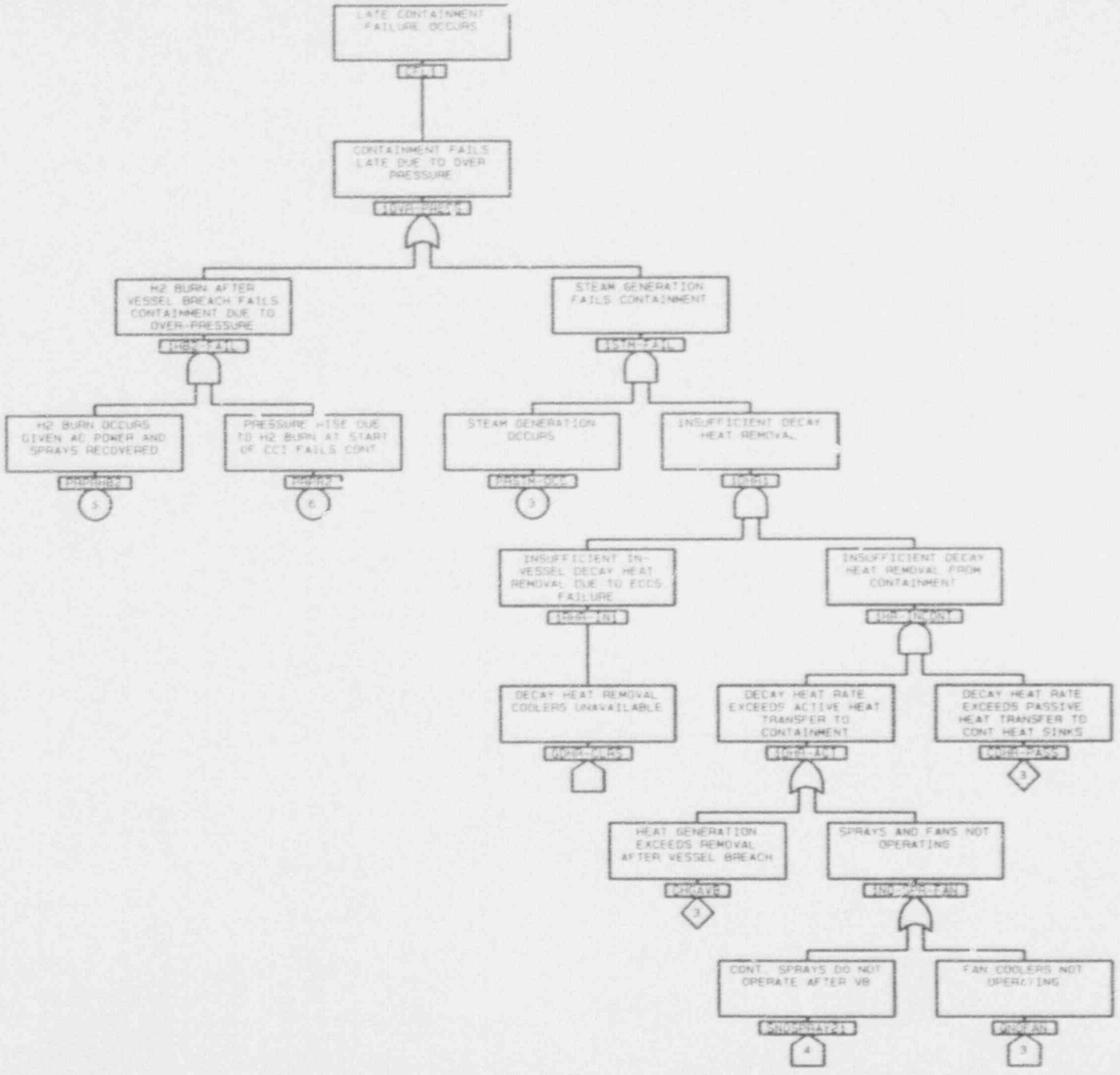

MASTER CONTAINMENT FAULT TREE	CP3.CAF	10-23-92	Fig4.5-15

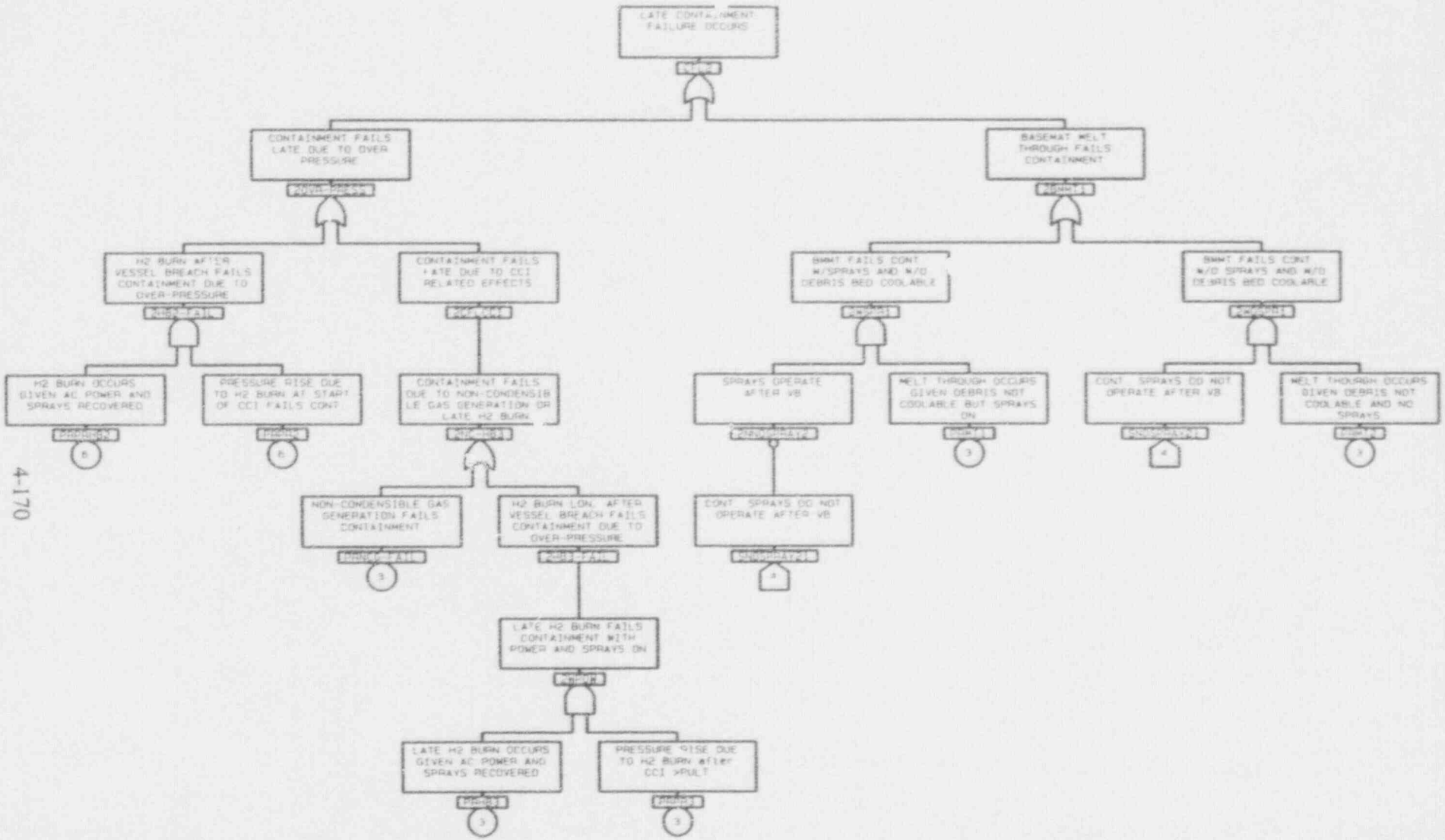

MASTER CONTAINMENT FAULT TREE	CP3.CAF	10-23-92	Fig4.5-16

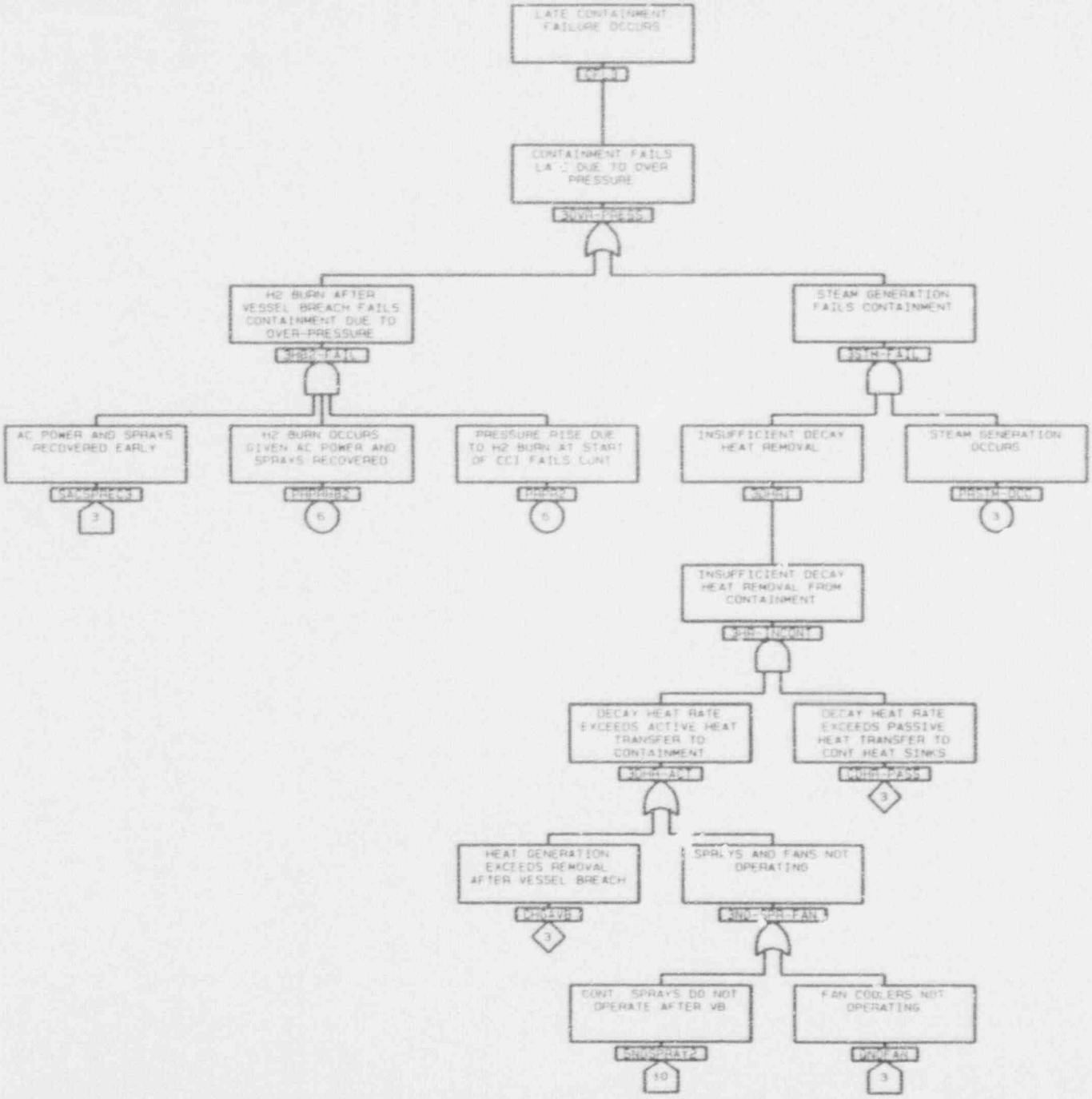

MASTER CONTAINMENT FAULT TREE | CP3.CAF | 10-23-9^ | Fig4.5-17

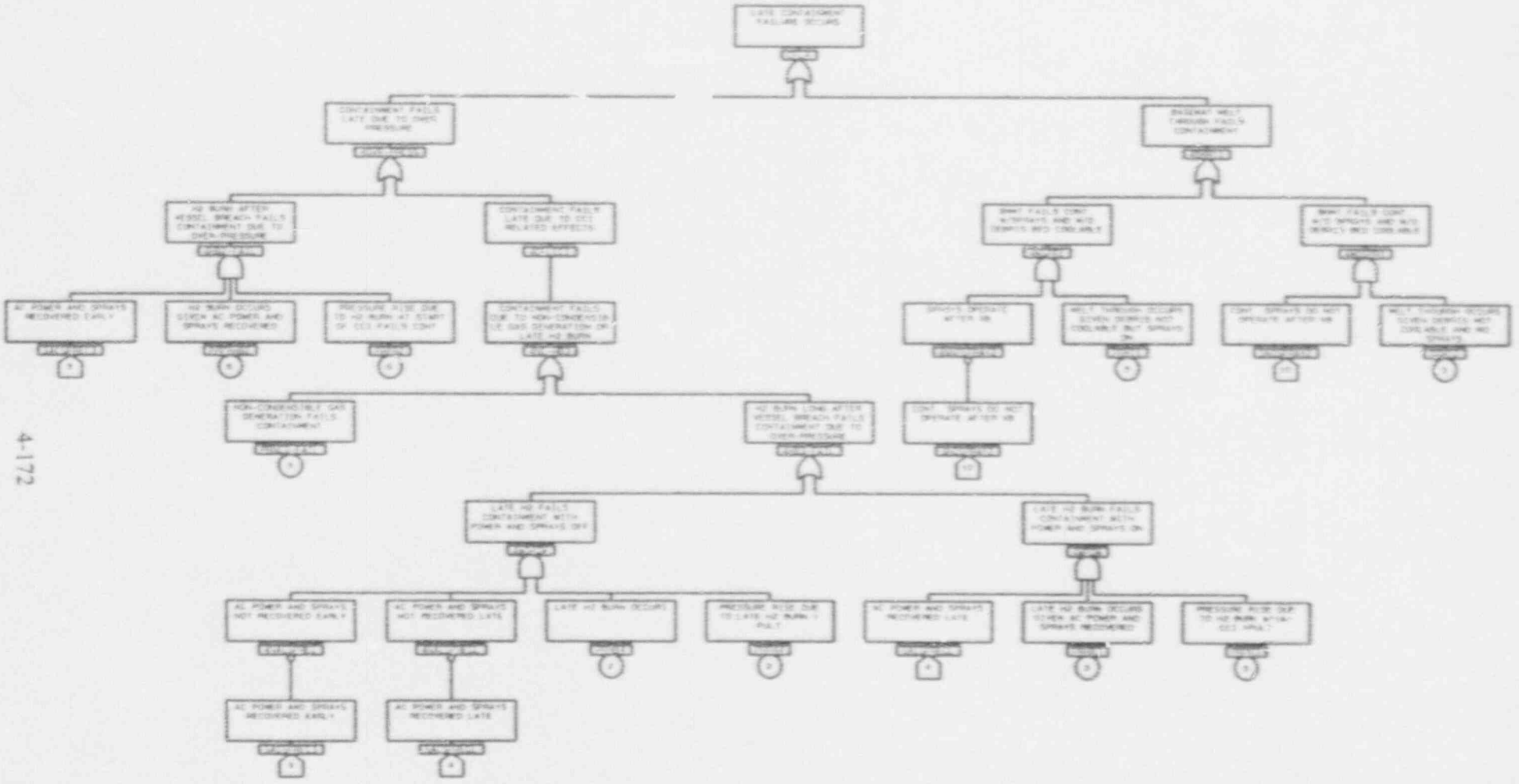

4-172

MASTER CONTAINMENT FAULT TREE	CP3.CAF	10-23-92	Fig4.5-18

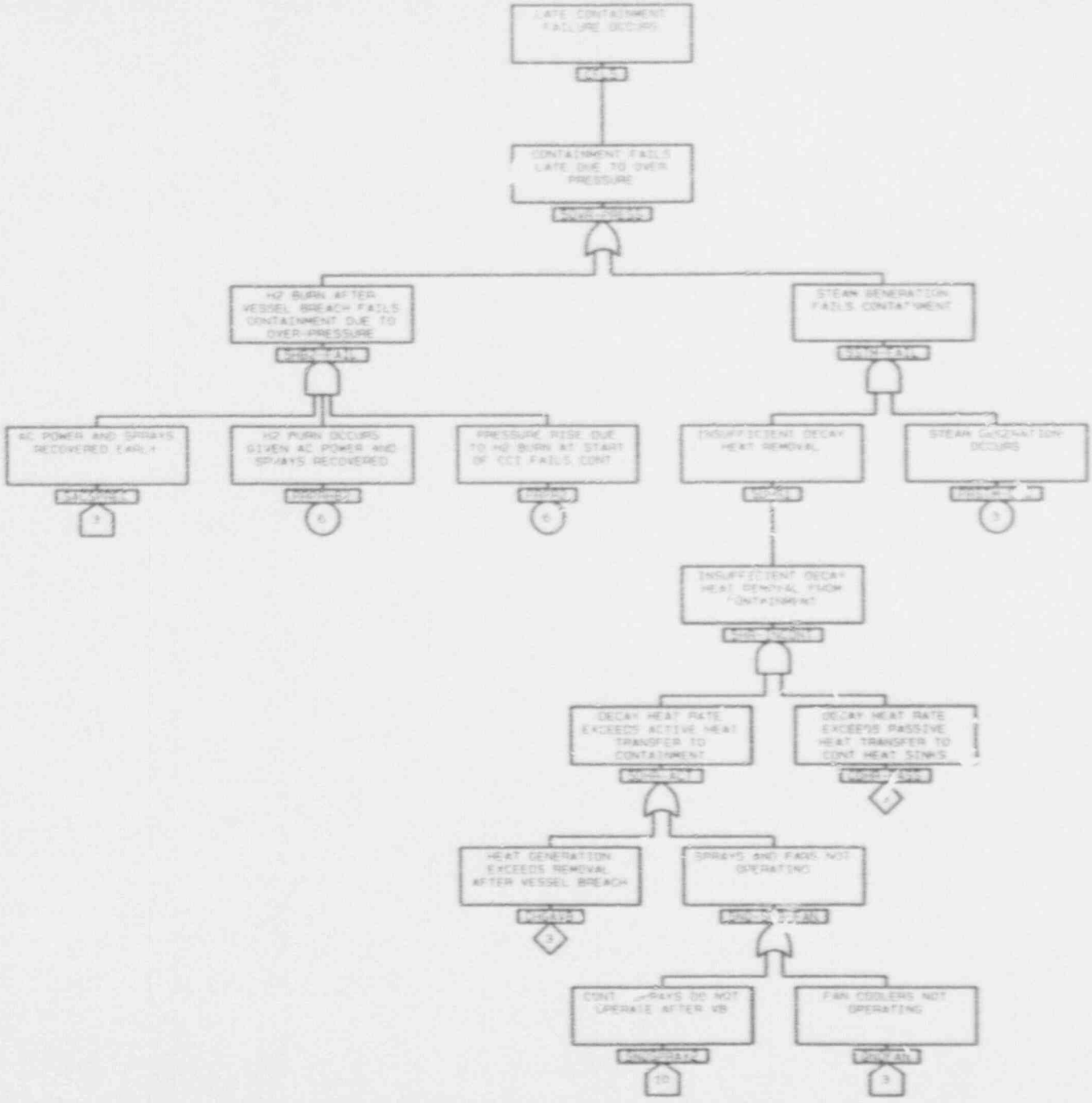

MASTER CONTAINMENT FAULT TREE	CP3.CAF	10-23-92	Fig4.5-1

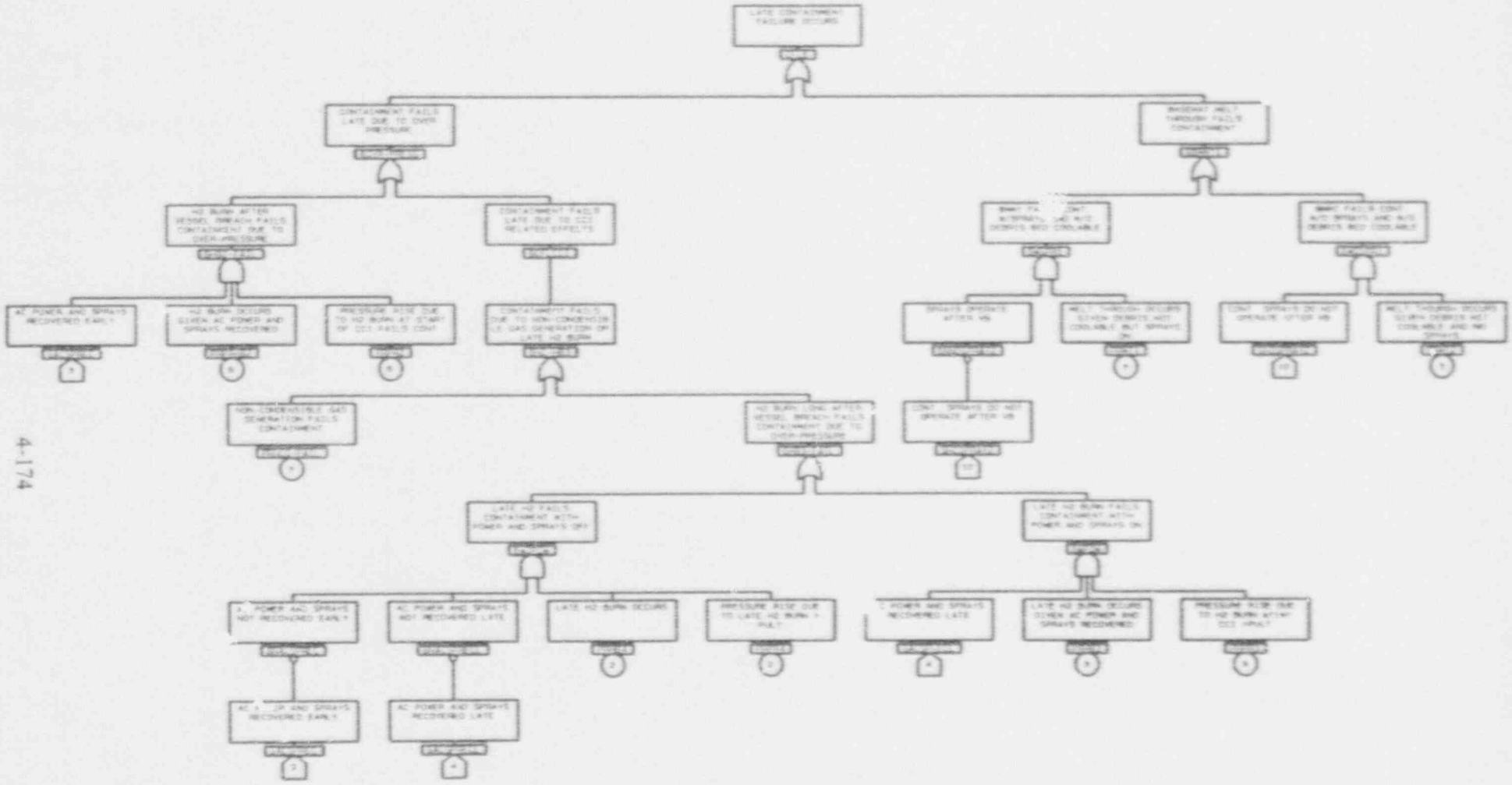

MASTER CONTAINMENT FAULT TREE | CP3.CAF | 10-23-92 | Fig4.5-20

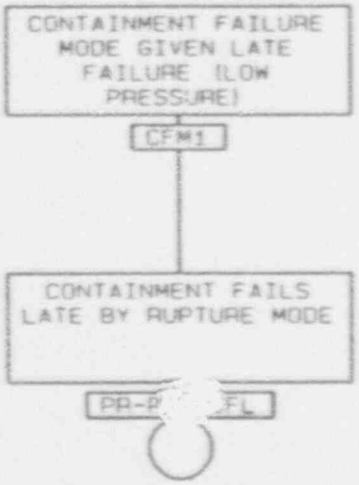

MASTER CONTAINMENT FAULT TREE	CP3.CAF	10-23-92	Fig4.5-21

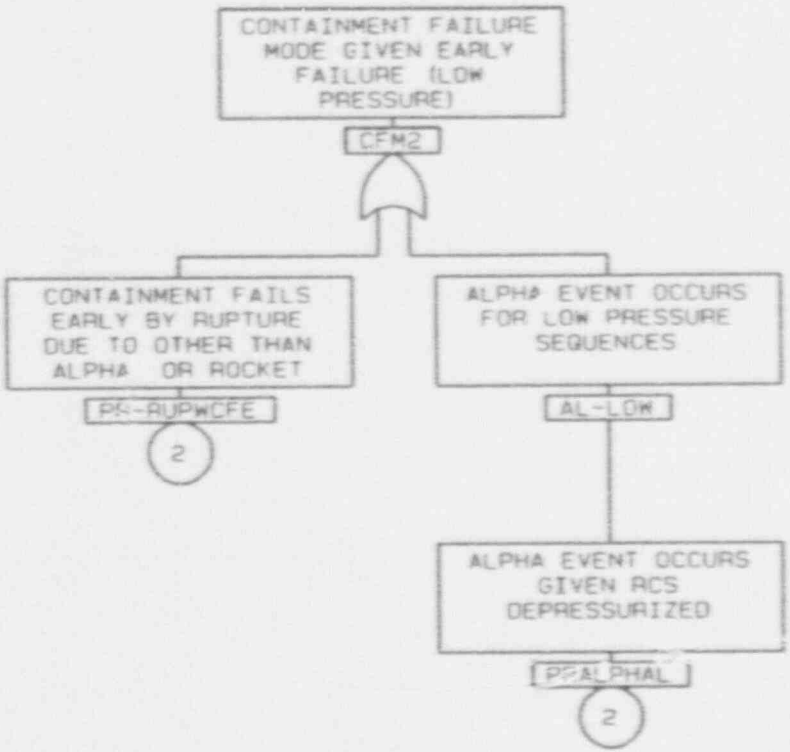

MASTER CONTAINMENT FAULT TREE	CP3.CAF	10-23-92	Fig4.5-22

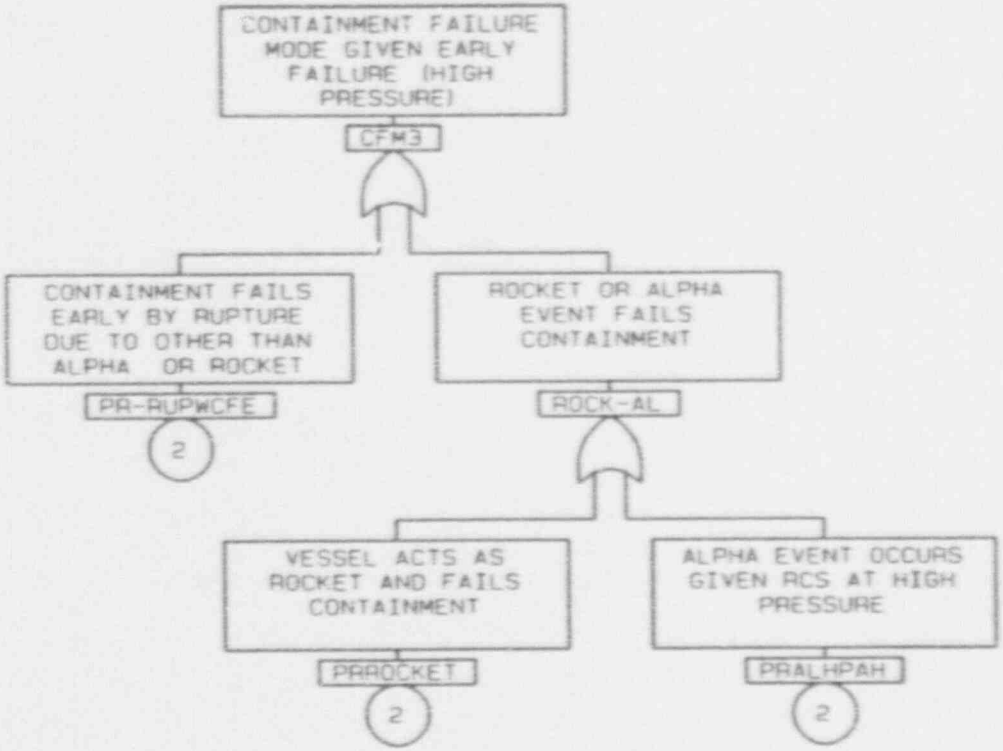

MASTER CONTAINMENT FAULT TREE	CP3.CAF	10-23-92	Fig4.5-23

4.6 Accident Progression and CET Quantification

Section 4.6.1 presents the conditional quantification of the CETs for each PDS, i.e, the method and results for determining CET end-state probability values assuming each PDS has occurred (1.0 probability for the first CET event, Figure 4.5-1).

Section 4.6.2 presents the coupling of the PDS frequencies determined in the binning process (Section 4.3) with the conditional CET probabilities determined in Section 4.6.1. It then goes on to rank the risk importance of the PDS, determines representative accident sequences and discusses accident progressions.

Section 4.6.3 describes the effect of the phenomenological uncertainties listed in NUREG-1335 Section 2.2.2.6 as significant, and expands that list to include a discussion on other uncertainties also considered important. The purpose of the uncertainties discussion is to show that the potential masking of vulnerabilities due to controversial assumptions regarding the likelihood of certain phenomena doesn't occur and that the findings of Section 4.6 are robust and insensitive to these uncertainty issues.

4.6.1 CET Quantification

The basic structure of the CPSES CETs is given in Figure 4.5-1 (Section 4.5) and the supporting logic trees of Figures 4.5-2 through 4.5-23. That basic structure is applied to each non-bypassed, successfully isolated containment PDS, which are listed in the top line of Table 4.3.3. Thus, there is one CET for each of those PDS.

There are two steps in the CET quantification process: (1) the determination of basic event (BE) probabilities and (2) the computation, interpretation and presentation of results for the conditional probabilities.

4.6.1.1 Determination of BE probabilities: Example, PRWCP-PULT for PDS 2H = 0.42

The first step in CET quantification is the determination of the basic event (BE) probabilities. These BEs are the events shown in Figures 4.5-2 through 4.5-23 that are flagged with either a circle (phenonmena-related), or a pentagon (system-related), or a diamond (operator action - related). Although the

determination of some of these BEs is trivial, when all PDS are considered, there are over one thousand BE values defined. Thus, the justification of each is not provided in this submittal but is available elsewhere (Ref. 8). Nevertheless, an example is given here in order to illustrate the process by which some BE probabilities are evaluated. This processes can be very detailed for some BE. A good example is presented below for PDS 2H. It is the determination of the BE probability value for PRWCP-PULT, under top event CFE2 on Figure 4.5-6. That BE reflects the probability that high pressure melt ejection (HPME) phenomena occurring at the time of vessel failure at high pressure will lead to a pressure spike that is greater than the containment capacity. It includes the effects of combustion of non-condensibles and direct containment heating (DCH) separately and combined, as well as their probability of occurrence.

Although the rapid thermal transient at vessel failure is not typically calculated by MAAP to induce the extremely high pressures and temperatures that threaten containment integrity, NUREG-1150 suggests that higher values than those computed with MAAP for the pressure rise are possible.

In the present assessment, the NUREG-1150 methodology was combined with plant specific MAAP analyses by adding the NUREG/CR-4551 pressure rise estimates for Zion (Table 4.6-1, (Ref. 1)), which is similar in volume to CPSES, to the initial containment pressure at vessel failure, determined through MAAP analyses for PDS 2H (Ref. 2). In addition, the entry or look-up conditions for the NUREG/CR-4551 pressure rise values were also based on CPSES-specific MAAP analyses for PDS 2H (Ref. 2) as follows.

There are four major parameters that control the pressure rise in the NUREG/CR-4551 approach, as indicated in Table 4.6-1, namely: (1) reactor vessel pressure prior to vessel breach, (2) fraction of molten debris ejected, (3) initial size of hole in the reactor vessel lower head and (4) presence or lack of water in the cavity. Although the pressure range for core damage bins 1 and 2 is 200 to 2000 psia, all Small Break LOCA PDS have RCS pressures at VF less than 1000 psia, as shown in Tables 2-6 (A and B) and Figure 2-2 of (Reference 2). This allows entry in Table 4.6-1 for all PDS into the MEDIUM RCS pressure line. The fraction of molten debris ejected is assumed to be less than 33% in all cases, so that the debris mass line entry is LOW. The RPV hole size is LOW based on the assumption that one penetration weld will fail first. Cavity status is WET in all cases as discussed in (Ref. 27) and according to MAAP CPSES-specific results, as summarized in Table 2-3 of Reference 8.

Based upon these considerations, a curve was obtained from the data in Table 4.6-1 for the probability that the pressure rise is less than the pressure shown. By adding to this distribution the initial value of the containment pressure, the probability that the final containment pressure is less than the value shown was estimated for each PDS. PDS 2H uses the Table 4.6-1 pressure rise plus 80 psi (per Table 2-3 of Reference 8). The curves obtained in this manner are shown in Figure 4.6-1, where they are compared with the curve for the probability of the containment surviving a given load: obtained specifically for CPSES, as described in Section 4.4 and represented in Table 4.4-4.

The probability that the HPME pressure does not exceed the ultimate pressure capacity of the containment is determined from these two cumulative distributions utilizing the concept of reliability (Ref. 28). The concept of containment reliability is that, if the challenge pressure induced by an event does not exceed its capacity, the containment is reliable. Specifically, in the present study the following are given:

F_1 (c): Cumulative probability distribution of the challenge pressure,

F_2 (s): Cumulative probability distribution of the containment surviving pressure,

where:

c: Challenge pressure,

s: Containment surviving pressure.

Both probability distributions are not in the form of known functions but, rather, the estimated cumulative probabilities at certain pressure points are available.

The containment reliability is defined as:

R (c < s): Probability distribution that the challenge pressure is less than the containment surviving pressure.

In order to determine the containment reliability, let f_1 (c) be the density function of the challenge pressure and f_2 (s) be the density function of the containment surviving pressure. The containment reliability is then calculated as:

$$R(c<s) = \int_{-\infty}^{\infty} f_1(c)\,[1 - \int_{c}^{\infty} f_2(s)\,ds]dc \qquad (4.6\text{-}1)$$

In order to compute the containment reliability directly by using the given data for both challenge pressure and containment surviving pressure, define:

$$1 - \int_{c}^{\infty} f_2(s)ds = F_2(c) \qquad (4.6\text{-}2)$$

and

$$dF_1(c) = f_1(c)dc \qquad (4.6\text{-}3)$$

The range of F_1 is obviously from 0 to 1. Substituting Eq. (4.6-2) and Eq. (4.6-3) into Eq. (4.6-1) yields:

$$R(c<s) = \int_{0}^{1} F_2 dF_1 \qquad (4.6\text{-}4)$$

Equation (4.6-4) suggests that the area under an F_1 versus F_2 plot would represent the reliability of the containment. It can also be obtained numerically utilizing the following expression:

$$R(c<s) = \sum_{i=1}^{2i} (F_{2i} + F_{2i-1})(F_{1i} - F_{1i-1})/2 \qquad (4.6\text{-}5)$$

Table 4.6-2 shows F_2, F_1 and calculates the reliability of the containment for BE PRWCP-PULT for PDS 2H.

4.6.1.2 CET Quantification Process and Discussion of Results

The CETs are input into the ETA-II (Ref. 29) code. The result of this stage is shown in Figure 4.5-1, which shows an ETA-II plot of the CPSES CET. The same CET structure is used for all PDS in which the containment is not bypassed or failed to isolate. ETA-II was used to generate logic for CAFTA (Ref. 30) by linking the various logic trees of Figures 4.5-2 through 4.5-23, each of which corresponds to a branch in the CET. This approach was taken in order to take into consideration the dependencies from earlier CET questions on later questions. There is a CAFTA file that contains all the logic trees and an associated BE file into which the PDS-specific BE probabilities were input. The logic trees are the same for all PDS. Basic event probabilities are distinguished in the BE file by suffixes, e.g., SNOSPRAY11F=0 vs. SNOSPRAY11H=1. The CAFTA file only contains one set of trees where the basic event names have no suffixes. In order to evaluate the logic trees, a flag file was developed that equates the unsuffixed BE name in the linked CAFTA file to the suffixed name in the BE file and its associated probability. The computation was actually performed by loading for each PDS: (1) the CAFTA logic trees and its associated BE file, (2) the flag files discussed above, and (3) the file containing the logic connecting the logic trees, as described above. Once these files were loaded into CAFTA, the actual computation of the probabilities was performed using the code GTPROB (Ref. 31). Since GTPROB does not yield cutsets but only probabilities, the logic trees were also quantified using CAFTA with the logic trees top event cutsets as the product. The CAFTA probability calculation is not sufficiently accurate for evaluating the CET end-state probabilities, hence the need for GTPROB.

The results of the quantification process described above are summarized in two sets of tables. The first set, Tables 4.6-3 through 4.6-6, lists the end-state probabilities. The second set, Tables 4.6-7 through 4.6-10, summarizes the same results in a more compact and descriptive form by grouping CET end-states. The key phenomena, systems considerations and operator actions which lead to the top event probability values in the CETs, which in turn lead to the end-state probability values, are discussed below for each PDS.

PDS 1E

This PDS groups Small Break LOCA with ECCS failure at injection and containment spray failure at recirculation. As previously discussed, these PDS involve the RCS at medium pressure, with only a 0.05 probability of depressurization to low pressure levels due to hot leg or surge line failure. Recovery is not considered and, therefore, vessel failure always occurs.

As a result, the first relevant branch probability is DP=0.95, representing the 0.95 probability that the vessel will be at an intermediate pressure at the time of vessel failure.

The next relevant branch probability is CFE1=8.0E-03, CONTAINMENT FAILS EARLY, along the successful DP path. This value is due to the probability of a low pressure alpha event. Along the non-depressurization path, CFE2=1.83E-03. This result is due primarily to the chance that HPME might occur and fail the containment. There is a small contribution due to the rocket event and one due to alpha at high pressure.

The next relevant event is DC2=7.37E-02, DEBRIS BED NOT COOLABLE, along the successful DP path. This results from judgment probabilities: (1) that a coolable debris bed does not form given no ex vessel steam explosion (PRCDB-LPNS = 0.1) times the probability that ex-vessel steam explosion does not occur (-PRVSE = 0.5), ORed with (2) the probability that an ex-vessel steam explosion occurs (PRVSE = 0.5) times the probability that a coolable debris bed does not form given that (PRCDB-LPSE = 0.05) an ex-vessel steam explosion occurs. That is:

$$DC = [(0.1x0.5) + (0.05x0.5)] - [(0.1x0.5)x(0.05x0.5)]$$

Along the non-depressurized path, DC3=0.05. This value is due primarily to the judgement that it is very unlikely (0.05, Table 2-1 of Ref. 8) that a coolable debris is not formed if the RCS is not depressurized before vessel breach, which then occurs in a blowdown mode, i.e., as high pressure melt ejection.

For LATE CONTAINMENT FAILURE OCCURS, CFL1 = CFL3 = CFL5 = 0.65, if the debris is coolable and CFL2 = CFL4 = CFL6 = 0.955, if it is not.

For FISSION PRODUCT REMOVAL MECHANISMS FAIL, FPR0 = FPR1 = FPR4 = 0.95 and FPR2 = FPR3 = 0.998 are high because of the probability that RCS heat up could cause revolatization of fission products, although RCS retention occurs due to spray operation before vessel breach.

For CONTAINMENT FAILURE MODES, CFM2=5.04E-01, CFM3=5.004E-01, if the failure is early and CFM1=5E-03, if it is late. These split fractions simply reflect the fact that an energetic failure is likely to result in a rupture mode failure and a puff release, while a late failure is likely to result in a leakage type failure.

As shown in Table 4.6-7, the combination of these branch probabilities results in a 0.67 total probability of no containment failure. There is a 2.1E-3 probability of early containment failure, where 22% are small or leakage type failures and 78% are rupture type. There is a 0.66 total probability of late containment failure. Of this, 92% are due to steam overpressure. The remaining 8% are due to non-condensible overpressure or basemat melt-through or H_2 burn, if the debris is not coolable and CCI occurs under the overlying pool of water. Ninety-five percent (95%) of both late and early failures are unmitigated since the releases are mostly due to revolatization within the RCS and cannot be scrubbed by an overlying pool in the reactor cavity. Of the late failures, 99.5% are benign, i.e., leakage as opposed to rupture.

PDS 1F

This PDS groups Small Break LOCA with ECCS failure at injection and containment sprays that operate during injection and recirculation. Except for the fact that an examination of the cutsets in this PDS shows that operator depressurization as quantified via BE HOP-DP is more likely here, the CET for this event is quite similar to that discussed previously for PDS 1E. The difference between the PDS is in the duration of spray operation. In this case, the containment would never fail due to overpressure, while in the previous case it can. The early failure probabilities are slightly higher than those for PDS 1E, namely a 7.71E-3 probability of early containment failure, where almost all of these failures are rupture-type from the steam explosion alpha event which became more likely due to the depressurization. The late failure probability is only 7.3E-2 due to the possibility that the debris may fall into a non-coolable configuration, even if the containment is flooded, and then fail by the same mechanisms presented for the non-coolable situation in PDS 1E. The total containment failure probability for PDS 1F is 8.1E-2.

PDS 1H

This PDS groups Small Break LOCA with ECCS and containment spray failure at injection. As previously discussed, these PDS involve the RCS at medium pressure, with only a 0.05 probability of depressurization to low pressure levels due to hot leg or surge line failure, but with possible operator depressurization. Recovery is not considered and, therefore, vessel failure always occurs.

As a result, the first relevant branch probability is DP=0.0475, representing the 0.0475 probability that the vessel will be at an intermediate pressure at the time of vessel failure.

The next relevant branch probability is CFE1=8.0E-03, CONTAINMENT FAILS EARLY, along the successful DP path. This value is due to the probability of a low pressure alpha event. Along the non-depressurization path, CFE2=1.83E-03. This result is due primarily to the chance that HPME might occur and fail the containment. There is a small contribution due to the rocket event and one due to alpha at high pressure.

The next relevant event is DC2=DC3=1.0, DEBRIS BED NOT COOLABLE. This results from the assumption that the debris bed is not coolable if the RWST water is not injected into the containment and the debris dries out.

For LATE CONTAINMENT FAILURE OCCURS, CFL1=CFL3=CFL5=0, if the debris is coolable and CFL2=0.996 and CFL4=CFL6=0.995, if it is not. If the debris is coolable, there is no containment failure because there is not enough H_2 generated in the core melt to threaten the containment in a burn and the amount of steam generated will not cause containment failure without the non condensibles in the CCI. If the debris is not coolable, there is CCI with enough attendant H_2 generated to yield a 2.49E-03 probability of a burn with enough energy to fail the containment, which must be combined with the 0.995 probability of failure due to non-condensible overpressurization and with the 0.05 probability of basemat melt-through. The burn probability is much lower than that for PDS 1E and 1F (6.0E-02) because for PDS 1H, the containment sprays are not in operation after vessel breach so the atmosphere is more likely to be inerted.

For FISSION PRODUCT REMOVAL MECHANISMS FAIL, FPR4=1.0 is higher than the value for PDS 1E and 1F because there is no overlying pool at the time of containment failure. This is because for PDS 1H the RWST water is not injected into the containment. Revolatization also occurs along with non-retention in this case, but the lack of an overlying pool at time of containment failure dominates this probability.

For CONTAINMENT FAILURE MODES, CFM2=5.04E-01 and CFM3=5.004E-01, if the failure is early and CFM1=5E-03, if it is late. These split fractions simply reflect the fact that an energetic failure is likely to result in a rupture type failure and a puff release, while a late failure is likely to result in a leakage type failure.

The combination of these branch probabilities results in a 0.996 probability of containment failure. This is much higher than for PDS 1E and 1F because the debris was found non-coolable due to the fact the RWST water was not injected into the containment. Thus, basemat melt-through, steam overpressure and late hydrogen burns would fail the containment with high likelihood. There is a 7.71E-3 probability of early containment failure. All of the late failures are unmitigated since the debris is not covered at containment failure, but 99.5% of these late failures are benign, i.e., leakage as opposed to rupture. Conversely, almost all of the early failures are rupture failures leading to a puff release.

PDS 2E

This PDS groups Small Break LOCA with both ECCS and containment spray failure at recirculation. The results for this PDS are nearly identical to those for PDS 1E. The only differences in the branch probabilities are that for FPR2=FPR4=1 in this case as opposed to 0.998 for PDS 1E. These differences are not significant so that PDS 1E and PDS 2E have essentially the same characteristics.

PDS 2F

This PDS groups Small Break LOCA with ECCS failure at recirculation and containment sprays that operate during injection and recirculation.

The logic tree top event probabilities for this PDS are identical to those discussed previously of PDS 1F except for event DP, which depends on the cutset composition of the PDS. As in PDS 1F, the containment would never fail due to overpressure. PDS 1F and PDS 2F thus have similar characteristics.

PDS 2H

This PDS groups Small Break LOCA with ECCS failure at recirculation and containment spray failure at injection. Because of the CT failure at injection, the RWST water lasts a very long time delaying the time to core damage significantly, while continuously pressurizing the containment with steam. Therefore, the time between vessel failure and containment failure becomes less for this PDS than for other PDS where the RWST water was injected into the containment, and the probability of late containment failure due to steam generation, PRSTM-OCC, is higher in this case, i.e., 0.95 as opposed to 0.65. This conclusion is conservative since the actual containment failure time for this PDS is 36 hours (vessel failure at 18 hours) which is similar to the corresponding times for PDS 1E (38 hours) and 2E (37 hours), but in those cases the vessel fails in 2 to 3 hours so the time after vessel failure is much larger. Thus, it appears that more containment failures than would be expected to occur in this case are

computed, so that results for PDS 2H are felt to be somewhat more conservative than those for other PDS.

The total containment failure probability for PDS 2H is 0.95. Of this, 0.03 are early failures and 0.92 are late failures. The early failures are due to HPME occurring with the containment at a relatively high initial pressure. The early failures are split almost 50-50 into rupture and leakage type and the late failures are mostly leakage. Since the RWST water is injected into the containment in this PDS, the late failure probability is 0.85, mostly due to steam overpressure, with a small contribution from non-condensible overpressurization (0.07) when the debris is found non-coolable with an overlying pool.

PDS 3E

This PDS groups Transients involving loss of all feedwater with RH and SI failure at injection, while two CCPs may or may not be available but if they are available, they do not inject until after vessel failure due to the high head and containment spray failure at recirculation. As previously discussed, these PDS involve the RCS at high pressure, with only a 0.05 probability of depressurization to low pressure levels due to hot leg or surge line failure. Recovery is not considered and, therefore, vessel failure always occurs.

As a result, the first relevant branch probability is DP=0.87, representing the 0.87 probability that the vessel will be at a high pressure at the time of vessel failure.

The next relevant branch probability is CFE1=8.0E-03, CONTAINMENT FAILS EARLY, along the successful DP path. This value is due to the probability of a low pressure alpha event. Along the non-depressurization path, CFE2=1.08E-02. This result is due primarily to the chance that HPME might occur and fail the containment. There is a small contribution due to the rocket event and one due to alpha at high pressure.

The next relevant event is DC2=7.37E-02, DEBRIS BED NOT COOLABLE, along the successful DP path. This results from judgment probabilities: (1) that a coolable debris bed does not form given no ex vessel steam explosion (PRCDB-LPNS = 0.1) times the probability that ex-vessel steam explosion does not occur (-PRVSE = 0.5), ORed with (2) the probability that an ex-vessel steam explosion occurs

(PRVSE = 0.5) times the probability that a coolable debris bed does not form given that (PRCDB-LPSE = 0.05) an ex-vessel steam explosion occurs. That is:

$$DC = [(0.1x0.5) + (0.05x0.5)] - [(0.1x0.5)x(0.05x0.5)]$$

Along the non-depressurized path, DC3=0.05. This value is due primarily to the judgement that it is very unlikely (0.05, Table 2-1, *Ref.* 8) that a coolable debris is not formed if the RCS is not depressurized before vessel breach, which then occurs in a blowdown mode, i.e, as high pressure melt ejection.

For LATE CONTAINMENT FAILURE OCCURS, CFL1 = CFL3 = CFL5 = 3E=0.65, if the debris is coolable and CFL2 = CFL4 = CFL6 = 3E=0.996, if it is not.

For FISSION PRODUCT REMOVAL MECHANISMS FAIL, FPR=0.175 is low because of the probability judged to be 0.175 that RCS heat up could cause revolatization of fission products, while RCS retention occurs due to spray operation before vessel breach and with a small path from the RCS to the containment.

For CONTAINMENT FAILURE MODES, CFM=5.04E-01, if the failure is early and CFM=5E-03, if it is late. These split fractions simply reflect the fact that an energetic failure is likely to result in a rupture mode failure and a puff release, while a late failure is likely to result in a leakage type failure.

The combination of these branch probabilities results in a 0.67 total probability of containment failure. There is an 9.13E-3 probability of early containment failure, where 22% are small or leakage type failures and 78% are large or rupture failures. There is a total 0.66 probability of late containment failure. Of this 0.60, are due to steam overpressure. The remaining 0.06 are due mostly to non-condensible overpressure and with small contributions from basemat melt-through and to H_2 burn, if the debris is not coolable and CCI occurs under the overlying pool of water. Only 17.5% of both late and early failures are unmitigated since the releases are mostly due to revolatization. Of the late failures, 99.5% are benign.

PDS 3F

This PDS is similar to PDS 3E except that containment sprays operate during injection and recirculation and with the exception of the potential for operator depressurization, which is cutset dependent as implemented in BE HOP-DP. Results for this event are quite similar to those discussed previously of PDS 3E. The difference between the PDS is in the duration of spray operation and the higher probability for event DP. In this case, the containment would never fail due to overpressure, while in the previous case it could. The early failure probabilities are slightly less than those for PDS 3E, namely a 8.19E-3 probability of early containment failure, where 22% are small or leakage type failures and 78% are rupture type. The late failure probability is only 0.07 due to the possibility that the debris may fall into a non-coolable configuration even if the cavity is full of water. The total containment failure probability for PDS 3F is 0.08.

PDS 3H

This PDS groups Transients involving loss of all feedwater with RH and SI failure at injection, while two CCPs may or may not be available but if they are available, they do not inject until after vessel failure due to the high head and containment spray failure at injection. As previously discussed, these PDS involve the RCS at high pressure, with only a 0.295 probability of not successfully depressurizing. Recovery is not considered and, therefore, vessel failure always occurs.

As a result, the first relevant branch probability is DP=0.295, representing the 0.295 probability that the vessel will be at low pressure at the time of vessel failure.

The next relevant branch probability is CFE=8.0E-03, CONTAINMENT FAILS EARLY, along the successful DP path. This value is due to the probability of a low pressure alpha event. Along the non-depressurization path, CFE=1.08E-02. This result is due primarily to the chance that HPME might occur and fail the containment. There is a small contribution due to the rocket event and one due to alpha at high pressure.

The next relevant event is DC=1.0, DEBRIS BED NOT COOLABLE. This results from assumption that the debris bed is not coolable if the RWST water is not fully injected into the containment and the debris dries out.

For LATE CONTAINMENT FAILURE OCCURS, CFL1 = CFL3 = CFL5 = 0, if the debris is coolable and CFL2 = CFL4 = CFL6 = 0.996, if it is not. If the debris is coolable, there is no coatainment failure becaute there is not enough H_2 generated in the core melt to threaten the containment in a burn and the amount of steam generated will cause containment failure without the non condensibles in the CCI. If the debris is not coolable, there is CCI with enough attendant H_2 generated to yield a 2.49E-03 probabilicy of a burn with enough energy to fail the containment, which must be combined with the 0.995 probability of failure due tc non-condensible overpressurization and with the 0.05 probability of basemat melt-through. The burn probability is much lower than that for PDS 3E and 3F (6.0E-02) because for PDS 3H, the containment sprays are not in operation after vessel breach so the atmosphere is more likely to be inerted.

For FISSION PRODUCT REMOVAL MECHANISMS FAIL, FPR4 = 1.0 is higher than the 0.175 value for PDS 3E and 3F because there is no overlying pool at the time of containment failure. This is because for PDS 3H, the RWST water is not injected into the containment. Revolatization also occurs along with non-retention in this case, but the lack of an overlying pool at time of containment failure dominates this probability.

For CONTAINMENT FAILURE MODES, CFM2 = 5.04E-01, if the failure is early and CFM1 = 5E-03, if it is late. These split fractions simply reflect the fact that an energetic failure is likely to result in a rupture mode failure and a puff release, while a late failure is likely to result in a leakage type failure.

The combination of these branch probabilities results in a 0.996 probability of containment failure. This is higher than for PDS 3E and 3F because the debris was found non-coolable due to the fact that the RWST water was not injected into the containment. Thus, basemat melt-through, steam overpressure and late hydrogen burns would fail the containment in high likelihood. There is a 8.83E-3 probability of early containment failure and a 0.987 probability of late failure. All of these late failures are unmitigated since the debris is not covered at containment failure, but 99.5% of these late failures are benign, i.e., leakage as opposed to rupture.

PDS 4E

This PDS groups Transients where the TDAFW operates for 4 hours after reactor trip and two CCPs inject on demand but fail at recirculation and containment spray also fails at recirculation. The results for this PDS are similar to those for PDS 3E. The main differences in the branch probabilities are: (1)

the CFL values for the coolable cases are higher for 4E because it takes longer to fail the containment after vessel failure and (2) FPR2 = FPR4 = 0.438 in this case as opposed to 0.0 for PDS 3E, due to the fact that, while there is an overlying pool in this case to provide scrubbing of material that ends up in the cavity, containment sprays do not operate after vessel breach and, thus, RCS retention does not occur.

The condensed end-state probabilities which are listed in Table 4.6-8 are similar to those for PDS 3E. The only significant difference is in the late containment failure probabilities due to steam overpressurization which are .37 for PDS 4E and .65 for PDS 3E. The difference is due to fact that the containment pressure reaches its mean failure pressure later for PDS 4E than for 3E because the TDAFW delays core melt and extends the duration of the ECCS.

PDS 4F

This PDS is similar to PDS 3F except that ECCS injects successfully in this case and fails only at recirculation. In both 3F and 4F, containment sprays inject and switchover successfully to recirculation, so there is no containment failure due to steam overpressurization.

The CET end-state probabilities for this event are identical to those discussed previously of PDS 3F except for event DP which is cutset dependent due to BE HOP-DP. As in PDS 3F, the containment would never fail due to overpressure.

PDS 4H

This PDS groups Transients where the TDAFW operates for 4 hours after reactor trip and two CCPs inject on demand but fail at recirculation and containment sprays fail at injection. The condensed end-state probabilities that are listed in Table 4.6-8 are similar to those for PDS 4E. The main difference are in the early failure probabilities, 0.16 versus 9.13E-03, and in the late containment failure probabilities due to steam overpressurization which are .37 for PDS 4E and .19 for PDS 4H. The former difference is due to differences in HPME failure probabilities and probabilities of operator action to depressurize. The latter difference is due to fact that the containment pressure reaches its mean failure pressure later for PDS 4H than for 4E because the failure of containment sprays extends the duration of the ECCS injection period.

PDS 3SBO AND 4SBO

This PDS groups Station Blackouts involving simultaneous loss of all feedwater (3SBOHR) and with 4 hours of auxiliary feedwater supplied by the TDAFW pump (4SBOHR). As previously discussed, these PDS involve the RCS at high pressure, with only a 0.068 probability of depressurization to low pressure levels for 4SBO due to hot leg or surge line failure and 0.98 for 3SBO due to operator action.

As a result, the first relevant branch probability is DP=0.387 for 4 SBO and DP=0.0225 for 3SBO, representing the probability that the vessel will be at high pressure at the time of vessel failure.

The next relevant branch probability is CFE1=8.0E-03, CONTAINMENT FAILS EARLY, along the successful DP path. This value is due to the probability of a low pressure alpha event. Along the non-depressurization path, CFE2=2.706E-01 for 3SBOHR and CFE2=5.078E-02 for 4SBOHR. This result is due primarily to the chance that HPME might occur and fail the containment. There is a small contribution due to the rocket event and one due to alpha at high pressure.

The next relevant event is DC3= 0.901 for 3SBOHR, DC3=0.991 for 4SBOHR and DC2= 0.904 for 3SBOHR, DC2= 0.991 for 4SBOHR, DEBRIS BED NOT COOLABLE. This results from assumption that the debris bed is not coolable if the RWST water is not fully injected into the containment and the debris dries out, combined with the probability of recovery of electrical power which would allow injection of the RWST into the containment to occur.

If the RWST is injected into the containment, DC1 = 7.38E-02, because the debris is coolable if it is geometrically coolable. Since this is along the path of successful recovery, the ECCS was injected into the containment. The value of 7.38E-02 results from the probability that a low pressure steam explosion may occur times the probability of forming a coolable debris bed in that case, ORed with the case were the bed is formed without the occurrence of a steam explosion at low pressure (Section 4.5). Top event DC1, Figure 4.5-7, applies only along the path of successful recovery.

For LATE CONTAINMENT FAILURE OCCURS, CFL1= CFL3=CFL5=0, if the debris is coolable and CFL2 = CFL4 = CFL6 = 0.996, if it is not. If the debris is coolable, there is no containment failure because there is not enough H_2 generated in the core melt to threaten the containment in a burn and the amount of steam generated will cause containment failure without the non condensibles of the CCI. If the debris is not coolable, there is CCI with enough attendant H_2 generated to yield a 2.49E-03

probability of a burn with enough energy to fail the containment, which must be combined with the 0.995 probability of failure due to non-condensible overpressurization and with the 0.05 probability of basemat melt-through.

For FISSION PRODUCT REMOVAL MECHANISMS FAIL, the discussion in the previous Section covers the issues.

For CONTAINMENT FAILURE MODES, CFM2 = 5.04E-01, if the failure is early and CFM1 = 5E-03, if it is late. These split fractions simply reflect the fact that an energetic failure is likely to result in a rupture mode failure and a puff release, while a late failure is likely to result in a leakage type failure.

The combination of these branch probabilities results in a 0.82 probability of containment failure for 3SBOHR and 0.98 for 4SBOHR. There is a 1.3% probability of early containment failure for 3SBOHR and a 2.5% probability of early failure for 4SBOHR. The difference is due to the higher initial pressure for 3SBOHR which yields a higher chance for a HPME event, but which is compensated by the depressurization probability. On the other hand, the late failure probabilities are 0.80 for 3SBOHR and 0.95 for 4SBOHR. The difference here is in part due to the probability of recovery which is higher for 3SBOHR because the time window begins at an earlier time (vessel failure) where the recovery probability curve is less flat and, in part, due to the depressurization probability. All of these late failures are due to CCI related effects and are mostly unmitigated since the debris is not covered at containment failure, but 99.5% of these late failures are benign, i.e , leakage as opposed to rupture.

PDS 5E

This PDS groups Large Break LOCA with ECCS failure at injection and containment spray failure at recirculation. As previously discussed, these PDS always involve the RCS at low pressure, recovery is not considered and, therefore, vessel failure always occurs.

As a result, the first relevant branch probability is CFE1 = 8.0E-03, CONTAINMENT FAILS EARLY. This value is due to the probability of a low pressure alpha event.

The next relevant event is DC2 = 7.37E-02, DEBRIS BED NOT COOLABLE. This results from judgment probabilities: (1) that a coolable debris bed does not form given no ex-vessel steam explosion

(PRCDB-LPNS = 0.1) times the probability that ex-vessel steam explosion does not occur (-PRVSE = 0.5), ORed with (2) the probability that an ex-vessel steam explosion occurs (PRVSE = 0.5) times the probability that a coolable debris bed does not form given that (PRCDB-LPSE = 0.05) an ex-vessel steam explosion occurs. That is:

$$DC = [(0.1 \times 0.5)+(0.05 \times 0.5)]-[(0.1 \times 0.5)(0.05 \times 0.5)]$$

For LATE CONTAINMENT FAILURE OCCURS, CFL3=0.65, if the debris is coolable and CFL4 = 7.38E-02, if it is not.

For FISSION PRODUCT REMOVAL MECHANISMS FAIL, FPR2= FPR4=0.95 is high because of the probability, judged to be 0.95, that RCS heat up could cause revolatization of fission products, although RCS retention occurs due to spray operation before vessel breach.

For CONTAINMENT FAILURE MODES, CFM2=5.04E-01, CFM3=5.004E-01, if the failure is early and CFM1=5E-03, if it is late. These split fractions simply reflect the fact that an energetic failure is likely to result in a rupture mode failure and a puff release, while a late failure is likely to result in a leakage type failure.

As shown in Table 4.6-10, the combination of these branch probabilities results in a 0.68 probability of containment failure. There is an 8.0E-3 probability of early containment failure and a 0.67 probability of late containment failure, of which 0.60 corresponds to overpressure failure due to steam generation and 0.07 corresponds to CCI related mechanisms: (a) overpressure due to non-condensibles, (b) basemat melt-through and (c) H_2 burn if the debris is not coolable and CCI occurs under the overlying pool of water. Ninety-five percent (95%) of these late failures are unmitigated since the releases are mostly due to revolatization, but 99.5% of these late failures are benign, i.e., leakage as opposed to rupture.

PDS 5F

This PDS groups Large Break LOCA with ECCS failure at injection and containment sprays that operate during injection and recirculation.

The CET for this event is quite similar to that discussed previously of PDS 5E. The difference between the PDS is in the duration of spray operation. In this case, the containment would never fail due to overpressure while in the previous case it can. Thus, the early failure probabilities are the same as those for PDS 5E, namely a 8E-3 probability of early containment failure, and all are rupture type since this is the alpha failure. The late failure probability is only 0.07 due to the possibility that the debris may fall into a non-coolable configuration even if the containment is flooded and then fail by the same mechanisms presented for the non-coolable situation in PDS 5E. The total containment failure probability for PDS 5F is 0.08.

PDS 5H

This PDS groups Large Break LOCA with ECCS and containment spray failure at injection. As previously discussed, these PDS always involve the RCS at low pressure, recovery is not considered and therefore, vessel failure always occurs.

As a result, the first relevant branch probability is CFE=8.0E-03, CONTAINMENT FAILS EARLY. This value is due to the probability of a low pressure alpha event.

The next relevant event is DC2=1.0, DEBRIS BED NOT COOLABLE. This results from the assumption that the debris bed is not coolable if the RWST water is not fully injected into the containment and the debris bed dries out prior to containment failure.

For LATE CONTAINMENT FAILURE OCCURS, CFL3=0, if the debris is coolable and CFL3 = 0.945, if it is not. If the debris is coolable, there is no containment failure because there is not enough H_2 generated in the core melt to threaten the containment in a burn and the amount of steam generated will not cause containment failure without the non condensibles in the CCI. If the debris is not coolable, there is CCI with enough attendant H_2 generated to yield a 2.49E-03 probability of a burn with enough energy to fail the containment, which must be combined with the 0.95 probability of failure due to non-condensible overpressurization and with the 0.05 probability of basemat melt-through. The burn probability is much lower than that for PDS 5E and 5F (6.0E-02) because for PDS 5H, the containment sprays are not in operation after vessel breach so the atmosphere is more likely to be inerted.

For FISSION PRODUCT REMOVAL MECHANISMS FAIL, FPR4=1.0 and FPR2=0.998 are higher than the 0.95 value for PDS 5E and 5F because there is no overlying pool at the time of containment

failure. This is because for PDS 5H the RWST water is not injected into the containment. Revolatization also occurs along with non-retention in this case, but the lack of an overlying pool at time of containment failure dominates this probability.

For CONTAINMENT FAILURE MODES, CFM2 = 5.04E-01, CFM3 = 5.004E-01, if the failure is early and CFM1 = 5E-03, if it is late. These split fractions reflect the fact that an energetic failure is likely to result in a rupture mode failure and a puff release, while a late failure is likely to result in a leakage type failure.

The combination of these branch probabilities results in a 0.995 probability of containment failure. This is much higher than for PDS 5E and 5F because the debris was found non-coolable due to the fact the RWST water was not injected into the containment. Thus, basemat melt-through, steam overpressure and late hydrogen burns would fail the containment with high likelihood. There is an 8E-3 probability of early containment failure from a low pressure alpha event. All of the late failures are unmitigated since the debris is not covered at containment failure, but 99.5% of these late failures are benign, i.e., leakage as opposed to rupture. Conversely, all the early failures are rupture failures leading to a puff release, the same as for 5E and 5F.

PDS 6E

This PDS groups Large Break LOCA with both ECCS and containment spray failure at recirculation. The results for this PDS are nearly identical to those for PDS 5E. The only differences in the branch probabilities are for the FPR values. These differences are not significant so that PDS 5E and PDS 6E have essentially the same end-state probabilities.

PDS 6F

This PDS groups Large Break LOCA with ECCS failure at recirculation and containment sprays that operate during injection and recirculation.

The end-state probabilities for this event are identical to those for PDS 5F. As in PDS 5F, the containment would never fail due to overpressure. PDS 5F and 6F have the same characteristics.

PDS 6H

This PDS groups Large Break LOCA with ECCS failure at recirculation and containment spray failure at injection. The CET split fractions for this PDS are nearly identical to those for PDS 6E. The only significant difference is in the late containment failure probabilities due to steam overpressurization which are .60 for PDS 6E and .64 for PDS 6H. The difference is due to fact that the failure of containment sprays extends the duration of the ECCS injection period for PDS 6H versus 6E, delaying the vessel failure time with minimal effect on the containment failure time resulting in a smaller time interval between vessel and containment failure times.

4.6.2 Ranking Accident Sequences and Accident Progression Analyses

The ranking of the accident sequences' risk importance was done according to their unconditional probabilities of the core melt leading to: (a) early containment failure, (b) late CCI-induced failure and (c) late steam-induced failures. The unconditional probabilities were obtained by combining the PDS probabilities of occurrence (core melt frequencies or CMF) with the conditional probabilities (i.e., given the occurrence) of each PDS leading to: (a) early containment failure, (b) late CCI-induced failure and (c) late steam-induced failure, respectively. The PDS probabilities of occurrence were taken from the bottom line of Table 4.3-3. The conditional probabilities for (a), (b) and (c) were determined in the containment event tree analysis (Ref. 2) summarized in Section 4.6.1 and in Tables 4.6-7, 4.6-8, 4.6-9, and 4.6-10. The combination of those results is listed in Table 4.6-14, which is sorted in decreasing order of PDS occurrence probability, i.e., core melt frequency (CMF). Tables 4.6-11, 4.6-12 and 4.6-13 provide the key to the notation describing the sequences.

In Table 4.6-15, the PDS are sorted according to the unconditional probabilities of early containment failure, and total unconditional containment failure probabilities. Table 4.6-16 sorts the PDS in decreasing order of the late CCI-induced failure and late steam-induced failure. This is done by extracting the relevant columns from Table 4.6-14 and resorting.

In Table 4.6-17, the PDS are given in decreasing order of contribution to early containment failure, along with their representative Level I functional sequences, which are taken from Table 4.3-3. Tables 4.6-11, 4.6-12 and 4.6-13 provide the key to the notation describing the sequences listed in Table 4.6-17.

For all of the PDS listed in Table 4.3-3, the following is discussed: (1) the reasons for the PDS contribution to risk, (2) identification and description of the front-end functional sequences making up most of the PDS frequency, and (3) selected accident progressions for these sequences obtained with MAAP. It is important to keep in mind that a particular front-end sequence may progress in various ways throughout the back-end portion of the analysis. In fact, that is what the CETs represent. The objective of the MAAP analyses is to obtain representative and/or bounding calculations for each of the CET end-states. As a result, the front-end sequences used as the basis to construct the MAAP analysis are not always the dominant sequence (i.e., the highest frequency contributor) in the PDS. Another point to remember is that most of the CET end-states do not correspond to the most likely outcome and require adjustments of MAAP parameters for the calculation to result in that outcome, for example obtaining an early containment failure due to DCH combined with a hydrogen burn. Each of these points is made below again on a case-by-case basis. Then for each PDS, functional sequences and select MAAP accident progression analyses are described in the following subsections.

4.6.2.1 PDS 2CB (SGTR & ISGTR)

PDS 2CB contains all Steam Generator Tube Rupture (SGTR) functional sequences that lead to core melt. In addition, it also groups the fraction of other PDS that result in induced SGTRs (ISGTR). The functional composition of this PDS is:

2CB = 95.5% RCM1, 3% RCM4, 1.5% ISGTR

The ISGTR frequency was calculated by subtracting the probability of depressurization in the CET (1-(top event DP probability)) as calculated for the base case (i.e., the case where the tubes could fail, BE PRSGOK = .982) from the case where the tubes are intact (BE PRSGOK = 1.0). This difference is the probability that the depressurization is due to the induced failure of the tubes and is listed in the left hand column of Table 4.6-18, for every high pressure PDS (3H, 3F, 4H, 4F, 3SBO, 4SBO). This is multiplied by the PDS frequency to obtain the unconditional ISGTR frequency for the PDS. The results of this calculation are summarized in Table 4.6-18. By consulting the functional sequence composition of each PDS, it is possible to determine the functional sequence contributions to ISGTR. These are listed in Table 4.6-19. The total frequency of ISGTR does not justify a separate PDS for this type of development, and since the release paths are identical, these sequences are binned with SGTR. Although the functional composition of the ISGTR is provided in Table 4.6-19, a special analysis of any of those

sequences is not warranted because of the comparatively low frequencies with respect to other SGTR. Thus, the representative sequence for PDS 2CB is RCM1, which accumulates the overwhelming majority of the frequency, 95.5% as shown above.

Description of The Representative Functional Sequences

RCM1:

This sequence involves a steam generator tube rupture initiating event. ECCS is available and safety injection is established. Following the "S" signal, secondary heat removal is established. However, the operators are not able to isolate break flow. This results in RWST depletion. Following that, operators are unable to perform closed loop recirculation switchover due to their own errors or power or equipment failures. Containment isolation is lost due to failure of atmospheric dump valves to reseat properly after steam generator overfill.

RCM4:

This is an SGTR where ECCS failed to inject due to failure of the CS and SI equipment. Following the generation of an "S" signal, secondary heat removal is established. However, the operator fails to terminate break flow within the 30 minute time window.

MAAP Calculations for The Representative Sequences

One calculation was performed to determine the accident progression and source term characteristics of the key sequence: calculation 2CB1 representing RCM1 described above, which represents 95.5% of the tube ruptures. Six additional tube rupture calculations are documented elsewhere (Ref. 2), and the case of RCM4 is considered there as well (SGTR03). However, since RCM1 has almost all the tube ruptures, it was selected as the representative sequence for PDS 2CB.

2CB1:

The calculation follows the accident description above for RCM1. Additional details are as follows: (1) MSIVs close at time of scram, (2) all AF is postulated to fail, and (3) a pre-calculation showed overfill occurs around 2 hours so the ARVs are postulated to fail to reseat at that time.

The accident progression calculation plots are given in Appendix A of Reference 7. Key times and pressures are summarized in Table 4.6-20. The RWST is depleted around 10 hours. Then, RCS pressure drops as there is no longer CCP injection to keep it up. The accumulator set point is reached

and they become depleted. Shortly after, RCS pressure reaches the broken SG pressure of about 2 MPa. After that, the broken SG drains into the RCS by gravity, delaying core uncovery for about 15000 seconds. When the gravity drain is over, the primary pressure rises again due to the increased steam production. Eventually the core begins to uncover and steam production decreases, reducing the RCS pressure. Vessel failure follows shortly after core uncovery and occurs at an intermediate pressure of 5 MPA (72[illegible]).

The 2CB1 calculation is similar to calculation SGTR06 done in Reference 2. In the actual sequence, operators isolate the AF to the faulted generator, but AF is available to the intact generator. Since MAAP cannot isolate AF to only one SG, AF is postulated to be lost for all steam generators. A case with AF available for all steam generators, SGTR02, was also run for comparison in Reference 2. That case led to qualitatively similar results as case SGTR06 except core uncovery occurs [illegible] hours sooner when there is AF available. However, that difference is primarily due to the fact that with AF available to the faulted SG, the CST keeps being fed into it. Therefore, the gravity drain from the faulted SG lasts 13 hours longer. Thus, case 2CB1 is somewhat conservative because it neglects the benefit of having AF to the intact SG and, furthermore, it does not provide CST water feed to the RCS through the faulted SG. Table 4.6-21 summarizes the release fraction for PDS 2CB based on the 2CB1 MAAP calculation.

4.6.2.2 PDS 4H and 4F

PDS 4H and 4F rank second and seventh, respectively, as contributors to early containment failures. In addition to being the second largest contributor to early containment failures, PDS 4H is also the second largest contributor to late steam-induced overpressure failures. PDS 4F does not contribute to steam overpressurization because the containment sprays work. The cause of the early failures is primarily HPME. The high HPME delta P resulted from the use of NUREG/CR-4551 pressure rise values, as shown in Table 4.6-1 . The table entry is based on a high RCS pressure at vessel failure of 2000 to 2500 psi, as described in Section 4.6.1.

Description of The Representative Functional Sequences

The functional sequence frequency composition for PDS 4H and 4F is:

4H: 95% IVSCM4, 5% VSCM4, 1% IVSCM1.

4F: 83% VSCM(14), 9% IVSCM4, 6% X(23)CM1.

The prefix notation for the above sequences is given in Table 4.6-11 and the suffix notation is given in Table 4.6-12.

IVSCM4:

The main cutsets in this sequence involve a loss of offsite power (loss of CC and SW also contribute to this category), which induces a very small seal LOCA greater than 21 GPM/PMP but less than 60 GPM/PMP 45 minutes after the initiating event. ECCS (CCPs and SIPs) is unavailable for establishment of safety injection due to loss of power or due to either: (a) loss of pump lube oil cooling on failure of SW or (b) failure of SW itself. Auxiliary feedwater is available.

IVSCM1:

This sequence is similar to IVSCM4 except that auxiliary feedwater is not available due to loss of turbine driven AF pump discharge control leading to steam generator over fill and eventual turbine drowning. The MDAFW pumps are lost due to either the initiator directly or due to failure of components on loss of room cooling. Feed and bleed was successfully completed, but recirculation was not established due to the initiator. The RCPs trip either at the time power is lost or on loss of AF by procedure FRH-0.1. Containment sprays failed at injection due to the loss of power or loss of supporting systems.

VSCM4:

The main cutsets in this sequence involve a very small break LOCA initiating event (less than 0.6 inch). High head injection (charging) fails due to the loss of various components associated with the Chemical and Volume Control System. Auxiliary feedwater is available for at least 24 hours. Containment spray is available in some cut sets. The operators fail to cool and depressurize the plant on loss of high head injection. The RCPs will be tripped if RCS subcooling is less than 25 °F and an ECCS pump, either one CCP or SIP, is operating. (Note: CCPs are unavailable for this sequence and if the RCS stays at high pressure, the SIPs will be unavailable). Upon initiation of containment spray (some cutsets have sprays failed), procedure EOP-0.0A calls for the operator to trip the RCPs.

VSCM1:

The main cutsets in this sequence also involve a very small break LOCA initiating event (less than 0.6 inch). In this case, ECCS is available for injection. Auxiliary feedwater is available for at least 24 hours. Containment spray is available as required. The operators fail to establish recirculation by failing

to re-align ECCS upon RWST depletion. The RCPs will be tripped if RCS subcooling is less than 25 °F and an ECCS pump is operating, either one CCP or SIP. Upon initiation of containment spray, procedure EOP-0.0A calls for the operator to trip the RCPs.

X(23)CM1:

This is an initiating event (loss of chilled water, loss of offsite power) that did not induce a seal LOCA. Thus a 21 GPM/PMP leak rate is postulated consistent with the thermal gradient leakage associated with loss of seal cooling where no RCP seal parts fail (Refs. 2,32). The MDAFW pumps fail due to a loss of supports or due to heat related failures associated with a loss of room cooling. The TDAFW pump fails due to its own faults or due to its supports which lead to an overfill condition that eventually drowns the turbine or fails its piping. Operators appropriately and successfully performed feed and bleed until the RWST is empty, but then recirculation fails due to the loss of chilled water which fails cooling to the RH pump room, or by the failure of the pumps supports. The RCPs were tripped at the loss of AF by procedure FRH-0.1. Sufficient ECCS injects on demand but fails at recirculation due to the loss of the RH pumps caused by a loss of supports or room cooling. By procedure FRH-0.1, operators will shutdown ECCS pumps, starting with the CCPs and followed by the SIPs, to preserve the RWST water as long as subcooling is maintained in the RCS, according to the criteria provided by the procedure.

MAAP Calculations for The Representative Sequences

PDS 4H:

From the thermohydraulics and accident progression perspectives, IVSCM4 and VSCM4 are similar. The only difference is that in one case, the leak is induced and in the other, it is the initiator. The IVSCM1 functional sequence is more severe for early containment failures because ECCS injection is successful and leads to a higher containment pressure at vessel failure. Therefore, it is picked as the basis for the representative MAAP calculation.

Two calculations were carried out for PDS 4H: (1) TRAN21, corresponding to the most likely outcome of sequence IVSCM1 and (2) TRAN22, where model parameters are adjusted to obtain HPME failure.

TRAN21:

This base case follows the sequence description above for IVSCM1 with the following additional assumptions:

- The seal leak rate is less than 60 GPM/PMP for IVSCM1 and 21 GPM/PMP for the MAAP calculation. That difference is not significant but since this is a high pressure PDS, the lower leak rate is slightly more representative.

- The RCPs and AFWPs are tripped simultaneously with the reactor for simplicity.

- One CCP is the only pumped ECCS. The success criteria is 1 of 4 pumps. This choice delays core damage while pressurizing containment leading to a maximum containment pressure at vessel failure. Since this sequence represents PDS 4H, which is a contributor to early HPME failure, it is appropriate to consider this situation as representative since it is the most conducive to early containment failure and does not impact the late failure time due to steam overpressurization.

- The PORV is closed after the RWST is depleted. Since the operators are executing feed and bleed, after they are no longer able to feed, operators will stop the bleed.

- When the containment failure pressure is reached, the containment failure mode is assumed to be by liner tear as discussed in Section 4.4. In that failure mode, the leak rate increases to a point where containment pressure is nearly constant or decreasing slowly, i.e., a leak type failure mode. This is accomplished in this sequence with a 0.005 m^2 liner tear leak area, which is approximately equivalent to a 3 inch diameter orifice.

The key event times and pressures for this analysis are summarized in Table 4.6-20. Calculated containment pressure and temperature histories are presented in Figure 4.6-2. Additional information on sequence development is presented in the corresponding Figures in Appendix A of Reference 7.

TRAN22:

Since PDS 4H is the number two contributor to early containment failure (HPME), MAAP model parameters were modified outside of their estimated values in order to obtain release fractions for the HPME failure mode. The parameter modifications for TRAN22 are identical to those discussed for SB2H5 follow the guidelines suggested in References 33 and 34. The key event times for this analysis are summarized in Table 4.6-20. Calculated containment pressure and temperature histories are presented in Figure 4.6-3. Additional information on sequence development is presented in the corresponding figures in Appendix A of Reference 7.

PDS 4F:

The frequency composition of PDS 4F is: 83% VSCM(14), 9% IVSCM4, 6% X(23)CM1. From the descriptions provided above, it is clear that IVSCM1 and VSCM1 are essentially identical from the thermohydraulic and phenomenological perspective and so are IVSCM4 and VSCM4. Since IVSCM1 was used as the basis for the representative MAAP analysis of PDS 4H, it is appropriate to examine VSCM4 for PDS 4F. This is done in VSB4F1.

VSB4F1:

This case follows the sequence description above for VSCM3 with the same additional assumptions made for TRAN22 to obtain HPME phenomena. Since PDS 4F is a contributor to early containment failure due to HPME, MAAP model parameters were modified outside of their estimated values in order to obtain release fractions for this failure mode. The parameter modifications for VSB4F1 are identical to those made for SB2H5 which followed the guidelines suggested in References 33 and 34.

The key finding from the analysis is that it was not possible to obtain containment failure due to HPME even after the parameter adjustments because of the low initial pressure due to spray actuation. In conclusion, since the CET end state corresponding to early containment failure with sprays available is represented by the 3SBO with recovery sequence IVSCM6 (MAAP calculation SBO31), and since another functional sequence which represents 4F has been analyzed as TRAN21 and TRAN22, only without sprays, it is not necessary to have a core melt sequence MAAP calculation specifically for 4F.

Table 4.6-21 summarizes the release fractions for CET end-state B6-L, represented by PDS 4H, based on the TRAN21 MAAP calculation. Table 4.6-22 describes that end-state and lists similar end-states.

4.6.2.3 PDS 1CB (V-Sequence) and 1CI (Isolation Failures)

PDS 1CB ranks third as contributor to early containment failures. It is not a high contributor with a frequency of 1.19 E-07 but is listed and analyzed for the sake of completeness. This section also includes PDS 1CI representing the core melt sequences in which the containment failed to isolate, because those frequencies are so low (9.92 E-09) that they do not warrant their own representative analyses and can have their consequences conservatively represented by the calculation used to represent PDS 1CB. The reason for the low frequency for isolation failures is the independence of the containment isolation from

the support systems failures that lead to most of the core melt sequences. As a result, the containment isolation failures are mostly the product of the conditional containment isolation failure probability as determined in Reference 6 and the frequency of each of the sequences leading to core melt. Thus, the dominant contributor to this PDS is the dominant contributor to the core melt frequency and is already analyzed elsewhere (PDS 1H).

Description of The Representative Functional Sequences

The functional sequence frequency composition for PDS 1CB is:

1CB: 83% SCM1, 9% MCM2, 7% ACM(12).

SCM1:

The cutsets in this sequence involve an interfacing systems LOCA of 2 to 4 inches in equivalent size. Based on the analyses of References 2 and 7, this is also a low pressure PDS. Auxiliary feedwater is available for at least 24 hours, but is worth very little for this break size. The RCPs are tripped when RCS subcooling is less than 25°F (criteria defined by procedure EOP-0.0A), which is almost immediately. Sufficient ECCS (1 of 4 pumps) injects on demand but fails at recirculation due to the operators failing to realign the systems or due to failure of components required for recirculation and because the water is not in the containment sump and, therefore, is not available for recirculation. By procedure EOS-1.1, operators shutdown ECCS pumps starting with the SI pumps followed by the RH pumps to preserve the RWST, as long as 25°F of subcooling is maintained in the RCS, but this situation is not realistically reached. The interfacing systems LOCA, by definition, provides a breach of containment leading to releases into the safeguards building.

MCM2:

The cutsets in this sequence involve an interfacing systems LOCA of 2-6 inches equivalent size. ECCS is unavailable for establishment of safety injection due to failure of the accumulators (loss of level or pressure) or due to failure of ESFAS equipment to generate an SI actuation signal, followed by the operator failure to manually initiate a safety injection signal or provide for manual actuation of injection equipment. The success criteria for a 2-6 inch LOCA requires accumulator injection and either CCPs (high head) or SIPs (intermediate head). The interfacing systems LOCA, by definition, provides a breach of containment leading to releases into the safeguards building.

ACM2:

The cutsets in this sequence involve an interfacing systems LOCA initiating event of more than 6 inches equivalent size. ECCS is unavailable for establishment of safety injection due to the failure of the RH pumps directly or due to supporting systems (ie. SW, CC or Chilled Water). The success criteria for a large break LOCA requires RH (low head) ar ccumulator injection and either CCPs (high head) or SIPs (intermediate head). The interfacing stems LOCA, by definition, provides a breach of containment leading to releases into the safeguards building.

ACM1:

Same as above except ECCS is available for injection.

MAAP Calculations for The Representative Sequences

From the thermohydraulics and accident progression perspectives, the significant differences between the sequences described above are the size of the break and availability of ECCS. In addition, the smaller break sequences are 88% RH pump seal failures where the leakage would be submerged in the safeguards building. Since the larger break and lack of ECCS makes the accident more severe, and since the overall frequency of the V-sequence is sufficiently small, the most severe sequence, namely ACM2, is selected to form the baseline for the development of the MAAP calculation: V1.

V1:

As described in ACM2 above, the calculation is a 10 inch large break LOCA in the cold leg into the safeguards b. ding. No ECCS injection is credited except for the accumulators. Containment sprays are also not credited since, in addition to their failure described above, the containment pressure does not reach their set point.

This sequence leads to the largest release fraction of all due to the combination of large early vessel and containment failure and lack of water in the containment leading to arly CCI.

The key event times and pressures for this analysis are summarized in Table 4.6-20. Calculated hydrogen production amounts are presented in Figure 4.6-4. Additional information on sequence development is presented in the corresponding figures in Appendix A of Reference 7.

Table 4.6-21 summarizes the release fraction for PDS 2CB based on the 2CB1 MAAP calculation. Table 4.6-22 describes the end-state and lists similar end-states.

4.6.2.4 PDS 1H and 1F (and 5H, 5F)

PDS 1H ranks fourth (2.3%) as a contributor to early containment failure (PDS 5H is sixteenth, 0.1%). However, PDS 1H is the first (57.1%) (5H is fifth, 1.5%) leading contributor to late CCI-induced failures and is also the leading contributor to total containment failures of any kind (46.7%) (5H is eighth, 1.2%). PDS 1F and 5F are not significant contributors to failures of any kind and have the same functional composition as PDS 1H and 5H, respectively. The only difference is that sprays work in PDS 1F and 5F. Since early failures with sprays operational are represented by another MAAP calculation (SBO31), it is not necessary to have an analysis for PDS 1F and 5F; their release fractions can be represented by that calculation as well. Since late CCI-induced failures are dominated by PDS 1H and since PDS 5H leads to a similar outcome, and since PDS 5H is not a significant contributor to early failures (0.1%) and is only a small contributor to CCI failures (1.2%), a calculation for 5H is also not necessary; it can be represented by the 1H representative as well.

Description of The Representative Functional Sequences

The functional sequence frequency composition for these PDSs is:

1H: 100% ISCM2

1F: 93% ISCM2, 7% SCM2

5H: 65% ACM2, 35% IMCM2

5F: 85% ACM2, 12% MCM2

ISCM2:

The majority of cutsets in this sequence involve a loss of offsite power, which induces a seal LOCA greater than 60 GPM/PMP (assumed 210 GPM/PMP, or approximately a 1 inch break) 45 minutes after the reactor trip. The remainder of the cutsets involve the loss of SW or CC initiators leading to the induced seal LOCA. All ECCS fails to inject on demand due to the loss of all power or supports. Containment sprays fail in some cutsets at injection due to loss of power, but are available in others.

SCM2:

This is similar to ISCM2 except the small break LOCA is the initiating event rather than induced.

ACM2, MCM2, IMCM2:

These are all large break LOCAs where the ECCS failed at injection.

MAAP Calculations for The Representative Sequences

ISCM2 is used as a basis for the MAAP analyses, primarily because it has 100% of PDS 1H frequency.

The objective of the present MAAP calculations was to obtain accident progression parameters and release fractions for CCI-induced failures in which the sprays do not operate and in which the non-coolability of the debris is caused by lack of a water pool above, rather than a non-coolable geometry situation which was represented via PDS 3F. Two scenarios were developed using ISCM2 as a guideline for the MAAP calculations: (1) SBO21, with a leakage-type late failure due to non-condensible overpressurization and (2) SBO22, with a rupture-type late failure due to a burn of the hydrogen generated in the CCI.

SBO21:

This is the base case calculation to represent ISCM2. The sequence development is that described for ISCM2 above; no additional assumptions were needed for the period prior to vessel failure, which occurs early at around 2.5 hours. After vessel failure, the assumption is that the non-coolable configuration of the debris is the 75 m^2 of cavity floor and not the unrealistic debris area of 7.5 m^2 that was used for PDS 3F. In that case, the change was necessary to obtain CCI in the presence of an overlying pool. In this case, since there is no ECCS injection, the RCS plus accumulator inventory eventually dries out and CCI can be expected to occur with near certainty.

The key event times for this analysis are summarized in Table 4.6-20. Calculated containment pressure and temperature histories are presented in Figure 4.6-5. Additional information on sequence development is presented in the corresponding figures in Appendix A of Reference 7.

SBO22:

In this calculation, a burn was forced to occur at approximately 29 hours by restarting calculation SBO21 at that time with a low TAUTO = 465°K, the temperature for autoignition of the hydrogen. The pressure

spike was sufficient to fail the containment. A rupture failure area was postulated for this calculation in order to evaluate release fractions for this case.

The key event times for this analysis are summarized in Table 4.6-20. Calculated containment pressure and temperature histories are presented in Figure 4.6-6. Additional information on sequence development is presented in the corresponding figures in Appendix A of Reference 7.

Table 4.6-21 summarizes the release fractions for CET end-states C6-L and C6-R, both represented by PDS 1H and based on the SBO21 and SBO22 MAAP calculations, respectively. Table 4.6-22 describes that end-state and lists similar end-states.

4.6.2.5 PDS 3H and 3F

PDS 3H and 3F rank fifth (1.5%) and sixth (1.0%) respectively as contributors to early containment failures. PDS 3H is the second (32.2%) leading contributor to late CCI induced failures and to all failures (26.3%) as well. PDS 3F does not contribute to steam overpressurization because the containment sprays work, and it ranks fourth (1.7%) in CCI induced late failures, which result only from the probability that the debris might fall in an non-coolable configuration under a water pool, since the RWST water is injected into containment via sprays. The cause of the early failures is also primarily HPME. The high HPME delta P results from the use of NUREG-1150 values for Zion based on a high RCS pressure at vessel failure of 2000 to 2500 psi, as described in Section 4.6.1 and illustrated in Table 4.6-1.

Description of The Representative Functional Sequences

The functional sequence frequency composition for PDS 3H and 3F is:

3H: 49% X(3617)CM2, 45% T(146)CM2 and 5% (CVCM2 & IVSCM3).

3F: 87% ATCM(631), 8% X(12)CM2 and 4% T(6)CM2.

The suffix and prefix notation for the above sequences are summarized in Tables 4.6-11 and 4.6-12.

ATCM(361):

The cutsets in this sequence involve various initiators leading to an ATWS and can be broken into two groups. The ATCM3 and ATCM6 group contains cutsets leading to core melt in which the initiators

cause, directly or indirectly, the loss of main feed water. The reactor fails to trip from either mechanical rod binding or the failure of the trip breakers (operator action to manually trip the breakers also fails). For this group, AF flow is lost mainly due to component failures. For several cutsets, the combination of loss of AF or PORVs will lead to RCS overpressurization. In the second group of cutsets, (ATCM7) the reactor fails to trip due to the failure of the trip breakers.

X(1367)CM2:

These are initiators (loss of a DC bus, loss of offsite power, loss of CC, loss of SW) that did not induce a seal LOCA. Thus, a 21 GPM/PMP leak rate is postulated consistent with the thermal gradient leakage associated with loss of seal cooling, where no RCP seal parts fail (Refs. 2,32). The MDAFW pumps fail either due to loss of support systems or room cooling to either the pump rooms or to the pumps electric equipment rooms. The TDAFW fails at that time as well, due to its own faults or loss of control power. Operators fail to perform feed and bleed mostly due to operator error but some cutsets also include the failure of the PORV to open. The RCP were tripped on loss of AFW by procedure FRH-0.1. There is no SI because the operators did not manually actuate SI in this scenario.

For sequences with initiating event X6 or X7, containment spray is not available due to supporting systems failures. A fraction of sequences with initiating events X1 and X3 also have containment spray unavailable depending upon the equipment that failed due to the initiator.

T(146)CM2:

The initiating event for these sequences is either a general plant transient or a loss of normal feedwater. The AF pumps are lost due to their failures or for the MDAFW pumps, due to heat related failures associated with a loss of room cooling. The TDAFW pump may also fail due supports that lead to either loss of turbine steam supply or to an overfill condition and subsequent drowning the turbine or causing its piping supports to break from static overloading. In cases of loss of support other than steam, the loss of safety chilled water (room cooling) leads to direct failures or indirect (electric power room cooling) failures, as safety chilled water requires manual actuation except in the case of SI actuation. Operators fail to perform feed and bleed mostly due to operator error, but some cutsets also include the failure of the PORV to open. The RCPs were tripped on loss of AF by procedure FRH-0.1. There is no SI because the operators did not manually actuate SI in this scenario. This bin's success/failure criteria is independent of ECCS injection.

A fraction of the cutsets in these sequences (those with initiating events T1, T4, or T6) also have containment spray unavailable due to failure of supporting system equipment. Another fraction of sequences with initiating events T1 and T6 have containment spray available.

CVCM2:

This is a loss of condenser vacuum initiating event. The MDAFW pumps fail either due to its own faults or due to a loss of support systems (including room cooling to the pump rooms or to the pumps electric equipment rooms). The TDAFW fails due to its own faults or loss of control power. Operators fail to perform feed and bleed mostly due to operator error, but some cutsets also include the failure of the PORV to open due to loss of power to the PORVs. The RCPs were tripped on loss of AF by procedure FRH-0.1. There is no SI because the operators did not manually actuate SI in this scenario. For this sequence containment spray will not be available due to supporting system failures.

IVSCM3:

The majority of cutsets in this sequence involve an induced small seal LOCA, that is, the leak rate is less than 60 GPM/PMP. ECCS was available for safety injection but feed and bleed was not implemented due mainly to loss of power to the PORV. Secondary heat removal is unavailable due to the initiating event or due to loss of AF. The MDAFW pumps are unavailable due to loss of cooling. The TDAFW controls are lost due to HVAC failure and battery depletion leading to overfill and eventual drowning of the turbine.

MAAP Calculations for The Representative Sequences

From the thermohydraulics and accident progression perspectives, all of the functional sequences described above are similar.

The objective of the present MAAP calculations is to obtain accident progression parameters and release fractions for CCI-induced failures in the event the debris is non-coolable, since catastrophic HPME failures and long term steam sequences are already represented in PDS 3SBO, 4SBO, 4H and 2H. Furthermore, since non-coolable sequences in which the sprays do not operate are dominated by PDS 1H, which is examined in another section and would have similar release fractions to the corresponding outcome for PDS 3H, it is not felt necessary to perform calculation for PDS 3H. Thus, only three non-coolable debris with the sprays in operation scenarios were developed using X(123)CM2 as a guideline for the MAAP calculations: VSB3F1, VSB3F2, VSB3F3.

VSB3F1:

This is the base case calculation to represent X(1367)CM2 with sprays in operation and a non-coolable debris configuration. The sequence development is that described for X(1367)CM2 above; no additional assumptions are needed for the period prior to vessel failure, which occurs early at around 2.5 hours.

After vessel failure, an assumption was made in order to obtain the non-coolable configuration of the debris. That is to assume a debris area in the cavity of 7.5 m^2 which is 10 times less than the 75 m^2 of cavity floor and not at all realistic. However, although the probability that the debris would fall in this configuration in high pressure PDS is highly unlikely, the probability itself is factored into the CET discussed in Section 4.6.1. In this section, the accident progression if that development occurs are evaluated.

The calculation was run for 220 hours (9 days) and stopped because the containment pressure was only 65 psig, well below the mean failure pressure of 114 psig.

Although overpressurization failure did not occur, a significant amount of hydrogen and CO were generated in the CCI (about 4000 Kg of hydrogen at 220 hours or 9 days). There were some burns at vessel failure and slightly afterwards but later on, the sprays kept the temperatures too low for burns. However, due to the large amount of hydrogen, another calculation was performed to evaluate the effect of a burn if it were to occur at such a low temperature, i.e., a burn was forced, and to calculate the release fractions if such a burn were to fail the containment. That is calculation VSB3F2.

Furthermore, in the present calculation (VSB3F1), there was a significant amount of concrete attack, and the 4m basemat depth was reached at 90 hours (3.75 days). The fast erosion depth was due to the small initial debris area. In order to estimate the release fractions if a failure were to occur at that time, another calculation was performed. That is calculation VSB3F3.

VSBF2:

In this calculation, a burn was forced to occur at approximately 208 hours by restarting calculation VSBF1 at that time with a low TAUTO = 315 °K, the temperature for autoignition of the hydrogen. The pressure spike was sufficient to fail the containment. A leak type failure area was postulated for this calculation in order to evaluate release fractions for a leak case, since the rupture case is seen above.

A rupture type failure area was postulated for VSBF3. The release fractions for this case were small due to spray operation and the leak type failure.

VSB3F3:

In view of the very low release fractions observed in VSB3F2 and considering the basemat erosion observed in VSB3F1, this calculation was performed to bound the release fractions for this PDS. That was done by forcing a burn just prior to the time of erosion of the 4m concrete basemat and postulating that the resulting containment failure would be of the rupture rather than leak type. The results show release fractions slightly higher than those for VSB3F2 but still very small. These values were then kept as bounding for this PDS for the non-coolable debris with fission product scrubbing path in the CET.

The key event times for these analyses are summarized in Table 4.6-20. Calculated containment pressure and temperature histories are presented in Figure 4.6-7 (VSB3F1), 4.6-8 (VSB3F2) and 4.6-9 (VSB3F3). Additional information on sequence development is presented in the corresponding figures in Appendix A of Reference 7.

Table 4.6-21 summarizes the release fractions for CET end-states C5-L and C5-R both represented by PDS 3F and based on the VSB3F3 and VSB3F2 MAAP calculations, respectively. Table 4.6-22 describes that end-state and lists similar end-states.

4.6.2.6 PDS 6F, 6H, 2F, 2H

PDS 6F, 6H and 2F and 2H are unimportant as contributors to early containment failure. PDS 6F and 6H can result in early failures from an alpha event, which is well known to be of very low probability, particularly for a cavity of the CPSES strength and configuration (see Section 4.1). PDS 2H and 2F, being situations of intermediate pressure at vessel failure, can result in early failures from HPME events. PDS 6H and 2H are important (ranked first and third respectively) as representatives of steam-induced overpressure failures.

Description of The Representative Functional Sequences

The representative functional sequences are:

6H: 99% IMCM1, 1% ACM1

6F: 62% ACM1, 29% MCM1, 8% XLCM1

2H: 100% ISCM1

2F: 87% SCM1, 13% ISCM1

IMCM1:

The main cutsets involve loss of CC or plant transient initiating events with the loss of the CC system components. This leads to an induced medium break LOCA (2-4 inches, which leads to a low pressure PDS), due to failure of safety valves to reclose after all have been opened to relieve pressure. Safety valves are required due to PORV unavailability from their own faults or due to closed block valves. ECCS injects successfully but fails at recirculation.

ACM1:

This has been previously described in connection with the V-sequence. It is a large break LOCA with successful ECCS injection but failure at recirculation.

MCM1:

This is a medium break LOCA (2-4 inches, which leads to a low pressure PDS) with successful ECCS injection but failure at recirculation due to operator error.

XLCM1:

This is an excessive LOCA, e.g., failure of the reactor vessel. ECCS injects but fails at recirculation.

ISCM1:

The majority of cutsets in this sequence involve a loss of CC, which induces a seal LOCA greater than 60 GPM/PMP (assumed 210 GPM/PMP, or approximately a 1 inch break) 45 minutes after the reactor trip. Auxiliary feedwater is available for at least 24 hours. The RCPs will only be tripped as RCS subcooling becomes less than 25°F (criteria defined by procedure EOP-0.0A). Sufficient ECCS (1 of 4 pumps) injects on demand but fails at recirculation due to the loss of CC directly or as a result of loss of room cooling. By procedure EOS-1.1, operators shutdown ECCS pumps starting with the SI pumps followed by the RH pumps to preserve the RWST as long as 25°F of subcooling is maintained in the RCS. Containment sprays fail at injection due to the loss of CC which causes failure of the pumps. Those sequences in which the spray pumps operate are binned into PDS 2F. Fan coolers are tripped at SI and are not available due to the loss of CC which causes a loss of chilled water for ventilation.

SCM1:

This is similar to ISCM1 except the small break LOCA is the initiator rather than being caused by loss of supports. As a result the containment sprays are available.

MAAP Calculations for The Representative Sequences

The importance of these sequences is as representatives of late steam overpressure failures. In that respect all the above sequences have similar accident progressions and the same most likely outcome. The representative MAAP calculations are based on ISCM1. Since ISCM1 is a small break rather than a large break for IMCM1, MCM1, ACM1 etc..., the vessel failure pressure tends to be somewhat higher than if the calculations were based on the LBLOCA sequences, but for long term steam failures this is irrelevant.

Two MAAP calculations were conducted for sequence ISCM1: (1) SB2H4 and (2) SB2H5. SB2H4 is a base case calculation representing the most likely outcome for the sequence if no recovery actions take place. This outcome is a late containment failure due to steam overpressure.

Albeit minor, this sequence is also a contributor to early containment failure due to HPME. MAAP model parameters were modified outside of their estimated values in order to obtain release fractions for this failure mode. The parameter modifications for SB2H5 followed the guidelines suggested in References 33 and 34.

SB2H4:

This base case follows the sequence description above with the following additional assumptions:

- CCP is the only pumped ECCS. The success criteria is 1 of 4 pumps. This choice delays core damage while pressurizing containment leading to a maximum containment pressure at vessel failure.

- When the containment failure pressure is reached, the containment is assumed to fail by rupture. This is not the most likely failure mode for slow steam overpressurization which is liner tear causing a leak-type failure. However, another sequence (TRAN21 for PDS 4H) is used to represent the leak-type failure and SB2H4 represents the rupture type.

SB2H5:

MAAP model parameters were modified outside of their estimated values in order to obtain release fractions for this failure mode. The parameter modifications for SB2H5 follow the guidelines suggested in References 33 and 34 and are as follows:

- TTRX = 1800. The time to fail a bottom head penetration after support plate failure was increased from 1 minute in the basic calculation to 30 minutes in order to accumulate more molten material for dispersion into containment at vessel failure.

- FCDMA = 1. The debris was assumed to be entrained directly into the upper compartment instead of the lower compartment. This leads to a greater pressure rise due to its larger volume.

- FENTR = 1E-06. This is the critical superficial gas velocity for entrainment of corium. The nominal value is around 1. A very low number suggests there is no threshold.

- FCMDCH = 1. This is the fraction of dispersed debris that contributes to DCH.

- FCDMH = 1. This is the fraction of debris that is dispersed.

- NVP = 1000. The equivalent area of 1000 bottom head penetrations was assumed to open at vessel failure.

- TAUTO = 460K. This is the critical temperature for a burn to occur. It incorporates steam inerting characteristics. Nominal value matching data is around 983°K. This is the most serious contributor to the pressure spike as it causes all hydrogen to burn at HPME simultaneously with the DCH.

Without the simultaneous hydrogen burn, the pressure at vessel failure does not approach the containment failure pressure, even when all parameters available in MAAP to maximize the DCH spike are adjusted to the maximum in that direction. Only with the simultaneous burn can the failure occur.

The key event times for these analyses are summarized in Table 4.6-20. Calculated containment pressure and temperature histories are presented in Figures 4.6-10 (SB2H4) and 4.6-11 (SB2H5). Additional

information on sequence development is presented in the corresponding figures in Appendix A of Reference 7.

Table 4.6-21 summarizes the release fractions for CET end-states B6-R and D6-R both represented by PDS 2H and based on the SB2H4 and SB2H5 MAAP calculations, respectively. Table 4.6-22 describes those end-states and lists similar end-states.

4.6.2.7 PDS 3SBO and 4SBO

PDS 4SBO is the third contributor to CCI-induced failures (2.2%) and tenth (0.3%) to early failures. PDS 3SBO is ninth (0.7%) and seventeenth (0.1%), respectively. The cause of the early failures is primarily High Pressure Melt Ejection (HPME). The high HPME delta P used is from the NUREG-1150 values for Zion (Section 4.6.1 and Table 4.6-1) based on a high RCS pressure at vessel failure.

Description of The Representative Functional Sequences

The representative functional sequence for PDS 3SBO is IVSCM6 which is 100% binned into PDS 3SBO and constitutes 100% of the total 3SBO frequency. The representative functional sequence for PDS 4SBO is IVSCM5 which is 100% binned into PDS 4SBO and constitutes 100% of the total 4SBO frequency.

IVSCM6:

The main cutsets in this sequence involve a loss of offsite power, which induces a very small seal LOCA, i.e., of less than 60 GPM/PMP, 45 minutes after the initiating event. All ECCS fails to inject on demand due to the loss of all power. Auxiliary feedwater is not available due to loss of power to the motor driven pumps and the loss of the turbine driven AF pump discharge control leading to steam generator overfill and eventual turbine drowning. Feed and bleed is not entered as it was not required. The RCPs will trip at the time power is lost or on the total loss of AF by procedure FRH-0.1. Containment sprays fail at injection due to the loss of power. Fan coolers trip at loss of power.

IVSCM5:

The main cutsets in this sequence involve a loss of offsite power, which induces a very small seal LOCA, i.e., of less than 60 GPM/PMP, 45 minutes after the initiating event. All ECCS fails to inject on demand due to the loss of all power or support systems. Auxiliary feedwater is not available since the motor

driven pumps have no power and the turbine fails due to its own faults. Feed and bleed is not entered as it was not required. The RCPs will trip at the time power is lost. Containment sprays fail at injection due to the loss of power. Fan coolers trip at loss of power.

MAAP Calculations for The Representative Sequences

PDS 3SBO and 4SBO are the only PDS for which the possibility of recovery after core uncovery and prior to vessel failure has been considered for CPSES. Although the most likely outcome for these PDS is CCI-induced failures, those failures are well represented in PDS 1H. As a result, it would be most appropriate to develop a representative sequence which would lead to early containment failure following recovery of power after core uncovery but where vessel failure could not be precluded (CET end-states D1 and D2). IVSCM5 was used as the base-case for that analysis.

SBO31:

Recovery of power is considered to occur after core uncovery and prior to vessel failure but not precluding vessel failure in order to have a calculation for the recovery CET end-state D1. Power recovery is assumed to take place after the fuel has already heated up significantly. In the simulation, the RCS pressure at time of power recovery is high so that an SI signal is not generated and injection does not occur. In practice, an SI signal would most likely be generated manually from the control room. However, as discussed in Reference 2 the injected amount would not be relevant unless the operators were to depressurize the RCS. That action is along the successful DP path and, therefore, it is not modeled here. Furthermore depressurization would simulate the situation which is already modeled in SB2H5 for PDS 2H. The effect of the additional amount of hydrogen that could be generated by the ECCS injection was investigated in sensitivity runs. However, since the containment fails in a burn-DCH event at time of containment failure anyway, the extra hydrogen is redundant.

Containment sprays operate since the power is recovered and mitigate the release as indicated in path D1 of the CET.

Since PDS 3SBO is the greatest contributor to early containment failure due to HPME, MAAP model parameters were modified outside of their estimated values in order to obtain release fractions for this failure mode. The parameter modifications for SBO31 followed the guidelines suggested in References 33 and 34 and were as follows:

- TTRX = 600. The time to fail a bottom head penetration after support plate failure was increased from 1 minute in the basic calculation to 10 minutes in order to accumulate more molten material for dispersion into containment at vessel failure.

- FCDMA = 1. The debris was assumed to be entrained directly into the upper compartment instead of the lower compartment. This leads to a greater pressure rise due to its larger volume.

- FENTR = 3E-02. This is the critical superficial gas velocity for entrainment of corium. The nominal value is around 1. A very low number suggests there is no threshold.

- FCMDCH = 1. This is the fraction of dispersed debris which contributes to DCH.

- FCDMH = 1. This is the fraction of debris which is dispersed.

- NVP = 100. The equivalent area of 100 bottom head penetrations was assumed to open at vessel failure.

- TAUTO = 700K. This is the critical temperature for a burn to occur. It incorporates steam inerting characteristics. Nominal value matching data is around 983°K. This is the most serious contributor to the pressure spike as it causes all hydrogen to burn at HPME simultaneously with the DCH.

Without the simultaneous hydrogen burn, the pressure at vessel failure does not approach the containment failure pressure, even when all parameters available in MAAP to maximize the DCH spike are adjusted to the maximum in that direction. Furthermore, only with a burn prior to spray actuation does the failure occur. Thus, it was necessary in the calculation to delay spray actuation until after the burn occurs following vessel failure. While this is not unrealistic given the closeness of the times involved, it should be noted that if de-inerting occurs, the initial pressure is too low and the pressure spike is too low for early containment failure following the burn. It should be remembered that burn probabilities of occurrence are not based on these findings but rather on the NUREG-1150 approach discussed in Section 4.6.1 and summarized in Table 4.6-1.

SBO41:

This calculation is similar to SBO31. In this case, CET end-states D2 are being obtained so that there is no fission product removal by sprays. Therefore, in order to model that situation, it is assumed that only the RH pumps are recovered and the sprays are not.

The key event times for these analyses are summarized in Table 4.6-20. Hydrogen produced in-vessel and in-containment due to CCI is shown in Figure 4.6-12 for SB031. Calculated containment pressure and temperature histories are presented in Figure 4.6-13 for SBO41. Additional information on sequence development is presented in the corresponding figures in Appendix A of Reference 7.

Table 4.6-21 summarizes the release fractions for CET end-states D1-R and D2-R, both represented by PDS 3SBO and based on the SBO31 and SBO41 MAAP calculations, respectively. Table 4.6-22 describes those end-states and lists similar end-states.

4.6.3 Treatment of Uncertainties and Sensitivity Studies

NUREG-1335 Section 2.2.2.6 requests a description of the methods employed for handling phenomenological uncertainties. The objective of this section is to comply with that request and also to describe the handling of non-phenomenological uncertainties which are important for accident management considerations.

The phenomenological uncertainties are addressed in Section 4.6.3.1 and are those considered in Table A.5 of NUREG-1335, Appendix A. In addition to those other uncertainties related to system characteristics and operator actions are addressed in Section 4.6.3.2.

The purpose of addressing uncertainties is to avoid masking the potential for vulnerabilities due to controversial assumptions regarding the likelihood of certain phenomena. In both Sections 4.6.3.1 and 4.6.3.2, the uncertainties are typically addressed in one of three ways: (1) via the CETs, by selection of basic event (BE) probability values, based on expert opinion probabilities from NUREG-1150 that cover the range of possible accident progression outcomes, thereby ensuring no potential vulnerabilities are masked; (2) by the NUREG-1335 Appendix A Step 8 sensitivity study approach, to address the consequence aspect of the uncertainties, i.e. the impact on accident progression or (3) by recalculating

CET end-state probabilities with variations in BE probabilities, in order to demonstrate that certain existing consequence uncertainties are irrelevant.

4.6.3.1 Phenomenological Uncertainties

The phenomenological uncertainties addressed in this section include all of those listed in Table A.5 of NUREG-1335 Appendix A, which are re-arranged and labeled a through m below.

a. Performance of containment heat removal during core meltdown accidents

The characteristics of the available containment heat removal equipment are part of the MAAP model, and therefore, their performance is reflected in the results of the analyses performed (Refs. 2, 7) for the core meltdown accidents. The adequacy of the available equipment was thus evaluated on a case- by-case basis. Nevertheless, general conclusions can drawn from these analyses and those are summarized below.

Containment heat removal during core meltdown accidents is via: (1) the residual heat removal system (RH) and/or the containment spray (CT) system, either or both operating in recirculation mode, or (2) the fan coolers. Fan cooler performance and availability is discussed in 4.6.3.2. MAAP calculations (VIIF2 and VIIF3, Ref. 2) were performed to investigate the minimum requirements in terms of RH and/or CT trains. It was found that as long as one RH train was able to switchover successfully to recirculation, with one RH heat exchanger available, the containment pressurization rate can be arrested. Since spray flow rates are much higher than RH flow rates, it is concluded that one spray train is also adequate. In either case, if switchover is successfully accomplished, a subsequent interruption in the sytem is unlikely, since all key components are located in the safeguards building outside containment. An additional calculation (VIIF5, Ref. 2) examined the case of total loss of component cooling water to the RH heat exchangers. Containment failure occured in almost the same time frame as of the case where switchover to recirculation failed altogether. However, when component cooling water flow to the RH exchangers was not totally lost, but merely impaired (up to 40% of its nominal value), the containment survived indefinitely (VIIF4, Ref. 2). While these findings are useful to the CPSES accident management knowledge base, they do not constitute success criteria for any of the front-end analyses. Those requirements are discussed in Section 3 of Volume I of this submittal and are typically more severe than the successful performance boundaries delineated above.

b. In-vessel hydrogen production at high and low RCS pressures and combustion in containment.

There is considerable uncertainty regarding how much hydrogen can be produced during the core melt progression. In addressing this issue for the CPSES IPE, the objective was to insure that the effect of very high quantities of hydrogen being produced in-vessel were examined. The main concern was whether in-containment burns from hydrogen produced in-vessel could cause early containment failure. Two situations are possible: (1) hydrogen combustion alone leads to containment failure for low RCS pressures and/or (2) combustion in combination with direct containment heating (DCH) for high RCS pressures leads to containment failure.

The CPSES IPE has been able to bypass much of the uncertainty regarding the problem of in-vessel hydrogen generation because the containment can resist a burn of all hydrogen produced in-vessel assuming 100% clad oxidation, as discussed in b.1 below. In an actual severe accident of course, the amount of hydrogen produced in-vessel would be much less than that corresponding to 100% clad oxidation. The NRC staff's summary of IDCOR/NRC issues 5 and 6, In-vessel Hydrogen Generation and Core Melt Progression and Vessel Failure, reflected disagreements on the effects of degradation in core geometry and on the rate and magnitude of hydrogen production. NRC considered that the IDCOR best-estimate position, i.e., that the onset of melt would quickly cause a complete stoppage of local Zircaloy oxidation, is not adequately substantiated by data. The applicable MAAP parameter relating to this issue is FCRBLK, a flag used to select the blockage model. In the calculations described (Ref. 7) below, the flag was set for no blockage. Typically, this resulted in approximately 60% clad reacted and is about twice what would occur if the blockage were turned on. One other parameter can be used to increase hydrogen production further, namely FAOX, which can be set to allow for one- or two- sided oxidation of the clad. This was set to two-sided oxidation in the cases that resulted in about 60% clad reacted. In any case, all these variations were bounded by the 100% clad reacted situation postulated for the adiabatic, isocoric, complete combustion (AICC) calculation discussed below. Thus, from a hydrogen production standpoint, there is a great deal of confidence that the amount produced in a severe accident would be somewhere between 30% and 60% of the clad reacted. From a consequence point of view, it is shown below that the combustion of even 100% clad reacted cannot fail the containment.

b.1. Low RCS pressures

In-containment combustion of hydrogen produced in-vessel was found not to be capable of causing early containment failure. This was concluded on the basis of an adiabatic, isocoric, complete combustion (AICC) calculation (Ref. 7), which postulated 100% Zircaloy clad reacted to maximize hydrogen

production, and also postulated the environment composition at the onset of the flammability limit, to maximize the post-burn pressure. Specifically, the pre-burn composition leading to the highest post-burn pressure is: (1) the existing air inventory of about 96000 Kg (43% molar fraction), (2) the upper bound 1000 Kg (6.5% molar fraction) of hydrogen (100% clad oxidized, i.e., 21316 Kg of Zr lead to 937 Kg of hydrogen) and (3) 69786 Kg (50.5% molar fraction) of steam (determined at the boundary of the flammability limit, given the above amounts of air and hydrogen). This composition is at the onset of the Shapiro and Moffette (Ref. 12) flammability limit. The pre-burn temperature is saturation at the steam specific volume for the composition above, because spray actuation is required to reduce the steam amount, i.e., the containment would always be inerted unless the sprays had come on. The final post-burn temperature, calculated by assuming adiabatic, isocoric, complete combustion of all hydrogen, is approximately 100 psia. The containment fragility curve, developed in Section 4.4 and represented by Table 4.4-4, shows clearly that the probability of CPSES containment failure at 100 psia is negligible.

b.2 High RCS pressures

In cases where both hydrogen burn and DCH can occur (assumed to be cases where vessel failure pressures are greater than 200 psia), the approach described in Section 4.6 (using Table 4.6-1 from NUREG/CR-4551) was used. The probability of early containment failure due to in-vessel production of hydrogen is included in the containment event tree for these cases because Table 4.6-1 includes, in the fractile pressure rises, the effects of hydrogen combustion and DCH. By using the values of Table 4.6-1, it appears that an upper bound on the pressure rises for all high pressure melt ejection (HPME) phenomena was obtained. There are two reasons for this conclusion: (1) the Zion cavity is considerably more favorable to particle entrainment into the upper compartment than CPSES' and (2) sensitivity calculations with MAAP (Ref. 7) were performed where parameters were modified to maximize the effect of DCH and even then, the containment failure pressure was only reached when a simultaneous burn was forced to occur under inerted conditions. Although recognized as somewhat excessive, the fractile pressure rises from Table 4.6-1 were utilized for CPSES because the resulting early containment failure probabilities were still low enough to show that HPME is not an important concern for CPSES, as discussed in Section 7.

c. Induced failure of the RCS pressure boundary at high RCS pressures

Three locations in the primary system boundary are considered in the CPSES IPE as possible locations for induced failures: (1) Reactor Coolant Pump Seals, (2) Hot Leg and/or Surge Line and (3) Steam Generator Tubes. All three types of induced failures are incorporated into the CETs, as shown in Figure

4.5-2. It should be noted that the RCP seal failures mentioned above are those occurring after core uncovery, assuming the seals were still intact at that time. The probability of pre-core melt induced seal LOCAs, due to loss of seal cooling, is addressed in the front-end of the IPE and is described in Volume I of the CPSES submittal.

Of these three types of failures, the first two, RCP seals and hot leg and/or surge line failures, are in a sense beneficial because they cause the RCS to depressurize and effectively eliminate the possibility of direct containment heating. From an accident progression point of view, RCP seal and hot leg/surge line failure effects are similar to the effects of operator depressurization of the RCS after core damage. The hot leg/surge line failure probability variations, shown as basic event PRHLSLOK in Figure 4.5-2, and the seal failure BE PRSEALOK, are bounded by variations in operator action to depressurize, BE HOP-DP, which is discussed in Section 4.6.3.2. Given this bounding consideration, and because the possibility of RCP seal failure and hot leg/surge line failure are included in the CETs, it is clear that all possibilities were considered and no potential vulnerabilities were masked.

Induced Steam Generator Tube Ruptures (ISGTR) are not desirable because of the containment bypass. The probability for these events is considered in BE PRSGOK, also shown in Figure 4.5-1. Thus, the potential for this vulnerability was also addressed via CETs. Furthermore, the frequency contribution to ISGTR from each PDS, given in Table 4.6-18, shows these progressions are almost two orders of magnitude less significant than for SGTRs as initiators, so additional sensitivities on this parameter are not warranted. The method for deriving ISGTR frequencies is described in Section 4.6.2.1. These probabilities are also bounded by the probability of operator action to depressurize the RCS, as discussed in Section 4.6.3.2.

The phenomenon which has the greatest impact on induced failures of the RCS is natural circulation. Several studies have been conducted to validate the natural circulation model in MAAP as discussed in Reference 33. The relative magnitude of the BE probabilities for hot leg/surge line failure, PRHLSLOK, versus steam generator tube failure, PRSGOK, with the hot leg/surge line failure being more likely, is based on the generic results reported in Reference 33 and on NUREG-1150 estimates as presented in Reference 1. In addition, CPSES-specific calculations for high pressure sequences (Figure 4.6-14) show hot leg temperatures around 900°C (1700°F), surge line temperatures around 800°C (1500°F), while the steam generator tubes are still around 500°C (900°F). The differential is less (Ref. 33) if the pump bowls are cleared by operator action to bump the pumps, because of the possibility of unidirectional natural

convection flows. However, hot leg/surge line failures are still more likely than ISGTRs in those cases, due to the higher temperatures at those locations.

In summary, these issues are all individually addressed via CETs. Furthermore, their main effect is RCS depressurization, which is investigated for a much wider probability range in Section 4.6.3.2 by examining variations in CET end-state probabilities resulting from perturbations in the probability of operator action to depressurize the RCS, namely BE HOP-DP.

d. Core relocation characteristics at high RCS pressures

e. Mode of reactor vessel melt-through at high RCS pressures

f. Direct Containment Heating (DCH)

Since direct containment heating is related to the core relocation characteristics and to the mode of vessel melt-through, these three issues are discussed together.

The mass of core debris released from the primary system at vessel failure, compared to that released later, can have a first-order effect on the subsequent containment response. Material released promptly from the primary system may be dispersed out of the reactor cavity and might participate in direct containment heating (DCH). Materials released later typically remain in the volume under the vessel. Dispersal processes also depend on the flow of gas from the primary system, which is affected by the mode of reactor vessel failure.

In the write-up for the NRC/IDCOR issue 6, the staff stated that the level of uncertainty in mechanistic calculations of core melt progression was high. Accordingly, they stated that parametric variations in the masses of core materials discharged at vessel failure should be used to investigate the impact of these uncertainties on the containment response in future IDCOR studies.

In the CPSES IPE, all the MAAP parameters related to these issues were varied from the base-case recommended values to extreme values, for the purpose of addressing these issues via sensitivity studies. More than one calculation was performed varying these parameters, as discussed in Section 4.6. However, one example is sufficient to show that the range was fully explored. For this purpose, consider MAAP calculations SB2H4 and SB2H5. SB2H4 has nominal expected values for the relevant parameters, while SB2H5 has extreme values, used to investigate the possibly of containment failure caused by DCH.

The parameter modifications for SB2H5 follow the guidelines suggested in Reference 33 and are as follows:

- TTRX=1800. The time to fail a bottom head penetration after support plate failure was increased from 1 minute in the basic calculation (SB2H4) to 30 minutes (SB2H5) in order to accumulate more molten material for dispersion into containment at vessel failure. Increasing the time any further leads to lower pressures at vessel failure because the steam production decreases as the lower plenum water boils away.

- FCDMA=1. The debris was assumed to be entrained directly into the upper compartment (SB2H5) instead of the lower compartment (SB2H4). This leads to a greater pressure rise due to its larger volume, but is somewhat unrealistic given the CPSES containment layout (see Section 4.1).

- FENTR=1E-06. This is the critical superficial gas velocity for entrainment of corium used for SB2H5. The nominal value is around 1, used for SB2H4. A very low number implies that there is no threshold and corium is entrained into the upper compartment at any gas speed. This is unrealistic but maximizes the amount of corium entrained to the upper compartment.

- FCMDCH=1. This is the fraction of dispersed debris that contributes to DCH in SB2H5. The base-case value in SB2H4 is 0.1.

- FCDMH=1. This is the fraction of debris that is assumed to be dispersed in SB2H5.

- NVP=1000. The equivalent area of 1000 bottom head penetrations was assumed to open at vessel failure in SB2H5. The base-case value in SB2H4 is 1.

- TAUTO=460°K. This is the critical temperature for a burn to occur. It incorporates steam inerting characteristics. Nominal value matching data is around 983°K, which is used in SB2H4. This is the most serious contributor to the pressure spike as it causes all hydrogen to burn at HPME simultaneously with the DCH.

The effect of these changes in parameters on the containment pressure history can be seen by comparing Figure 4.6-10 and 4.6-11. (Other examples of HPME failures obtained as outlined above are seen in Figures 4.6-3, 4.6-12 and 4.6-13). It should be noted that in all cases, even with the extreme variations in values for parameters 1 through 6 listed above, without the simultaneous hydrogen burn forced by the change in parameter 7, the pressure at vessel failure did not approach the containment failure pressure. The extreme variations in all parameters 1 through 6 available in MAAP are to maximize the DCH spike and were adjusted to the maximum in that direction. Only with the burn can the failure occur. However, the burn would not be likely due to inerting conditions. If inerting were not to occur, the initial pressure would also be too low for early containment failure. These findings are part of the rationale for why, by using the values of Table 4.6-1 and the NUREG/CR-4551 HPME pressure rise fractiles for Zion, it was felt that an upper bound on the corresponding CPSES pressure rises was obtained.

g. Core relocation characteristics at low RCS pressures

h. Mode of reactor vessel melt-through at low RCS pressures

i. Fuel/coolant interactions at high and low pressures

All the above issues are important because of the possibility of in-vessel and ex-vessel steam explosions with the potential for the so-called alpha failure mode of the containment. This issue has been addressed on a generic basis in the open literature, and it is not a likely threat for large dry PWR containments. However, for the sake of completeness the issue is addressed in the CPSES CETs via BE PRALPAL under top event CFE1, Figure 4.5-5. Due to the small likelihood of this event, a probability of 8E-3 is used for it, based on NUREG-1150 expert judgement as reported in Reference 1. The alpha mode failure at high pressures is considered to be an order of magnitude less likely based on the same reference and is also considered via BE PRALPAH under top event CFE2, Figure 4.5-6. Consideration of this phenomenon in the way described assures that no vulnerabilities for it are masked. Furthermore, due to the unlikelihood of the alpha failure mode for CPSES, particularly in view of the concrete thickness and configuration of the cavity region, as described in Section 4.1, it is felt that additional sensitivity studies on this issue are not warranted.

j. Potential for early containment failure due to pressure loads

In the case of CPSES, the potential for early containment failure due to pressure loads is addressed in the CET under top event CFE1, Figure 4.5-5, and under top event CFE2, Figure 4.5-6. The phenomena considered are: (a) HPME, including DCH, combustion of hydrogen produced in-vessel and steam spikes

(PRWCP-PULT, PRDCP-PULT), which are discussed in Section 4.6.1 and under d,e,f above; and (2) as alpha failure mode at high and low RCS failure pressures (PRALHPH and PRALPL), which are discussed in Section 4.6.1 and under g,h,i above.

k. Potential for early containment failure due to direct contact by core debris

Although this event is formally considered in the CETs under logic tree top events CFE1 and CFE2, there is no possibility of direct contact of the debris with the containment liner other than in particulate form in a DCH event, which is already addressed as discussed in Section 4.6.1 and under d,e,f above. This conclusion comes from an examination of plant drawings and a walkdown of the plant cavity area. As a result, the BE probability for this event (PRIMPINGE) is set to zero.

l. Long term disposition of core debris (coolable or not coolable)

m. Long-term core-concrete interactions: water availability and coolability of debris

The issues of debris coolability and core-concrete interactions are addressed in the CPSES CETs. The treatment of these issues is comprehensive, all possibilities are considered, and thus, the potential for vulnerabilities is adequately explored via CETs in the manner explained in this sub-section.

The debris coolability issue is addressed in top events DC1, DC2 and DC3, Figures 4.5-7, 4.5-8 and 4.5-9, respectively. When the debris is coolable, there is no CCI. When the debris is not coolable, there is CCI. CCI sequences dominate the containment failure modes with 49% of the CMF. There are two types of PDS which result in CCI related failure of the containment: (1) PDS where the debris is not coolable because it is in a non-coolable configuration, i.e., an insulating crust has formed which prevents heat transfer to an existing overlying water pool, and (2) PDS where the debris was originally in a coolable configuration with water over it and the water dried out and CCI began. Top events DC1, DC2 and DC3 consider both these cases, via events DEBFORM and WTRPOOL. Distinction is also made between low and high pressure cases, because the debris is more likely to be coolable when it is forcefully expelled from the vessel at high pressure, although the occurrence of a steam explosion which is more likely at low pressure, also increases the chances a coolable configuration. The approach is conservative because it assumes that when the debris is found non-coolable due to dry-out, it then becomes definitely non-coolable and cannot be recovered, as if it had become also geometrically or crust-wise non-coolable. The result of this approach is that, typically, there is a 3% to 6% probability of the debris being non-coolable if there is an overlying pool, and a 100% probability if there is not.

Given the size of the CPSES containment and the amount of concrete and metal, the containment cannot fail from steam overpressurization from RCS and accumulator inventories alone. Therefore, all sequences where ECCS fails to inject lead to dry-out prior to containment failure. All these sequences are then, after dry-out, assumed to be unrecoverable and result in CCI-induced containment failure.

CCI-induced containment failure can occur in three ways: (1) from overpressurization due to non-condensibles generated in the CCI, (2) from basemat melt-through and from (3) combustion of non-condensibles generated in the CCI.

In cases where the pool above the debris dries out, i.e., when the debris is initially in a coolable configuration, the most likely outcome is overpressurization. Combustion of non-condensibles, which is considered in the CETs under top events CFL1-6, Figures 4.5-15 through 4.5-20, accounts for only a small fraction of these late failures, primarily because they are dry-out type situations with high steam content, and therefore are inerted. In order to determine whether the overpressurization or the melt-through mechanism prevails at CPSES, a dry-out debris bed situation maximizing CCI was simulated with MAAP. This was done by obtaining an early vessel failure time with minimum cavity inventory, in order to obtain an early cavity dry-out as well. The early vessel failure time was obtained by a station blackout initiator with no ECCS and no auxiliary feedwater from time zero. The early dry-out of the cavity was obtained by shutting off all sprays and failing all accumulators. Results of this bounding calculation are shown in Figure 4.6-16 for two types of concrete composition: (1) high limestone (SBOCCI) and (2) limestone/common sand (SBOCCI2). Some of the initial MAAP calculations assumed a high limestone composition based on the soil composition. A subsequent investigation revealed the composition is very near the CORCON default for the limestone/common sand type. The two calculations illustrate that for either type of concrete, overpressurization precedes melt-through by a large margin. In these calculations (Figure 4.6-16), it would take more than 240 hours to erode the 4.0 m thick basemat. On the other hand, Figure 4.6-16 shows that overpressurization due to non-condensibles could occur in about 30 to 36 hours. Therefore, while there are uncertainties involved and differences due to the type of concrete, it is felt that due to the difference of a factor of about ten (based on extrapolation of Figure 4.6-16) between failure times for these modes, basemat melt-through would be very unlikely at CPSES for dry-out cases. The two main reasons why basemat melt-through is highly unlikely in these cases are: (1) the CPSES large cavity area (70 m^2) results in a low erosion depth for a given eroded volume and allows for a higher radiation heat transfer area, and (2) the boiling off of the steam prior to dry-out takes the containment pressure to a high level prior to the onset of CCI. The non-coolable configuration by reason of dry-out

applies to PDS where the ECCS failed to inject, namely, 1H, 3H, 5H, 3SBO, 4SBO, and represents 93.7% of the CCI failures or 46% of the CMF.

In cases where the debris is non-coolable by reason of crust formation, the mode of CCI-induced failure is less clear cut. That is because in these cases, the atmosphere may not be inerted since the debris is insulated from its overlying water pool, and the debris may not occupy the entire cavity area and thus moves downward more rapidly. This type of progression has been simulated with MAAP (e.g., VSB3F1, Figure 4.6-7) by reducing the cavity area from 70 m^2 to 7 m^2 and reducing the heat transfer coefficient between the water pool and the debris to a very low number. That calculation shows that when the cavity area is reduced by a factor of 10, then basemat melt-through (90 hours) can precede overpressurization (over 400 hours). In this case, burns prior to 90 hours would also be possible as shown in calculation VSB3F4, Figure 4.6-9. Thus, while uncertainty exists in the mode of CCI failure in cases where the debris is non-coolable by reason of crust formation, these cases are not statistically significant. This is because the non coolable configuration by reason of crust formation applies only to a small (3% to 6%) fraction of PDS 3F, 4F, 6F, 1F, 2F, 6H, 4H, 5F, 2H, for a total frequency of only 6.3% of the CCI failures or 3.1% of the CMF. This is much less significant than the dry-out situation, which represents 93.7% of the CCI failures or 46% of the CMF. Furthermore, the magnitude of the uncertainty discussed here exists because it was assumed that: (a) the debris occupies only 10% of the cavity area and (b) there is no heat transfer to the pool, i.e., no steam formation. Both of these assumptions are extreme and unlikely in themselves. Therefore, it is still likely that in the case of CPSES non-coolable debris CCI would also lead to overpressurization failure, as in the dry-out case.

A final point to be clarified is how debris coolability issues are addressed in the CPSES IPE in the cases of early containment failure. There are two groups of early failure PDSs, each of which is assumed to have a definite coolable or non-coolable progression for the reasons discussed below.

The first group involves bypass PDSs 1CB and 2CB, namely SGTR and V-Sequences (containment isolation failures are statistically negligible, as discussed in Section 4.6). This group is non-coolable by virtue of dry-out and, therefore, all these sequences have the MAAP-calculated core-concrete interaction following vessel failure and dry-out.

The second group includes all other early failures, which are either from HPME or alpha-type events. In these cases, the debris is finely dispersed and suspended in the containment atmosphere from where

it would have a very large settling area and, therefore, could not form a deep pool,i.e., it would have to be coolable. In order to illustrate this point, consider Table 4.5-4, which provides an indication of potential debris bed thicknesses. Knowing that the core barrel and upper internals would not be molten at the time of vessel failure, and would, therefore, not be expelled from the vessel at that time, and would either stay in place or fail off later as large solid pieces with no decay heat, it can be inferred from Table 4.5-4 that the maximum cavity debris depth would be 23 cm (30 cm if an average corium density of 7000 Kg/m^3 is used). Further, knowing that in the HPME events the MAAP calculations required 100% debris dispersion in order to fail the containment, when the entire containment settling areas are considered, it is obvious that the debris bed cannot be deep enough not to be coolable. Even if only 50% debris dispersion were enough to fail containment, the cavity depth alone would be less than 15 cm. Therefore, when HPME and/or alpha are the containment failure modes, the debris must be coolable at CPSES.

4.6.3.2 System and Operational Uncertainties

In addition to the phenomenological uncertainties discussed in Section 4.6.3.1, there are a number of system and operational uncertainties which warrant discussion particularly due to their applicability towards accident management. These are presented below.

a. Effect of operator action to depressurize the RCS at the onset of core damage

Procedure FRC-0.1A instructs operators to depressurize the RCS when core exit thermocouples reach 1200°F. This action reduces the RCS pressure at vessel failure and reduces the probability of DCH. Since the action is proceduralized, the base case CET end-state probabilities in this report includes credit for it in the CETs, by appropriately calculating BE HOP-DP, shown in logic tree DP, Figure 4.6-2. It should be noted that the calculation includes consideration of the availability of power and equipment (PORVS) as well as human factors, i.e., the probability that operators will act given a proceduralized action.

In spite of the foregoing, a sensitivity study was conducted to examine the impact of assuming operators fail to depressurize the RCS. The driving force for the study is to verify that no vulnerabilities will surface in this hypothetical case, rather than concern that the action might not be taken. The key concerns are increases in the early containment failure frequency due to increases in DCH and ISGTR probabilities. The study was conducted by setting BE HOP-DP to 1.0 and comparing the key frequencies with those obtained using the base case values for HOP-DP. It should be noted that the variation in top

event DP, Figure 4.6-2, is much greater from varying HOP-DP, given its range, than it would be from variations in other parameters affecting depressurization, namely PRHLSLOK, PRSEALOK, etc... Therefore, this study also illustrates the sensitivity of early containment failure frequency to other the uncertainties related to RCS depressurization, as was pointed out in Section 4.6.3.1 item c.

The early containment failure probability for the sensitivity case is 4.29E-06, while the base case value shown in Table 4.6-4 is 4.12E-06. This variation is small and confirms that no vulnerabilities to HPME phenomena exist at CPSES. The narrow difference is in part due to the fact that depressurization increases the alpha mode failure probability. In other words, HPME and alpha are in competition and of similar weight as early failure contributors.

b. Potential benefits of the fan coolers

Fan coolers can reduce the frequency of early failures, but the attendant risk reduction is insignificant. If functioning at time of core uncovery, they would reduce the HPME-induced containment failure frequency by reducing the base pressure in containment at vessel failure. However, these are only 5.4% of the early failures (which are 9.4% of CMF), i.e., 0.5% of the CMF, and the fans would improve this by a fraction at best.

Fan coolers can reduce the frequency of steam-induced late containment failures, but the attendant risk reduction is also insignificant. Steam-induced late containment failures are 2.1% of the CMF. Again, fans could only improve this by a fraction at best, so the potential gain for these cases is also marginal.

The greatest potential for Fan cooler benefit is in the CCI sequences which dominate the containment failure modes with 49% of the CMF.

The key is just how effective can the fans be in these CCI cases. There are two types of PDS which contribute to this kind of failure: (1) PDS where the debris is not coolable because it is in a non-coolable configuration and/or an insulating crust has formed which prevents heat transfer to an existing overlying water pool and (2) PDS where the debris was originally in a coolable configuration with water over it and the water dried out and CCI began.

The first situation cannot be helped by fan coolers because while they can stop overpressurization, they cannot preclude the basemat melt-through. The effect of fan coolers for these PDS would simply be to

switch the likelihood of CCI-induced failure from non-condensible overpressurization to basemat penetration. While this is an improvement in source term, it is not an improvement in containment integrity probability. This first situation applies to a small fraction of almost all PDS, namely 3F, 4F, 6F, 1F, 2F, 6H, 4H, 5F, 2H. Its total frequency is 6.3% of the CCI failures or 3.1% of the CMF, which is significantly less than the second situation.

The second situation, namely PDS 1H, 3H, 5H, 3SBO, 4SBO, represent 93.7% of the CCI failures or 46% of the CMF. This is a situation where the debris was originally in a coolable configuration with water over it, the water dried out and CCI began. If a sufficient number of fan coolers had been in operation, the overlying water pool would never have dried out. The potential benefit of the fan coolers for these cases is clearly high. This is the situation for which the fan coolers are considered.

While the PDS where potential benefits exist has been established, it remains to determine for each of these, namely PDS 1H, 3H, 5H, 3SBO, 4SBO: (1) how many fan coolers will keep the overlying pool from drying out, (2) for what fraction of the frequency of these PDS are the fans available, and (3) can the operating fan coolers be expected to continue to operate, if they are started and their importance is understood by the operators.

In order to determine the number of fan coolers required, a bounding scenario was established based on PDS 5H, which is a large break LOCA without ECCS. Since all the PDS under consideration are dry, all involve ECCS failure to inject. Thus, while 5H is bounding due to the early core melt, it is also a representative scenario. Calculations were performed for 0, 2, 3, and 4 fan cases. The most significant result is shown in Figure 4.6-15 which shows the mass of water in the cavity (MWC1) for each case. While the time to dry out increases, as expected, with increasing the number of fans in operation, only when all four fans are in operation does the cavity remain wet indefinitely. Therefore, all four fans would be required to prevent containment failure for PDS 1H, 3H, 5H, 3SBO, 4SBO.

The next step is to examine PDS 1H, 3H, 5H, 3SBO, 4SBO, to determine for what fraction of their frequencies of occurrence could fans be available or recovered. A preliminary examination revealed that this fraction would be negligible, unless recovery actions are undertaken. Therefore, the benefits of containment failure probability reduction from fan coolers have not been included in the present IPE. Nevertheless, the present discussion is relevant as part of a knowledge base for accident management.

Table 4.6-1: NUREG-1150 HPME Pressure Rise Probability Distributions for Zion

RCS Pressure		Cavity Status	RPV Debris Mass	Hole Size	PRESSURE RISE FOR FRACTILES (psi) 0.01	0.05	0.10	0.25	0.50	0.75	0.90	0.95	0.99
1	HI	WET	HI	HI	19.55	35.12	47.47	75.24	98.17	116.83	140.64	156.81	177.97
2	HI	WET	HI	LO	18.22	30.71	39.53	59.52	88.62	104.34	121.24	142.11	164.15
3	HI	WET	LO	HI	17.64	29.83	36.59	51.58	66.87	82.30	95.23	102.43	112.57
4	HI	WET	LO	LO	16.31	26.75	32.33	43.21	59.52	71.42	82.74	94.50	111.98
5	HI	DRY	HI	HI	28.07	41.88	55.40	85.68	108.46	125.21	141.96	150.9[illegible]	166.06
6	HI	DRY	HI	LO	27.04	37.62	46.73	69.81	98.76	114.63	126.39	136.08	156.37
7	HI	DRY	LO	HI	27.19	35.71	43.21	59.08	73.04	86.12	100.23	106.69	116.98
8	HI	DRY	LO	LO	21.75	29.83	35.71	49.38	66.28	79.36	90.23	95.82	107.28
9	MED	WET	HI	HI	17.49	28.95	37.33	53.79	78.18	94.79	107.87	119.63	141.08
10	MED	WET	HI	LO	14.11	24.54	30.27	43.06	65.84	82.18	101.40	113.31	140.64
11	MED	WET	LO	HI	15.25	23.95	29.25	39.68	53.64	65.99	75.54	80.53	87.00
12	MED	WET	LO	LO	13.37	18.37	22.34	3[illegible].48	46.00	58.34	65.54	69.51	76.71
13	MED	DRY	HI	HI	29.39	36.74	44.09	60.84	88.03	104.78	116.39	124.92	142.38
14	MED	DRY	HI	LO	20.87	30.57	36.45	49.38	73.77	96.85	108.90	114.48	132.85
15	MED	DRY	LO	HI	24.54	30.42	33.95	43.50	59.08	70.25	77.30	82.00	88.03
1[illegible]	MED	DRY	LO	LO	15.72	24.54	28.80	36.15	51.14	63.78	71.72	75.83	82.89
17	LOW	WET	--	--	6.61	11.02	13.52	17.93	25.72	36.45	44.38	49.08	62.90

RCS HI = 2000-2500 PSI
RCS MED = 500-1000 PSI
RCS LO = 50-200 PSI
MASS HI = 75%
MASS LO = 33%
HOLE HI = 2 M^2
HOLE LO = 0.1 M^2

Table 4.6-2: Calculation of Containment Reliability for HPME Events

CONT. PRES. (PSI)	CPSES CONT. SURVIVAL PROB.	HPME PRES. PROB. PDS 2H	A = $F_{2i} + F_{2i-1}$	B = $F_{1i} - F_{1i-1}$	(A*B)/2
0	1	0			
80	0.999	0	1.998	0	0
93	0.999	0.01	1.997	0.01	0.00998
98	0.999	0.05	1.997	0.04	0.0399
102	0.999	0.1	1.997	0.05	0.0499
105	0.999	0.16	1.997	0.06	0.0599
112	0.999	0.23	1.997	0.07	0.0698
113	0.977	0.31	1.975	0.08	0.0790
121	0.841	0.39	1.818	0.08	0.0727
126	0.7	0.5	1.541	0.11	0.0847
129	0.5	0.61	1.2	0.11	0.066
137	0.159	0.7	0.659	0.09	0.0296
138	0.04	0.8	0.199	0.1	0.00995
145	0.0228	0.9	0.063	0.1	0.00314
150	0.0121	0.95	0.035	0.05	0.00087
153	0.0014	0.975	0.014	0.025	0.000168
154	0	0.985	0.0014	0.01	0.000007
157	0	0.989	0	0.004	0
159	0	0.99	0	0.001	0
185	0	1	0	0.01	0
CONTAINMENT RELIABILITY FOR PDS 2H= = = >					0.576
		PDSs 1E, 1F,1H,2E,2F			
33	0.999	0	1.999	0	0
46	0.999	0.01	1.999	0.01	0.00999
51	0.999	0.05	1.999	0.04	0.03997
55	0.999	0.1	1.999	0.05	0.04996
65	0.999	0.25	1.998	0.15	0.14988
79	0.999	0.5	1.998	0.25	0.24976
91	0.998	0.75	1.998	0.25	0.2497
99	0.998	0.9	1.997	0.15	0.1498
103	0.998	0.95	1.997	0.05	0.0499
105	0.998	0.9814	1.997	0.0313	0.0313
110	0.998	0.99	1.997	0.00865	0.00863
112	0.998	1	1.997	0.01	0.009985
113	0.977	1	1.976	0	0
121	0.841	1	1.818	0	0
129	0.5	1	1.341	0	0
137	0.159	1	0.659	0	0
138	0.07	1	0.229	0	0
145	0.0228	1	0.0928	0	0
153	0.0014	1	0.0242	0	0
CONTAINMENT RELIABILITY FOR PDS 1E,1F,1H,2E,2F= = = >					0.999

Table 4.6-3: End-State Probabilities for Small Break LOCA PDS

	1H	1E	1F	2H	2E	2F
PDS	1	1	1	1	1	1
A1	0.00	0.00	0.00	0.00	0.00	0.00
A2	0.00	0.00	0.00	0.00	0.00	0.00
B1	0.00	0.00	0.00	0.00	0.00	0.00
B2-L	0.00	0.00	0.00	0.00	0.00	0.00
B2-R	0.00	0.00	0.00	0.00	0.00	0.00
C1-L	0.00	0.00	0.00	0.00	0.00	0.00
C1-R	0.00	0.00	0.00	0.00	0.00	0.00
C2-L	0.00	0.00	0.00	0.00	0.00	0.00
C2-R	0.00	0.00	0.00	0.00	0.00	0.00
D1-L	0.00	0.00	0.00	0.00	0.00	0.00
D1-R	0.00	0.00	0.00	0.00	0.00	0.00
D2-L	0.00	0.00	0.00	0.00	0.00	0.00
D2-R	0.00	0.00	0.00	0.00	0.00	0.00
B3-L	0.00	7.42E-05	0.00	2.06E-03	7.42E-05	0.00
B3-R	0.00	3.73E-07	0.00	1.04E-05	3.73E-07	0.00
B4-L	0.00	2.96E-02	0.00	8.23E-01	2.96E-02	0.00
B4-R	0.00	1.49E-04	0.00	4.14E-03	1.49E-04	0.00
C3-L	0.00	9.21E-06	7.02E-02	1.75E-04	9.21E-06	1.07E-02
C3-R	0.00	4.62E-08	3.53E-03	8.81E-07	4.62E-08	5.37E-05
C4-L	9.36E-01	3.68E-03	0.00	6.99E-02	3.68E-03	0.00
C4-R	4.70E-03	1.85E-05	0.00	3.51E-04	1.85E-05	0.00
D3-L	0.00	0.00	0.00	1.18E-06	0.00	0.00
D3-R	0.00	1.00E-06	7.62E-03	2.02E-05	1.00E-06	1.16E-03
D4-L	0.00	0.00	0.00	4.71E-04	0.00	0.00
D4-R	7.62E-03	3.99E-04	0.00	8.07E-03	3.99E-04	0.00
B5-L	0.00	1.46E-03	0.00	6.18E-05	1.46E-03	0.00
B5-R	0.00	7.32E-06	0.00	3.10E-07	7.32E-06	0.00
B6-L	0.00	5.81E-01	0.00	2.47E-02	5.81E-01	0.00
B6-R	0.00	2.92E-03	0.00	1.24E-04	2.92E-03	0.00
C5-L	0.00	1.17E-04	2.35E-03	3.41E-06	1.17E-04	4.23E-02
C5-R	0.00	5.90E-07	1.18E-05	1.71E-08	5.90E-07	2.12E-04
C6-L	4.70E-02	4.68E-02	0.00	1.36E-03	4.68E-02	0.00
C6-R	2.36E-04	2.35E-04	0.00	6.83E-06	2.35E-04	0.00
D5-L	5.93E-08	1.19E-06	2.37E-05	2.49E-05	1.19E-06	4.27E-04
D5-R	1.57E-07	3.15E-06	6.30E-05	2.50E-05	3.15E-06	1.13E-03
D6-L	2.37E-05	4.73E-04	0.00	9.94E-03	4.73E-04	0.00
D6-R	6.28E-05	1.26E-03	0.00	9.98E-03	1.26E-03	0.00
TOT	0.995	0.043	0.0806	0.955	0.668	0.056

Table 4.6-4: End-State Probabilities for Transient PDS

	3H	3E	3F	4H	4E	4F
PDS	1	1	1	1	1	1
A1	0.00	0.00	0.00	0.00	0.00	0.00
A2	0.00	0.00	0.00	0.00	0.00	0.00
B1	0.30	0.00	0.00	0.00	0.00	0.00
B2-L	0.00	0.00	0.00	0.00	0.00	0.00
B2-R	0.00	0.00	0.00	0.00	0.00	0.00
C1-L	0.00	0.00	0.00	0.00	0.00	0.00
C1-R	0.00	0.00	0.00	0.00	0.00	0.00
C2-L	0.00	0.00	0.00	0.00	0.00	0.00
C2-R	0.00	0.00	0.00	0.00	0.00	0.00
D1-L	0.00	0.00	0.00	0.00	0.00	0.00
D1-R	0.00	0.00	0.00	0.00	0.00	0.00
D2-L	0.00	0.00	0.00	0.00	0.00	0.00
D2-R	0.00	0.00	0.00	0.00	0.00	0.00
B3-L	0.00	3.54E-01	0.00	9.58E-02	1.48E-01	0.00
B3-R	0.00	1.78E-03	0.00	4.81E-04	7.45E-04	0.00
B4-L	0.00	0.00	0.00	4.49E-02	6.95E-02	0.00
B4-R	0.00	0.00	0.00	2.26E-04	3.50E-04	0.00
C3-L	0.00	4.39E-02	6.86E-02	3.09E-02	2.99E-02	4.42E-02
C3-R	0.00	2.21E-04	3.45E-04	1.55E-04	1.50E-04	2.22E-04
C4-L	6.93E-01	0.00	0.00	1.45E-02	1.40E-02	0.00
C4-R	3.48E-03	0.00	0.00	7.29E-05	7.05E-05	0.00
D3-L	0.00	0.00	0.00	0.00	0.00	0.00
D3-R	0.00	4.77E-03	7.45E-03	3.36E-03	3.25E-03	4.80E-03
D4-L	0.00	0.00	0.00	0.00	0.00	0.00
D4-R	5.64E-03	0.00	0.00	1.58E-03	1.52E-03	0.00
B5-L	0.00	2.45E-01	0.00	3.58E-02	1.03E-01	0.00
B5-R	0.00	1.23E-03	0.00	1.80E-04	5.16E-04	0.00
B6-L	0.00	0.00	0.00	1.68E-02	4.82E-02	0.00
B6-R	0.00	0.00	0.00	8.43E-05	2.42E-04	0.00
C5-L	0.00	1.98E-02	3.36E-03	7.49E-03	1.35E-02	1.96E-02
C5-R	0.00	9.94E-05	1.69E-05	3.76E-05	6.76E-05	9.84E-05
C6-L	2.89E-01	0.00	0.00	3.51E-03	6.32E-03	0.00
C6-R	1.45E-03	0.00	0.00	1.77E-05	3.17E-05	0.00
D5-L	1.03E-03	2.02E-03	3.43E-04	5.48E-02	1.37E-03	2.00E-03
D5-R	1.17E-03	2.35E-03	4.00E-04	5.50E-02	1.60E-03	2.33E-03
D6-L	4.70E-04	0.00	0.00	2.57E-02	6.44E-04	0.00
D6-R	5.48E-04	0.00	0.00	2.58E-02	7.51E-04	0.00
TOT	0.995	0.675	0.0806	0.417	0.444	0.0733

Table 4.6-5: End-State Probabilities for Station Blackout PDS

	3S	4S
INI	1	1
A1	0.00	0.00
A2	0.00	0.00
B1	0.00	0.00
B2-L	0.00	0.00
B2-R	0.00	0.00
C1-L	3.53E-03	1.70E-04
C1-R	1.77E-05	8.54E-07
C2-L	6.56E-04	3.57E-05
C2-R	3.29E-06	1.79E-07
D1-L	0.00	0.00
D1-R	3.83E-04	1.85E-05
D2-L	0.00	0.00
D2-R	7.12E-05	3.87E-06
B3-L	0.00	0.00
B3-R	0.00	0.00
B4-L	0.00	0.00
B4-R	0.00	0.00
C3-L	5.60E-03	3.24E-04
C3-R	2.81E-05	1.63E-06
C4-L	7.80E-01	5.76E-01
C4-R	3.92E-03	2.89E-03
D3-L	0.00	0.00
D3-R	6.08E-04	3.51E-05
D4-L	0.00	0.00
D4-R	6.47E-03	4.70E-03
B5-L	0.00	0.00
B5-R	0.00	0.00
B6-L	0.00	0.00
B6-R	0.00	0.00
C5-L	6.26E-05	1.41E-04
C5-R	3.14E-07	7.08E-07
C6-L	1.31E-02	3.76E-01
C6-R	6.57E-05	1.89E-03
D5-L	1.89E-03	6.88E-05
D5-R	1.91E-03	7.10E-03
D6-L	8.27E-04	3.21E-03
D6-R	8.34E-04	3.31E-03
TOT	0.82	0.983

Table 4.6-6: End-State Probabilities for Large Break LOCA PDS

	5H	5E	5F	6H	6E	6F
PDS	1	1	1	1	1	1
A1	0.00	0.00	0.00	0.00	0.00	0.00
A2	0.00	0.00	0.00	0.00	0.00	0.00
B1	0.00	0.00	0.00	0.00	0.00	0.00
B2-L	0.00	0.00	0.00	0.00	0.00	0.00
B2-R	0.00	0.00	0.00	0.00	0.00	0.00
C1-L	0.00	0.00	0.00	0.00	0.00	0.00
C1-R	0.00	0.00	0.00	0.00	0.00	0.00
C2-L	0.00	0.00	0.00	0.00	0.00	0.00
C2-R	0.00	0.00	0.00	0.00	0.00	0.00
D1-L	0.00	0.00	0.00	0.00	0.00	0.00
D1-R	0.00	0.00	0.00	0.00	0.00	0.00
D2-L	0.00	0.00	0.00	0.00	0.00	0.00
D2-R	0.00	0.00	0.00	0.00	0.00	0.00
B3-L	0.00	1.48E-03	0.00	1.60E-03	1.48E-03	0.00
B3-R	0.00	7.45E-06	0.00	8.03E-06	7.45E-06	0.00
B4-L	0.00	5.92E-01	0.00	6.37E-01	5.92E-01	0.00
B4-R	0.00	2.98E-03	0.00	3.20E-03	2.98E-03	0.00
C3-L	0.00	1.84E-04	7.37E-02	1.84E-04	1.84E-04	7.37E-02
C3-R	0.00	9.25E-07	3.70E-04	9.25E-07	9.25E-07	3.70E-04
C4-L	9.82E-01	7.35E-02	0.00	7.35E-02	7.35E-02	0.00
C4-R	4.94E-03	3.69E-04	0.00	3.69E-04	3.69E-04	0.00
D3-L	0.00	0.00	0.00	0.00	0.00	0.00
D3-R	0.00	2.00E-05	8.00E-03	2.00E-05	2.00E-05	8.00E-03
D4-L	0.00	0.00	0.00	0.00	0.00	0.00
D4-R	8.00E-03	7.98E-03	0.00	7.98E-03	7.98E-03	0.00
B5-L	0.00	0.00	0.00	0.00	0.00	0.00
B5-R	0.00	0.00	0.00	0.00	0.00	0.00
B6-L	0.00	0.00	0.00	0.00	0.00	0.00
B6-R	0.00	0.00	0.00	0.00	0.00	0.00
C5-L	0.00	0.00	0.00	0.00	0.00	0.00
C5-R	0.00	0.00	0.00	0.00	0.00	0.00
C6-L	0.00	0.00	0.00	0.00	0.00	0.00
C6-R	0.00	0.00	0.00	0.00	0.00	0.00
D5-L	0.00	0.00	0.00	0.00	0.00	0.00
D5-R	0.00	0.00	0.00	0.00	0.00	0.00
D6-L	0.00	0.00	0.00	0.00	0.00	0.00
D6-R	0.00	0.00	0.00	0.00	0.00	0.00
TOT	0.995	0.678	0.0821	0.724	0.678	0.0821

Table 4.6-7: Summary of Conditional Containment Failure Probabilities for Small Break LOCA PDS

	1H	1E	1F	2H	2E	2F
Early, Leak	2.38E-05	4.74E-04	2.37E-05	1.04E-02	4.74E-04	4.27E-04
Early, Rupture	7.68E-03	1.66E-03	7.68E-03	1.81E-02	1.66E-03	2.29E-03
CCI, Leakage	9.83E-01	5.06E-02	7.26E-02	7.14E-02	5.06E-02	5.30E-02
CCI, Rupture	4.94E-03	2.54E-04	3.65E-04	3.59E-04	2.54E-04	2.66E-04
Steam, Leakage	0.00	6.12E-01	0.00	8.50E-01	6.12E-01	0.00
Steam, Rupture	0.00	3.08E-03	0.00	4.27E-03	3.08E-03	0.00
Early, Total	7.71E-03	2.14E-03	7.71E-03	2.85E-02	2.14E-03	2.72E-03
Late, Leak	9.83E-01	6.63E-01	7.26E-02	9.21E-01	6.63E-01	5.30E-02
Late, Rupture	4.94E-03	3.33E-03	3.65E-04	4.63E-03	3.33E-03	2.66E-04
CCI Total	9.88E-01	5.09E-02	7.29E-02	7.18E-02	5.[illegible]	5.33E-02
Steam Total	0.00	6.15E-01	0.00	8.54E-01	6.15E-01	0.00
TOTAL	9.96E-01	6.68E-01	8.06E-02	9.54E-01	6.68E-01	5.60E-02

Table 4.6-8: Summary of Conditional Containment Failure Probabilities for Transient PDS

	3H	3E	3F	4H	4E	4F
Early, Leak	1.47E-03	2.02E-03	3.43E-04	8.05E-02	2.01E-03	2.00E-03
Early, Rupture	7.35E-03	7.12E-03	7.85E-03	8.57E-02	7.12E-03	7.13E-03
CCI, Leakage	9.82E-01	6.37E-02	7.20E-02	5.64E-02	6.37E-02	6.38E-02
CCI, Rupture	4.93E-03	3.20E-04	3.62E-04	2.83E-04	3.20E-04	3.20E-04
Steam, Leakage	0.00	5.99E-01	0.00	1.93E-01	3.69E-01	0.00
Steam, Rupture	0.00	3.01E-03	0.00	9.71E-04	1.85E-03	0.00
Early, Total	8.83E-03	9.14E-03	8.19E-03	1.66E-01	9.14E-03	9.13E-03
Late, Leak	9.82E-01	6.63E-01	7.20E-02	2.50E-01	4.32E-01	6.38E-02
Late, Rupture	4.93E-03	3.33E-03	3.62E-04	1.25E-03	2.17E-03	3.20E-04
CCI Total	9.87E-01	6.40E-02	7.23E-02	5.67E-02	6.40E-02	6.41E-02
Steam Total	0.00	6.02E-01	0.00	1.94E-01	3.71E-01	0.00
TOTAL	9.96E-01	6.75E-01	8.05E-02	4.17E-01	4.44E-01	7.33E-02

Table 4.6-9: Summary of Conditional Containment Failure Probabilities for Station Blackout PDS

	3S	4S
Early, Leak	2.72E-03	1.01E-02
Early, Rupture	1.03E-02	1.52E-02
CCI, Leakage	8.03E-01	9.53E-01
CCI, Rupture	4.04E-03	4.78E-03
Steam, Leakage	0.00	0.00
Steam, Rupture	0.00	0.00
Early, Total	1.30E-02	2.53E-02
Late, Leak	8.03E-01	9.53E-01
Late, Rupture	4.04E-03	4.78E-03
CCI Total	8.07E-01	9.57E-01
Steam Total	0.00	0.00
TOTAL	8.20E-01	9.83E-01

Table 4.6-10: Summary of Conditional Containment Failure Probabilities for Large Break LOCA PDS

	5H	5E	5F	6H	6E	6F
Early, Leak	0.00	0.00	0.00	0.00	0.00	0.00
Early, Rupture	8.00E-03	8.00E-03	8.00E-03	8.00E-03	8.00E-03	8.00E-03
CCI, Leakage	9.82E-01	7.37E-02	7.37E-02	7.37E-02	7.37E-02	7.37E-02
CCI, Rupture	4.94E-03	3.70E-04	3.70E-04	3.70E-04	3.70E-04	3.70E-04
Steam, Leakage	0.00	5.93E-01	0.00	6.39E-01	5.93E-01	0.00
Steam, Rupture	0.00	2.99E-03	0.00	3.21E-03	2.99E-03	0.00
Early, Total	8.00E-03	8.00E-03	8.00E-03	8.00E-03	8.00E-03	8.00E-03
Late, Leak	9.82E-01	6.67E-01	7.37E-02	7.12E-01	6.67E-01	7.37E-02
Late, Rupture	4.94E-03	3.36E-03	3.70E-04	3.58E-03	3.36E-03	3.70E-04
CCI Total	9.87E-01	7.41E-02	7.41E-02	7.41E-02	7.41E-02	7.41E-02
Steam Total	0.00	5.96E-01	0.00	6.42E-01	5.96E-01	0.00
TOTAL	9.95E-01	6.79E-01	8.21E-02	7.24E-01	6.79E-01	8.21E-02

Table 4.6-11: Accident Sequence Initiator Notation (Prefixes)

INITIATOR	DESCRIPTION		INITIATOR	DESCRIPTION
X1	LOSS OF 125 V DC BUS 1ED1		T1	GENERAL TRANSIENT
X2	LOSS OF CHILLED WATER		T6	LOSS OF FEEDWATER
X3	LOSS OF OFFSITE POWER		T4	MAIN STEAM LINE BREAK
X4	LOSS OF BUS 1A3		IS	INDUCED SMALL BREAK (0.6 TO 2 IN) OVER 60 GPM/PMP IF SEAL LOCA
X5	LOSS OF PROTECTION CHANNEL 1PC1		IVS	INDUCED VERY SMALL BREAK (UP TO 0.6 IN) 21 TO 60 GPM/PMP SEAL LOCA
X6	LOSS OF CC		AT	ATWS
X7	LOSS OF SW		R	STEAM GENERATOR TUBE RUPTURE
X8	LOSS OF INSTRUMENT AIR		CV	LOSS OF CONDENSER VACUUM

Table 4.6-12: Accident Sequence Functions Notation (Suffixes)

FUNCTION LOST (SUFFIX)	DESCRIPTION
CM1	Failure to switchover to recirculation after successful injection.
CM2	Loss of secondary cooling and failure to perform feed and bleed (for T,X,CV). Injection failure (for S,M,A, i.e. LOCA).
CM3	Failure of secondary heat removal and bleed and feed (for VS). Injection failure (for XL).
CM4	Injection failure (VS)
CM5	Injection and Secondary heat removal failure (VS)
CM6	Same as CM5 but TDAFW runs until battery depletion (VS).

Table 4.6-13: Level II Characteristics of Level I Break Size Ranges

RANGE (INCHES)	LEVEL I NOMENCLATURE [MAIN CAUSES]	LEVEL II CHARACTERISTICS (VF PRESSURE)
0 TO 0.6	VS - VERY SMALL [SMALL SEAL LOCA, 60 GPM/PMP]	SAME AS NO BREAK, HIGH PRESSURE AT VF (OVER 2000 PSIA)
0.6 TO 2	VS - VERY SMALL [LARGE SEAL LOCA, 250 GPM/PMP, STUCK OPEN PORV]	INTERMEDIATE PRESSURES AT VF (400 TO 1000 PSIA)
2 TO 4[a]	S - SMALL [STUCK OPEN SRV]	LOW PRESSURES AT VF (LT 200 PSIA)
4 TO 6	M - MEDIUM [PIPE BREAK]	LOW PRESSURES AT VF (LT 200 PSIA)
OVER 6	L - LARGE [PIPE BREAK]	LOW PRESSURES AT VF (LT 200 PSIA)

[a] Breaks greater than 2 inches all lead to low pressures at vessel failure but have different Level I success criteria.

Table 4.6-14: Containment Failure Probabilities Sorted by PDS Frequency

PDS NAME	PDS FREQ	REP SEQ	SEQ PCT	COND EARLY	UNCOND EARLY	COND CCI	UNCOND CCI	COND STEAM	UNCOND STEAM	TOTAL FAIL. PROB.
1H	1.25E-05	ISCM2	100%	7.71E-03	9.65E-08	9.88E-01	1.24E-05	0.00	0.00	1.25E-05
3F	7.06E-06	*CM2	99%	8.83E-03	6.23E-08	9.87E-01	6.97E-06	0.00	0.00	7.03E-06
3F	5.05E-06	ATCM(36)	86%	8.19E-03	4.14E-08	7.23E-02	3.65E-07	0.00	0.00	4.07E-07
4F	4.40E-06	VSCM1	74%	9.13E-03	4.02E-08	6.41E-02	2.82E-07	0.00	0.00	3.22E-07
SGTR	3.48E-06	RCM1	97%	1.00E+00	3.48E-06	0.00	0.00	0.00	0.00	3.48E-06
6F	3.29E-06	ACM1	62%	8.00E-03	2.63E-08	7.41E-02	2.44E-07	0.00	0.00	2.70E-07
1F	2.57E-06	ISCM2	93%	7.71E-03	1.96E-08	7.29E-02	1.88E-07	0.00	0.00	2.07E-07
2F	1.70E-06	SCM1	87%	2.72E-03	4.63E-09	5.33E-02	9.07E-08	0.00	0.00	9.54E-08
4H	1.12E-06	IVSCM4	93%	1.66E-01	1.87E-07	5.67E-02	6.36E-08	1.9E-01	2.2E-07	4.68E-07
6H	9.00E-07	IMCM2	99%	8.00E-03	7.20E-09	7.41E-02	6.66E-08	6.4E-01	5.8E-07	6.51E-07
5F	6.96E-07	ACM2	85%	8.00E-03	5.57E-09	7.41E-02	5.15E-08	0.00	0.00	5.71E-08
4SBO	5.02E-07	IVSCM5	100%	2.53E-02	1.27E-08	9.57E-01	4.81E-07	0.00	0.00	4.93E-07
5H	3.27E-07	ACM2	65%	8.00E-03	2.61E-09	9.87E-01	3.22E-07	0.00	0.00	3.25E-07
3SBO	1.85E-07	IVSCM6	100%	1.30E-02	2.40E-09	8.07E-01	1.49E-07	0.00	0.00	1.52E-07
2H	1.41E-07	ISCM1	100%	2.85E-02	4.02E-09	7.18E-02	1.01E-08	8.5E-01	1.2E-07	1.35E-07
V-Seq	1.19E-07	SCM1	83%	1.00E+00	1.19E-07	0.00	0.00	0.00	0.00	1.19E-07
CI	9.92E-09	ISCM2	37%	1.00E+00	9.92E-09	0.00	0.00	0.00	0.00	9.92E-09
Total	4.41E-05 100%				4.12E-06 9.4%		2.16E-05 49%		9.1E-07 2.1%	2.67E-05 60.5%

Table 4.6-15: PDS in Order of Increasing Early and Total Unconditional Containment Failure Probabilities

PDS NAME	EARLY FAILURE PROB.	PCT OF EARLY TOTAL		PDS NAME	TOTAL CONT FAIL. PROB.	PCT OF TOTAL FAIL
SGTR	3.48E-06	84.4%		1H	1.25E-05	46.7%
4H	1.87E-07	4.5%		3H	7.03E-06	26.3%
V-Seq	1.19E-07	2.9%		SGTR	3.48E-06	13.0%
1H	9.65E-08	2.3%		6H	6.51E-07	2.4%
3H	6.23E-08	1.5%		4SBO	4.93E-07	1.8%
3F	4.14E-08	1.0%		4H	4.68E-07	1.8%
4F	4.02E-08	1.0%		3F	4.07E-07	1.5%
6F	2.63E-08	0.6%		5H	3.25E-07	1.2%
1F	1.98E-08	0.5%		4F	3.22E-07	1.2%
4SBO	1.27E-08	0.3%		6F	2.70E-07	1.0%
CI Fail.	9.92E-09	0.2%		1F	2.07E-07	0.8%
6H	7.20E-09	0.2%		3SBO	1.52E-07	0.6%
5F	5.57E-09	0.1%		2H	1.35E-07	0.5%
2F	4.63E-09	0.1%		V-Seq.	1.19E-07	0.4%
2H	4.02E-09	0.1%		2F	9.54E-08	0.4%
5H	2.61E-09	0.1%		5F	5.71E-08	0.2%
3SBO	2.40E-09	0.1%		CI Fail.	9.92E-09	0.0%
TOTAL:	4.12E-06	100.0%		TOTAL	2.67E-05	100.0%

Table 4.6-16: PDS in Order of Increasing Late CCI and Steam-Induced Unconditional Containment Failure Probabilities

PDS NAME	CCI-INDUCED CONT FAIL PROB.	PCT OF CCI-INDUC FAIL.		PDS NAME	STEAM-INDUC FAIL. PROB.	PCT OF STEAM-INDUC FAIL.
1H	1.24E-05	57.1%		6H	5.78E-07	63.0%
3H	6.97E-06	32.2%		4H	2.18E-07	23.8%
4SBO	4.81E-07	2.2%		2H	1.20E-07	13.1%
3F	3.65E-07	1.7%		3H	0.00	0.0%
5H	3.22E-07	1.5%		5F	0.00	0.0%
4F	2.82E-07	1.3%		4SBO	0.00	0.0%
6F	2.44E-07	1.1%		6F	0.00	0.0%
1F	1.88E-07	0.9%		5H	0.00	0.0%
3SBO	1.49E-07	0.7%		2F	0.00	0.0%
2F	9.07E-08	0.4%		3SBO	0.00	0.0%
6H	6.66E-08	0.3%		3F	0.00	0.0%
4H	6.36E-08	0.3%		4F	0.00	0.0%
5F	5.15E-08	0.2%		1F	0.00	0.0%
2H	1.01E-08	0.0%		SGTR	0.00	0.0%
SGTR	0.00	0.0%		1H	0.00	0.0%
V-Seq	0.00	0.0%		V-Seq	0.00	0.0%
CI FAIL	0.00	0.0%		CI FAIL.	0.00	0.0%
TOTAL	2.16E-05	100.0%		TOTAL	9.16E-07	100.0%

Table 4.6-17: Key PDS and Their Functional Sequences Probability Composition

PDS NAME	PDS FREQUENCY	PRINCIPAL FUNCTIONAL SEQUENCES	PCT		SECONDAY FUNCTIONAL SEQUENCES	PCT		TERTIARY FUNCTIONAL SEQUENCES	PCT		TOTAL
SGTR	3.48E-06	RCM1	97%		RCM4	3%					100%
4H	1.12E-06	IVSCM4	93%		VSCM4	5%		IVSCM1	1%		99%
V-Seq	1.19E-07	SCM1	83%		MCM2	9%		ACM(12)	7%		99%
1H	1.25E-05	ISCM2	100%								100%
3H	7.06E-06	X(3617) CM2	49%		T(146) CM2	45%		CVCM2 IVSCM3	5%		99%
3F	5.05E-06	ATCM(631)	87%		X(12)CM2	8%		T6CM2	4%		99%
4F	4.40E-06	VSCM(14)	83%		IVSCM4	9%		X(23)CM1	6%		98%
6F	3.29E-06	ACM1	62%		MCM1	29%		XLCM1	8%		99%
1F	2.57E-06	ISCM2	93%		SCM2	7%					100%
4SBO	5.02E-07	IVSCM5	100%								100%
CI	9.92E-09	ISCM2	37%		ALL	63%					100%
6H	9.00E-07	IMCM2	99%		ACM1	1%					100%
5F	6.96E-07	ACM2	85%		MCM2	12%		IMCM1	3%		100%
2F	1.70E-06	SCM1	87%		ISCM1	13%					100%
2H	1.41E-07	ISCM1	100%								100%
5H	3.27E-07	ACM2	65%		IMCM1	35%					100%
3SBO	1.85E-07	IVSCM6	100%								
ISGTR	5.64E-08	VSCM(14)	33%		X(3617) CM2	19%		T(146) CM2	17%		69%

Table 4.6-18: Contribution to ISGTR by PDS

ISGTR CONDITIONAL PROBABILITY	PDS FREQUENCY	ISGTR UNCONDITIONAL PROBABILITY	PERCENT OF ISGTR TOTAL	PDS NAME
3.00E-03	7.06E-06	2.12E-08	38%	3H
1.00E-03	5.05E-06	5.05E-09	9%	3F
5.00E-03	1.12E-06	5.61E-09	10%	4H
5.00E-03	4.40E-06	2.20E-08	39%	4F
3.00E-04	1.85E-07	5.55E-11	0%	3SBO
5.00E-03	5.02E-07	2.51E-09	4%	4SBO
TOTAL ===>		5.64E-08	100%	

Table 4.6-19: Contribution to ISGTR by Functional Sequence

FUNCTIONAL SEQUENCE	ISGTR FREQUENCY
VSCM(14)	1.83E-08
X(3617)CM2	1.04E-08
T(146)CM2	9.53E-09
IVSCM4	5.22E-09
ATCM(631)	4.40E-09
IVSCM5	2.51E-09
IVSCM4	1.98E-09
X(23)CM1	1.32E-09
CVCM2 IVSCM3	1.06E-09
X(12)CM2	4.04E-10
VSCM4	2.81E-10
T6CM2	2.02E-10
IVSCM1	5.61E-11
IVSCM6	5.55E-11
TOTAL	5.57E-08

Table 4.6-20: Summary of MAAP Calculations for Representative Sequences

Calc Label [PDS]	Sequence Description	CONTAINMENT		Core Uncovery Time (hr) [RCS Pres]	Core Melt Time (hr)	Vessel Failure Time (hr) [RCS Pres]	RWST Depleted Time (hr)	Containment Failure Time (hr)
		Fail Mode	Pres. @ VF, Psia					
SBO21 [1H]	SBO, 250 GPM/PMP seal LOCA, 4 hrs TDAFW, NO ECCS, Late, non-condensible induced (CCI), overpressure failure.	L	21.7	2.70 [1100 psia]	3.2	3.71 [798 psia]	N/A	38.54
SBO22 [1H]	Same as SBO21 except a burn was forced to yield containment failure by rupture rather than leakage.	L	21.7	2.70 [1100 psia]	3.2	3.71 [798 psia]	N/A	29.1
SBO31 [3SBO]	SBO, 60 GPM/PMP seal LOCA, NO AFW, ECCS recovers but vessel fails. HPME fails containment with sprays on.	R	29.0	1.66 [2300 psia]	2.08	2.55 [2300]	RECIRC OK	2.55
SBO41 [3SBO]	Same as SBO31 but sprays are failed to yield unscrubbed release.	R	29.0	1.66 [2300 psia]	2.08	2.55 [2300 psia]	RECIRC OK	2.55
2CB [2CB1]	Steam Generator Tube Rupture, ECCS injects, operators fail to stop break flow by depressurization, SG overfills, SG safety sticks open.	BY-PASS	14.7	16.76 [2100 psia]	17.78	18.60 [800 psia]	10.15	16.76
V1 [1CB]	V-Sequence simulation. 10" CL LBLOCA, no pumped ECCS, 4 Accumulators	BY-PASS	N/A	0.04	0.5	0.82	NO ECCS	0.

Table 4.6-20: Summary of MAAP Calculations for Representative Sequences (continued...)

Calc. Label [PDS]	Sequence Description	CONTAINMENT		Core Uncovery Time (hr) [RCS Pres]	Core Melt Time (hr)	Vessel Failure Time (hr) [RCS Pres]	RWST Depleted Time (hr)	Containment Failure Time (hr)
		Fail Mode	Pres. @ VF, Psia					
SB2H4 [2H]	AFW, 0 RHR, 4 ACC, 1 CCP, 0 SIP, 0 CSP, Inject but Fail @ Recirc., late steam-induced overpressure failure.	R	83.42	24.69 [1100 psia]	25.6	26.2 [435 psia]	21.46	38.1
SB2H5 [2H]	Same as SB2H4. Model Parameters modified to yield containment failure at VF due to HPME	R	127	25.27 [1100 psia]	26.4	30.46 [1100 psia]	21.71	30.46
TRAN21 [4H]	NO FW, 1 PORV @ 20 min for F&B, 4 ACC, 1 CCP, 0 SIP, 0 CSP, 0 RHR, Fail @ Recirc, 21 GPM/PMP, late steam-induced overpressure failure.	L	94.3	21.86 [2300 psia]	22.22	23.78 [2300]	18.94	29.62
TRAN22 [4H]	Same as TRAN21. Model Parameters modified to yield containment failure at VF due to HPME.	L	94.3	21.68 [2300 psia]	22.22	23.78 [2300 psia]	18.94	23.78
VSB3F1 [3F]	21 GPM/PMP seal LOCA. ALL ECCS & AFW FAIL. 2 CSP. Non coolable debris configuration.	N/A	26	1.63 [2300]	2.05	2.53 [2300]	NO ECCS CT OK	OVER 220.0[1]
VSB3F2 [3F]	Restart of VSB3F1 with a forced Burn at 208 hours.	L	26	1.63 [2300 psia]	2.05	2.53 [2300 psia]	NO ECCS CT OK	208.33
VSB3F3 [3F]	Restart of VSB3F1 with a forced Burn at 83 hours.	R	26 [No]	1.63 [2300] [2250 psia]	2.05	2.53 [2250 psia]	NO ECCS CT OK	83.34

[1] Basemat 4m thickness was reached at 90 hours.

Table 4.6-21: Release Fractions for CET End-States and Respective PDS Representatives

END-STATE[5]	PDS	MAAP RUN	NOBLE GASES	CSI	TEO2	SRO	MOO2	CSOH	BAO	LA2O3	CEO2	SB
D2-R	3SBO	SBO41	8E-01	5E-02	4E-02	1E-03	6E-02	4E-02	1E-03	3E-06	9E-06	4E-02
D1-R	3SBO	SBO31	2E-01	3E-03	0	1E-05	3E-04	2E-03	9E-05	3E-07	5E-07	2E-03
D1-L	3SBO	SBO32	5E-02	2E-04	0	5E-07	2E-05	2E-04	5E-06	1E-08	3E-08	8E-05
B6-L	4H	TRAN21	8E-01	2E-03	0	2E-05	7E-04	2E-03	2E-04	1E-06	1E-06	2E-03
B6-R	2H	SB2H4	9E-01	9E-03	0	3E-04	2E-03	9E-03	2E-03	3E-[illegible]	4E-06	6E-03
C5-L	3F	VSB3F2	8E-01	1E-10	1E-09	2E-13	1E-10	1E-09	1E-11	1E-11	1E-11	4E-09
C5-R	3F	VSB3F3	1E+00	7E-07	1E-09	5E-13	1E-10	5E-06	4E-11	1E-11	1E-11	1E-05
C6-L	1H	SBO21	9E-01	3E-02	8E-03	7E-06	2E-05	2E-02	2E-03	2E-06	2E-05	6E-02
C6-R	1H	SBO22	1E+00	2E-01	7E-01	1E-03	1E-08	2E-01	3E-03	4E-04	4E-03	4E-01
D6-L	4H	TRAN22	1E+00	6E-02	0	5E-04	1E-02	6E-02	6E-03	3E-05	3E-05	6E-02
[illegible]	2H	SB2H5	1E+00	3E-02	0	4E-04	2E-02	3E-02	4E-03	3E-05	6E-05	4E-02
V-SEQ	1CB	V1	1E+00	8E-01	1E+00	1E-01	2E-03	8E-01	5E-02	2E-02	2E-01	8E-01
SGTR & ISGTR	2CB	2CB1	9E-01	8E-01	3E-02	3E-03	1E-01	8E-01	3E-02	4E-04	7E-04	5E-01
CI FAIL	1CI	V1	1E+00	8E-01	1E+00	1E-01	2E-03	8E-01	5E-02	2E-02	2E-01	8E-01

[5] End-States in this column are those actually represented by the MAAP runs listed. TABLE 3-3 provides additional information on the end state characteristics and lists similar ends states which can be represented by the same MAAP calculation.

Table 4.6-22: Description of Calculated End-States

CAUSE OF CONTAINMENT FAILURE	CONT. FAIL. MODE	FISSION PRODUCT REMOVAL	CALC NAME [END STATE]	PDS	SIMILAR END STATES
Late Steam-Induced Overp. Failure	L	Pool No Sprays	TRAN21 [B6-L]	4H	B4-L B2-L
Late Non-Cond (CCI) Induced Overp. Fail.	L	No	SBO21 [C6-L]	1H	C4-L C2-L
Late Non-Cond. (CCI) Induced Overp. Failure	R	Sprays	VSB3F3 [C5-R]	3F	C3-R C1-R
Late Non-Cond. (CCI) Overp. Failure	R	No	SB022 [C6-R]	1H	C4-R C2-R
Late Steam - Induced Overp. Failure	R	Pool But No Sprays	SB2H4 [B6-R]	2H	B4-R B2-R
Recovered Early-HPME	R	Sprays	SBO31 [D1-R]	3SBO	D3-R D5-R
Recovered Early-HPME	R	No	SBO41 [D2-R]	3SBO	
Early-HPME	R	No	SB2H5 [D6-R]	2H	D4-R
Early-HPME	L	No	TRAN22 [D6-L]	4H	D4-L D2-L
Early-HPME	L	Sprays	SBO32 [D5-L]	3SBO	D1-L D3-L
Late Non. Cond. (CCI) Induced Overp. Failure	L	Sprays	VSB3F2 [C5-L]	3F	C3-L C1-L

Figure 4.6-1: Comparison of Probabilities for HPME Final Pressures with Containment Survival Probabilities for; Above: PDS 1E, 1F, 1H, 2E and 2F; Below: PDS 2H

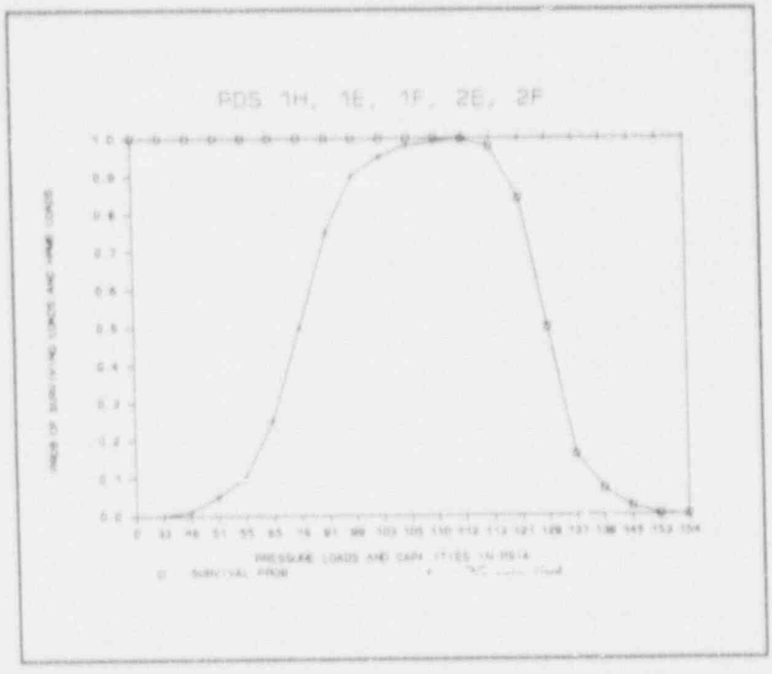

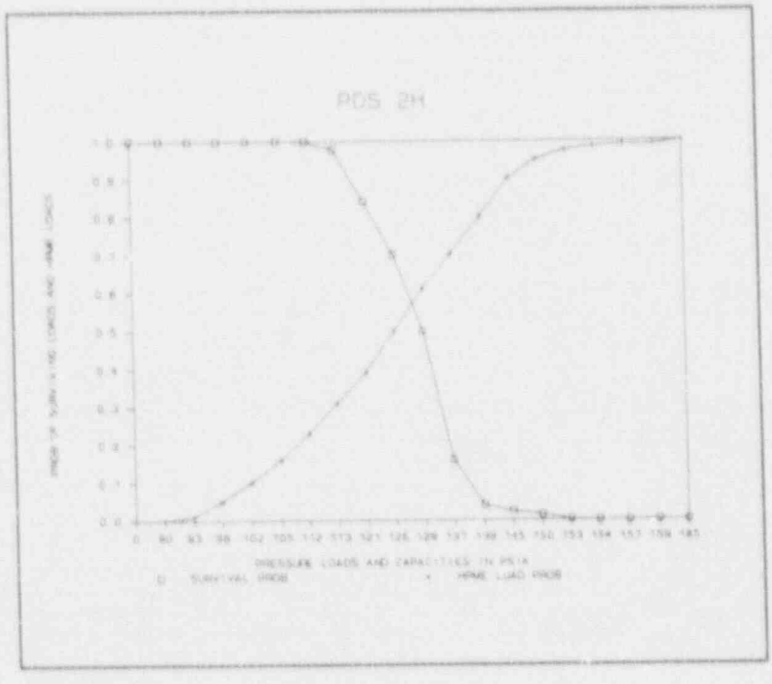

Figure 4.6-2: Containment Temperatures (TG) and Pressures in (A=upper, B=lower and C=cavity) Compartments

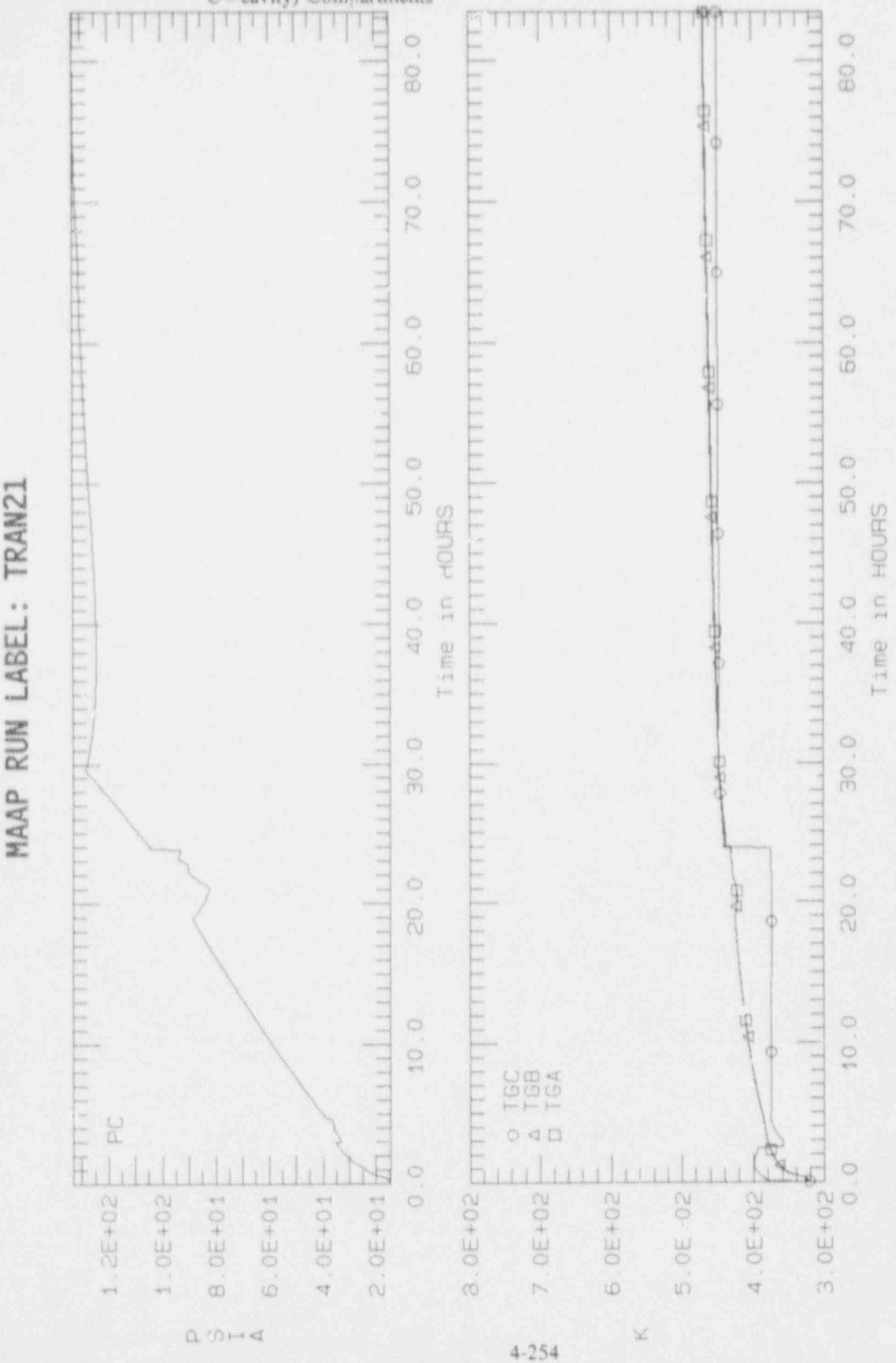

Figure 4.6-3: Containment Temperatures (TG) and Pressures in (A = upper, B = lower and C = cavity) Compartments

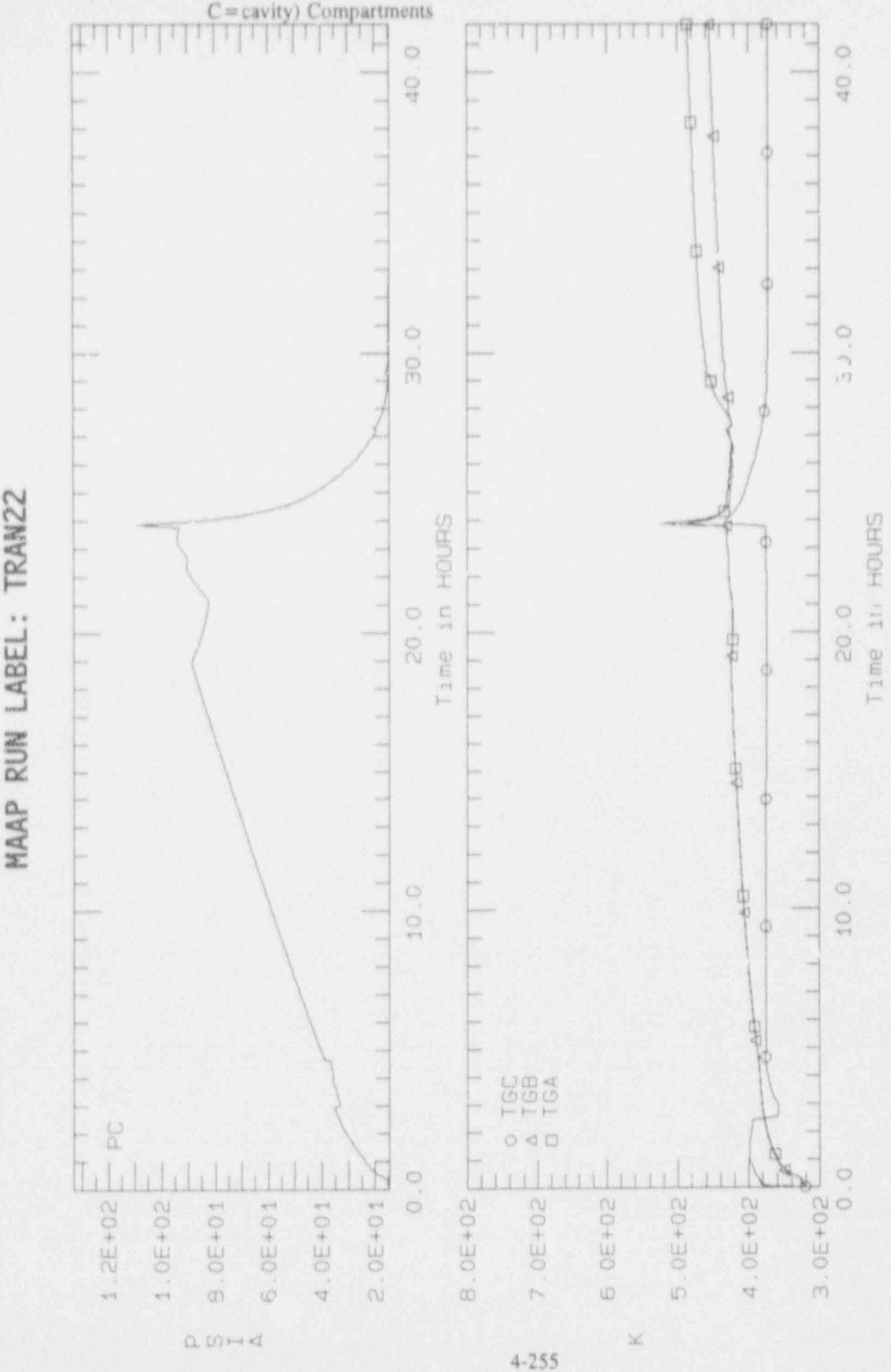

Figure 4.6-4: Masses of Hydrogen Produced in Core (CR1) and in Containment (CB1)

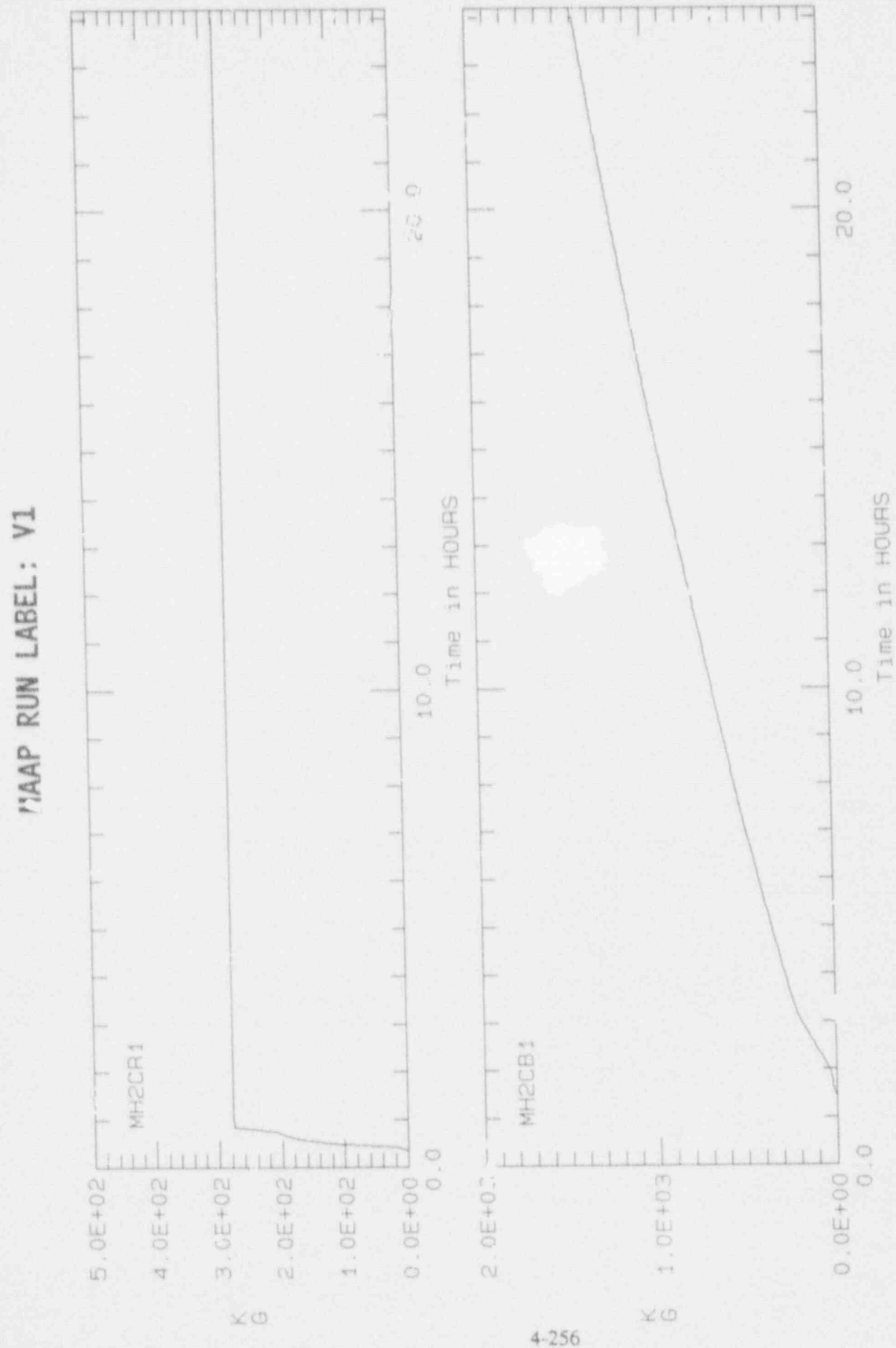

Figure 4.6-5: Containment Temperatures (TG) and Pressures in (A=upper, B=lower and C=cavity) Compartments

Figure 4.6-6: Containment Temperatures (TG) and Pressures in (A=upper, B=lower and C=cavity) Compartments

Figure 4.6-7: Basemat Erosion Depth (XCNC1) and Pressures in (B=lower and C=cavity) Compartments

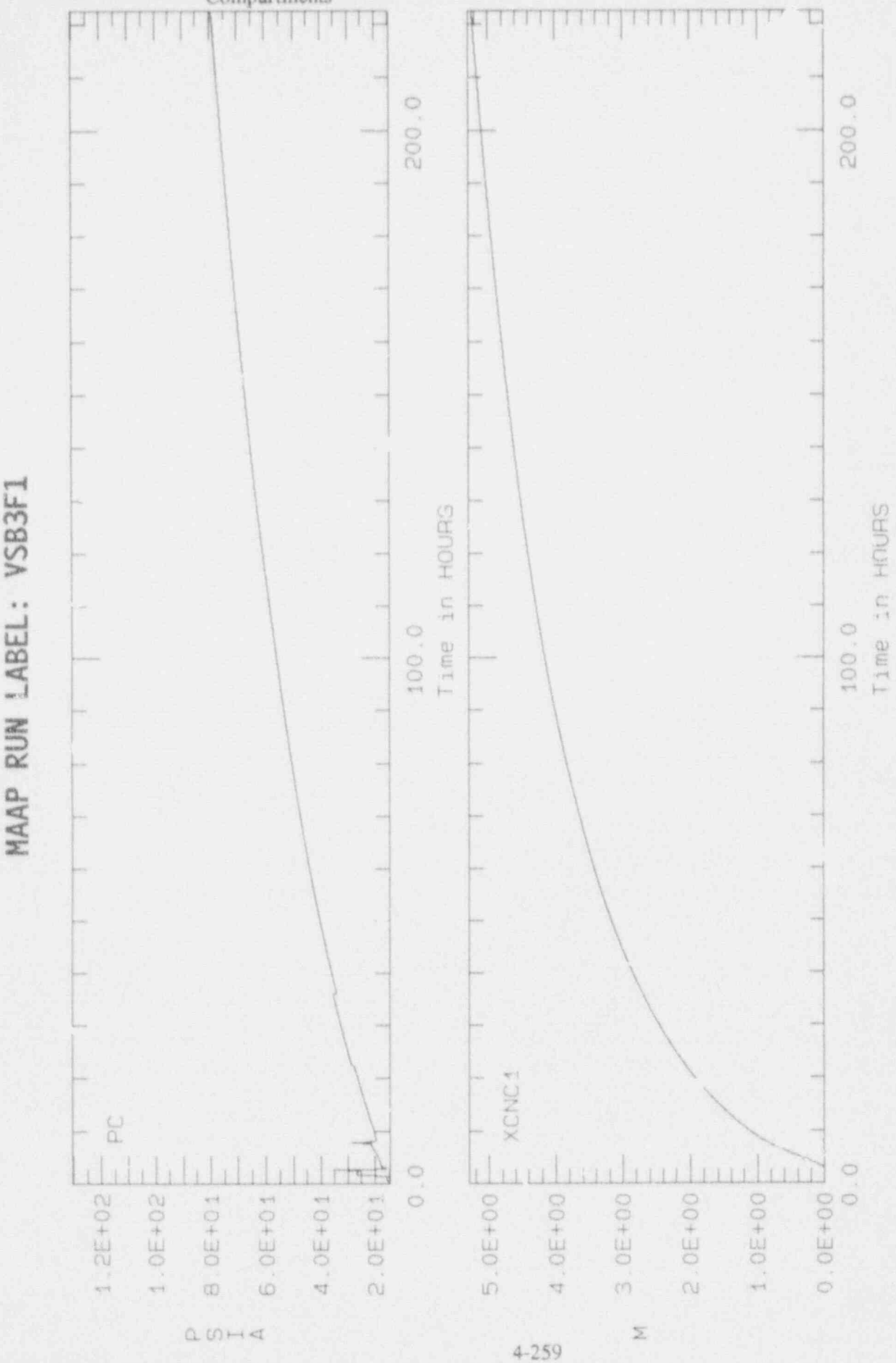

Figure 4.6-8: Containment Temperatures (TG) and Pressures in (A=upper, B=lower and C=cavity) Compartments

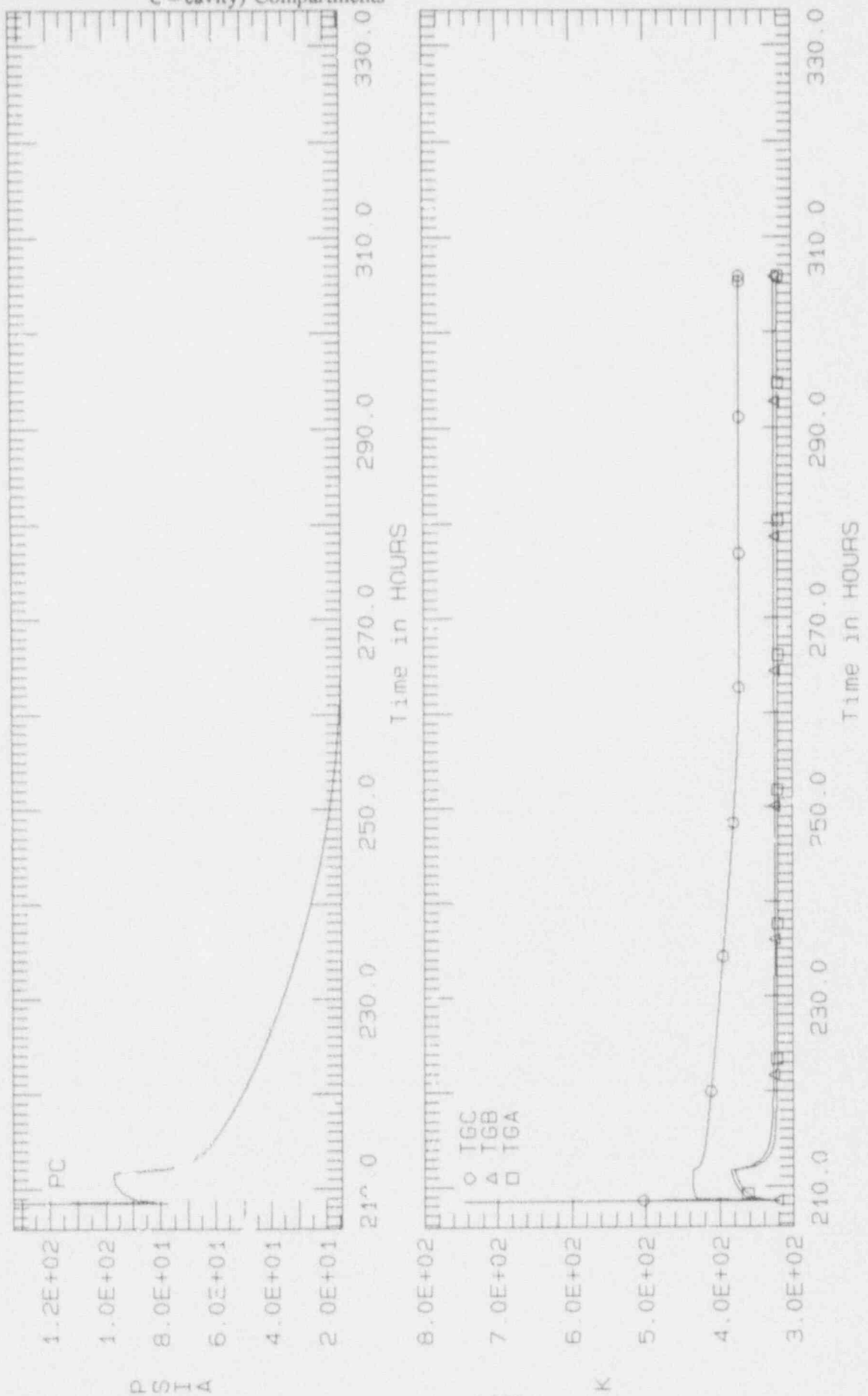

Figure 4.6-9: Containment Temperature (TG) and Pressures in (A=upper, B=lower and C=cavity) Compartments

Figure 4.6-10: Containment Temperatures (TG) and Pressures in (A=upper, B=lower and C=cavity) Compartments

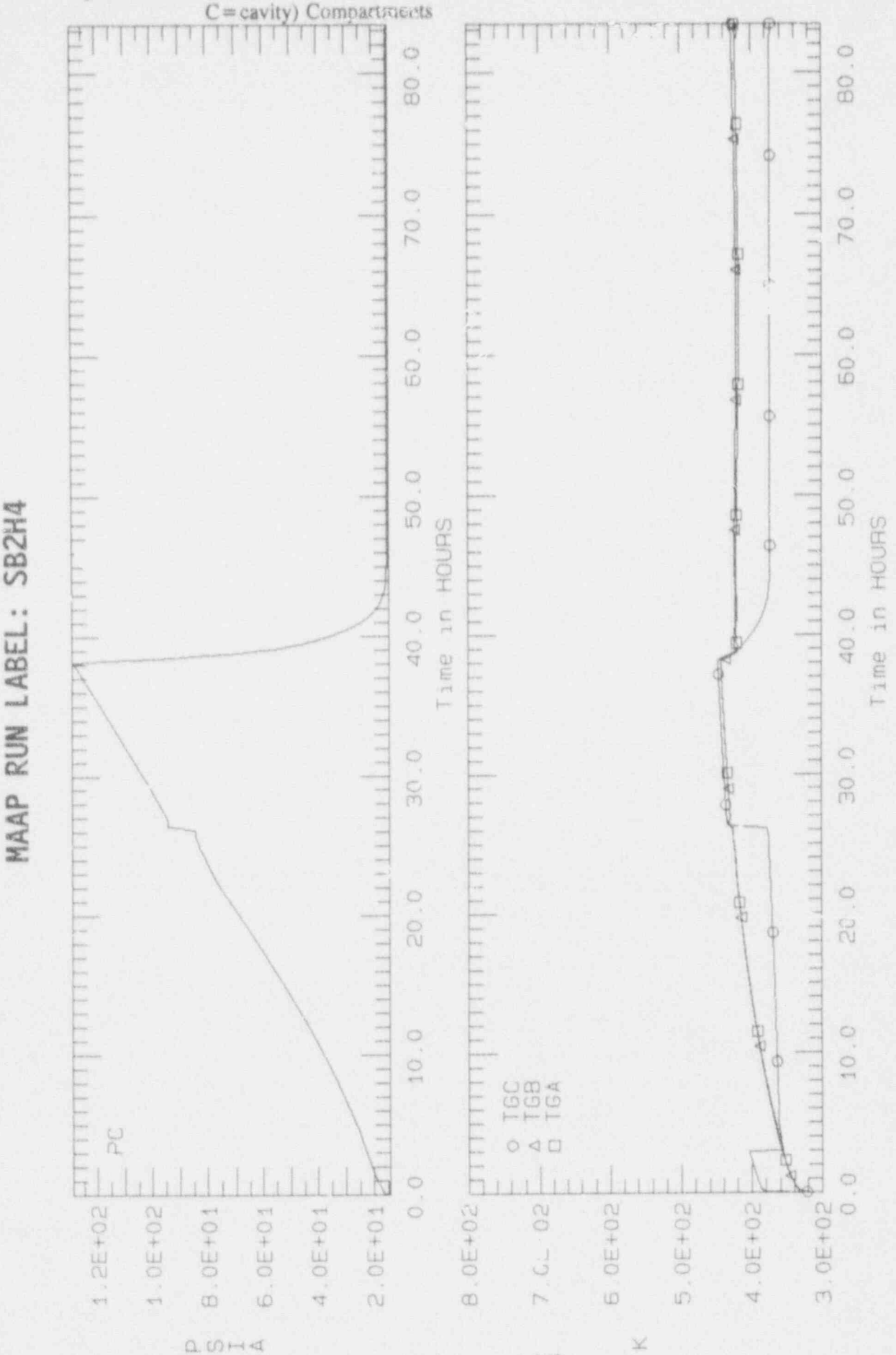

Figure 4.6-11: Containment Temperatures (TG) and Pressures in (A=upper, B=lower and C=cavity) Compartments

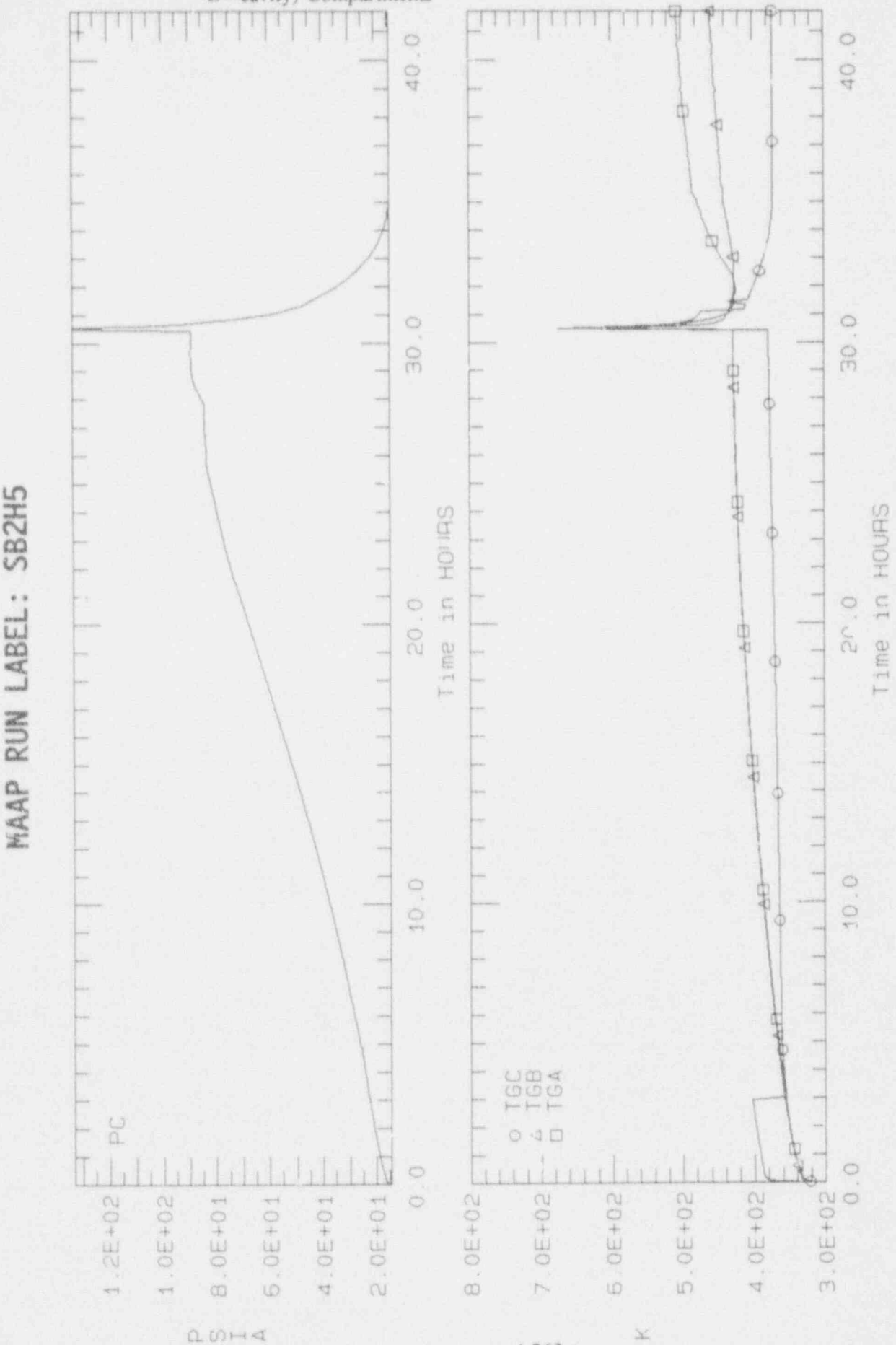

Figure 4.6-12: Containment of Temperatures (TG) and Pressures in (A=upper, B=lower, and C=cavity) Compartments

Figure 4.6-13: Containment Temperatures (TG) and Pressures in (A=upper, B=lower and C=cavity) Compartments

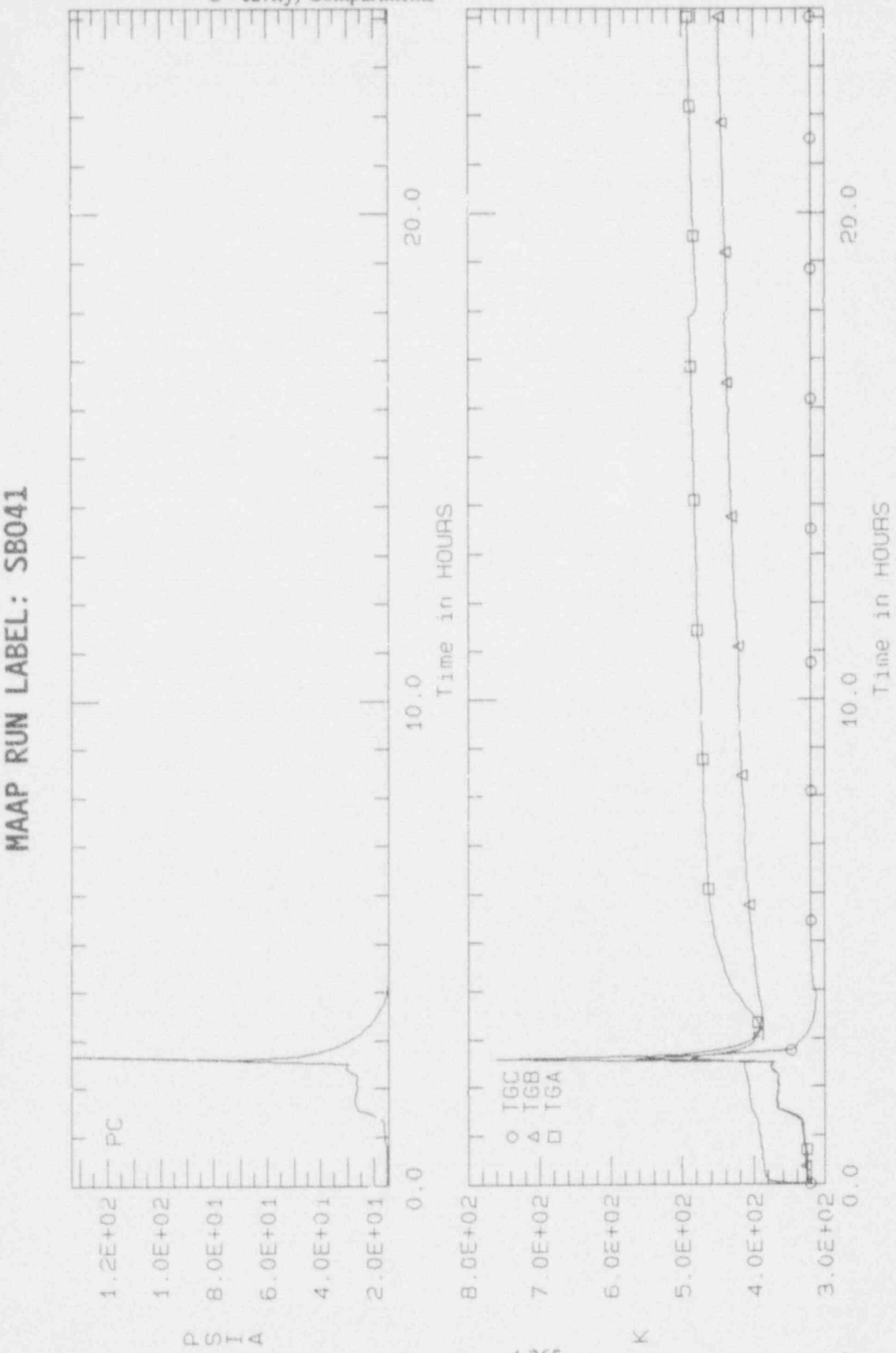

Figure 4.6-14: TRAN21 (A) and TRAN22 (B) Surge Line (TSR1), Hot Leg (TUH), SG Tube (TPHSF) Temperatures

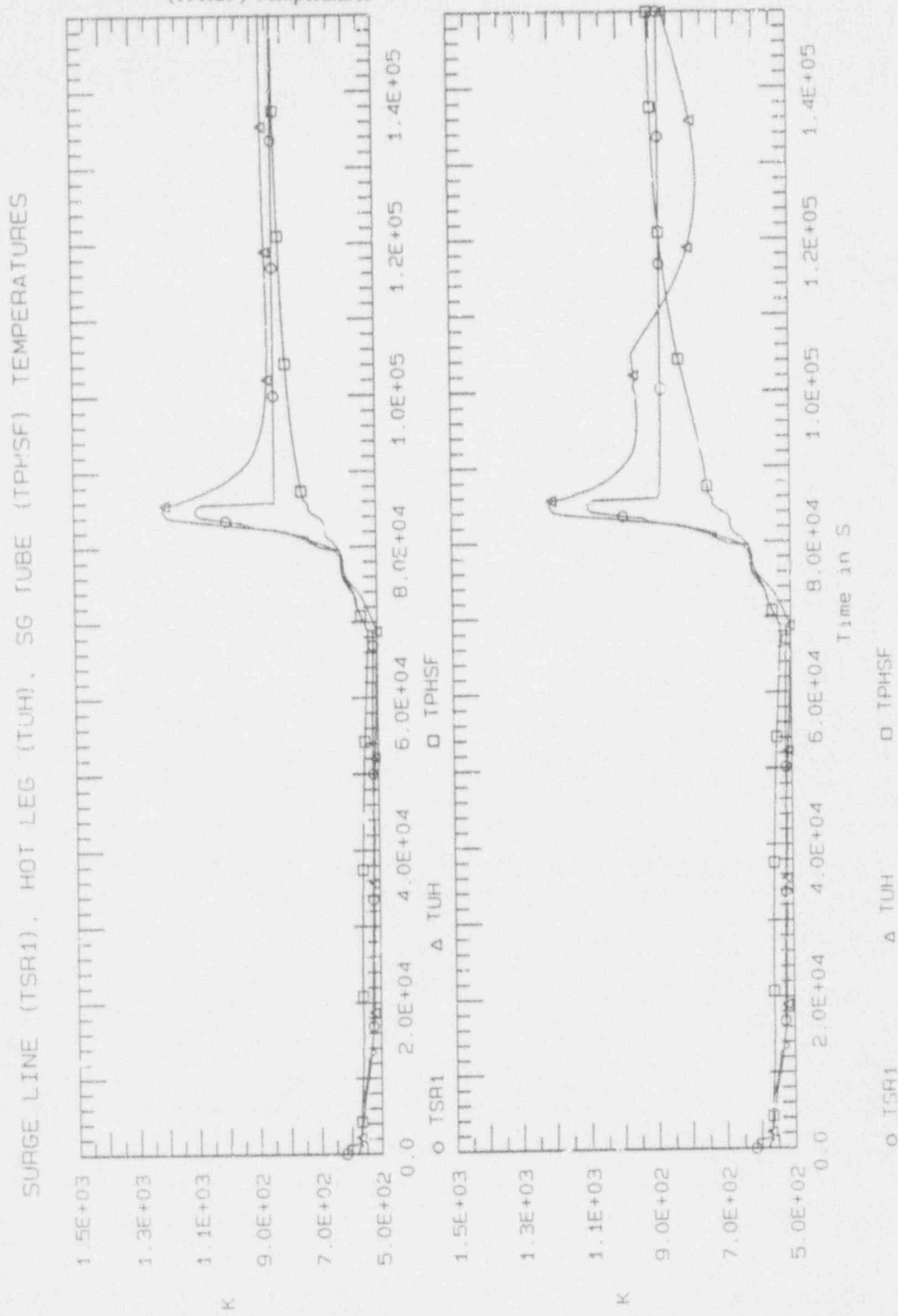

Figure 4.6-15: Effect of Fan Coolers for Dry PDS

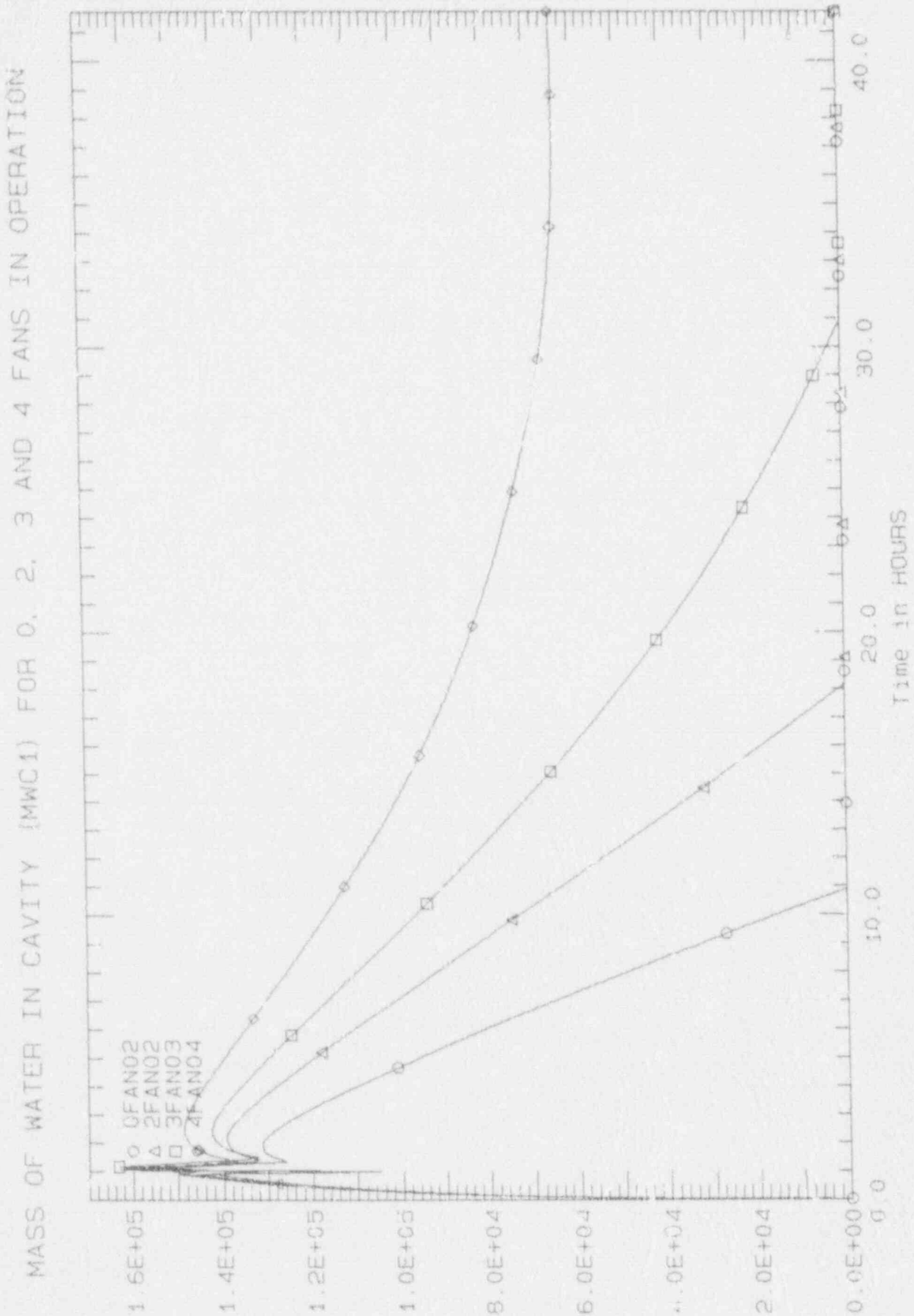

Figure 4.6-16: CCI Failure Modes for CPSES Concrete: Overpressurization vs Melt-through for Two Types of Concrete

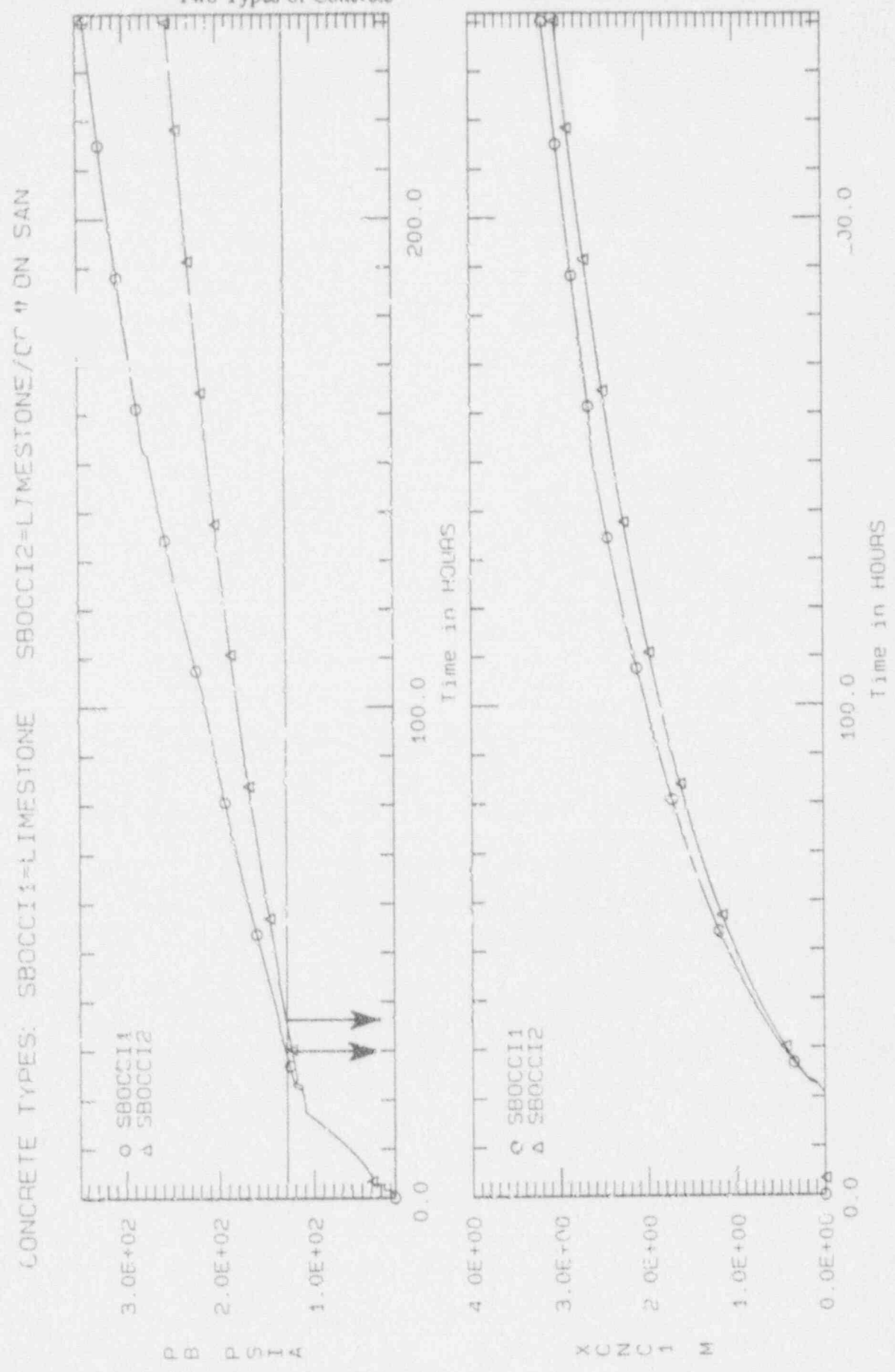

4.7 Radionuclide Release Characterization

In this section, CPSES release categories are defined and the combined frequency contributions from all PDS to each CPSES release category are computed and presented. Then representative values for the energy or type of the release (i.e., whether continuous or puff), the timing of the release, and the release fractions or composition are presented for each of the previously defined CPSES release fractions. The section concludes by ranking the release categories on the basis of both their conditional and unconditional probabilities (i.e., including front-end results).

4.7.1 The CPSES Release Categories

The primary considerations for defining the CPSES release categories are whether: (1) the containment is intact at the time of core melt or whether (2) the release involves a bypassed or unisolated containment.

4.7.1.1 Isolated, Non-bypass (Intact Containment at Vessel Failure) Release Categories

The isolated, non-bypass release categories are defined by grouping CET end-states with similar characteristics. There are four groups of characteristics that are considered to be the most relevant to the CPSES release grouping for the CPSES isolated, non-bypass release categories. These four groups, which are not necessarily independent, are:

Timing

Early: if the containment fails at or shortly after vessel breach.

Late: if the containment fails much after vessel breach.

Size of Breach and/or Mode of Failure

This establishes the type or energy level of release, i.e., whether a puff or a continuous release, as associated with two modes:

Rupture: when there is a large gross failure of the containment leading to quick depressurization and a puff release, and

Leakage: when there is a small breach of the containment associated with liner tearing in the vicinity of penetrations. This leads to a slow, almost negligible depressurization of the

containment corresponding to a continuous protracted release. The breach diameter is 2 to 3 inches depending on whether the sequence is wet or dry.

Cause of Failure

- The Alpha failure mode
- High Pressure Melt Ejection (HPME) including direct containment heating (DCH) and/or a hydrogen burn at the time of vessel failure
- Steam Overpressurization No Core Concrete Interaction (CCI)
- CCI leading to a Hydrogen Burn
- CCI leading to Non-Condensible Overpressure Failure
- CCI leading to Basemat Melt-through

Release Mitigation

Pool

Sprays

None

These four characteristics are not independent due to the following considerations, of which the first two are actual restrictions and the others are reasonable and conservative simplifying assumptions:

- If the Timing is Early, the only non-negligible failure modes are Alpha and HPME (DCH and/or Burn). In either case, the debris is coolable, i.e., there will be no subsequent CCI because the depth of any debris pool would be much less than 25 cm, as discussed in Section 4.5.

- If the Timing is Late and the Cause is Steam Overpressurization, then mitigation is either Pool or None, i.e., Sprays is impossible in that case. This is because, although failure of the RH heat exchangers with sprays operational would be possible, those sequences are not statistically significant, and furthermore, they are binned as failed sprays cases.

- If the Failure Mode is CCI leading to a Hydrogen Burn, CCI Non-Condensible Overpressure Failure or CCI leading to Basemat Melt-through, then mitigation is assumed to be either Sprays or None. Although an overlying pool exists in some of the end-states in this category, those cases result merely from non-coolable debris formations, which is unlikely at CPSES and are not numerous enough to justify segregation.

- When the Timing is Late and the Mode is Leakage and the Cause is CCI leading to Non-Condensible Overpressure Failure or CCI leading to Basemat melt-through, the releases are placed in the same category and calculated based on CCI leading to Non-Condensible Overpressure Failure.

Based upon these considerations, the CET end-states of Figure 4.5-1 and Table 4.5-2 were collapsed into the ten CPSES Release Categories, labeled by Roman Numerals I through X in Table 4.7-1. The gray areas in Table 4.7-1 represent the combinations of characteristics that are either impossible or that have been binned with others, as discussed in the preceding paragraph.

4.7.1.2 Unisolated or Bypass Release Categories

The non-isolated or bypassed containment CPSES Release Categories are defined as follows:

XI. V-Sequence
XII. SGTR and ISGTR
XIII. Failure to Isolate

4.7.2 Release Category Frequencies

Table 4.7-2 shows in each column the unconditional frequencies for the CET end-states contained in each Release Category according to the grouping shown in Table 4.7-1. The bottom row corresponds to the total frequency for each Release Category, i.e., the sum of Release Category frequencies over all PDS. The lowest rightmost total is the total containment failure probability, which corresponds to approximately 60% of the total CMF, as discussed in Section 4.6.1.

Table 4.7-3 ranks the CPSES Release Categories in order of decreasing frequency. The dominant Release Category is VI, with 76% of the total containment failure probability. It corresponds to an unmitigated, late, leakage-type failure due to CCI-induced non-condensible gas overpressurization (it includes basemat failures as well), where the ECCS and the containment sprays fail at injection.

The next most likely is Category XII, which is Steam Generator Tube Ruptures (SGTR), both as initiators and induced (ISGTR), although the induced are not a significant fraction of the total Category XII frequency. Their actual frequency is 5.57E-08 or 1.6% of the total Release Category Frequency, as

shown in Tables 4.6-18 and 4.6-19. Release Category XII (SGTR & ISGTR) has 13% of the containment failure probability.

The next likely Release Category is VIII (4.7% of the containment failures), corresponding to late, CCI-induced (i.e., basemat melt-through or non-condensible overpressurization), leakage-type failure with sprays operating.

That is followed by Release Category X (3.4% of the containment failures), corresponding to late, steam-induced overpressure, leakage-type failures without sprays, but with an overlying water pool.

After that come the Early Failures by Rupture, Categories III (with sprays) and I (no sprays), corresponding to 0.7% of the containment failures each. These are followed by the V-sequence (0.4% of the containment failures), Category XI. Finally are Categories IV (0.3%) and II (0.1%), which are Early Failures by Leakage with and without sprays, respectively. The remaining Categories (combined) account for 0.4% of the containment failures and all have individual frequencies of less than 1E-08.

The conditional frequencies (i.e., assuming the occurrence probability of all PDS binning into the Release Category is 1.0) are given in Table 4.7-4.

4.7.3 Release Fractions and other Characteristics for the Release Categories

Table 4.6-21 presents release fractions for the similar groups of CET end-states which are shown in Table 4.6-22. The correspondence between CET end-states and Release Categories is given in Table 4.7-1. The release fractions for each Release Category are listed in Table 4.7-5.

Principal CPSES Release Category characteristics other than release fractions are summarized in Table 4.7-6. These key characteristics are: (a) core melt time, (b) release timing, where the actual time of release is given, (c) the type of release, i.e., whether a puff or continuous release, and (d) the type of mitigation as defined by the Release Category. The values correspond to the release fractions of Table 4.7-5 since they result from the same MAAP calculations, which in turn are based on the representative functional sequences for the PDS that are the greatest contributors to risk, as discussed in Section 4.6-2. These PDS, the representative functional sequences, and the MAAP run labels are also included in Tables 4.7-5 and 4.7-6, and represent a summary of the Level II analysis source term results and origins.

Table 4.7-1: CPSES Release Category Definition and CET End-States

TIME	FAILURE MODE	HPME (DCH and/or BUR.4)		STEAM OVER-PRESSURE		CCI AND BURN OR NC OVERPRESSURE		CCI AND BASEMAT MELT-THROUGH OR NC OVERPRESSURE	
	MITIGATION->	SPRAY	NONE	SPRAY[6]	POOL/NONE	SPRAY	NONE	SPRAY	NONE
EARLY	LEAKAGE	[SBO32] IV[7] D(135)L	[TRAN22] II D(246)L						
	RUPTURE	[SBO31] III D(135)R	[SBO32] I D(246)R						
LATE	LEAKAGE				[TRAN21] X B(23456)L			[VSB3F2] VIII C(135)L	[SBO21] VI C(246)L
	RUPT[7]				[SB2H4] IX A(12), B1 B(23456)R	[VSB3F3] VII C(135)R	[SBO22] V C(246)R		

[6] Shaded areas are either impossible or insignificant.

[7] Roman Numerals are CPSES RELEASE CATEGORY Labels.

Table 4.7-2: Binning PDS into the CPSES Release Categories

	XIII	XII	XI	X	IX	VIII	VII	VI	V	IV	III	II	I	TOTAL
1H								1.23E-05	6.18E-08	7.42E-13	1.97E-12	2.97E-10	9.62E-08	1.25E-05
1F						1.87E-07	9.39E-10			6.10E-11	1.98E-08			2.07E-07
2H				1.20E-07	6.03E-10	2.52E-11	1.27E-13	1.00E-08	5.04E-11	3.68E-12	6.37E-12	1.47E-09	2.54E-09	1.35E-07
2F						9.03E-08	4.53E-10			7.27E-10	3.93E-09			9.54E-08
3H								6.93E-06	3.48E-08	7.06E-09	8.26E-09	3.32E-09	4.37E-08	7.03E-06
3F						3.64E-07	1.83E-09			1.73E-09	3.97E-08			4.07E-07
4H				2.17E-07	1.09E-09	4.31E-08	2.16E-10	2.02E-08	1.02E-10	6.15E-06	6.55E-08	2.89E-08	3.07E-08	4.68E-07
4F						2.81E-07	1.41E-09			8.80E-09	3.14E-08			3.22E-07
5H								3.21E-07	1.61E-09				2.61E-09	3.25E-07
5F						5.13E-08	2.57E-10				5.57E-09			5.71E-08
6H				5.75E-07	2.89E-09	1.66E-10	8.32E-13	6.61E-08	3.32E-10		1.80E-11		7.18E-09	6.51E-07
6F						2.42E-07	1.22E-09				2.63E-08			2.70E-07
3S						1.70E-09	8.53E-12	1.47E-07	7.38E-10	3.49E-10	5.36E-10	1.53E-10	1.36E-09	1.52E-07
4S						3.19E-10	1.60E-12	4.78E-07	2.40E-09	3.45E-09	3.59E-09	1.61E-09	4.02E-09	4.93E-07
V-SEQ			1.19E-07											1.19E-07
SGTR		3.48E-06												7.48E-06
C* FAIL	9.92E-09													9.92E-09
TOTALS	9.92E-09	3.48E-06	1.19E-07	9.12E-07	4.58E-9	1.26E-06	6.33E-09	2.03E-05	1.02E-07	8.37E-08	2.05E-07	3.57E-08	1.88E-07	2.67E-05

Table 4.7-3: CPSES Release Categories in Order of Absolute Unconditional Frequency

RELEASE CATEGORY	FREQUENCY
VI	2.03E-05
XII	3.48E-06
VIII	1.26E-06
X	9.12E-07
III	2.05E-07
I	1.88E-07
XI	1.19E-07
V	1.02E-07
IV	8.37E-08
II	3.57E-08
XIII	9.92E-09
VII	6.33E-09
IX	4.58E-09
TOTAL	2.67E-05

Table 4.7-4: CPSES Release Categories in Order of Relative Conditional Frequency

RELEASE CATEGORY	PERCENT OF TOTAL CONDITIONAL FREQUENCY
VI	36.21%
X	35.76%
XIII	7.07%
XII	7.07%
XI	7.07%
VIII	3.99%
III	0.87%
I	0.79%
IV	0.50%
II	0.30%
V	0.18%
IX	0.18%
VII	0.02%
TOTAL	100.00%

Table 4.7-5: Release Fractions for Release Categories and Respective PDS Representatives

RELEASE CATEGORY	PDS	MAAP RUN	NOBLE GASES	CsI	TeO2	SrO	MoO2	CsOH	BaO	La2O3	CeO2	Sb
NON-BYPASS & ISOLATED												
X	4H	TRAN21	8E-01	2E-03	0	2E-05	7E-04	2E-03	2E-04	1E-06	1E-06	2E-03
IX	2H	SB2H4	9E-01	9E-03	0	3E-04	2E-03	9E-03	2E-03	3E-06	4E-06	6E-03
VIII	3F	VSB3F2	8E-01	1E-10	1E-09	2E-13	1E-10	1E-09	1E-11	1E-11	1E-11	4E-09
VIi	3F	VSB3F3	1E+00	7E-07	1E-09	5E-13	1E-10	5E-06	4E-11	1E-11	1E-11	1E-05
VI	1H	SBO21	9E-01	3E-02	8E-03	7E-06	2E-05	2E-02	2E-03	2E-06	2E-05	6E-02
V	1H	SBO22	1E+00	2E-01	7E-01	1E-03	1E-08	2E-01	3E-03	4E-04	4E-03	4E-01
IV	3SBO	SBO32	5E-02	2E-04	0	5E-07	2E-05	2E-04	5E-06	1E-08	3E-07	8E-05
III	3SBO	SBO31	2E-01	3E-03	0	1E-05	3E-04	2E-03	9E-05	3E-07	5E-07	2E-03
II	4H	TRAN22	1E+00	6E-02	0	5E-04	1E-02	6E-02	6E-03	3E-05	3E-05	6E-02
I	3SBO	SBO41	8E-01	5E-02	4E-02	1E-03	6E-02	4E-02	1E-03	3E-06	9E-06	4E-02
BYPASSED OR UNISOLATED												
XIII	1CB	V1	1E+00	8E-01	9E-01	1E-01	2E-03	8E-01	5E-02	2E-02	2E-01	8E-01
XII	2CB	2CB1	9E-01	8E-01	3E-02	3E-03	1E-01	8E-01	3E-02	4E-04	7E-04	5E-01
XI	1CI	V1	1E+00	8E-01	9E-01	1E-01	2E-03	8E-01	5E-02	2E-02	2E-01	8E-01

Table 4.7-6: Principal Release Category Characteristics (Besides the Release Fractions)

RELEASE CATEGORY	REL. CAT. FREQ.	PDS	REPRESENTATIVE FUNCT. SEQUENCE (PCT OF PDS FREQ)	MAAP RUN LABEL	MELT TIME (HR)	RELEASE TIME	RELEASE TYPE / ENERGY	MITIGATION
NON-BYPASS & ISOLATED								
X	9.12E-07	4H	IVSCM1 (1%)[a]	TRAN21	22.2	29.6	CONTINUOUS	NONE
IX	4.58E-09	2H	ISCM1 (100%)	SB2H4	25.6	38.1	PUFF	NONE
VIII	1.26E-06	3F	X(12)CM2 (8%)	VSB3F2	2.05	208.3	CONTINUOUS	SPRAYS
VII	6.33E-09	3F	X(12)CM2 (8%)	VSB3F3	2.05	83.3	PUFF	SPRAYS
VI	2.03E-05	1H	ISCM2 (100%)	SBO21	3.2	38.5	CONTINUOUS	NONE
V	1.02E-07	1H	ISCM3 (100%)	SBO22	3.2	29.1	PUFF	NONE
IV	8.37E-08	3SBO	IVSCM6 (100%)	SBO32	2.08	2.55	CONTINUOUS	SPRAYS
III	2.05E-07	3SBO	IVSCM6 (100%)	SBO31	2.08	2.55	PUFF	SPRAYS
II	3.57E-08	4H	IVSCM1 (1%)	TRAN22	22.2	23.8	CONTINUOUS	NONE
I	1.88E-07	2H	ISCM1 (100%)	SB2H5	26.4	30.5	PUFF	NONE
BYPASSED OR UNISOLATED								
XIII	9.92E-09	1CB	ACM2 (7%)	V1	0.5	0.5	CONTINUOUS	NONE
XII	3.48E-06	2CB	RCM1 (97%)	2CB1	17.5	17.5	CONTINUOUS	NONE
XI	1.19E-07	1CI	ACM2 (<1%)	V1	0.5	0.5	CONTINUOUS	NONE

[a] Low percentages can occur when the representative sequences are chosen conservatively, i.e. when they lead to higher release fractions than the dominant sequences.

6. PLANT IMPROVEMENTS AND UNIQUE SAFETY FEATURES

Back-end plant improvements and unique safety features are discussed in this section. This section does not address the general plant improvements and unique safety features from the front-end analysis, since those were addressed in Volume I of the IPE submittal.

Plant improvements

The back-end analysis did not reveal any vulnerabilities nor the need for any plant improvements beyond those outlined in Volume I of the IPE submittal regarding the front-end portion.

Unique Containment Safety Features

CPSES exhibits three specific design features that are the underlying causes for the good performance of the CPSES containment.

The first is the very large containment free volume, which renders the CPSES containment relatively invulnerable to early hydrogen burn events and to the direct containment heating phenomena associated with high pressure melt ejection sequences. Calculations performed for the CPSES containment show that the containment would not reach the failure pressure even if a hydrogen burn from a 100% Zirconium oxidation were postulated. Furthermore, the assessment of the direct containment heating phenomena for CPSES, which is based on the conservative analyses for the Zion plant under the NUREG-1150 program, has shown that the CPSES containment is unlikely to fail as a result of a DCH overpressure transient.

The second and third important containment features are associated with the reactor cavity configuration. First, the reactor cavity has a large flat floor area of over 70 m^2 (800 ft^2). This results in a shallow debris bed of only a few inches thickness, which is coolable by an overlaying layer of water, and which would result in a slow concrete penetration rate if the debris is dry and not self cooled by convection to the atmosphere. Second, there is no curb at the containment floor elevation surrounding the reactor cavity exit for the instrument guide tubes that would prevent the return of water from the main containment floor to the reactor cavity. As a result, all the water injected into the containment or released inside the containment has to boil off before the debris in the reactor cavity can dry out. Accident sequences with failure of RWST injection dominate the plant damage states that dominate the

containment failures. Therefore, the absence of a reactor cavity curb means that even if only the RCS water inventory is released to the containment, this entire water inventory must boil off and be in the form of steam in the containment before the debris in the reactor cavity can dry out. After that, containment pressurization proceeds very slowly, due only to non-condensible gas generation in the core-concrete attack. This characteristic results in delaying the containment failures, and would increase the chances of maintaining containment integrity as any condensation or water injected into the containment by accident management would drain back to the reactor cavity and to the debris.

7. SUMMARY AND CONCLUSIONS

The summary and conclusions of the front-end of the IPE are presented in Volume I of the IPE submittal. The following are the back-end summary and conclusions.

The main conclusion to be drawn from these findings is that the CPSES containment provides adequate protection to the public.

The principal concerns in this regard are the frequency and timing of potential early containment failures. With the exception of Steam Generator Tube Ruptures (SGTR), all other possible modes of early containment failure have frequencies nearly at or below the reporting cut off levels of 1E-7. Although classified as early failures, most SGTR events would take several hours to reach core melt, allowing that time to be used for accident diagnosis and management.

Regarding the late containment failures, almost all are due to overpressurization from non-condensibles originating in a post dry-out core-concrete attack. This type of failure is protracted over approximately 36 hours, allowing for accident management.

CPSES exhibits three specific design features that are the underlying causes for the good performance of the CPSES containment.

The first is the very large containment free volume which renders the CPSES containment relatively invulnerable to early hydrogen burn events and to the direct containment heating phenomena associated with high pressure melt ejection sequences. Calculations performed for the CPSES containment show that the containment would not reach the failure pressure even if a hydrogen burn from a 100% Zirconium oxidation were postulated. Furthermore, the assessment of the direct containment heating phenomena for CPSES, which is based on the conservative analyses for the Zion plant under the NUREG-1150 program, has shown that the CPSES containment is unlikely to fail as a result of a direct containment heating overpressure transient.

The second and third important containment features are associated with the reactor cavity configuration. First, the reactor cavity has a large flat floor area of over 70 m^2 (800 ft^2). This results in a shallow

debris bed of only a few inches thickness. This shallow bed is coolable by an overlaying layer of water and results in a slow concrete penetration rate even if the debris is dry and not self cooled by convection to the atmosphere. Second, there is no curb at the containment floor elevation surrounding the reactor cavity exit for the instrument guide tubes that would prevent the return of water from the main containment floor to the reactor cavity. As a result, all the water injected into the containment or released inside the containment has to boil off before the debris in the reactor cavity can dry out. Accident sequences with failure of RWST injection dominate the plant damage states that dominate the containment failures. Therefore, the absence of a reactor cavity curb means that even if only the RCS water inventory is released to the containment, this entire water inventory must boil off and be in the form of steam in the containment before the debris in the reactor cavity can dry out. After that, containment pressurization proceeds very slowly, due only to non-condensible gas generation in the core-concrete attack. This characteristic results in the protracted containment failures. Furthermore, any condensation or water injected into the containment by accident management would drain back to the reactor cavity and to the debris.

Finally, the back-end analysis did not reveal any vulnerabilities nor the need for any plant improvements.

The overall containment performance is summarized in Figure 7-1. The containment survives in 40% of the core melt sequences, with 49% leading to late CCI-induced failures, 9% to early failures and 2% to late steam-induced failures.

The dominant contributors to early containment failure are summarized in Figure 7-2.1. The fraction of the Core Melt Frequency (CMF) leading to early containment failure (9%) is low and shows that the containment provides excellent protection against early releases. Approximately 8% of the core melt frequency is due to SGTR. The remaining early failures correspond to approximately 1% of the core melt frequency. Various transients (PDS 4H, 3H, 3F, 4F), V-Sequence and Small break LOCAs (PDS 1H, 1F) contribute 4.2% (0.4% CMF), 2.9% (0.3% CMF), 1.4% (0.13% CMF), respectively, to early failures.

The distribution of early containment failure by phenomenological causes is shown in Figure 7-3. Of the early failures, 84% are due to SGTR, 7% are due to alpha mode failures of the containment, 5.4% are

due to HPME including burns, and 2.9% are V-Sequences. Isolation failures are insignificant because of the independence of containment isolation on support systems.

The breakdown of late containment failure resulting from core-concrete interaction effects is shown in Figures 7-4.1 and 7-4.2. These represent the majority (49%) of all containment failures. The main contributors are PDS 1H (mostly induced small break LOCAs) and PDS 3H (transients), both with ECCS failure to inject, which together lead to almost 90% of the CCI-induced failures.

The breakdown of the late steam induced failures which total up to only 2% of the containment failures is shown in Figure 7-5. Steam-induced failures are low because they can only occur if the RWST is successfully injected and subsequently fails. If ECCs fails to inject, boil off of the RCS plus accumulator inventory cannot take the pressure to containment failure. Additional pressurization from CO_x non-condensible gas generation is required. The main contributors are PDS 2H (small break LOCAs), PDS 4H (transients) and PDS 6H (large break LOCAs) where ECCS injection was initially successful but failed at recirculation.

Figure 7-1: CPSES Overall Containment Performance

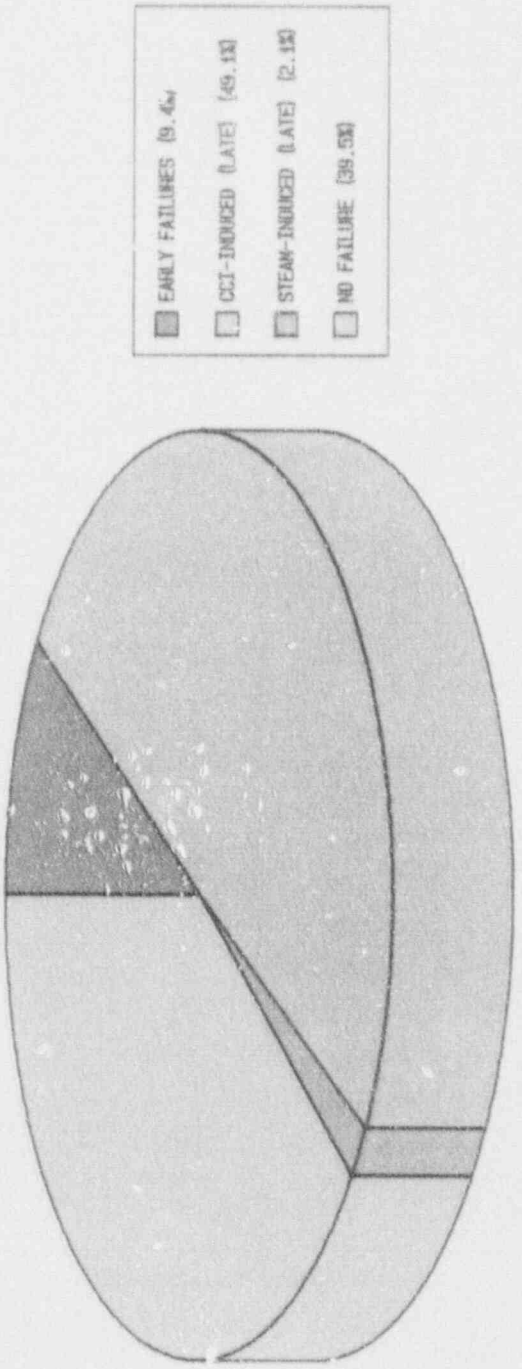

Figure 7-2.1: Breakdown of Early Failures by PDS

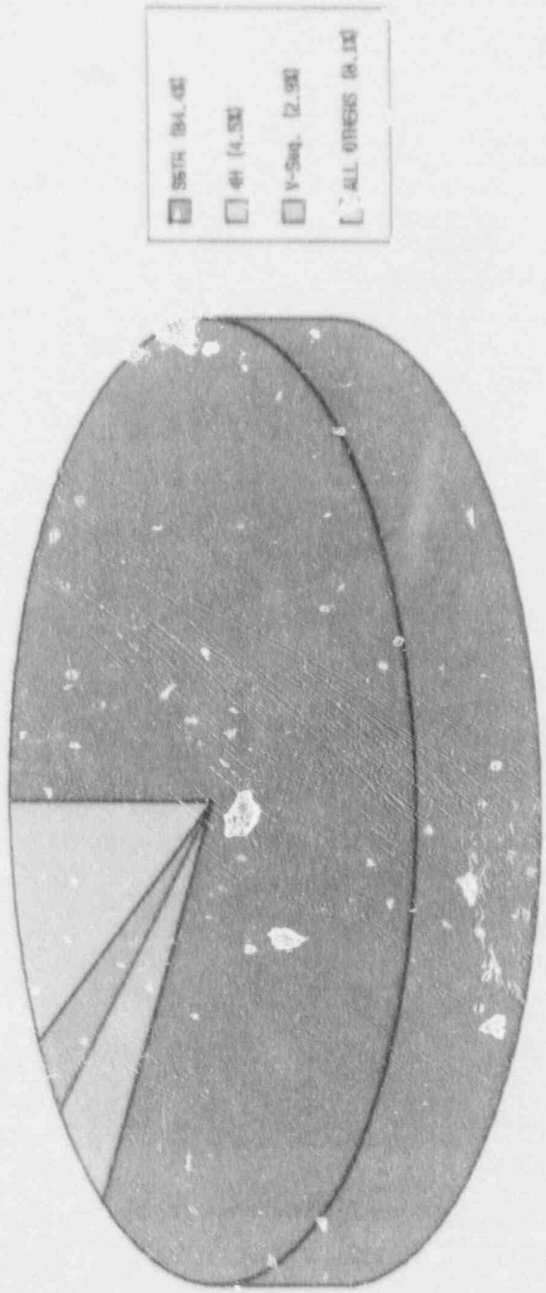

Figure 7-2.2: Early Failures (except SGTR) by PDS

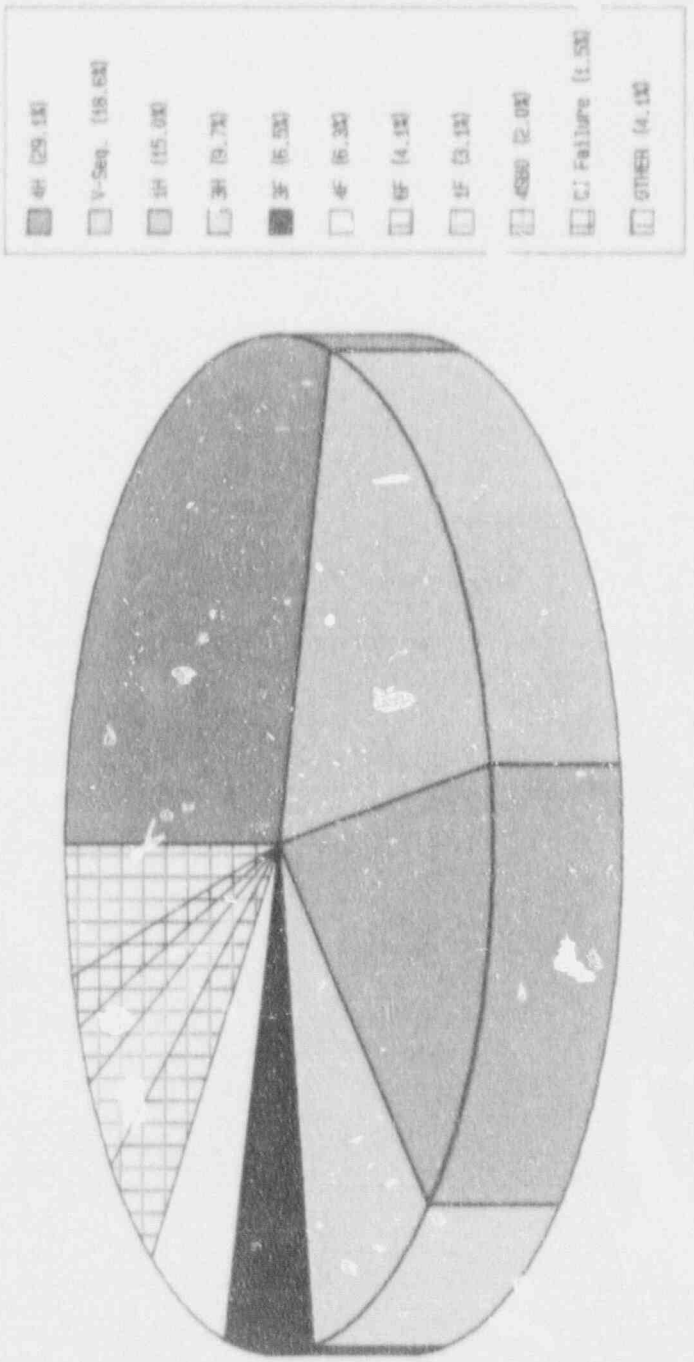

Figure 7-3: Breakdown of Early Failures by Cause

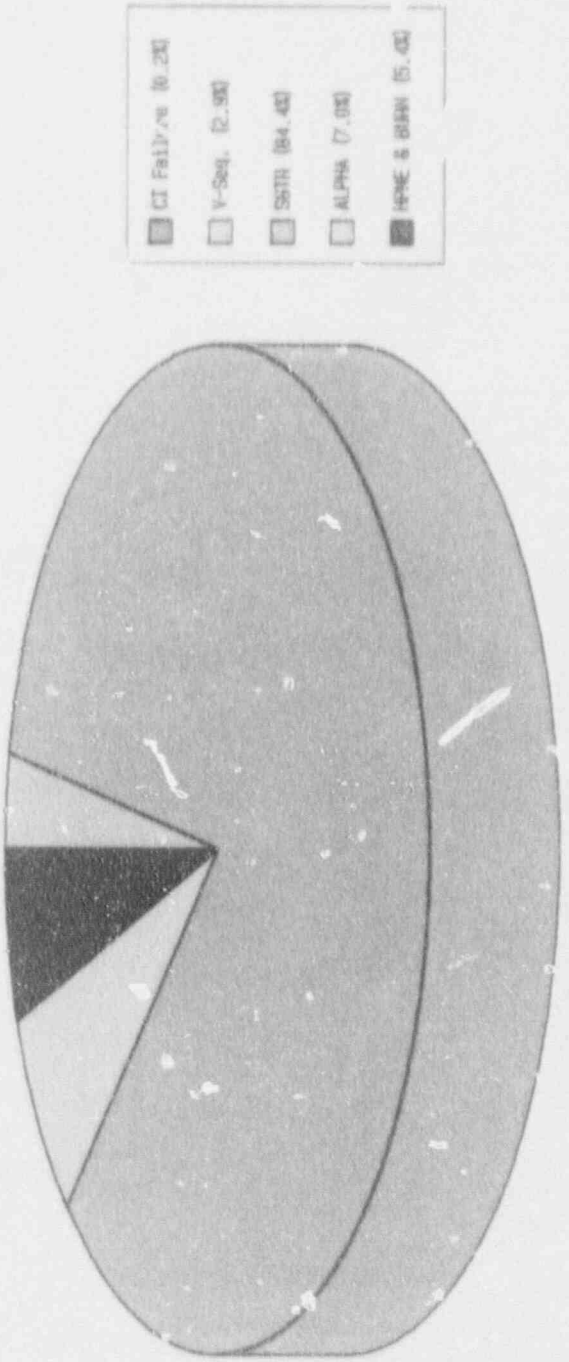

Figure 7-4.1: Breakdown of CCI-Induced Late Failures by PDS

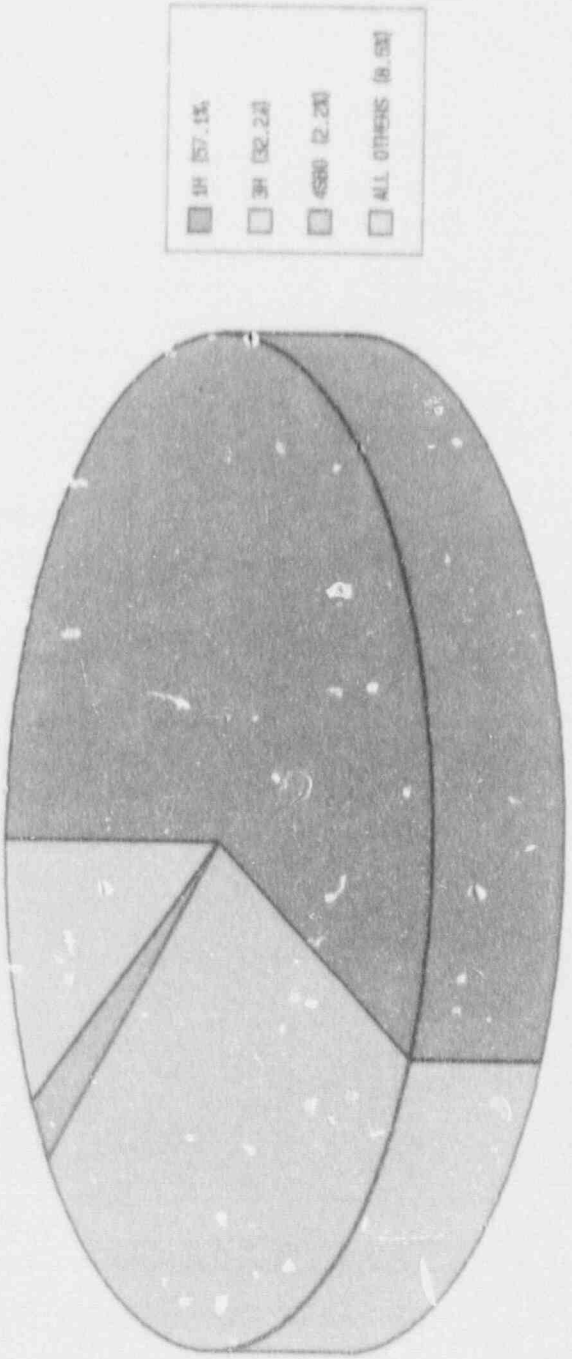

Figure 7-4.2: Detail of ALL OTHERS (8.5%) CCI-Induced Failures

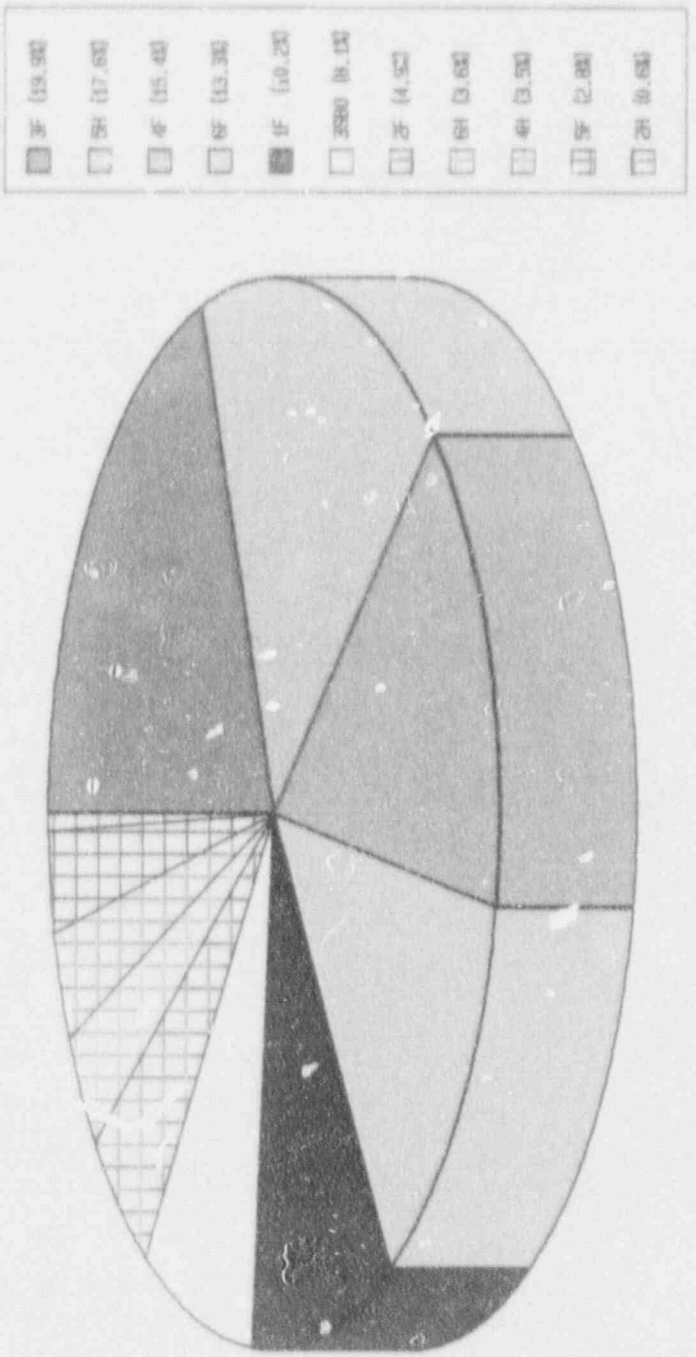

Figure 7-5: Breakdown of Steam-Induced Failures by PDS

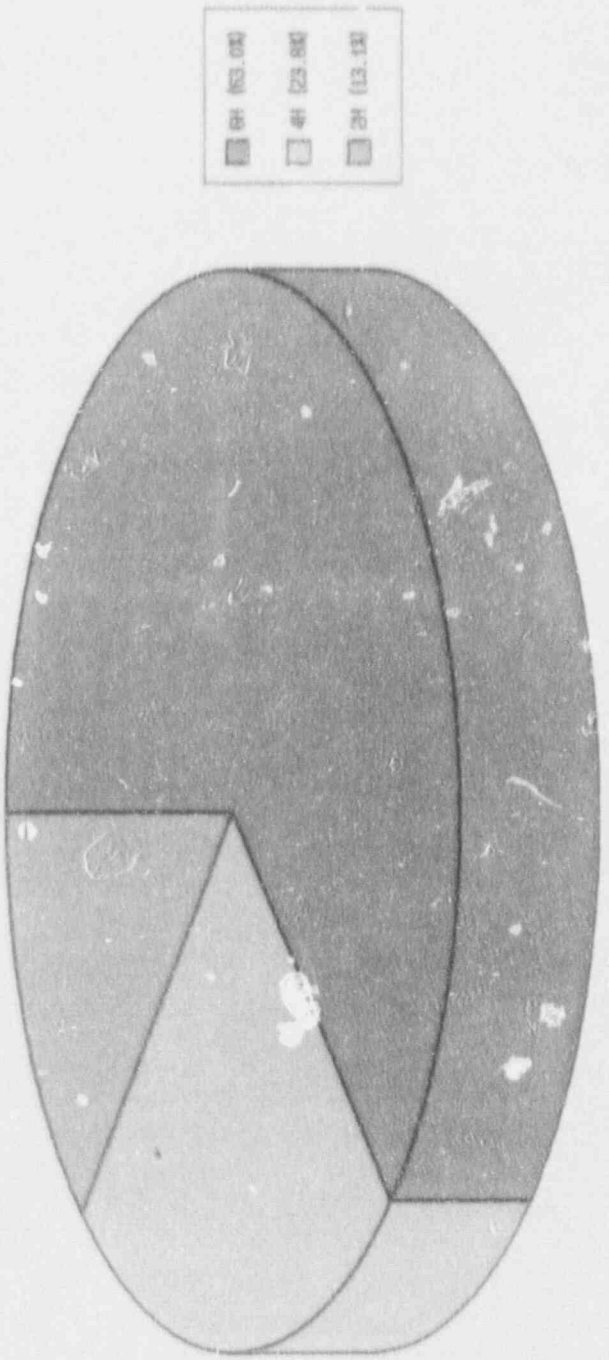

8. REFERENCES

There is a list of references in each of the volumes of the CPSES IPE report. The references in section 8 of Volume I pertain to the Front-End analysis and are unique to that volume. The references in section 8 of Volume II presented here pertain to the Back-End analysis and are unique to Volume II.

1. Z. T. Mendoza, et. al., "Generic Framework for IPE Level 2 Analysis," NSAC 159, October 1991.

2. H. da Silva, "MAAP Calculations of Accident Progression Baselines for CPSES IPE PDS," TU Electric, RXE-LA-TBD, 1991.

3. U.S. Nuclear Regulatory Commission, "Severe Accident Risks: An Assessment for Five U.S. Nuclear Power Plants," NUREG-1150, June 1989.

4. C. Cragg, "Accident Sequence Analysis," TU Electric, RXE-SY-CP1/1-013, 1991.

5. D. Tirsun, "Interfacing Systems LOCA," TU Electric, RXE-SY-CP1/1-026, 1992.

6. Y. Shen, "System Notebook: Containment Isolation," TU Electric, RXE-SY-CP1/1-024C, 1992.

7. H. da Silva, "The CPSES Containment Performance During Severe Accidents," TU Electric, RXE-LA-TBD, 1992.

8. H. da Silva, "Containment Event Tree Analysis," TU Electric, RXE-LA-TBD, 1992.

9. G. Bozoli, P. Kohut, R. Fitzpatrick, "Interfacing Systems LOCA: Pressurized Water Reactors," NUREG/CR-5102, February 1989.

10. R. Henry et. al, "MAAP 3.0B Computer Code Manual," Volumes 1 and 2, EPRI NP-7071-CCML, November 1990.

11. U.S. Nuclear Regulatory Commission, "Containment Performance Working Group Report," NUREG-1037, Draft Report for comment, May 1985.

12. Z. M. Shapiro and T. R. Moffette, "Hydrogen Flammability Data and Application to PWR Loss-of-Coolant Accidents," WAPD-SC-545, Westinghouse Electric Corporation, 1957.

13. Dameron, R.A., Dunham, R. S. Rashid, Y. R. and Sullaway, M. F. "Criteria and Guidelines for Predicting Concrete Containment Leakage," Electric Power Research Institute NP-6260-M, Research Project 2172-1, Interim Report, Palo Alto, CA, April 1989.

14. Comanche Peak Steam Electric Station Design Basis Document, "Penetration Seals," DBD-ME-002, Rev. 2, March 1992.

15. W. Sebrell, "The Potential for Containment Leak Paths Through Electrical Penetration Assemblies under Severe Accident Conditions," NUREG/CR-3234, June 1983.

16. Dunham, R. S., Rashid, Y.R., Yuan, K. A. and Lu, Y.M., "Methods for Ultimate Load Analysis of Concrete Containments," Electric Power Research Institute, NP-4046, Research Project 2172-1, Interim Report, Palo Alto, CA, June 1985.

17. Technology for Energy Corporation, "Technical Report 10.1, Containment Structural Capability of Light Water Nuclear Power Plants," IDCOR (Industry Degraded Core Rulemaking Program) Atomic Industrial Forum, Inc., Bethesda, MD, July 1983.

18. U.S. Nuclear Regulatory Commission, "Proceedings of the Workshop on Containment Integrity," by Sandia National Laboratories, SAND82-1659, NRC NUREG/CP-0033, Albuquerque, NM, October 1982.

19. U.S. Nuclear Regulatory Commission, "Containment Analysis Techniques: A State-of-the-Art Summary," by Sandia National Laboratories, NUREG/CR-3653, April 1984.

20. Dameron, R. A., Dunham, R.S., Rashid, Y.R. and Sullaway, M.F., "Methods for Ultimate Load Analysis of Concrete Containments," Electric Power Research Institute, NP-6263-SD, Research Project 2172-1, Palo Alto, CA, January 1989.

21. Dameron R. A., Dunham R. S., Rashid, Y. R. and Sullaway, M.F., "Analysis of the Sandia One-Sixth Scale Reinforced Concrete Containment Model," Electric Power Research Institute, Research Project 2172-1, Interim Report, Palo Alto, CA, March 1989.

22. Correspondence, Letter to H.T. Tang (EPRI) from R. A. Dameron (Anatech), August 30, 1990.

23. Hald, A., Statistical Theory with Engineering Applications, John Wiley & Sons, New York: 1975.

24. Fardis, M. N. A. Nacar, and M. A. Delichatsios, "Reinforced Concrete Containment Safety Under Hydrogen Explosion Loading," Massachusetts Institute of Technology, Department of Civil Engineering, NUREG/CR-2898, September 1982.

25. H. da Silva, "MAAP Parameter File Development," TU Electric, RXE-LA-CP1/1-025, Volumes I and II, 1992.

26. Parker Seals Co., O-Ring Handbook, OR5700, Copyright 1977.

27. H. da Silva, "PDS for CPSES IPE," TU Electric, RXE-LA-CP1/1-002, 1991.

28. Y. Shen, "Containment Reliability Estimation," TU Electric, RXE-SY-CP/TBD, 1992.

29. Science Applications International Corporation, "ETA-II version 2.0, USERS MANUAL," January 1991.

30. Electric Power Research Institute, "CAFTA, Version 1.7," prepared by Science Applications International Corporation, 1987.

31. Science Applications International Corporation, "GTPROB/GTPROB386 version 2.1d, Reference Guide," December 1991.

32. C.J. Ruger and W.J. Luckas, Jr. "Technical Findings Related to Generic Issue 23: Reactor Coolant Pump Seal Failure," NUREG/CR-4948, March 1989.

33. M.A. Kenton and J.R. Gabor, "Recommended Sensitivity Analyses for An Individual Plant Examination Using MAAP 3.0B," EPRI NP-TBD, 1991.

34. G. Lowenhielm, "MAAP 3.0B Sensitivity Analysis for PWR Station Blackout Sequences Sequences," EPRI NP-7192, January 1991.